

**FORAMINIFERAL BIOFACIES AND HOLOCENE SEDIMENTS FROM
SAANICH INLET, BRITISH COLUMBIA: IMPLICATIONS FOR
ENVIRONMENTAL AND NEOTECTONIC RESEARCH**

by

ANDRÉE BLAIS, B. Sc., M. Sc.

A thesis submitted to the Graduate Studies and Research

in partial fulfilment of

the requirements for the degree of

Doctor of Philosophy

Ottawa-Carleton Geoscience Centre

and

Department of Earth Sciences

Carleton University

Ottawa, Ontario

May, 1995.

©copyright

1995, Andrée Blais.



Carleton University
Ottawa, Canada K1S 5B6

**Thesis contains black & white
photographs &/or explanatory tables
which when microfilmed may lose their
significance. The hardcopy of the
thesis is available upon request from
Carleton University Library.**

The undersigned hereby recommend to
the Faculty of Graduates Studies and Research
acceptance of the thesis,

**"FORAMINIFERAL BIOFACIES AND HOLOCENE SEDIMENTS FROM
SAANICH INLET, BRITISH COLUMBIA: IMPLICATIONS FOR
ENVIRONMENTAL AND NEOTECTONIC RESEARCH"**

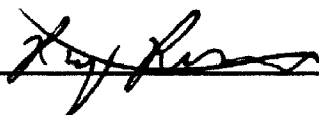
submitted by

ANDRÉE BLAIS, B. Sc., M. Sc.

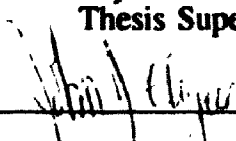
in partial fulfilment of the requirements
for the degree of Doctor of Philosophy



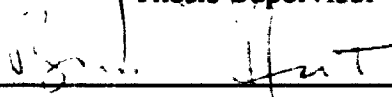
Chair, Department of Earth Sciences



Thesis Supervisor



Thesis Supervisor



External Examiner

Carleton University

May 1995

To Wayne, my companion for life.

ABSTRACT

This dissertation has been divided into three separate but related parts. The first describes the Saanich Inlet setting and gives a brief review of possible sedimentary processes in a submarine environment, the second establishes the environmental significance of foraminiferal biofacies from Saanich Inlet and the third, a paleoseismic study, describes and interprets sediments from cores collected in the central part of the basin. Foraminiferal analyses conducted on certain units in the paleoseismic study helped determine their origin.

In a reconnaissance study, foraminiferal biofacies identified in Saanich Inlet appear to be closely linked to a variety of environmental parameters including water quality. Five biofacies were defined based on Q-mode cluster analysis and faunal distribution profiles of foraminifera-bearing sediment surface samples from Saanich Inlet. Biofacies 1 (*Eggerella advena* Biofacies), is found nearshore in two densely populated bays. This assemblage appears to have an affinity to areas contaminated by sewage outfall and septic system drainage. Biofacies 2 (*Eggerella advena*-*Spiroplectammina biformis* Biofacies) and 3 (*Millammina fusca* Biofacies) characterize shallow, brackish waters, and are distributed in shallow bays near Biofacies 1. Biofacies 4 (*Lobatula fletcheri* Biofacies), the only biofacies dominated by a calcareous fauna, has been subdivided into two subbiofacies: Sub-biofacies 4A (*Stainforthia feylingi* Sub-biofacies) and 4B (*Buccella frigida* Sub-biofacies). Sub-biofacies 4A is found in deep water, low oxygen environments and Sub-biofacies 4B characterizes shallow water, normal marine environments. The patchy distribution of Sub-biofacies 4B samples is probably due to vagaries of water circulation in the restricted basin. Biofacies 5 (*Leptohalysis catella*-*Spiroplectammina biformis* Biofacies) defines a relatively deeper muddy environment with a high proportion of plant debris and low oxygen levels. The main environmental control is restricted water circulation which is guided by the shape of the basin, i.e., presence of the sill.

Eight sediment piston cores spanning the last 1500 years were collected from Saanich Inlet to obtain information on sedimentation and prehistoric earthquake activity. The cores consist mainly of silty clay varved sediments and massive beds deposited by debris flows. The debris flows may have been triggered by earthquakes or by the build-up of fine sediment on the walls of the inlet. Cesium-137 and ^{210}Pb data, ^{14}C ages, and varve counts were used to correlate massive layers in the eight cores. The uppermost massive layer in two cores may record a magnitude 7.2 earthquake in 1946 near Comox, B.C., 200 km north-northwest of Saanich Inlet. Five older layers, found in two or more cores are about 200, 550, 800-850, 1050-1100, and 1100-1150 years old. Some of these ages correspond to the times of documented seismic events. There is an average of one massive layer per 116 varves (range of 15-336) in the core with the greatest number of such layers. These results are broadly consistent with the expected periodicity of moderate to large earthquakes in the region (on average, one earthquake of local Modified Mercalli Intensity VII or VIII per 100 years). Saanich Inlet may contain a proxy record of all moderate and large earthquakes that have affected southwestern British Columbia during Holocene

time, but the set of massive layers likely includes both seismically and nonseismically generated deposits.

RÉSUMÉ

Ce mémoire traite de trois sujets différents mais liés. Le premier est une description de l'encadrement de l'inlet Saanich en Colombie-Britannique et une révision de quelques processus de déposition sédimentaire et sous-marine. Le deuxième est une étude qui détermine la signification environnementale des biofaciès de foraminifères dans l'inlet Saanich. Le troisième est une étude paléosismique décrivant et interprétant des sédiments prélevés avec un carottier à piston dans la partie centrale du même inlet Saanich. L'étude des foraminifères a permis d'identifier l'origine de certaines unités de l'étude paléosismique.

L'étude préliminaire des foraminifères semble indiquer que les biofaciès identifiés sont reliés à des paramètres environnementaux, tels que la contamination de l'eau associés au déversement de vidanges et au drainage de fosses septiques. Sur la côte ouest de l'inlet Saanich, on planifie un aménagement de la banlieue au nord de Victoria, la plus grande ville sur l'île de Vancouver. L'étude des foraminifères peut servir à mesurer le stress qu'un tel aménagement fera subir au délicat écosystème de l'inlet.

En combinant les résultats d'une analyse statistique appelée "Q-Mode cluster analysis" et ceux de profils de distribution de la faune foraminifère, cinq biofaciès ont été définis. Le biofaciès 1 (biofaciès *Eggerella advena*) est localisé dans deux baies densément peuplées de l'inlet Saanich. Il semble y avoir un rapport entre ce type d'assemblage et le déversement de vidanges et le drainage de fosses septiques dans ces baies. Le biofaciès 2 (biofaciès *Eggerella advena-Spiroplectammina biformis*) et le biofaciès 3 (biofaciès *Miliammina fusca*) représentent un environnement d'eaux saumâtres peu profondes situé dans des baies sises à proximité de celles du biofaciès 1. Le biofaciès 4 (biofaciès *Lobatula fletcheri*), le seul représenté par une faune calcaire, a été subdivisé en deux sous-biofaciès, soient 4A (sous-biofaciès *Stainforthia feylingi*) et 4B (sous-biofaciès *Bucella frigida*). Le sous-biofaciès 4A représente des conditions d'eaux profondes à faibles teneurs en oxygène. Le sous-biofaciès 4B représente des conditions d'eaux peu profondes et un environnement marin normal. La distribution sporadique de ce dernier sous-biofaciès est probablement liée aux variations de circulation des eaux dans un bassin restreint. Le biofaciès 5 (biofaciès *Leptohalysis catella-Spiroplectammina biformis*) représente un environnement d'eaux profondes, à faibles teneurs en oxygène et riches en matières végétales. Le principal facteur contrôlant la distribution des biofaciès est le manque de circulation des eaux qui est influencé par la présence d'un seuil.

Huit carottes prélevées dans l'inlet Saanich représentent une sédimentation au cours des 1500 dernières années. Le but des prélèvements est d'obtenir de l'information sur la sédimentation et l'activité pré-historique des tremblements de terre. Les sédiments sont constitués de varves dans lesquelles des couches massives résultant supposément de séismes, sont interstratifiées. La présence de foraminifères dans les couches massives a pu confirmer que celles-ci sont des coulées de boue. Ces coulées de boue peuvent avoir été déclenchées par des tremblements de terre ou par l'éboulement de sédiments fins, mous et instables sur les murs du bassin. Les

résultats d'analyses radiométriques du ^{137}Cs , ^{210}Pb , ^{14}C et du comptage de varves ont été utilisés pour établir la corrélation entre les couches massives de diverses carottes. La plus haute couche massive dans deux carottes représente possiblement le tremblement de terre qui a eu lieu en 1946 à Comox, situé quelques 200 km au nord-ouest de l'inlet Saanich. Cinq autres couches massives ont été identifiées dans deux ou plusieurs carottes et sont âgées de 200, 550, 800-850, 1050-1100 et 1100-1150 ans. Trois de celles-ci ont possiblement été mises en place lors d'autres tremblements de terre documentés dans la région. Il y a en moyenne 116 varves pour chaque couche massive (écart de 15 à 336) dans la carotte contenant le plus grand nombre de ces couches. Ces résultats concordent avec les prédictions de la périodicité des séismes moyens à grands dans la région. En moyenne, on calcule qu'il y a dans cette région un séisme par 100 ans de niveau VII ou VIII à l'échelle Mercalli. La séquence sédimentaire de Saanich documente possiblement tous les tremblements de terre qui ont secoué la région du sud-ouest de la Colombie-Britannique pendant l'Holocène supérieur. Une mise en garde- la séquence peut également inclure des sédiments résultant d'éboulements de sédiments, non occasionnés par des séismes, à partir des murs de bassin.

ACKNOWLEDGEMENTS

This research was funded by the Geological Survey of Canada (GSC; J. J. Clague's Project Number 870017) and by Natural Sciences and Engineering Research Council of Canada Operating Grant OGP0041665 to R. T. Patterson. I am grateful to Dr. Clague for offering me this project in a unique setting of our country, his enlightening discussions, and his editorial suggestions. Dr. Patterson is thanked also for initiating my work in southern B.C. and for his helpful editorial comments and suggestions.

Dr. P.T. Bobrowsky is acknowledged for proposing that I work on Saanich Inlet sediments. Drs. J.-S. Vincent, R.N.W. DiLabio, and R.J. Fulton are thanked for hiring me and giving me permission to complete my thesis while an employee of the Geological Survey of Canada. Dr. Vincent helped me translate the thesis abstract.

Radiocarbon ages were provided by IsoTrace Laboratory (University of Toronto). Cesium-137 determinations were made by Dr. T.S. Hamilton and Ms. W. Bentkowski at Pacific Geoscience Centre. R. McDonald and G. Jewsbury collected the piston cores. T. Forbes facilitated sedimentological analyses at the GSC laboratory at Pacific Geoscience Centre. Technical support from the Geological Survey of Canada Library and Photomechanical Unit is appreciated. Ms. S. Burbidge (Carleton University Ph.D. student) is thanked for her sound advice during preparation of my defence presentation. E. Keane and M. Taylor (summer students) drafted some of the figures.

I am greatly indebted to Mr. and Mrs. Stevens for inviting me into their home

while I was working as a student. I appreciate their kindness and generosity. Ms. A. Collins is also thanked for providing room and board during my first summer at Pacific Geoscience Centre.

In addition, I thank my parents (Doreen and Marcel Blais), Denyse and Elie, and the rest of my family for their encouragement.

Last but not least, I am very grateful to Wayne Stevens, my spouse, for his technical assistance, encouragement, and emotional support.

ORIGINAL CONTRIBUTION

The economy of southern Vancouver Island relies heavily on fishing, tourism, and aquaculture, all of which are adversely affected by water pollution. Plans to build 5000 new houses with septic system sewage treatment on the southwestern side of Saanich Inlet could have considerable environmental impact on the inlet.

Foraminifera are used as environmental indicators of pollution sources but no work of this type has been carried out on the northwest coast. Consequently, there is an interest and a need to conduct a reconnaissance foraminiferal study to establish the biofacies of this fiord, which is anoxic at depth.

The foraminiferal biofacies project evolved from discussions with Dr. R. T. Patterson about the effects of restricted water circulation and pollution in Saanich Inlet and the use of foraminifera as proxies of slumping. For this portion of my dissertation research, I collected grab samples from a small boat during a period of three weeks in July 1992. I also processed the samples, identified, and quantitatively analyzed the foraminiferal populations over a period of 14 months (September 1992- October 1993).

Furthermore, there is concern that a moderate to large earthquake may damage cities and the economic infrastructure. In southwestern British Columbia, the search for paleoseismic evidence in the sediment record may provide insights into the frequency and magnitude of past earthquakes. Since the sediments in the central part of Saanich Inlet consist of varves intercalated with massive layers which have been attributed to earthquakes, a paleoseismic study was conducted on eight piston cores

containing sediments that span the last 1500 years to determine the origin of the massive layers.

The original proposal for the project on sediment cores evolved from a post-doctorate fellowship project carried out by Dr. P. T. Bobrowsky (who, at the time was stationed at Pacific Geoscience Centre) under Dr. J. J. Clague's supervision (GSC). Their interesting results led to the collection of additional cores, which I utilized in my dissertation research.

With assistance, I split, described in detail, and subsampled both sets of cores over eight summer months in 1992 and 1993. I prepared samples for ^{14}C , ^{210}Pb , and ^{137}Cs dating, and conducted most of the ^{137}Cs analyses. I performed clay fraction separations on sediment samples and prepared them for X-ray analyses. I also processed sediment samples for identification and point-counting of foraminiferal species.

My contribution to the field of micropaleontology is that I have provided the first baseline foraminiferal study in Saanich Inlet in which biofacies were established. I have initiated interest in using foraminifera for detecting subtle environmental changes. In the field of sedimentology, I have documented the sedimentation pattern in Saanich Inlet and confirmed the origin of the massive layers as sediment gravity flow deposits, more precisely, debris flows deposits. Foraminifera were used to confirm the sediment gravity flow origin of the deposits. Furthermore, I have documented that some debris flow deposits are coincident with known seismic events.

I have benefitted from discussions with my advisors, colleagues, and students

but take full responsibility for the data and interpretations presented in this thesis.

TABLE OF CONTENTS

DEDICATION	i
TITLE PAGE	ii
ACCEPTANCE SHEET	iii
ABSTRACT	iv
RÉSUMÉ	vi
ACKNOWLEDGEMENTS	viii
ORIGINAL CONTRIBUTION	x
TABLE OF CONTENTS	xiii
LIST OF TABLES	xx
LIST OF FIGURES	xxi
LIST OF PLATES	xxiv
LIST OF APPENDICES	xxv
CHAPTER 1: Introduction	1
Method of presentation	1
Location and description of Saanich Inlet and the area	1
Climate, temperature, and precipitation	1
Runoff	7
Winds	9
Physical oceanography	9
Tides	9
Currents	9

Flushing	10
Temperature, oxygenation, salinity, and density of the water column	12
Bedrock geology	12
Surficial geology	16
Sediment distribution in Saanich Inlet	20
Sedimentary processes	20
Classifications of sediment gravity flows	20
Classification utilized in the thesis	22
1) Turbidity currents	24
Sedimentary structures of turbidites	24
2) Liquified flows	27
Sedimentary structures of liquefied flow deposits	29
3) Grain flows	29
Sedimentary structures of grain flow deposits	29
4) Debris flows	30
Sedimentary structures of debris flow deposits	32
Objectives	32
References	34
CHAPTER 2: Biofacies of benthic foraminiferal Saanich Inlet, Vancouver Island, British Columbia: valuable environmental indicators.	39
Abstract	39

Introduction	41
Study area	43
Previous work	51
Methods and materials	52
Results	57
Species abundance and preservation	57
% live vs. depth of sample	58
Cluster analysis	58
Faunal distribution of dominant species	63
Bays/shore	63
Basin trough	68
Biofacies	73
Biofacies 1: <u>Eggerella advena</u> Biofacies	73
Biofacies 2: <u>Eggerella advena-Spiroplectammina biformis</u>	
Biofacies	73
Biofacies 3: <u>Miliammina fusca</u> Biofacies	77
Biofacies 4: <u>Lobatula fletcheri</u> Biofacies	77
Sub-biofacies 4A: <u>Stainforthia feylingi</u>	
Sub-biofacies	77
Sub-biofacies 4B: <u>Bucella frigida</u>	
Sub-biofacies	78
Biofacies 5: <u>Leptohalysis catella Spiroplectammina biformis</u>	

Biofacies	78
Discussion	78
% live vs. depth of sample	78
Biofacies	79
Biofacies 1: <u>Eggerella advena</u> Biofacies	79
Biofacies 2: <u>Eggerella advena-Spiroplectammina biformis</u>	
Biofacies	80
Biofacies 3: <u>Miliammina fusca</u> Biofacies	81
Biofacies 4: <u>Lobatula fletcheri</u> Biofacies	82
Sub-biofacies 4A: <u>Stainforthia feylingi</u> Sub-biofacies	
	82
Sub-biofacies 4B: <u>Bucelia frigida</u> Sub-biofacies	83
Biofacies 5: <u>Leptohalysis catella Spiroplectammina biformis</u>	
Biofacies	84
Environmental control of the biofacies	85
Conclusions	86
Faunal reference list	88
Acknowledgements	93
References	95
PLATE 2-1	104
PLATE 2-2	106
PLATE 2-3	108

PLATE 2-4	110
PLATE 2-5	112
Appendix 2-1	114
CHAPTER 3: Paleoseismic evidence in late Holocene sediments, Saanich Inlet,	
British Columbia.	146
Abstract	146
Introduction	147
Study area	152
Previous work	156
Methods and materials	158
Results	162
Sedimentology	162
Varved sediments	162
Massive layers	166
Particle-size analyses	172
Clay mineralogy	183
Micropaleontology	183
Dating	187
Cesium-137	187
Lead-210	189
Carbon-14	191
Varve chronology	191

Discussion	194
Debris flow deposits	194
Correlation of the cores	195
Regional correlations	196
Style and pattern of sedimentation	200
Causes of the of the debris flows	205
Model 1: None of the debris flows were triggered by earthquakes	205
Model 2: All of the debris flows were triggered by earthquakes	206
Model 3: Some, but not all of the debris flows, were triggered by earthquakes	209
Error analysis	210
Lack of a precise datum	210
Missing varves	213
Contamination	213
Dating using varves	214
Conclusions	214
Acknowledgements	217
References	218
Appendix 3-1	230
Appendix 3-2	235

Appendix 3-3	237
Appendix 3-4a	243
Appendix 3-4b	250
Appendix 3-5	257
Appendix 3-6	259
Appendix 3-7	263
Appendix 3-8	272
CHAPTER 4: Conclusions	277

LIST OF TABLES

Table 2-1. Location of sample sites.	54
Table 2-2. Characteristics of the five foraminiferal biofacies.	76
Table 3-1. Location of core sites.	159
Table 3-2. Average varve thickness per core.	167
Table 3-3. Distribution of massive layers within the cores.	177
Table 3-4. Foraminiferal faunal reference list.	188
Table 3-5. Radiocarbon ages.	192
Table 3-6. Cumulative number of varves between massive layers.	193
Table 3-7. Age of massive layers (core TUL89A-003).	197
Table 3-8. Scenario (a). Possible correlations based on adjusted cumulative number of varves.	199
Table 3-9. Summary of correlations based on scenarios (a), (b), and (c).	201

LIST OF FIGURES

Figure 1-1. Location map of Saanich Inlet, British Columbia.	2
Figure 1-2. Detailed location map of Saanich Inlet.	4
Figure 1-3. Watershed boundaries, Saanich Inlet.	8
Figure 1-4. Oxygen structure in Saanich Inlet.	11
Figure 1-5. Temperature structure in Saanich Inlet.	13
Figure 1-6. Salinity structure in Saanich Inlet.	14
Figure 1-7. Density structure in Saanich Inlet.	15
Figure 1-8. Bedrock geology map of Saanich Inlet area.	18
Figure 1-9. Subdivisions of Quaternary events and deposits.	19
Figure 1-10. Location of surface sediments in Saanich Inlet.	21
Figure 1-11. Classification of subaqueous sediment gravity flows.	23
Figure 1-12. Sedimentary structures associated with sediment gravity flows.	25
Figure 1-13. Hydraulics of turbidity currents.	26
Figure 1-14. Turbidite; Bouma sequence.	28
Figure 1-15. Cross-section of a debris flow.	31
Figure 2-1. Location map of Saanich Inlet, British Columbia.	42
Figure 2-2. Sample location map.	45
Figure 2-3. Oxygen structure in Saanich Inlet.	47
Figure 2-4. Sediment map, Saanich Inlet.	48
Figure 2-5. Temperature structure in Saanich Inlet.	49
Figure 2-6. Salinity structure in Saanich Inlet.	50

Figure 2-7. Scattergram of % live specimens per sample v.s. depth of sample.	60
Figure 2-8. Dendrogram from Q-mode cluster analysis.	62
Figure 2-9. Profile 1; Cumulative abundance of dominant species per sample depth.	65
Figure 2-10. Profile 2; Cumulative abundance of dominant species per sample depth.	67
Figure 2-11. Profile 3; Cumulative abundance of dominant species per sample depth.	70
Figure 2-12. Profile 4; Cumulative abundance of dominant species per sample depth.	72
Figure 2-13. Biofacies map.	75
Figure 3-1. Schematic diagram showing subduction of the oceanic Juan de Fuca plate beneath North America.	148
Figure 3-2. Location map of Saanich Inlet, British Columbia.	151
Figure 3-3. Location map of core sites.	153
Figure 3-4. Sediment map, Saanich Inlet.	155
Figure 3-5. Scattergrams of varve thicknesses versus core depth.	165
Figure 3-6. Summary of core stratigraphy and radiometric ages.	176
Figure 3-7. Particle size distribution of all samples.	178
Figure 3-8. Particle-size distribution of samples of varved sediments and massive layers.	179
Figure 3-9. Percent clay abundances in massive layers (core TUL91A-003).	181

Figure 3-10. Comparison between varve particle-size distribution and sedimentation rates for two cores (TUL89A-001 and TUL91-001)	182
Figure 3-11. Particle-size distribution of samples of massive clayey silt from core TUL91A-005.	186
Figure 3-12. Semi-log plots of ^{210}Pb data from (A) core TUL89A-003 and (B) TUL91A-005.	190
Figure 3-13. Schematic diagram showing the inferred origin of massive layers within the varved sequence in Saanich Inlet.	202
Figure 3-14. Three interpretations of a hypothetical sequence of massive layers deposited by debris flows in Saanich Inlet.	212

LIST OF PLATES

Plate 1-1. Bathymetric map of Saanich Inlet, B.C.	6
Plate 2-1. Common agglutinated specimens.	104
Plate 2-2. Common agglutinated specimens.	106
Plate 2-3. Common agglutinated specimens.	108
Plate 2-4. Common calcareous specimens.	110
Plate 2-5. Common calcareous specimens.	112
Plate 3-1. Typical varved sediments.	164
Plate 3-2. Massive layer overlain and underlain by varved sediments.	169
Plate 3-3. Brecciated laminae at the base of a massive layer.	171
Plate 3-4. Deformed overturned varves at the base of a massive layer.	174
Plate 3-5. Clayey silt containing scattered shells and shell fragments (core TUL91A-005).	185

LIST OF APPENDICES

Appendix 2-1. Percent abundance, percent live specimens, and percent error.	114
Appendix 3-1. Particle-size data.	230
Appendix 3-2. T-test calculations.	235
Appendix 3-3. Percent clay fractions in massive layers.	237
Appendix 3-4a. Particle-size fractions in varves.	243
Appendix 3-4b. Particle-size fractions in massive layers.	250
Appendix 3-5. Clay mineralogy.	257
Appendix 3-6. Foraminiferal content in the massive layers.	259
Appendix 3-7. Lead-210 data.	263
Appendix 3-8. Possible correlations of the massive layers.	272

CHAPTER 1. Introduction

Method of presentation

This dissertation is presented, in part, in the form of scientific journal articles. The first chapter is an introduction to Saanich Inlet and a review of sedimentary processes in the fiord. The main chapters (2 and 3) detail the contents of two separate projects. The last chapter outlines the conclusions. Due to the format, there is some repetition of introductory material in Chapters 1, 2, and 3.

Location and description of Saanich Inlet and the surrounding area

Saanich Inlet is a fiord located on southern Vancouver Island, approximately 15 km north of Victoria, British Columbia (Fig. 1-1). It is 26 km long, up to 8 km wide, and has an average and maximum depths of 120 m and 236 m, respectively (Fig. 1-2 and Plate 1-1). A bedrock sill is located at the north end of the inlet at 70 m depth (Herlinveaux, 1962). In the northern part of the basin, wall slopes are shallow and in the southern part, steep.

Saanich Inlet lies in the Nanaimo Lowlands physiographic region (Holland, 1964). The terrain surrounding the inlet ranges from gently rolling in the north to steeply sloping in the south. Relative to much of Vancouver Island, the area has generally low relief (Holland, 1964).

Climate, temperature, and precipitation

The climate is temperate maritime with wet winters and dry summers (Herlinveaux, 1962; Gucluer and Gross, 1964; EnviroEd Consultants Ltd., 1995). Air temperature at Victoria is coldest in January with a mean of 4°C and

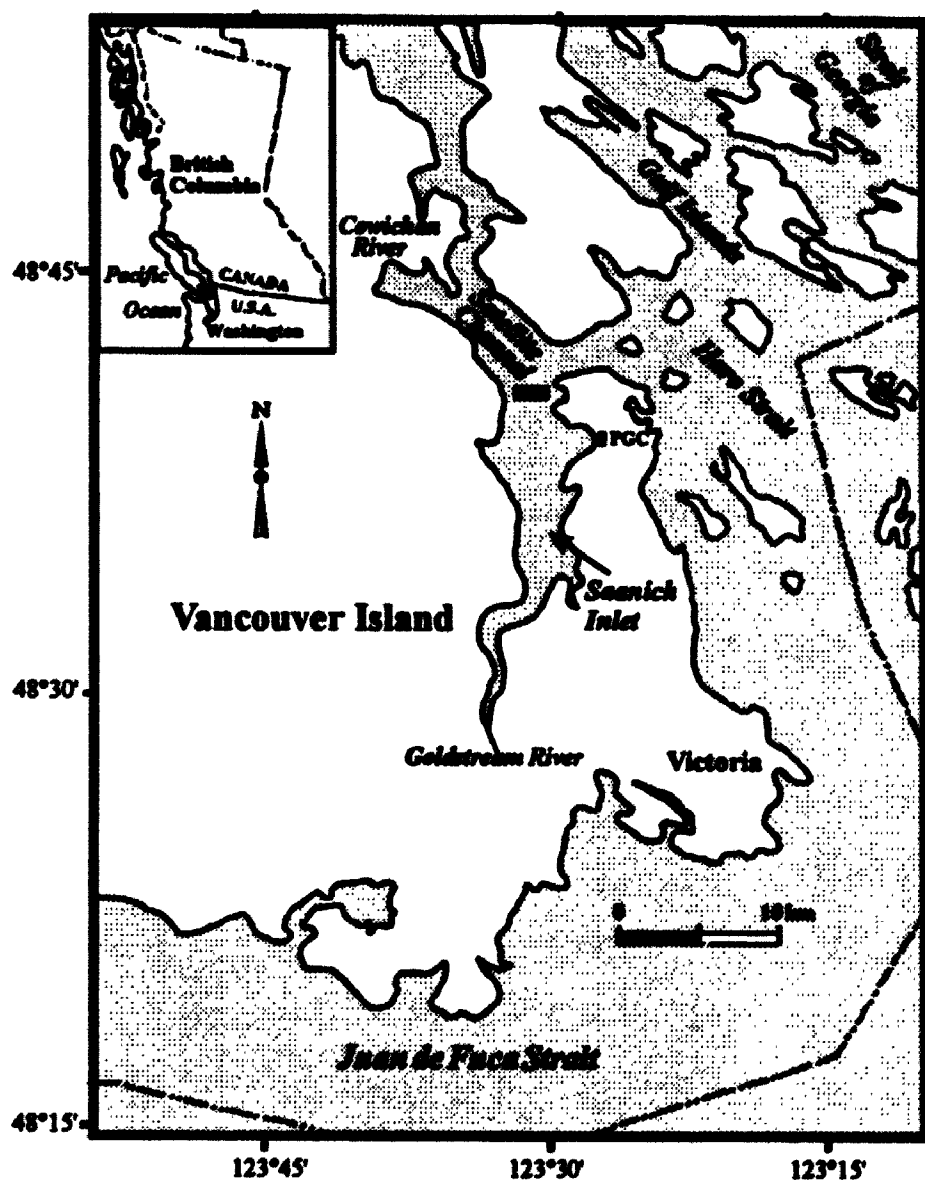


Figure 1-1. Location map, Saanich Inlet, British Columbia. The shaded box locates the bedrock sill at the north end of the inlet. PGC=Pacific Geoscience Centre.

Figure 1-2. Map of Saanich Inlet, British Columbia. PGC= Pacific Geoscience Centre. Stations O, M, L, J, H, and B are from a hydrological study by Herlinveaux (1962). They are referred to in Figs. 1-4, 1-5, 1-6, and 1-7.

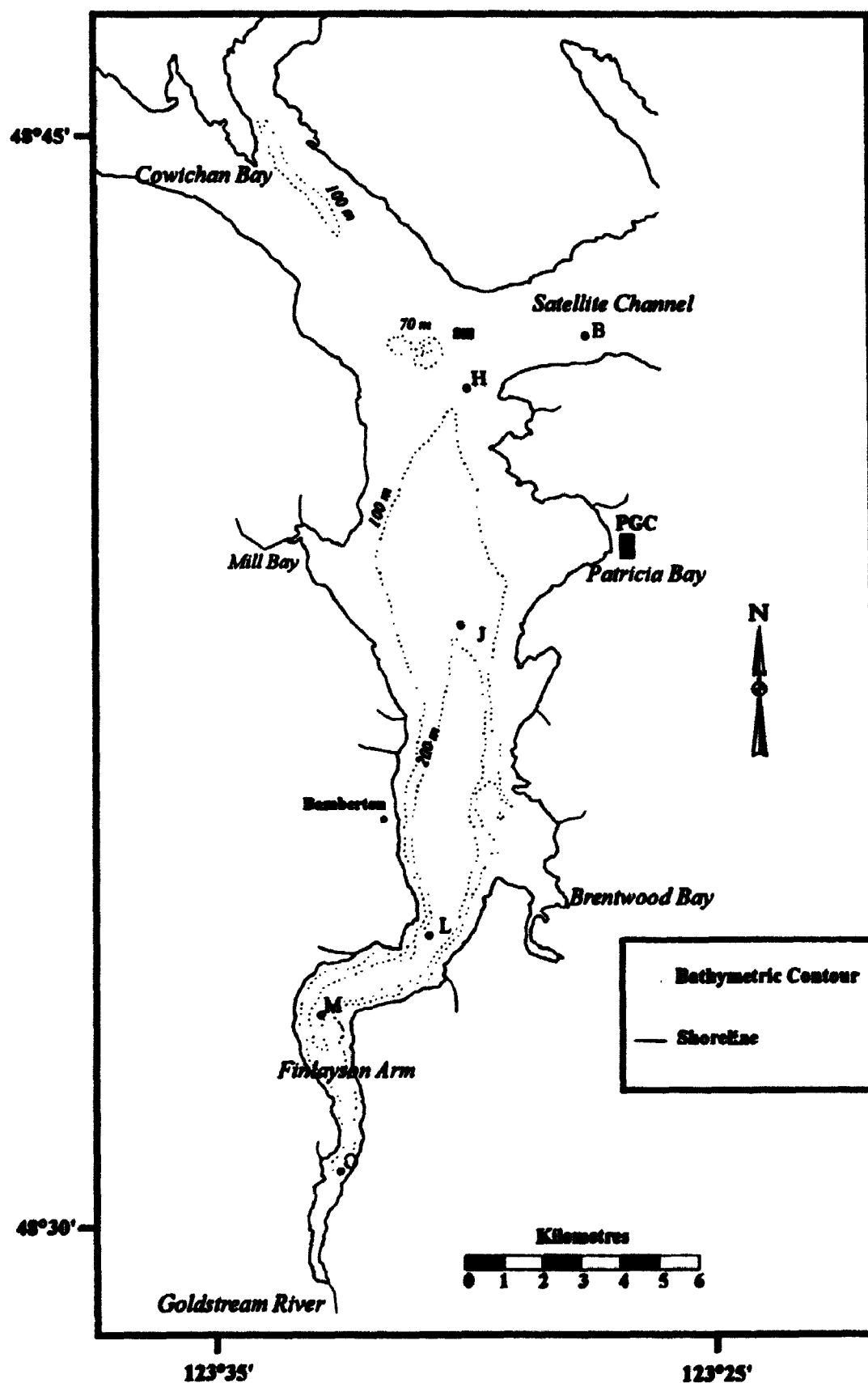
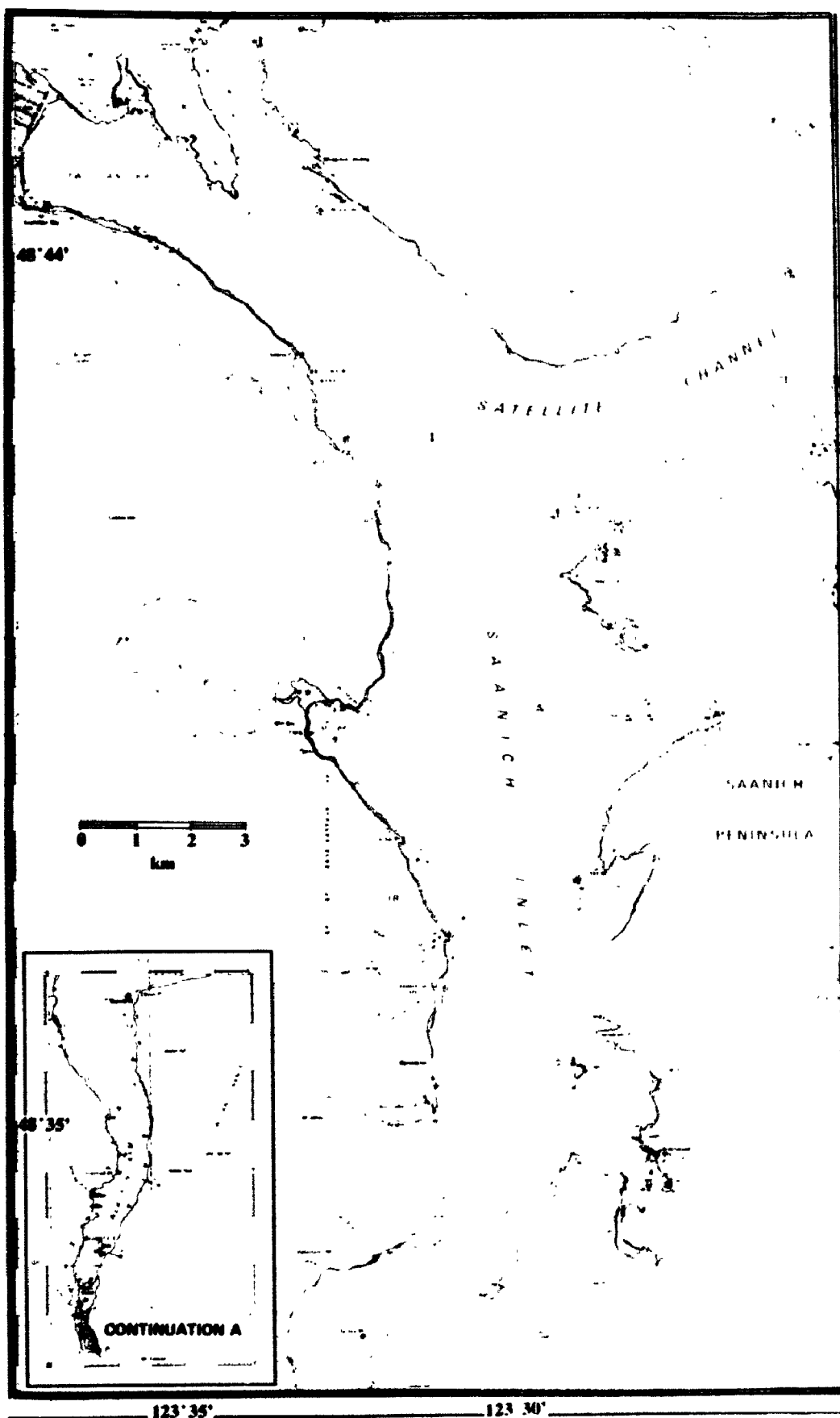


Plate 1-1. Bathymetric map of Saanich Inlet.



warmest in July with a mean of 16°C (Kendrew and Kerr, 1955; Herlinveaux, 1962). The mean annual temperature at the Victoria International Airport is 9.5 °C (Atmospheric Environment Service, 1982; EnviroEd Consultants, 1995).

Precipitation is usually in the form of rain. The average annual precipitation is 81.5 cm. Precipitation is greatest in December (13.7 cm) and least in July (1.8 cm; Herlinveaux, 1962).

Runoff

The main source of freshwater and sediment is Cowichan River northwest of the mouth of the inlet. In addition, Saanich Inlet is surrounded by a number of small watersheds which cover approximately 395 km² (Fig. 1-3). The only significant stream flowing into Saanich Inlet is Goldstream River, and it contributes only a small percentage of the 9×10^4 tonnes of sediments that accumulate in Saanich Inlet each year (Gross and others, 1963). In most British Columbia fiords, the runoff enters at the head and develops a two-layer flushing system. In contrast, the freshwater runoff at the head of Saanich Inlet (Goldstream River) is negligible, and the dominant freshwater source originates from the approaches (Cowichan River).

Between 1892 and 1910, the Greater Victoria Water District began diverting water from the Goldstream River watershed by building reservoirs. As the population of Victoria increased, the demand for freshwater grew and diversions from Goldstream River also increased. Records of water supply for the area in the late 1800's are either nonexistent or very poor, and there are no quantitative observations for the watershed prior to dam construction. Nevertheless, from observations using a

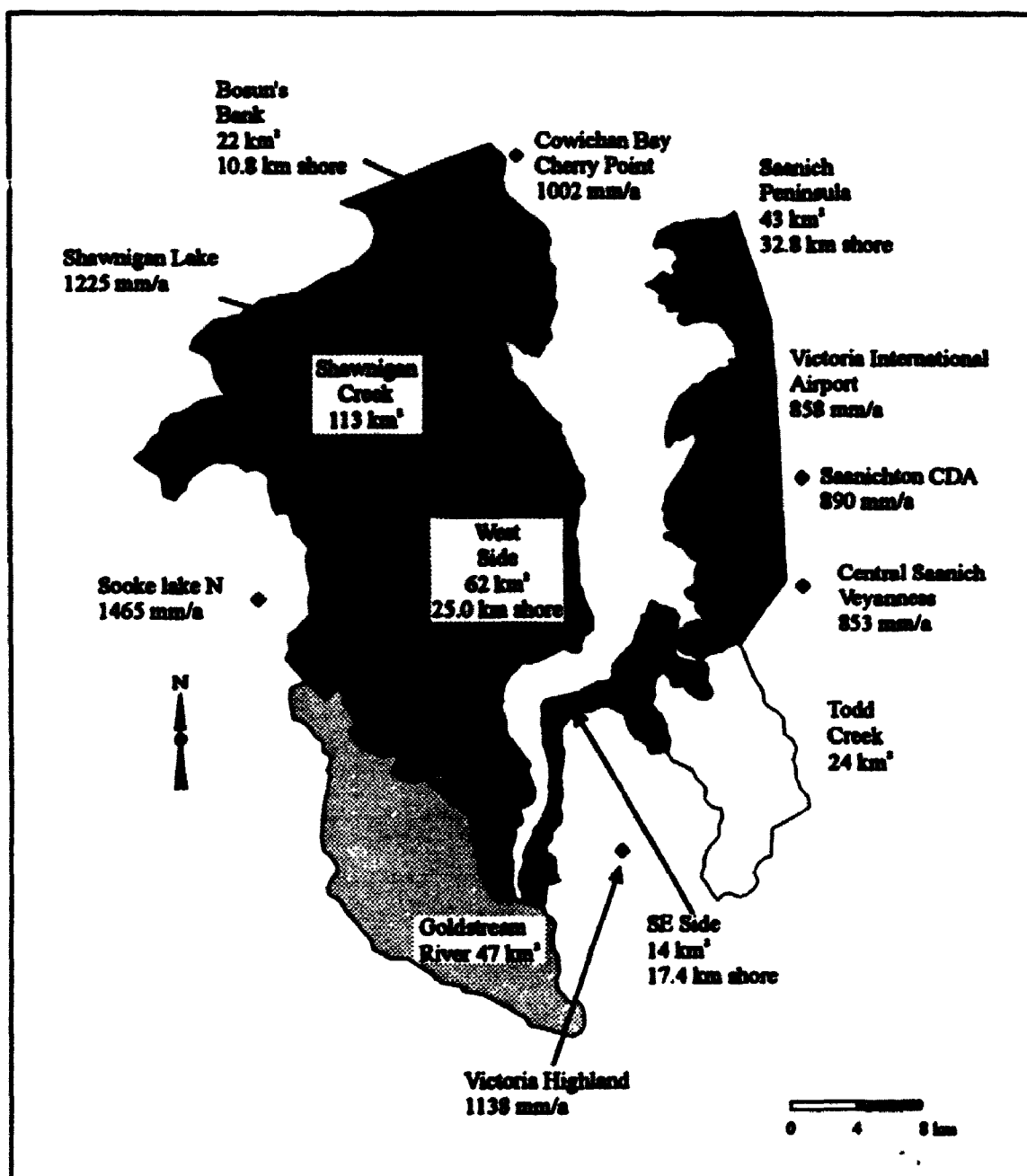


Figure 1-3. Watershed boundaries and precipitation stations with annual mean precipitation (modified from EnviroEd Consultants Ltd., 1995).

topographic map (NTS: 92B/05; 1:50 000 scale), it is apparent that the base widths of the tributary stream channels flowing into Goldstream River and of Goldstream River itself are on average small (<100 m wide) and therefore, do not indicate that the water supply was considerably greater before water supply diversion. This is discussed further in Chapter 3.

Winds

Winds generally blow from the southeast in summer and from the west in winter (Kendrew and Kerr, 1955; Herlinveaux, 1962). From measurements at Patricia Bay, the mean speed is highest at 9.6 km/h in winter and lowest, at 8 km/h in summer (Kendrew and Kerr, 1955).

Physical oceanography

Tides

Tides in Saanich Inlet are intermediate in range. The mean range is 2.44 m and the maximum is 3.8 m (Herlinveaux, 1962). They are classified as mixed semi-diurnal tides with the diurnal components dominant (Stucchi and Giovando, 1984; EnviroEd Consultants Ltd., 1995; D. Stucchi, oral communication, 1995).

Currents

A compilation by EnviroEd Consultants Ltd. (1995) describes currents in Saanich Inlet in plan view and in elevation. In plan view, currents are divided in two components: one north of Mill Bay and Patricia Bay, and the other to the south. Currents north of the Mill Bay/Patricia Bay line are thought to be associated with currents from Satellite Channel travelling from the west to east. South of the Mill

Bay/Patricia Bay line, currents are thought to travel longer and may come from any direction. It is not known whether they are wind-driven or an expression of tidal resonance.

In depth, currents are divided in three components: one above sill depth (70 m); the second at sill depth; and the third below sill depth. In the northern part of the inlet, currents from the upper two components (sill depth and above) are thought to be products of estuarine circulation from Satellite Channel presumably from fresh water flowing from Cowichan River. These currents are typically slow (e.g., mean at 14 m depth = 4.9 cm/s) but can occasionally be rapid (e.g., maximum at 44 m depth = 26.4 cm/s). In the southern part of the inlet, below the sill, currents usually travel at low speed (mean at 88 m depth = 5.7 cm/s; EnviroEd Consultants Ltd., 1995).

Flushing

The sill at 70 m depth restricts water circulation into the inlet, creating anoxic conditions below 70-150 m (Carter, 1934; Gross and others, 1963). However, in late summer or fall, cold water usually enters the north end of the inlet from Haro Strait through Satellite Channel (Herlinveaux, 1962; Anderson and Devol, 1973; Stucchi and Giovando, 1984). This causes flushing and oxygen renewal in the inlet (Fig. 1-4). The amount of flushing varies from year to year (Anderson and Devol, 1973) and sometimes does not take place (Stucchi and Giovando, 1984). Flushing rates are thought to be high and residence times short although no detailed data are available (EnviroEd Consultants Ltd., 1995). Due to the short residence time and low

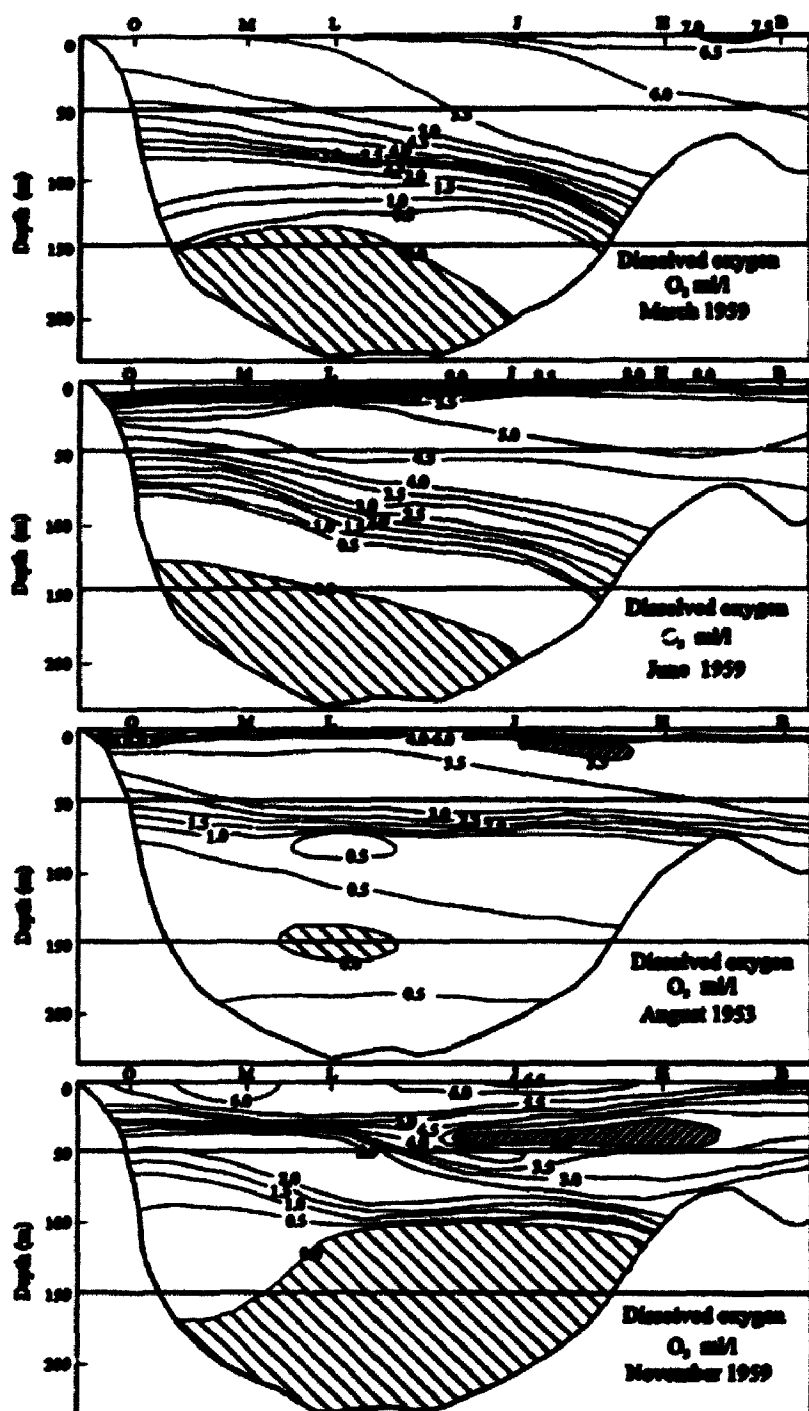


Figure 1-4. Oxygen structure along a longitudinal profile of Saanich Inlet. Stations are plotted on Fig. 1-2 (modified from Herlinveaux, 1962).

concentrations of oxygen, conditions below 150 m are considered anoxic.

Temperature, salinity, density, and oxygen in the water column

Water temperatures in the fiord fall within the expected range for fiords in British Columbia (Pickard, 1975). At <50 m depth, temperature changes are seasonal, ranging from ~5°C in January to ~18°C in July. Below 50 m, temperatures are stable at 8-9°C. Figure 1-5 shows observed temperature structure along a longitudinal section of the inlet (Herlinveaux, 1962). It shows that temperature varies along the inlet, with patches of warmer or cooler water at different depths.

Surface water salinities range widely depending on precipitation and drainage (Herlinveaux, 1962). Waters below sill depth appear to be isolated from the approaches, i. e., waters entering from Satellite Channel (Fig. 1-6; Herlinveaux, 1962). Moreover, water density concentrations reflect similar patterns (Fig. 1-7).

Bedrock geology

Vancouver Island is part of the Insular mountain belt, which is one of five northwest-southeast trending mountain belts that make up the Canadian Cordillera. The island, along with much of the rest of British Columbia and the Yukon, is thought to consist of a series of exotic terranes originating in distant latitudes in an ancient Pacific Ocean. These exotic terranes were accreted to the edge of North America over a period of 170 million years. Most of Vancouver Island belongs to a piece of the earth's crust known as Wrangellia which ranges in age from Lower Paleozoic to Upper Cretaceous. The south and west part of the island are part of the

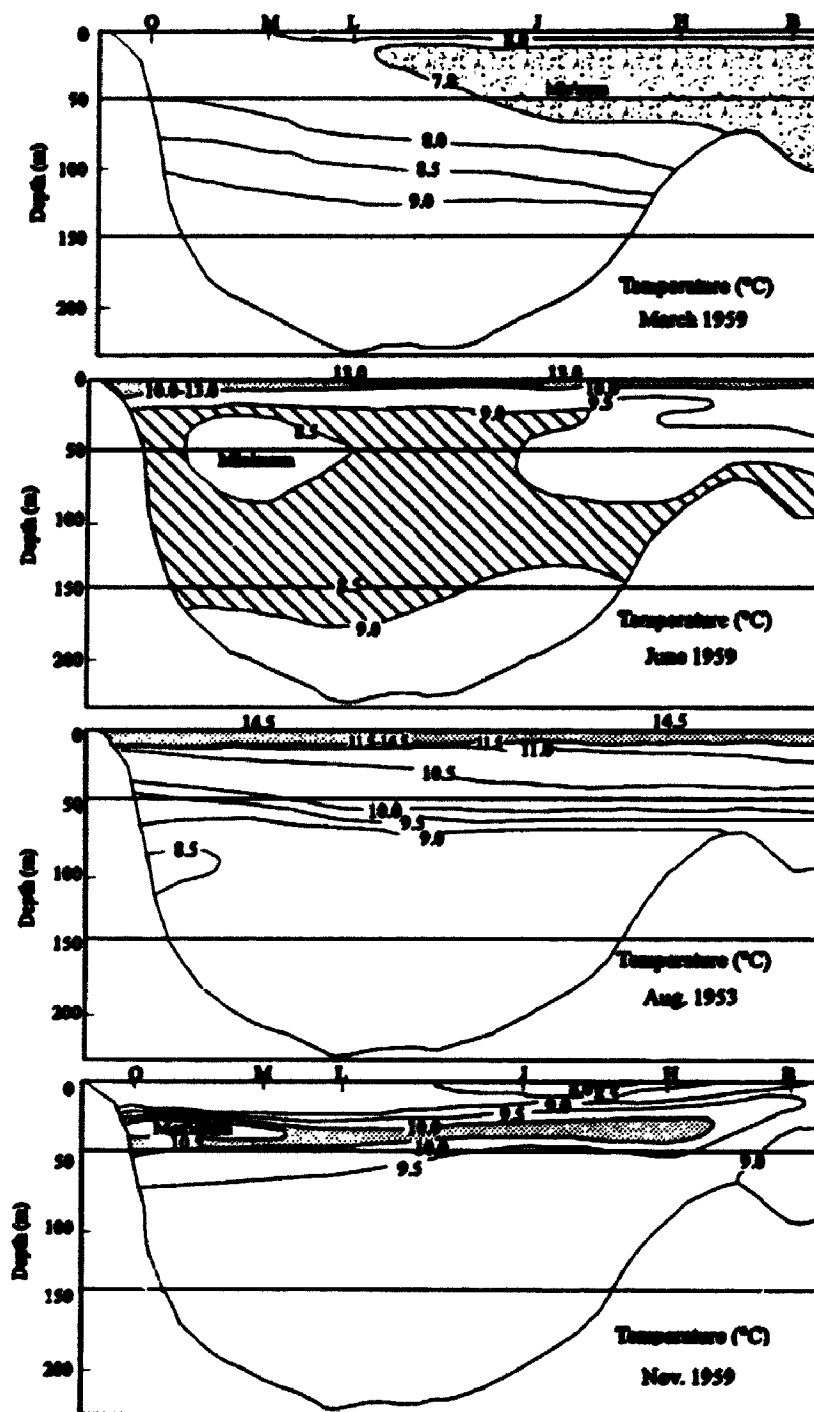


Figure 1.5. Temperature structure along a longitudinal profile of Saanich Inlet. Stations are plotted on Fig. 1-2 (modified from Herlinveaux, 1962).

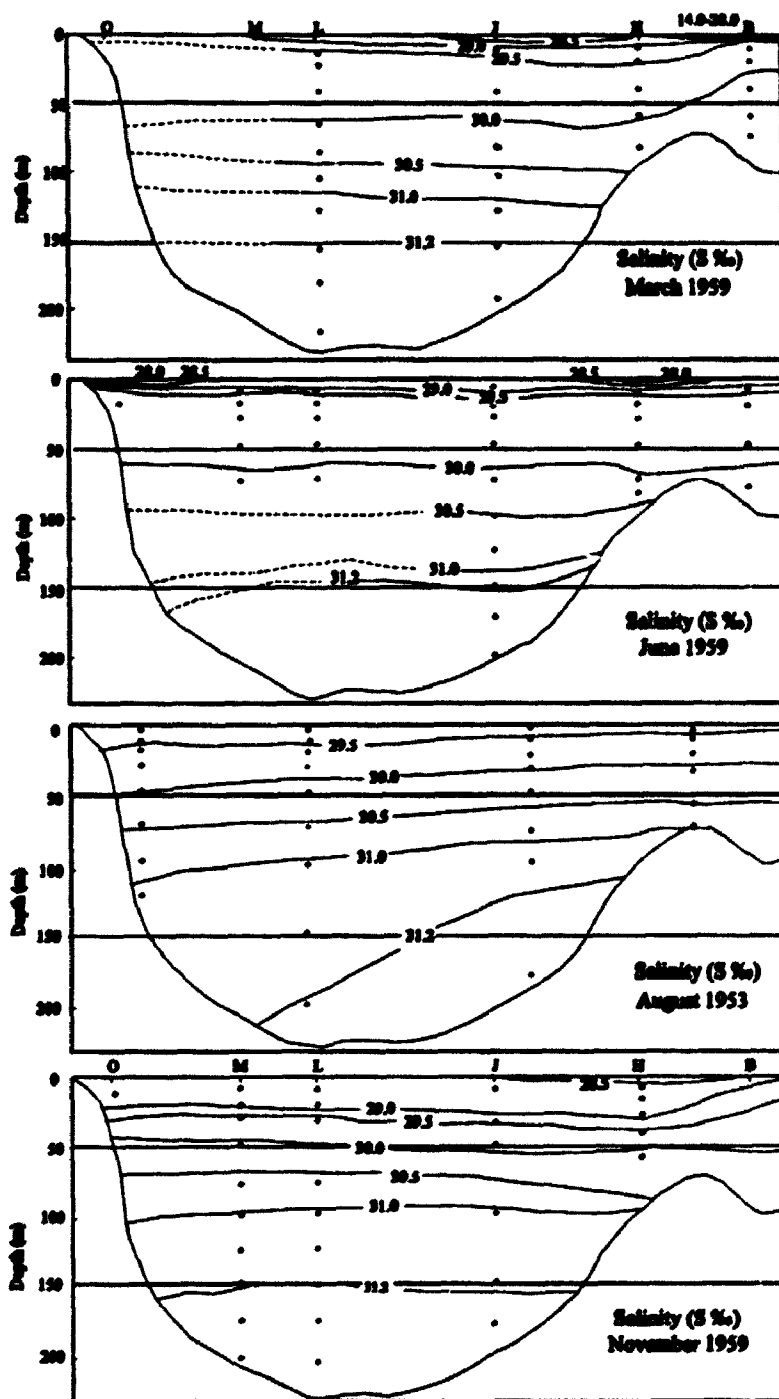


Figure 1-6. Salinity structure along a longitudinal profile of Saanich Inlet. Stations are plotted on Fig. 1-2 (modified from Herlinveaux, 1962).

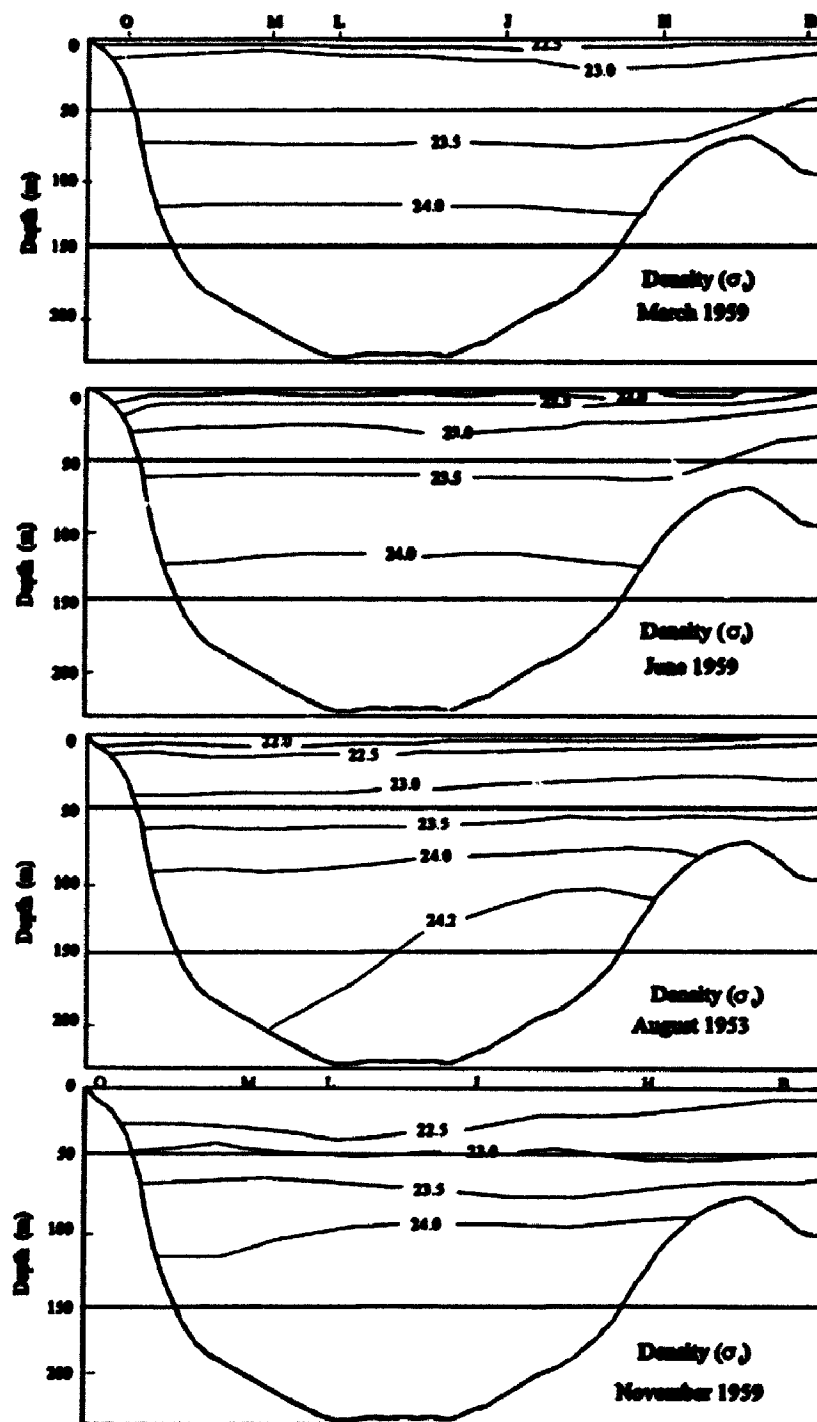


Figure 1-7. Density structure along a longitudinal section of Saanich Inlet. Stations are plotted on Fig. 1-2 (modified from Herlinveaux, 1962).

Pacific Rim and Crescent terranes of Eocene age (Yorath and Nasmith, 1995).




Bedrock surrounding Saanich Inlet includes components of all three terranes (Fig. 1-8; Muller, 1981). Wrangellia bedrock comprises a variety of island-arc assemblages: plutonic and metaplutonic rocks including granodiorite, diorite, metadiorite, metagabbro; volcanic rocks such as tuff and basalt; and marine sedimentary rocks, including limestone, chert, argillite, greywacke, and sandstone. Pacific Rim rocks consist mainly of metasedimentary and metavolcanic rocks. The Crescent terrane consists mainly of volcanic rocks (Yorath and Nasmith, 1995).

Surficial geology

Surficial sediments surrounding Saanich Inlet were deposited during the last (Wisconsin) glaciation and during post-glacial (Holocene) time. These sediments are shown on Muller's 1981 bedrock geology map (Fig. 1-8) and, more recently, were mapped in detail by Blyth and Rutter (1993) and Blyth and others (1993). Three principal units are found in the Saanich Inlet area. The oldest unit is Vashon drift¹ (Qv; Fig. 1-8), deposited by a lobe of Cordilleran ice sheet during the Fraser Glaciation (Clague, 1994; Fig. 1-9). Vashon Drift consists till, sand, and gravel. The Capilano Sediments (Qc; Fig. 1-8) deposited in the sea at the end of the Fraser Glaciation (Clague, 1994) consist of sand, gravel, silt, and clay. Postglacial sediments (Q; Fig. 1-8) are of Holocene age (Clague, 1994), consist of fluvial, marine, lacustrine and organic deposits.

¹ Some surficial units may be slightly older in age (Quadra Sands).




QUATERNARY

-  Recent sediments
-  Capilano Sediments: *sand, gravel; silt, clay*
-  Vashon Drift: *gravel, sand, till*



TERTIARY - EOCENE (AND OLDER ?)

-  Metchosin Volcanics: *mainly basaltic lava*



CRETACEOUS - Upper Cretaceous

-  Extension - Protection Formation: *sandstone, conglomerate; minor siltstone, shale*
-  Haslam Formation: *shale, siltstone, minor sandstone*
-  Comox Formation: *sandstone, conglomerate; minor siltstone, shale*

TRIASSIC TO CRETACEOUS - Leech River Formation

-  Argillite - Metagreywacke Unit: *thinly bedded greywacke and argillite, slate, phyllite, quartz-biotite schist*
-  Chert - Argillite - Volcanic Unit: *ribbon chert, cherty argillite, metarhyolite, metabasalt, chlorite schist*



JURASSIC - Lower to Middle Jurassic

-  Island Intrusions: *granodiorite, quartz diorite*
-  Bonanza Group: *Basaltic to rhyolitic tuff, breccia, flows, minor argillite, greywacke*

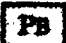
TRIASSIC - Upper Triassic

-  Karmutsen Formation: *pillow basalt, breccia tuff, minor flows*

PERMIAN AND/OR TRIASSIC

-  Unnamed volcanics (San Juan Island, Saanich Peninsula): *basaltic to dacitic lava, breccia, tuff; minor limestone*
-  Limestone



PENNSYLVANIAN AND PERMIAN

-  Buttle Lake Formation: *limestone, greywacke, argillite*



PENNSYLVANIAN AND MISSISSIPPIAN

-  Sediment - Sill Unit: *argillite, greywacke, chert, diabase sills*

LOWER DEVONIAN AND OLDER

-  Saltspring Intrusions: *metagranodiorite, metaquartz porphyry, quartz sericite schist*
-  Myra Formation: *well bedded silicic tuff and breccia, argillite, rhyodacite in flows and domes, minor basic tuff; quartz-sericite schist, phyllite; massive sulphides*

LOWER PALEOZOIC (OR YOUNGER ?)

-  Colquitz Gneiss: *quartz-feldspar gneiss*
-  Wark Gneiss: *massive and gneissic metadiorite, metagabbro, amphibolite*



Geological boundary, (approximate)..... 
Fault, (approximate)..... 



Figure 1-8. Bedrock geology map of Saanich Inlet area (modified from Muller, 1981).

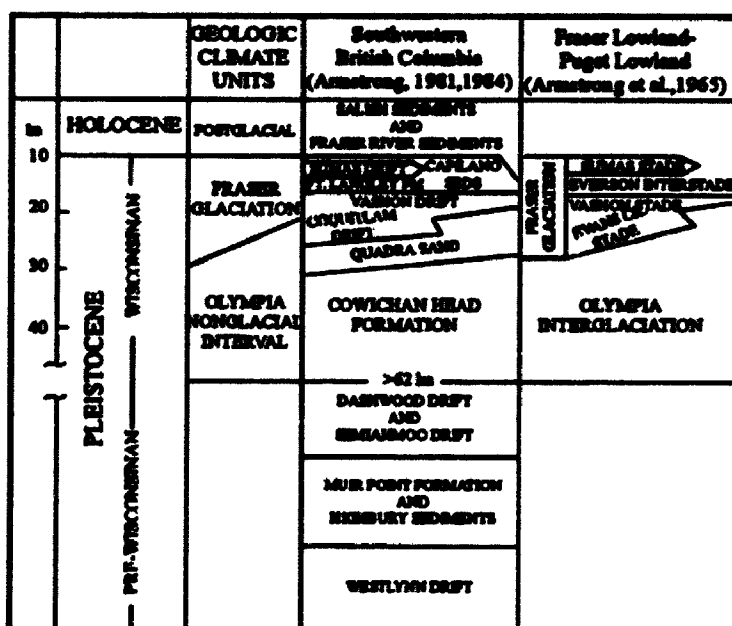


Figure 1-9. Subdivisions of Quaternary events and deposits in southwestern British Columbia (from Clague, 1994).

Sediment distribution in Saanich Inlet

There are three main types of sediment in Saanich Inlet (Fig. 1-10; Gucluer and Gross, 1964): (1) silt on the sill at the mouth of the inlet; (2) poorly- to moderately-sorted fine sand in nearshore environments; and (3) diatomaceous silty clay in deep water. The last group of sediments consists primarily of alternating laminae of terrigenous silty clay deposited during fall and spring freshets and diatoms deposited during spring and summer blooms. Individual couplets have been shown to be annual deposits and thus may be termed varves (Sancetta and Calvert, 1988; Sancetta, 1989).

Intercalated between the varves are massive layers of silty clay thought to be sediment gravity flow deposits (Bobrowsky and Clague, 1990; Blais, 1992; Blais and others, 1993). Some of these deposits are interpreted as products of earthquakes and are discussed in Chapter 3.

Sedimentary processes

Much of the sediment in Saanich Inlet was deposited from suspension (Gucluer and Gross, 1964). However, some strata, which were central to this study, were deposited by sediment gravity flows. Thus, some classifications of sediment gravity flows are reviewed below.

Classifications of sediment gravity flows

Lowe (1979, 1982) classified sediment gravity flows on the basis of rheology of the flow (plastic or fluid) and dominant coarse-particle support mechanism (turbulence, fluidization, escaping pore fluid, dispersive pressure, matrix

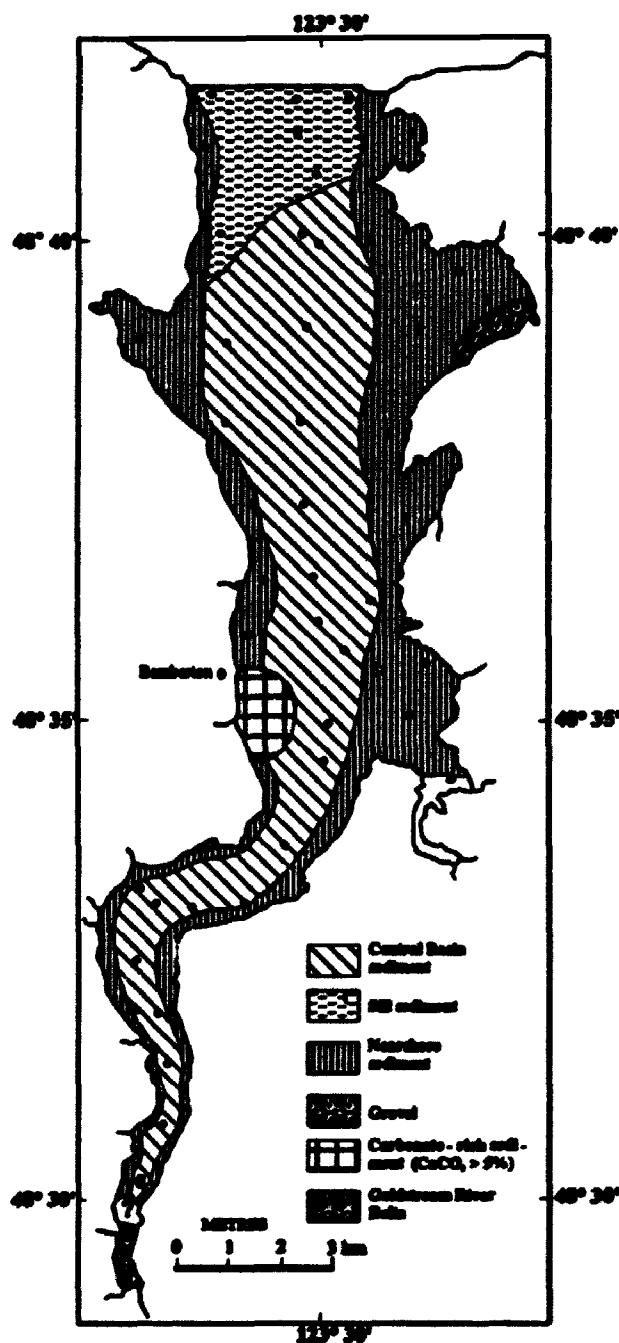


Figure 1-10. Surface sediment samples (black dots) and distribution of sediment types in Saanich Inlet. Central Basin sediment= silt and clay with abundant diatom frustules. Silt sediment= silt. Nearshore sediment= poorly sorted, fine sand and some gravel. Carbonate-rich sediment= near limestone quarry in Bamberton. (Modified from Gucluer and Gross, 1964).

cohesiveness). Another classification presented by Postma (1986) is based on the flow character of a sediment gravity flow implanted during the depositional stage of the flow, which is more likely to be reflected in the deposit. The flow character can be laminar or turbulent, plastic or fluid, low or high density. Comparing his classification to Lowe's, Postma disagreed with Lowe's classification of liquified flows, fluidized flows, grain flows, and modified grain flows. Postma classified these as part of the same rheological model, namely, a high concentration, laminar, cohesionless sediment flow.

The classification used in this thesis is that of Middleton and Hampton (1973, 1976) and Middleton and Southard (1984) with additional information taken from Prior and Coleman (1984), Johnson and Rodine (1984), and Arnott and Hand (1989). This classification is based on how grains are supported during flow. It was chosen because it added textural and structural interpretations of the flows and their associated deposits. This classification is briefly described in the following sections.

Classification utilized in the thesis

Sediment gravity flows are described as "flows consisting of sediment moving downslope under the action of gravity" (Middleton and Hampton, 1976, p. 197). The physical behaviour, (i.e., flow mechanism) determines the type of sediment gravity flow. There are four types of sediment gravity flows based on how grains are supported above the bed (Fig. 1-11): (1) turbidity currents, in which sediment grains are supported by fluid turbulence; (2) liquified sediment flows, in which sediment is supported by the upward flow of fluid as grains settle out; (3) grain flows, in which

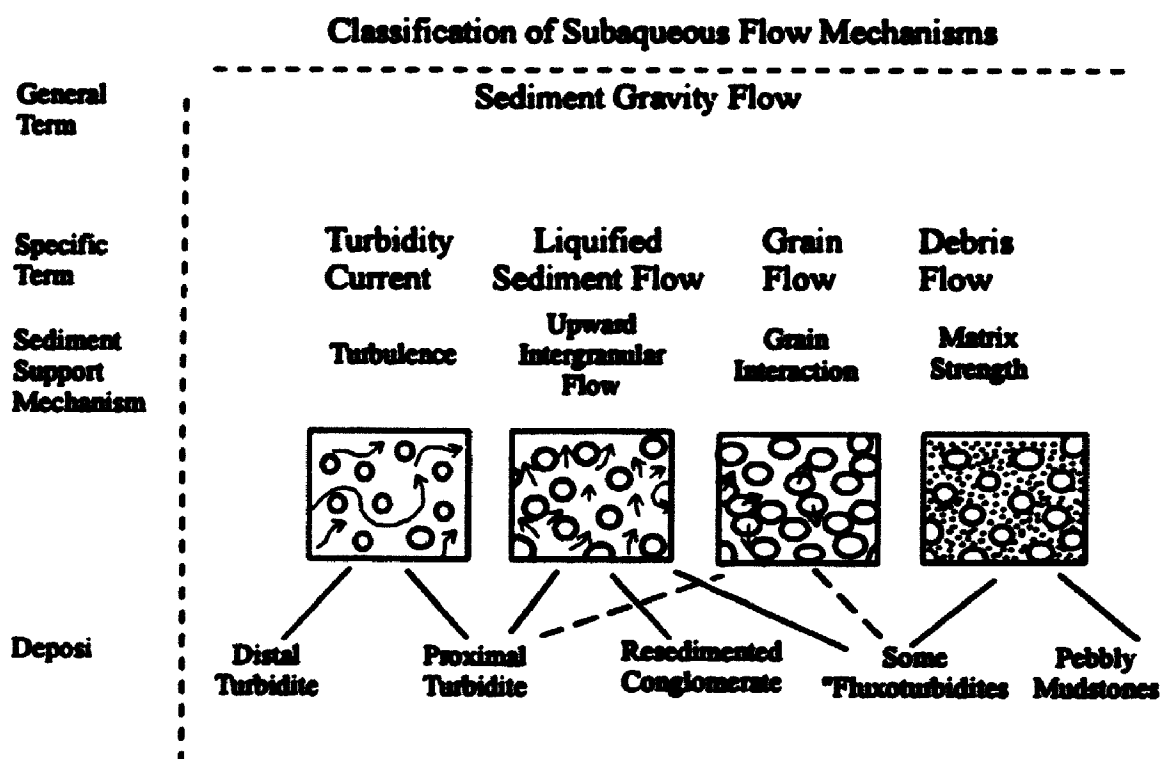


Figure 1-11. Classification of subaqueous sediment gravity flows (modified from Middleton and Southard, 1984).

sediment is supported by grain-to-grain interaction, either collisions or as a result of viscous forces produced by near approaches of grains; and (4) debris flows, in which sediment is supported by matrix strength. There can be more than one type of flow during a single event. The four flow mechanisms outlined above are conceptual end members. Distinctive sedimentary structures are associated with each of these end members (Fig. 1-12).

1) Turbidity currents

Most turbidity currents appear to be initiated as surges. Travelling away from the source, the surge will develop into a turbulent flow consisting of four parts: the head, neck, body, and tail (Fig. 1-13).

For a steady uniform turbidity flow, fluid and sediment sweep forward and upward through the head and circulate around to the back of the head where some sediment is lost in eddies torn away by separating flow (Fig. 1-13). The coarser sediment is circulated back into the flow, but finer sediment is incorporated into a dilute cloud that trails behind the head and is swept along by entrainment. This flow pattern has three important consequences: (1) the head may be a region of erosion even while deposition is taking place from the main body of the flow; (2) dense fluid must continuously be supplied to the head to replace that lost in eddies, resulting in a concentration of coarsest sediment in the head; and (3) the head is slower and thus thicker than the body.

Sedimentary structures of turbidites

A turbidity current leaves a sediment package that has been described as the

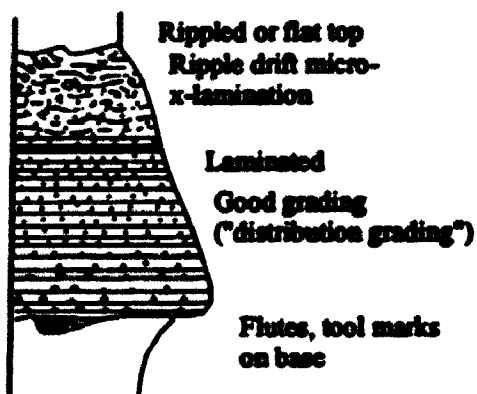
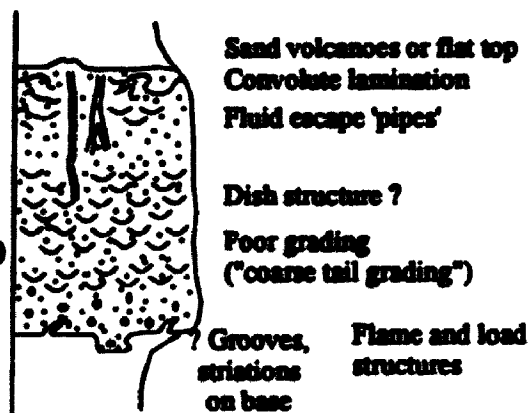
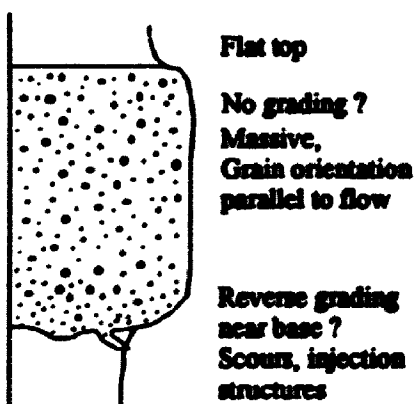
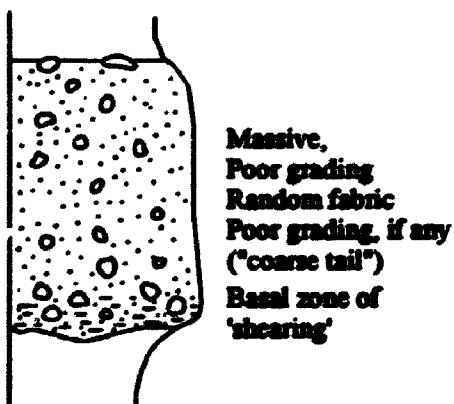
Turbidity flow**Liquified flow****Grain Flow****Debris flow**

Figure 1-12 . Sequence of sedimentary structures in hypothetical single-mechanism deposits (modified from Middleton and Hampton, 1976).

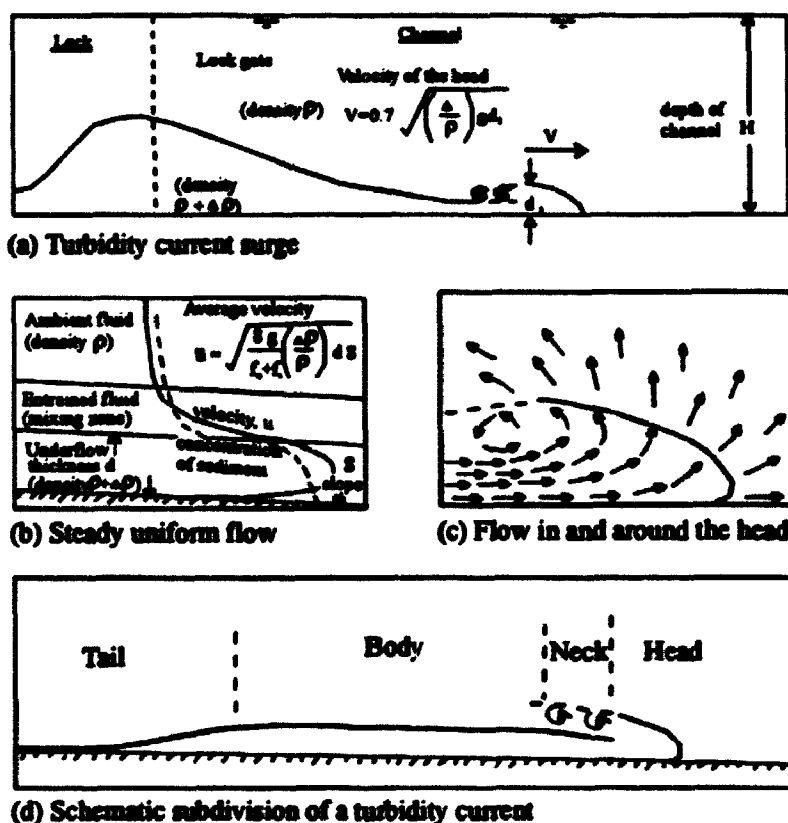


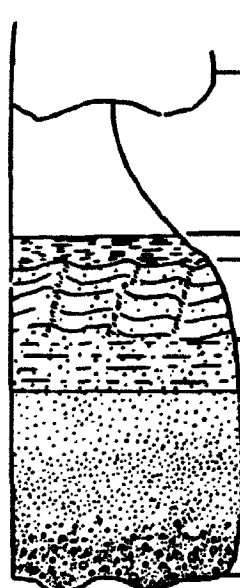
Figure 1-13. Hydraulics of turbidity currents. (a) Turbidity current surge, as observed in a horizontal channel after releasing suspension from a lock at one end. The velocity, v , is related to the thickness of the head, d_h , the density difference between the turbidity current and the water above, $\Delta\rho$, the density of the water, ρ , and the acceleration due to gravity, g . (b) Steady, uniform flow of a turbidity current down a slope, s . The average velocity of flow, u , is related to the flow thickness, d , the density difference, and the frictional resistance at the bottom, f_b , and upper interface, f_i . (c) Flow pattern within and around the head of a turbidity current. (d) Schematic division of a turbidity current into head, neck, body, and tail (modified from Middleton and Hampton, 1976).

Bouma sequence (Bouma, 1962; Blatt and others, 1972; Middleton and Hampton, 1973, 1976), also called a turbidite. It is composed of a set of five units that usually grade upward (Figs. 1-12, 1-14). Sole marks formed by erosion are common at the base of the sequence. Load structures are present where the base of the turbidite is denser than the underlying sediment, e.g, sand over mud; but the viscosity of both materials has to be low enough to permit deformation of the interface between them.

Most sedimentary structures associated with turbidites are formed by a combination of erosion at the head and more or less rapid deposition from the body and tail of the flow. Rapid deposition will produce a unit that is structureless. Slower deposition will produce parallel lamination. With less energy, plane lamination and cross-ripple lamination are produced, reflecting more traction in the flow. Grain fabric will tend to be parallel to current (Arnott and Hand, 1989). Generally, the Bouma sequence indicates a decrease in flow intensity with decreased deposition from suspension, from bottom to top.

2) Liquified flows

Liquified flows, originally called fluidized flows by Middleton and Hampton (1973, 1976), are produced when grains in a loosely packed sand temporarily lose contact with one another and become suspended by pore fluid. Contact between the grains and the strength of the mass are restored when the grains settle through the interstitial fluid, part of which escapes vertically upward to the surface. Sand units that are subject to liquefaction are ones that are loosely packed so that the liquid can expand the fabric and support the grains. A liquified sand can flow rapidly down



Grain Size	Bouma (1962) Divisions	Interpretation
Mud	E Interturbidite (generally shale)	Pelagic sedimentation or fine grained, low density turbidity current deposition
	D Upper parallel laminae	? ? ?
Sand Silt	C Ripples, wavy or convoluted laminae	Lower part of lower flow regime
	B Plane parallel laminae	Upper flow regime plane bed
Sand Silt (to granule at base)	A Massive, graded	? Upper flow regime Rapid deposition and quick bed (?)

Figure 1-14. Ideal sequence of structures in a turbidite bed (the Bouma sequence; modified from Bouma, 1962; Blatt and others, 1972; Middleton and Hampton, 1976).

relatively gentle slopes (3° - 10°). Deposition takes place when pore fluid is lost.

Sedimentary structures of liquified flow deposits

Excess pore fluid can produce liquefaction structures either during deposition or after deposition. Sedimentary structures that are common in liquified flow deposits include dish and pillar features, convolute laminae, and load structures (Fig. 1-12).

3) Grain flows

Grain flows are cohesionless flows in which grains are supported by a dispersive pressure that causes the grains to bounce off one another. The dispersive pressure is proportional to the shear stress transmitted between the grains; it counteracts the tendency for the grains to settle out of the flow. Dispersive pressure is generated by the downslope pull of gravity on the grains, which varies with the slope angle. This process applies specifically to the movement of loose sand grains without clay or silt (Prior and Coleman, 1984). The expected slope angle necessary to sustain movement is high whether the flow is a viscous regime or an inertial regime (37° , viscous ; 18° , inertial). Since such slopes are uncommon on the ocean floor, it is thought that pure grain flows do not travel long distances in submarine environments. Deposition of grain flows occurs "en masse" in layers several grains thick when the driving force becomes less than the force necessary to propel the flow. This is different from deposits formed by traction (turbidites) where grains are deposited particle by particle.

Sedimentary structures of grain flow deposits

Lateral and inverse grading, dish structures, diffuse or swirled laminae, and

intraclasts are common in grain flow deposits (Fig. 1-12). Sole structures may or may not be present at the base. In addition, elongate grains are parallel to flow. Some deposits are massive and structureless.

4) Debris flows

The term debris flow "implies a process by means of which granular solids, in general admixed with minor amounts of clay, entrained water and air (in subaerial flows), move readily on low slopes" (Johnson and Rodine, 1984, p. 257). Other terms have been used to identify similar processes including debris slide, mudflow, rocky mudflow, mud slide, earth flow, mudspate, lahar. According to Johnson and Rodine (1984), all these sediment gravity flows reflect the same mechanism. Differentiations are based on the rate of movement and percentage of fine particles which tend to mask the similarities of these types of flows.

A typical debris flow is a large wave of admixed solid and fluid materials moving steadily though a channel with superimposed, smaller waves travelling at velocities higher than those of the debris flow itself (Johnson and Rodine, 1984). The debris flow acts as a cohesive fluid that carries coarser particles. These particles are supported by floating within the matrix. Deposition of debris flows occurs instantly, "en masse", when the driving force decreases below the strength of the debris.

Lateral and medial deposits commonly are left by debris flows. During flow, sediment is deposited along the sides of the channel in terraces or levees. Medial deposits form in the centre of the channel (Fig. 1-15). A rigid plug forms in the centre of the flow and is rafted along downslope. In some subaqueous flows with

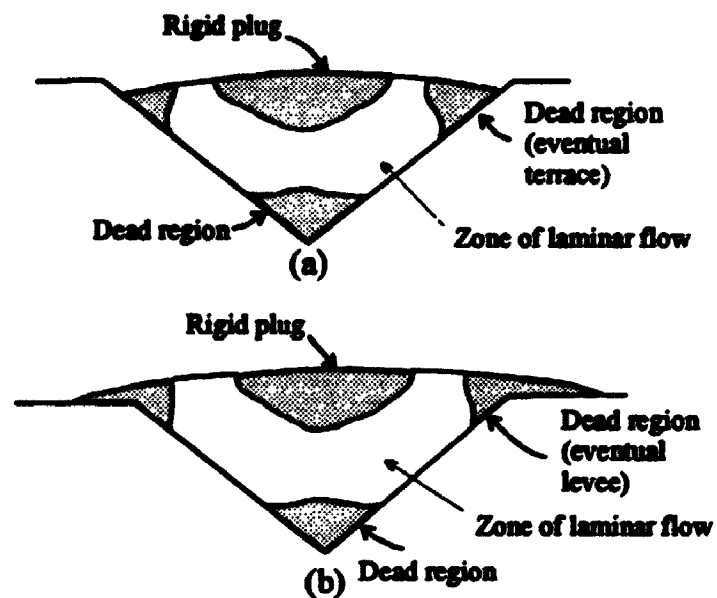


Figure 1-15. Idealized cross-sections of debris flow in a V-shaped channel. (a) Flow is contained within the channel. (b) Flow overlaps the channel (modified from Johnson, 1970; Middleton and Hampton, 1976).

large stress imposed by the water on the upper interface, the rigid plug will flow below the surface of the flow. Around the plug, there is a zone of laminar flow where shearing occurs (Middleton and Hampton, 1976; Johnson and Rodine, 1984; Fig. 1-15). The thickness of the rigid plug will vary directly with strength and inversely with density and slope angle. The flow will stop when the thickness of the plug becomes equal to the thickness of the flow.

Sedimentary structures of debris flow deposits

Bouldery debris flow deposits are typically massive and have a random fabric. Fine-grain debris flow deposits may contain normally or inversely graded laminae. Such laminae would form in the area of flow below the rigid plug in the zone of shearing (Johnson and Rodine, 1984). The base of a debris flow deposit may contain load casts or erosional features, such as slide marks (Fig. 1-12). Generally, debris flows do not abrade the underlying bed unless pull-apart or rigid block sliding occurs, in which case there may be slide marks at the base of the bed. Pull-apart involves tensile separation of a debris flow, for example when the channel is smooth and wet. Blocks produced by separation slide rigidly ahead of the main flow.

Objectives

Saanich Inlet, a fiord on southern Vancouver Island, is a quiet basin in terms of water circulation and sediment deposition. These conditions make it a natural laboratory for studying foraminiferal assemblages and Holocene sediments. Chapter 2 is focused on understanding the response of foraminiferal assemblages to restricted water circulation and the potential environmental implications. Chapter 3 considers

the paleoseismic implications of the sediments in the inlet.

The objectives of the foraminiferal study are: (1) to document the distribution of foraminifera in Saanich Inlet and to determine the effects of this intermittently anoxic basin on foraminiferal ecology; (2) to provide baseline data for a paleoseismic study of sediment cores from Saanich Inlet (Chapter 3); and (3) to assess the environmental impact of industry and encroaching urban development on the fragile fiord ecosystem.

The objectives of the paleoseismic study are fourfold: (1) to determine the source and age of the sediments in Saanich Inlet; (2) to ascertain whether the massive silty clay layers are indeed sediment gravity flow deposits; (3) to determine whether the massive layers are products of earthquakes, and (4) to attempt to use varves as a precise dating tool.

REFERENCES

- Anderson, J. J. and Devol, A. H., 1973, Deep water renewal in Saanich Inlet, an intermittently anoxic basin: *Estuarine and Coastal Marine Science*, vol. 1, p. 1-10.
- Armstrong, J. E., 1981, Post-Vashon Wisconsin glaciation, Fraser Lowland, British Columbia, Canada: *Geological Survey of Canada, Bulletin 322*, 34 p.
- Armstrong, J. E., 1984, Environmental and engineering applications of the surficial geology of the Fraser Lowland, British Columbia: *Geological Survey of Canada, Paper 83-23*, 54 p.
- Armstrong, J. E., Crandell, D. R., Easterbrook, D. J., and Noble, J. B., 1965, Late Pleistocene stratigraphy and chronology in southwestern British Columbia and northwestern Washington: *Geological Society of America Bulletin*, vol. 76, p. 321-330.
- Arnott, R.W.C. and Hand, B.M., 1989, Bedforms, primary structures and grain fabric in the presence of suspended sediment rain: *Journal of Sedimentary Petrology*, vol. 59, p. 1062-1069.
- Atmospheric Environment Service, 1982, Canadian climate normals, 1951-1980: *Environment Canada*, vol. 2, 306 p.
- Blais, A., 1992, Holocene sediments from Saanich Inlet, British Columbia and their neotectonic implications: *Current Research, Part A*; *Geological Survey of Canada, Paper 92-1A*, p. 195-198.

- Blais, A., Clague, J. J., and Bobrowsky, P. T., 1993, Marine geological studies of coastal areas: Saanich Inlet to the Fraser River delta: Canadian Quaternary Association, Program with Abstracts and Field Guide, p. G19-G23.
- Blatt, H., Middleton, G. V., and Murray, R., 1972, Origin of sedimentary rocks, Prentice-Hall, New Jersey, 634 p.
- Blyth, H. E. and Rutter, N. W., 1993, Surficial geology of the Sidney area: Ministry of Energy, Mines, and Petroleum of British Columbia, Open file map 1993-24, NTS 92B/11.
- Blyth, H. E., Rutter, N. W., and Sankeralli, L. M., 1993, Surficial geology of the Shawnigan Lake area: Ministry of Energy, Mines, and Petroleum of British Columbia, Open file map 1993-26, NTS 92B/12.
- Bobrowsky, P. T. and Clague, J. J., 1990, Holocene sediments from Saanich Inlet, British Columbia, and their neotectonic implications: Current Research, Part E, Geological Survey of Canada, Paper 90-1E, p. 251-256.
- Bouma, A. H., 1962, Sedimentology of flysch deposits: Elsevier, Amsterdam, 168 p.
- Carter, N. M., 1934, Physiography and oceanography of some British Columbia fiords: Proceedings of the Fifth Pacific Science Congress, Pacific Science Association, Vancouver, B.C., 1933, vol. 1, p. 721-733.
- Clague, J. J., 1994, Quaternary stratigraphy and history of south-coastal British Columbia: Geology and geological hazards of the Vancouver region, southwestern British Columbia, (J. W. H. Monger, ed.): Geological Survey of Canada, Bulletin 481, p. 181-192.

- EnviroEd Consultants Limited, 1995, Saanich Inlet study synthesis workshop, Information package, April 25-26: hosted by Ministry Lands and Parks of British Columbia, Saanich Native Heritage Society, Institute of Ocean Sciences, 46 p.**
- Gross, M. G., Gucluer, S. M., Creager, J. S., and Dawson, W. A., 1963, Varved marine sediments in a stagnant fjord: Science, vol. 141, p. 918-919.**
- Gucluer, S. M. and Gross, M. G., 1964, Recent marine sediments in Saanich Inlet, a stagnant marine basin: Limnology and Oceanography, vol. 9, p. 359-376.**
- Herlinveaux, R. H., 1962, Oceanography of Saanich Inlet in Vancouver Island, British Columbia: Fisheries Research Board of Canada Journal, vol. 19, no. 1, p. 1-37.**
- Holland, S. S., 1964, Landforms of British Columbia -A physiographic outline: British Columbia Department of Mines and Petroleum Resources, Buletin 48, 138 p.**
- Johnson, A. M., 1970, Physical processes in geology, Freeman, San Fransisco, 577 p.**
- Johnson, A. M. and contributions from Rodine, J. R., 1984, Debris flow (D. Brunsden and D. B. Prior, eds.): Slope instability, John Wiley and Sons, Toronto, p. 257-361.**
- Kendrew, W. G. and Kerr, D., 1955, The climate of British Columbia and the Yukon Territory: Queen's Printer and Controller of stationary, Ottawa, 222 p.**

- Lowe, D. R., 1979, Sediment gravity flows: their classification and some problems of application to natural flows and deposits: The Society of Economic Paleontologists and Mineralogists (SEPM), Special publication, no., 27, p. 75-82.**
- Lowe, D. R., 1982, Sediment gravity flows: II. Depositional models with special reference to the deposits of high density turbidity currents: Journal of Sedimentary Petrology, vol. 52, no. 1, p. 279-297.**
- Middleton, G. V. and Hampton, M. A., 1973, Sediment gravity flows: mechanics of flow and deposition (G. V. Middleton and A. H. Bouma, eds.): Turbidites and deep-water sedimentation, The Society of Economic Paleontologists and Mineralogists (SEPM), Short course 1, p. 1-38.**
- Middleton, G. V. and Hampton, M. A., 1976, Subaqueous sediment transport and deposition of sediment gravity flows (D.J. Stanley, D.J.P. Swift, eds.): Marine transport and environmental management, John Wiley and Sons, Toronto, p. 197-218.**
- Middleton, G. V. and Southard, J. B., 1984, Mechanics of sediment movement: The Society of Economic Paleontologists and Mineralogists (SEPM), Short course 3, second edition, 401 p.**
- Muller, J.A., 1981, Geology of Victoria: Geological Survey of Canada, Map 1553A.**
- Pickard, 1975, Annual and longterm variations of the deepwater properties in the coastal waters of southern B.C.: Journal of Fisheries and Oceans Board of Canada, vol. 32, no. 9, p. 1561-1587.**

- Postma, G., 1986, Classification for sediment gravity flow deposits based on flow conditions during sedimentation: *Geology*, v. 14, p. 291-294.**
- Prior, D.B. and Coleman, J. M., 1984, Submarine slope instability (D. Brunaden and D. B. Prior, eds.): *Slope instability*, John Wiley and Sons, Toronto, p. 419-455.**
- Sancetta, C., 1989, Spatial and temporal trends of diatom flux in British Columbian fjords: *Journal of Plankton Research*, vol. 11, p. 503-520.**
- Sancetta, C. and Calvert, S. E., 1988, The annual cycle of sedimentation in Saanich Inlet, British Columbia: Implications for the interpretation of diatom fossil assemblages: *Deep-Sea Research*, vol. 35, p. 71-90.**
- Stucchi, D. J. and Giovando, 1984, Deep water renewal in Saanich Inlet (S. K. Juniper and R. O. Brinkhurst, eds.): *Proceedings of a multidisciplinary symposium on Saanich Inlet, 2nd February, 1983*, Institute of Ocean Sciences, Technical report of Hydrography and Ocean Sciences, no. 38, p. 7-15.**
- Yorath, C.J. and Nasmith, H.W., 1995, The geology of southern Vancouver Island, a field guide, Orca Book Publishers, Victoria, B.C., 172 p.**

CHAPTER 2. Biofacies of benthic foraminifera from Saanich Inlet, Vancouver Island, British Columbia: valuable environmental indicators.

ABSTRACT

Foraminiferal biofacies identified in Saanich Inlet appear to be closely linked to a variety of environmental parameters including water quality. The area adjacent to this fiord is slated for a large suburban development as Victoria, the largest city on Vancouver Island, continues to rapidly expand. Foraminifera may thus prove to be good indicators of the stress that this development may place on the delicate Saanich Inlet ecosystem.

Five biofacies are defined based on Q-mode cluster analysis and faunal distribution profiles of foraminifera-bearing sediment surface samples from Saanich Inlet. Biofacies 1 (*Eggerella advena* Biofacies), is found nearshore in two densely populated bays. This assemblage appears to have an affinity for areas contaminated by sewage outfall and septic system drainage. Biofacies 2 (*Eggerella advena-Spiroplectammina biformis* Biofacies) and 3 (*Miliammina fusca* Biofacies) characterize shallow, brackish waters, and are distributed in shallow bays near Biofacies 1. Biofacies 4 (*Lobatula fletcheri* Biofacies), the only biofacies dominated by a calcareous fauna, has been subdivided into two subbiofacies: Sub-biofacies 4A (*Stainforthia feylingi* Sub-biofacies) and 4B (*Buccella frigida* Sub-biofacies). Sub-biofacies 4A is found in deep water, low oxygen environments and Sub-biofacies 4B characterizes shallow water, normal marine environments. The patchy distribution of

Sub-biofacies 4B samples is probably due to vagaries of water circulation in the restricted basin. Biofacies 5 (*Leptohalysis catella*-*Spiroplectammina biformis* Biofacies) defines a relatively deeper muddy environment with a high proportion of plant debris and low oxygen levels. Hence, the main environmental control defining the biofacies is water circulation (or lack thereof) which is influenced by the shape of the fiord (presence of the sill).

INTRODUCTION

The economy of southern Vancouver Island, British Columbia, relies heavily on fishing, tourism, and aquaculture, all of which are adversely affected by water pollution. As the population of greater Victoria, the largest city on the island, continues to burgeon, water pollution caused by sewage outfall and industrial waste has become a matter of concern (Vancouver Sun; The Province; Times Colonist; 1993, 1994, 1995). Encroaching housing developments (Development Services Department of the Cowichan Valley Regional District, oral communication, 1994) also may threaten the ecosystem of Saanich Inlet (Fig. 2-1). Foraminifera are used as environmental indicators of pollution sources but no work of this type has been carried out on the northwest coast. Consequently, there is an interest and a need to conduct a reconnaissance study to establish the foraminiferal biofacies in Saanich Inlet.

Southwestern British Columbia is also one of the most tectonically active regions of North America. In light of recent major earthquake damage to other west coast cities, there is increasing concern about the effects that a moderate to large earthquake would have on the region. In response to this concern, research has been initiated by the Geological Survey of Canada, primarily in southwestern British Columbia, to determine the times and effects of large prehistoric earthquakes (Clague and Bobrowsky, 1994a, b; Mathewes and Clague, 1994).

Analysis of foraminiferal assemblages and biofacies distribution is a proven tool in the paleoceanographic interpretation of marine sediments worldwide (Culver,

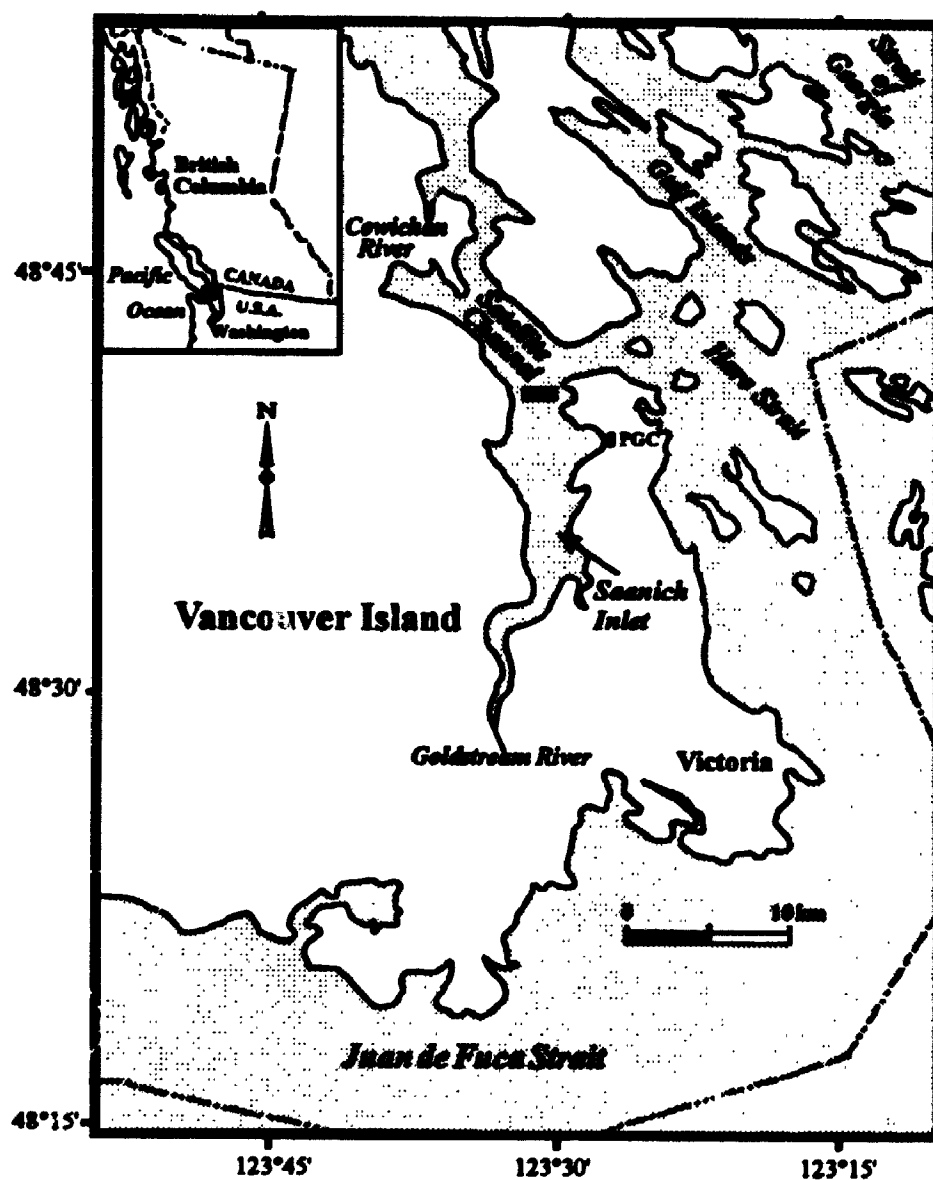


Figure 2-1. Location map, Saanich Inlet, British Columbia. The shaded box locates the bedrock sill at the north end of the inlet. PGC=Pacific Geoscience Centre.

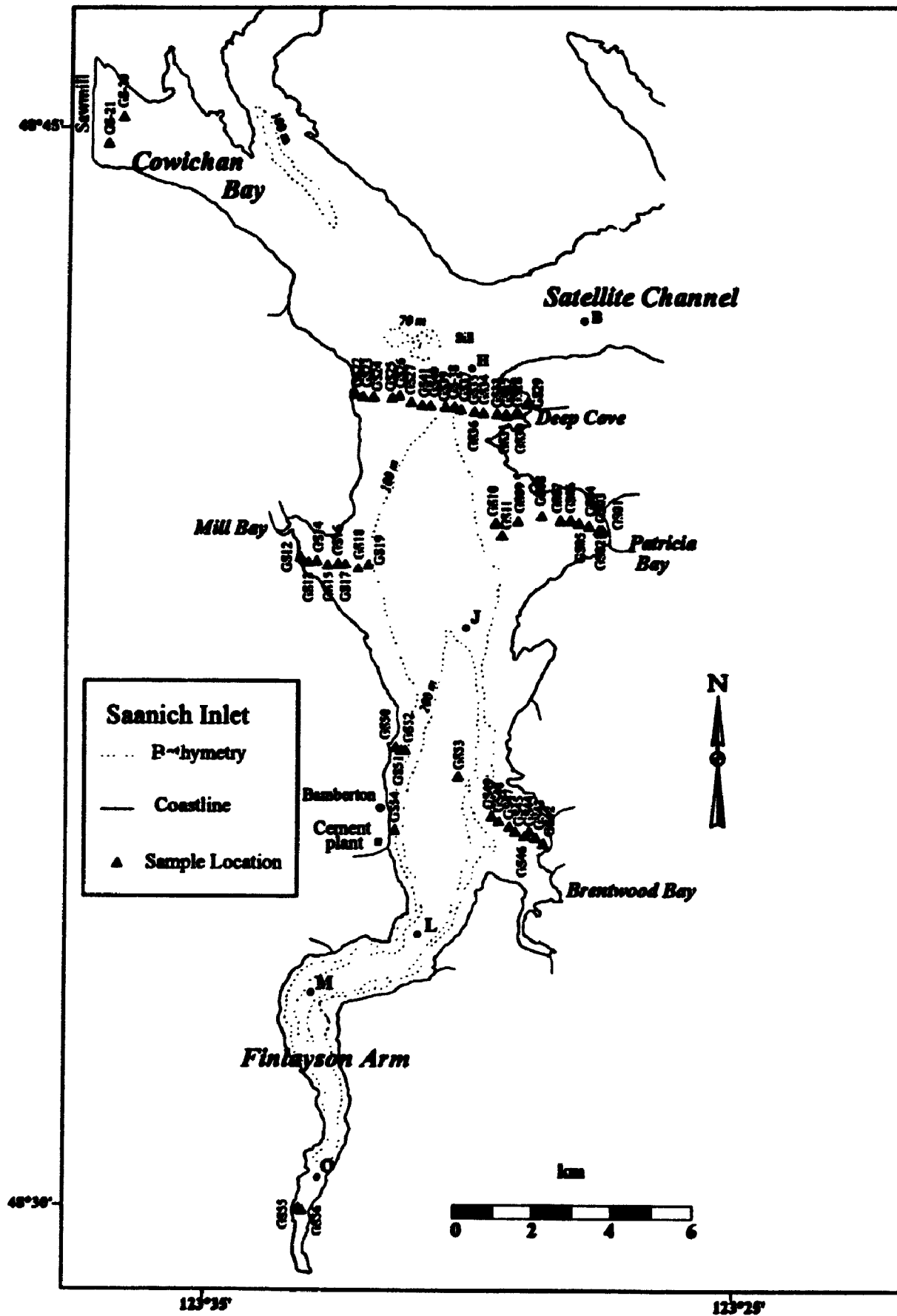
1993). With the concerns outlined above, the purpose of this reconnaissance study is threefold: (1) to document the foraminiferal distribution in Saanich Inlet and to determine the effects of an intermittently anoxic basin on foraminiferal ecology; (2) to provide baseline data for a paleoseismic study of sediment cores (Chapter 3); and (3) to assess the environmental impact of industry and urban development on the fragile fiord ecosystem.

STUDY AREA

Saanich Inlet, located at the southern end of Vancouver Island (Fig. 2-1), is 26 km long, up to 8 km wide, and has average and maximum depths of 120 m and 236 m, respectively. It is indented by five bays into which small ephemeral streams flow (Fig 2-2).

Unlike other inlets in British Columbia, freshwater runoff into Saanich Inlet is negligible as a flushing mechanism (Herlinveaux, 1962). Goldstream River, the only significant stream flowing into the inlet, discharges only a small amount of freshwater. The main source of freshwater and sediment is Cowichan River which flows into Satellite Channel northwest of the inlet (Fig. 2-1). A bedrock sill at 70 m depth at the mouth of the inlet (Figs. 2-1 and 2-2) restricts water circulation, creating anoxic conditions below depths of 70-150 m (Carter, 1934; Gross and others, 1963). In late summer or fall, dense cold water enters the inlet from Haro Strait. This water flushes the upper part of the anoxic zone, and increases the amount of dissolved oxygen in the water (Herlinveaux, 1962; Anderson and Devol, 1973; Stucchi and

Figure 2-2. Location map of grab sample sites in Saanich Inlet. Stations O, M, L, J, H, and B are from a hydrological study by Herlinveaux (1962). They are referred to in Figs. 2-3, 2-5, and 2-6.



Giovando, 1984). The amount of flushing differs from year to year, and, as a result, the thickness of the anoxic layer is highly variable to the extent that it sometimes does not take place (Anderson and Devol, 1973; Stucchi and Givando, 1984). An example of oxygen replenishment in Saanich Inlet is shown in Figure 2-3 (Herlinveaux, 1962) where oxygen concentrations decrease with depth throughout the year, except in late summer, for a short period of time, there is a minor increase in oxygen at lower depths.

In the shallower oxygenated areas of the inlet, sediments range from silt to fine sand with gravel in some areas. In the anoxic part of the basin, the sediments are mainly muddy diatomaceous ooze (Fig. 2-4; Gucluer and Gross, 1964).

Annual water temperatures in the fiord fall within the expected range for fiords in British Columbia (Pickard, 1975). At <50 m, temperature changes are seasonal ranging from $\sim 5^{\circ}\text{C}$ in January to $\sim 18^{\circ}\text{C}$ in July. Below 50 m, temperatures are stable at $8\text{--}9^{\circ}\text{C}$. Figure 2-5 represents observed temperature structures in a longitudinal section of the inlet (Herlinveaux, 1962). These show that water temperature is not constant longitudinally throughout the inlet. There are patches of warmer or cooler water at various depths.

Furthermore, water salinities compiled by Herlinveaux (1962) indicate that surface water salinities vary widely depending on the precipitation and the local land drainage. However, waters below the sill appear to be isolated from the approaches, i. e., waters entering from Satellite Channel (Fig. 2-6; Herlinveaux, 1962).

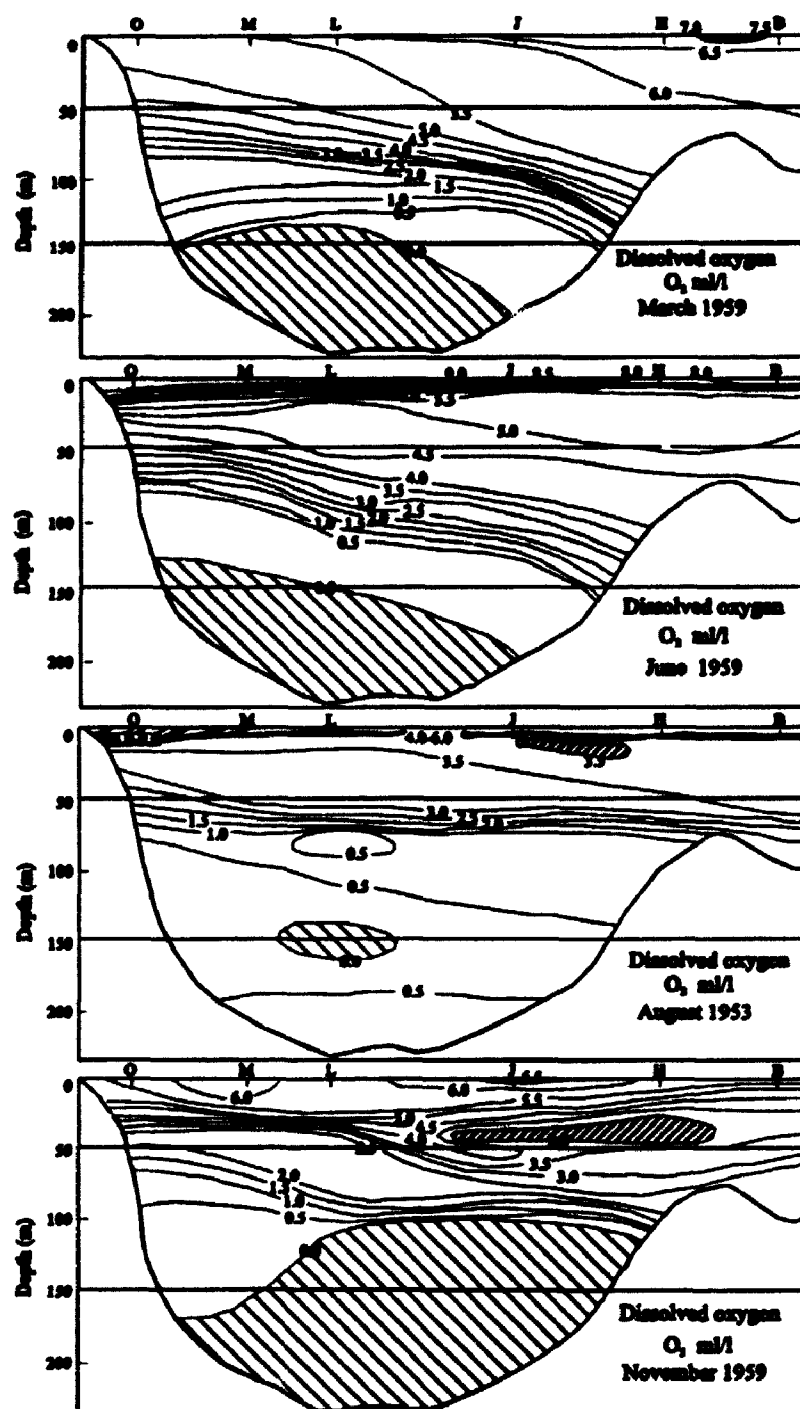


Figure 2-3. Oxygen structure in a longitudinal profile of Saanich Inlet. Stations are plotted on Fig. 2-2 (modified from Herlinveaux, 1962).

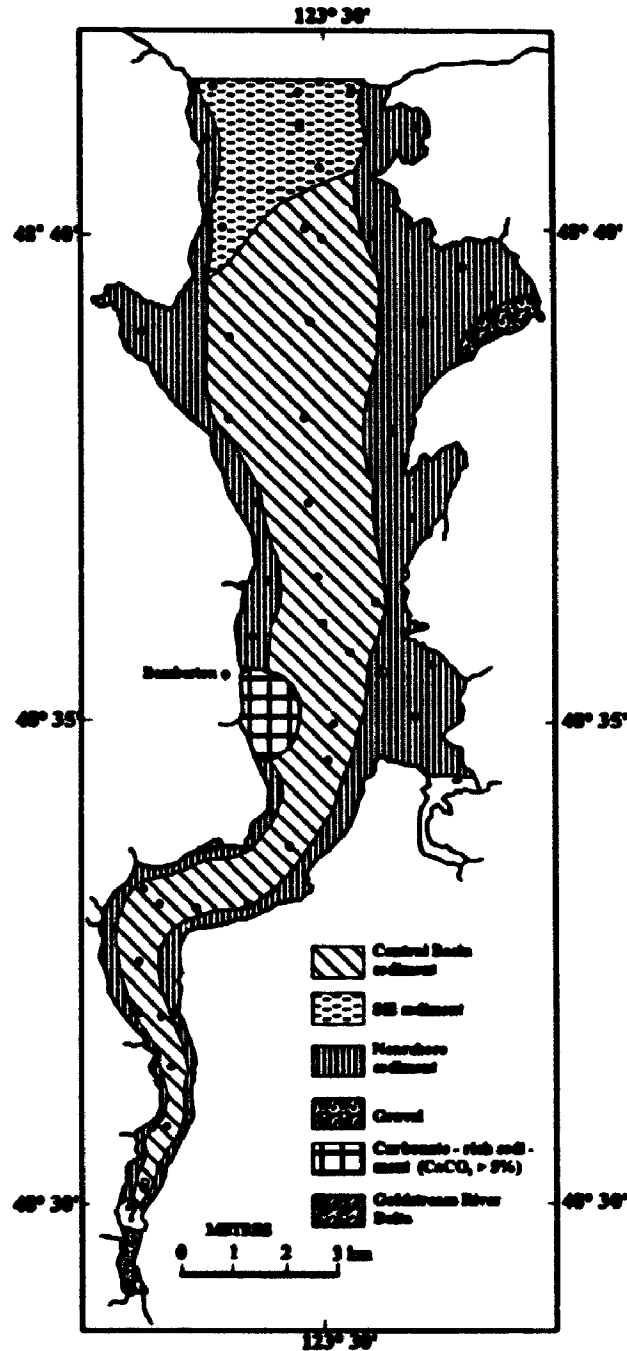


Figure 2-4. Location of surface sediment samples (black dots) and distribution of sediment types in Saanich Inlet. Central Basin sediments= silt and clay with abundant diatom frustules. Sill sediments= silt. Nearshore sediments= poorly sorted, fine sand and some gravel. Carbonate-rich sediments= Near limestone quarry in Bamberton. (Modified from Gucluer and Gross, 1964).

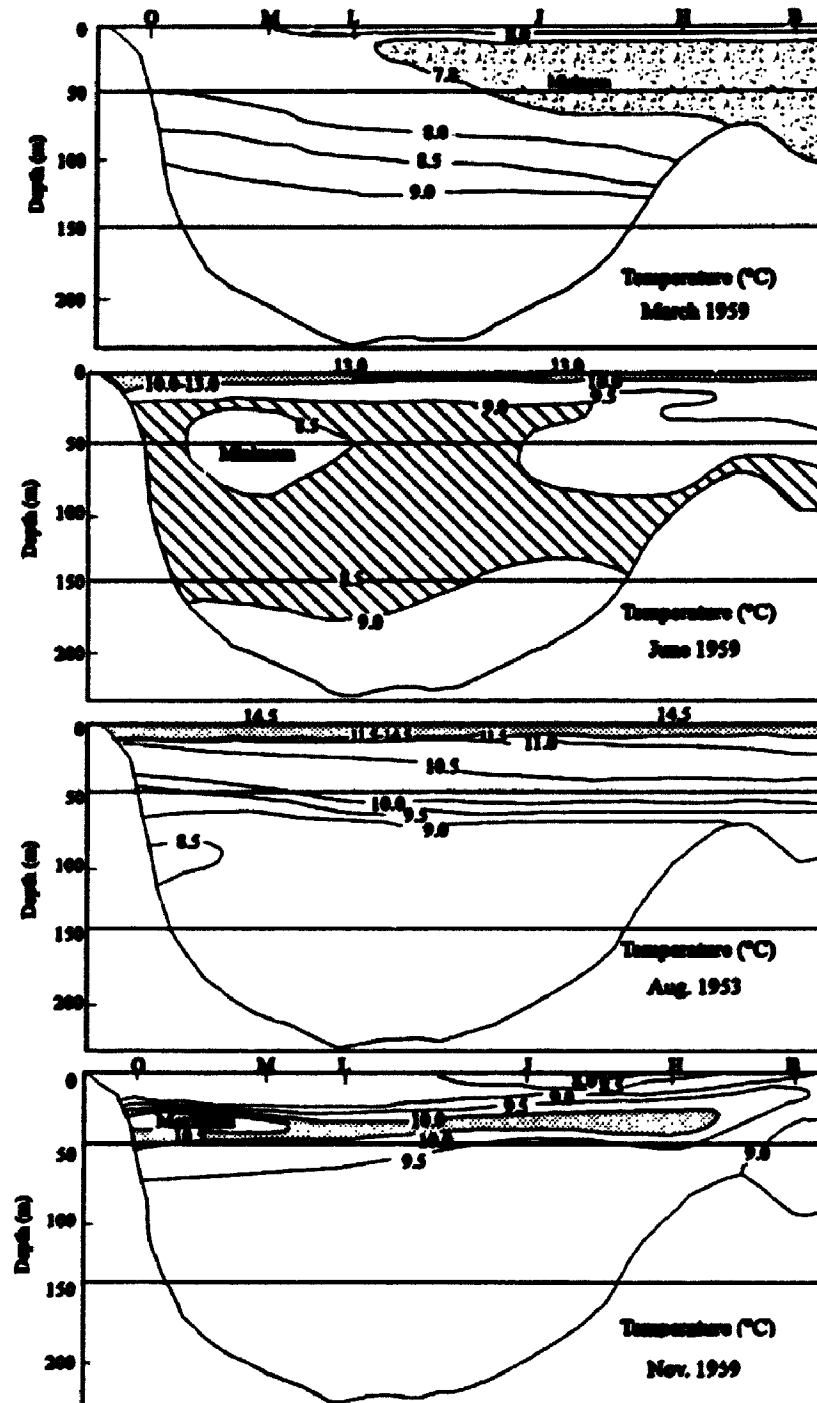


Figure 2-5. Temperature structure in a longitudinal profile of Saanich Inlet. Stations are plotted on Fig. 2-2 (modified from Herlinveaux, 1962).

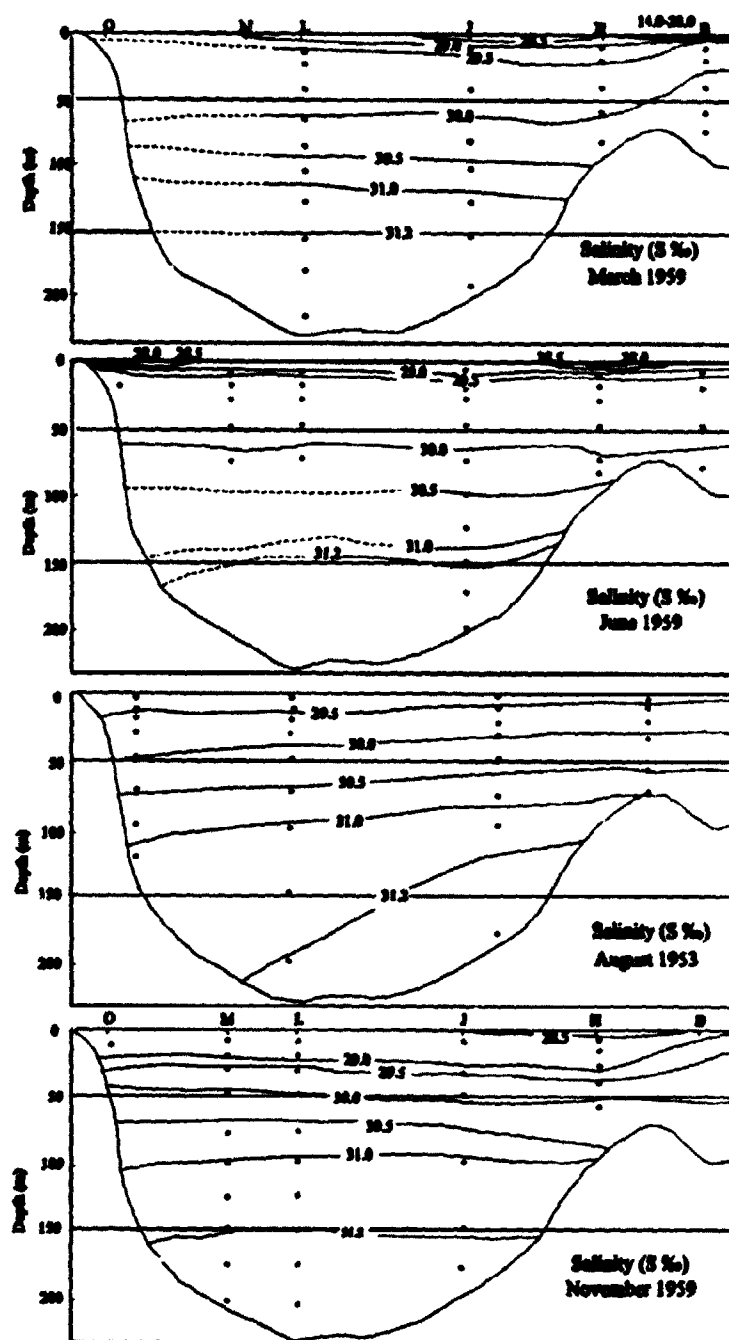


Figure 2-6. Salinity structure in a longitudinal profile of Saanich Inlet. Stations are plotted on Fig. 2-2 (modified from Herlinveaux, 1962).

PREVIOUS WORK

Until recently, very few studies of recent foraminifera had been carried out along the coast of British Columbia and adjacent Washington state. In addition, most of these studies were of a reconnaissance nature or targeted to specific stratigraphic problems and thus provided little ecological information.

Systematic studies on recent shelf foraminifera in the northeast Pacific Ocean along the coast of British Columbia and Washington have been carried out by Cushman (1925), Cushman and Todd (1947), Phleger (1967), McCulloch (1977), and Patterson (1991). As the study of foraminifera developed, some foraminiferal species names were changed, which led to some confusion. Thus, to standardize nomenclature and assist subsequent researchers in the area, Patterson and others (in press) prepared a monograph on the foraminiferal faunas of the British Columbia shelf. The results of several stratigraphic, distributional and paleoenvironmental studies in the region are of limited use in the Saanich Inlet work as none was carried out in fiords (Scott, 1974; Gallagher, 1979; Jones and Ross, 1979; Williams, 1989; Patterson, 1989; 1990; 1991; 1993; Patterson and Cameron, 1991; Jonasson and Patterson, 1992; Snyder and others, 1990 a, b; and Patterson and Luternauer, 1993). The only foraminiferal distribution study geographically close to Saanich Inlet was carried out by Cockbain (1963) in the Strait of Georgia (Fig. 2-1).

Studies of diatoms in Saanich Inlet sediments (Gucluer and Gross, 1964; Sancetta and Calvert, 1988; Sancetta, 1989) have confirmed that rhythmites in the central anoxic part of the basin are varves. One varve consists of a dark, terrigenous-

rich, silty-clay, winter layer and a light, diatom-rich, summer layer. These layers are deposited annually from settling of pelagic matter.

METHODS AND MATERIALS

Fifty-six grab samples were collected from sites distributed throughout the inlet (Fig. 2-2) using a Dietz-Lafond grab sampler with a sampling area of 11 X 14.7 cm and a capacity of 480 cm³; only the top 5 cm were saved for analysis. The initial idea was to sample in transects across the basin. However, sampling in the central part of the fiord was not always possible because the grab sampler employed did not always snap shut at greater depths in the soft diatomaceous ooze. Locations of sample sites were determined using a Trimble-NAVTRAC Global Positioning System (GPS) instrument. Sampling depths (in metres below sea level) were recorded with a 200 kHz Ross echosounder (Table 2-1). After qualitative sedimentological description (Table 2-1), each sample was transferred to a vial and immersed in a formalin Rose Bengal solution for 24 hours to help distinguish live (stained pink) from dead (unstained) specimens. The following day, samples were rinsed through a 0.5 mm screen to remove coarse organic matter and rock fragments and a 0.063 mm screen to retain the foraminifera. The 0.063-0.50 mm fractions were wet split for quantitative analysis using a wet splitter described by Scott and Hermelin (1993) and preserved in buffered formalin solution. The amount of sediment retained for examination ranged from 20 to 100 cm³.

For identification and point-counting of specimens, samples were immersed in

Table 2-1. List of samples with their location, depth, brief qualitative sediment description (not using Wentworth scale) and total percent of live specimens. In the last column, the samples with no number have less than 100 specimens and were not included in the scattergram of Figure 2-7. Sample GS-04 was included because it was statistically significant (Fishbein and Patterson, 1989).

Sample	Latitude °W	Longitude °N	Depth (m)	Description	Total % live
GS01	48° 39.37"	123° 26.83"	1	Grey coarse sand	
GS02	48° 39.37"	123° 26.90"	3	Grey coarse sand high organics	12.5
GS03	48° 39.33"	123° 26.86"	6	Grey coarse sand high organics	15
GS04	48° 39.43"	123° 27.11"	12	Olive coarse sand	48
GS05	48° 39.47"	123° 27.32"	15	Olive coarse sand	36
GS06	48° 39.51"	123° 27.49"	20	Olive coarse sand	48.3
GS07	48° 39.51"	123° 27.70"	26	Olive coarse sand	33.1
GS08	48° 39.57"	123° 28.09"	23	Olive coarse sand	19.2
GS09	48° 39.50"	123° 28.57"	36	Olive coarse sand	8
GS10	48° 39.47"	123° 29.03"	72	Sand and mud	
GS11	48° 39.30"	123° 28.90"	73	Olive coarse sand	1.4
GS12	48° 39.92"	123° 33.08"	5	Sand and mud	23.5
GS13	48° 38.93"	123° 32.89"	15	Olive coarse sand	23.7
GS14	48° 38.90"	123° 32.67"	13	Coarse sand	1
GS15	48° 38.94"	123° 32.55"	21	Medium-coarse olive sand	4.6
GS16	48° 38.95"	123° 32.43"	34	Medium-coarse olive sand	14.8
GS17	48° 38.90"	123° 32.12"	42	Medium-coarse olive sand	21.2
GS18	48° 38.72"	123° 31.77"	90	Olive mud	
GS19	48° 38.79"	123° 31.72"	90	Olive mud	0
GS20	48° 45.14"	123° 36.75"	53	Olive mud high organic content	0
GS21	48° 44.77"	123° 37.05"	40	Olive mud high organic content	0
GS22	48° 41.27"	123° 31.95"	19	Olive coarse sand	44.6
GS23	48° 41.23"	123° 31.79"	67	Olive mud high organic content	0
GS24	48° 41.22"	123° 31.57"	72	Olive mud and sand	0
GS25	48° 41.21"	123° 31.19"	73	Olive-grey mud and sand	0
GS26	48° 41.24"	123° 31.04"	73	Olive mud and sand	0.8
GS27	48° 41.15"	123° 30.79"	76	Olive mud and sand	1.6
GS28	48° 40.99"	123° 28.58"	18	Coarse dark grey sand	0

Sample	Latitude °W	Longitude °N	Depth	Description	Total % live
GS29	48° 41 13"	123° 28 41"	2	Coarse sand	—
GS30	48° 41 01"	123° 28.62"	25	Olive coarse sand	46.6
GS31	48° 40 98"	123° 28.84"	30	Medium-coarse olive sand	40.1
GS32	48° 40.96"	123° 28.82"	30	Medium-coarse olive sand	12
GS33	48° 40.99"	123° 29.02"	41	Medium-coarse olive sand	20.6
GS34	48° 41.00"	123° 29.30"	49	Medium-coarse olive sand	23.2
GS35	48° 41 02"	123° 29.49"	57	Medium-coarse olive sand	5.9
GS36	48° 41 02"	123° 29.49"	56	Medium-coarse olive sand	2.1
GS37	48° 41.05"	123° 29.77"	95	Olive mud high organic content	1.2
GS38	48° 41.09"	123° 29.90"	97	Olive mud and sand	1.5
GS39	48° 41 08"	123° 30.08"	112	Olive mud high organic content	0
GS40	48° 41.10"	123° 30.40"	84	Olive mud and sand	0.5
GS41	48° 41.11"	123° 30.57"	78	Olive mud and sand	5.6
GS42	48° 35.02"	123° 28 03"	10	Coarse sand and mud	38
GS43	48° 35.10"	123° 28 18"	44	Coarse sand and mud	23.3
GS44	48° 35.18"	123° 28.30"	52	Olive mud high organic content	3.2
GS45	48° 35.18"	123° 28 60"	78	Olive mud high organic content	2
GS46	48° 35 12"	123° 28 40"	62	Olive mud + high organic content	0
GS47	48° 35.25"	123° 28 72"	42	Medium-coarse olive sand	7
GS48	48° 35 32"	123° 28.93"	62	Sand and mud	—
GS49	48° 35 39"	123° 29 08"	31	Coarse sand and mud	0.3
GS50	48° 36 34"	123° 31.08"	2	Olive-grey coarse sand	80.7
GS51	48° 36 30"	123° 30 97"	35	Coarse sand	—
GS52	48° 36 30"	123° 30 88"	74	Olive coarse sand and mud	10.8
GS53	48° 35 82"	123° 30 87"	221	Black mud and H ₂ S odor	0
GS54	48° 35 20"	123° 31 09"	88	Light grey med. sand	0.2
GS55	48° 29 97"	123° 33 01"	16	Medium-coarse olive sand	30.2
GS56	48° 29 94"	123° 32 94"	14	Coarse sand + high org. content	0.9

water and examined with an Olympus (Model 219142) binocular microscope. Total abundances (live and dead) of specimens were tabulated (Appendix 2-1). Specimens were considered live when globules of stained protoplasm were identified. In addition, the percent abundance and the percent error for each species were calculated (Appendix 2-1) using the methods of Patterson and Fishbein (1989). These authors suggest that percent abundance and percent error values be included in the data compilation to provide an indication of accuracy of species estimates. The percent error (95% confidence level) was calculated using the standard error equation

("X_i):

$$s_{x_i} = 1.96 \sqrt{\frac{[X_i(1-X_i)]}{N}}$$

where (N) is the total number of counts, and (X) is the fractional abundance of a species (Patterson and Fishbein, 1989).

A Q-mode cluster analysis was carried out on the data using a technique that has been demonstrated to closely emulate the results of the statistically significant "error weighted maximum likelihood" clustering method of Fishbein and Patterson (1993). This method requires that only the species present in statistically significant² populations be analyzed. From a total of 96 observed species, the Q-mode cluster analysis was carried out on the 34 statistically significant species using SYSTAT (v. 5.2; SYSTAT Inc. 1992). Euclidean distance correlation coefficients were used to

² Percent abundance of species > standard error (Fishbein and Patterson, 1993).

measure similarity between pairs of species, and the Ward's linkage method was utilized to arrange sample pairs and sample groups into a hierarchic dendrogram.

Four faunal distribution profiles of the dominant species were plotted against sample depth (i.e., water depth) in order to help define, along with the cluster analysis, the ecological parameters.

Selected specimens of common species were mounted, gold coated, and examined using a LECA Cambridge S360 scanning electron microscope at the Geological Survey of Canada, Ottawa.

RESULTS

Species abundance and preservation

All 56 grab samples with the exception of GS-53, collected at 221 m (deepest), contain benthic foraminifera. Eight samples have less than 100 specimens and are not included in Appendix 2-1 (where relative abundances are tabulated) because the species makeup in these samples is not statistically significant (Patterson and Fishbein, 1989; Fishbein and Patterson, 1993). However, one sample (GS-04) containing less than 100 specimens is included as it only contains two species and is considered statistically significant. Of the 49 samples that are tabulated (Appendix 2-1), 39 contained specimens with protoplasm that stained with Rose Bengal.

In general, most specimens are well preserved. Some post-mortem dissolution is indicated by the presence of variably dissolved Cibicides spp. tests in 36 of the 49 samples. It is also apparent that some dissolution has continued after collection

because stained specimens of Criboelphidium spp. and Quinqueloculina spp. are partially to completely dissolved, in some cases with only the organic linings remaining.

Agglutinated species characterize the foraminiferal fauna of most samples. Only six samples contain relatively more calcareous specimens than agglutinated ones. However, the calcareous faunas are more diverse than agglutinated faunas where they dominate an assemblage. No planktic foraminifera are observed in any sample.

% live vs. sample depth

The percentage of live specimens per total (live and dead) abundance of sample (Table 2-1) is plotted against depth of sample (Fig. 2-7). The scattergram indicates a negative relationship, which means, the deeper the sample, the lower the percentage of live specimens. Furthermore, in samples collected at deeper depths (73-97 m), only trace abundances of live specimens are found. These live specimens are Trochammina pacifica and Spiroplectammina biformis.

Cluster analysis

Q-mode cluster analysis on the foraminiferal data (total abundance=live and dead) for 34 statistically significant species (Appendix 2-1), yields six clusters (Fig. 2-8). Each cluster also has a slightly different sediment texture (Table 2-1).

These clusters are: (1) Eggerella advena Cluster, found in grey sand at depths ranging from 15-26 m; (2) Eggerella advena-Spiroplectammina biformis Cluster found in olive coarse sand at depths ranging from 12-57 m; (3) Miliammina fusca Cluster found in coarse sand with a high proportion of plant debris at depths ranging from 3-

Figure 2-7. Scattergram of the total percent abundance of live specimens versus sample depth. "Best-fit" regression line shows negative relationship as calculated by Delta Graph version 3.0 (for Apple Macintosh). Correlation coefficient (r)= -0.5325.

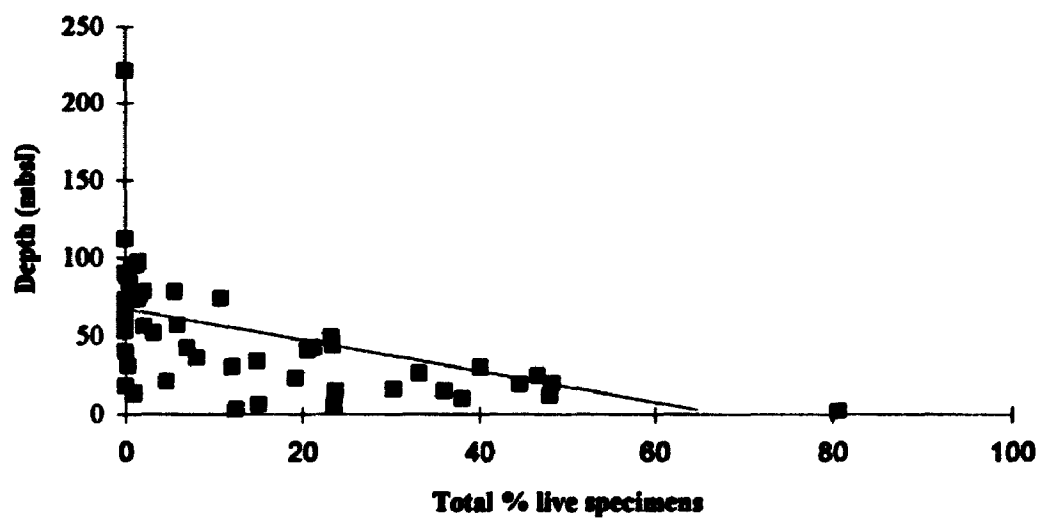
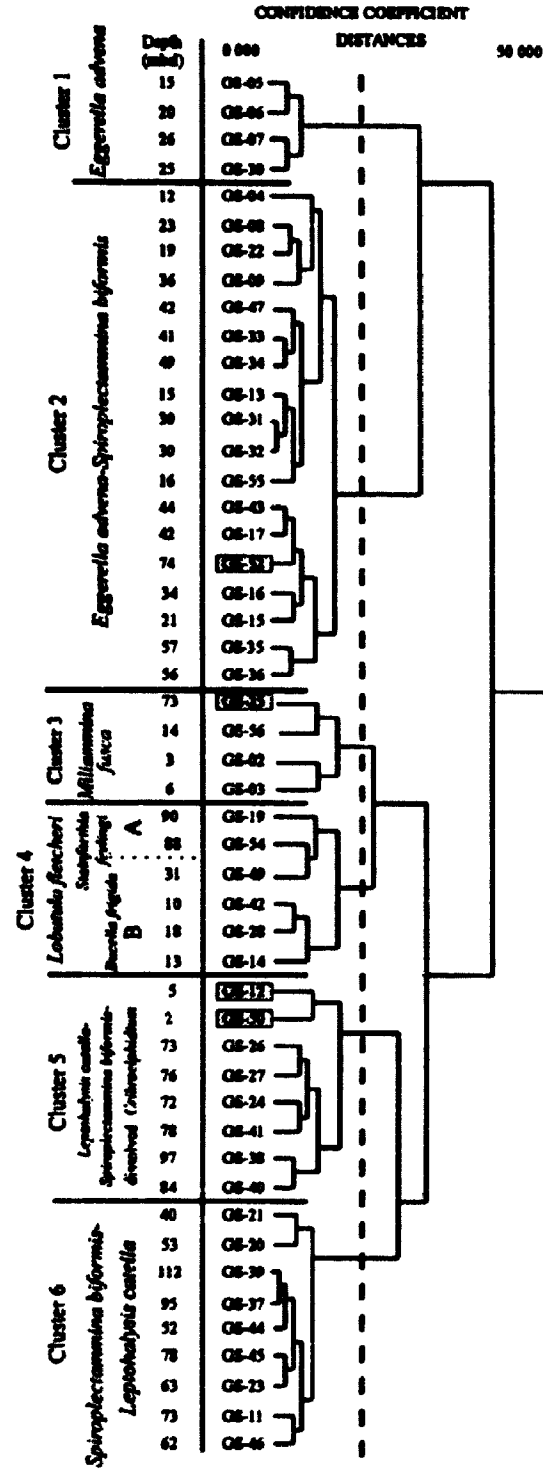
% live vs. sample depth

Figure 2-8. Q-mode cluster dendrogram defining six clusters. Cluster 4 is divided into two sub-clusters: 4A and 4B. Dashed line defines confidence level. Shaded boxes indicate anomalous clustering.



14 m; (4) Lobatula fletcheri Cluster characterized by calcareous foraminifera and divided into two sub-clusters based on dominant species, depth ranges, and sediment texture: (4A) Stainforthia feylingi found in two samples; one of olive mud and one of grey medium sand at depths of 88-90 m and (4B) Buccella frigida found in coarse sand at depths ranging from 10-31 m; (5) Dissolved Criboelphidium-Spiroplectammina biformis-Leptohalysis catella Cluster found in olive mud at depths ranging from 72-97 m; and (6) Spiroplectammina biformis-Leptohalysis catella Cluster found in olive mud with a high proportion of plant material (with the exception of GS-11, which was found in olive sand) at depths ranging from 40-112 m. In Clusters 2, 3 and 5, some samples are anomalously distributed within a cluster because of their differing taxa, sediment texture, and sample depths.

Faunal distribution of dominant species

To examine faunal changes with depth across the fiord, cumulative abundances of dominant foraminiferal species, i.e., dominant in at least one sample (Appendix 2-1), are plotted against sample depth in four profiles (Figs. 2-9, 2-10, 2-11, and 2-12), which are located on Figure 2-13. Five samples (GS-20, 21, 54, 55, and 56; Fig. 2-13) are not in line with the profiles and therefore are excluded.

Bays/shore

Eggerella advena dominates the assemblages in Deep Cove (Profile 1; Fig. 2-9) and in Patricia Bay (Profile 3; Fig. 2-11), two bays subject to septic tank drainage and sewage outfall; only trace amounts of other species are present in these areas.

Miliammina fusca dominates the agglutinated foraminiferal assemblages (Profile 3;

Figure 2-9. Profile 1: Cumulative percent abundance of the dominant foraminiferal species plotted against sample depth. See Fig. 2-13 for location of profile.

Profile 1

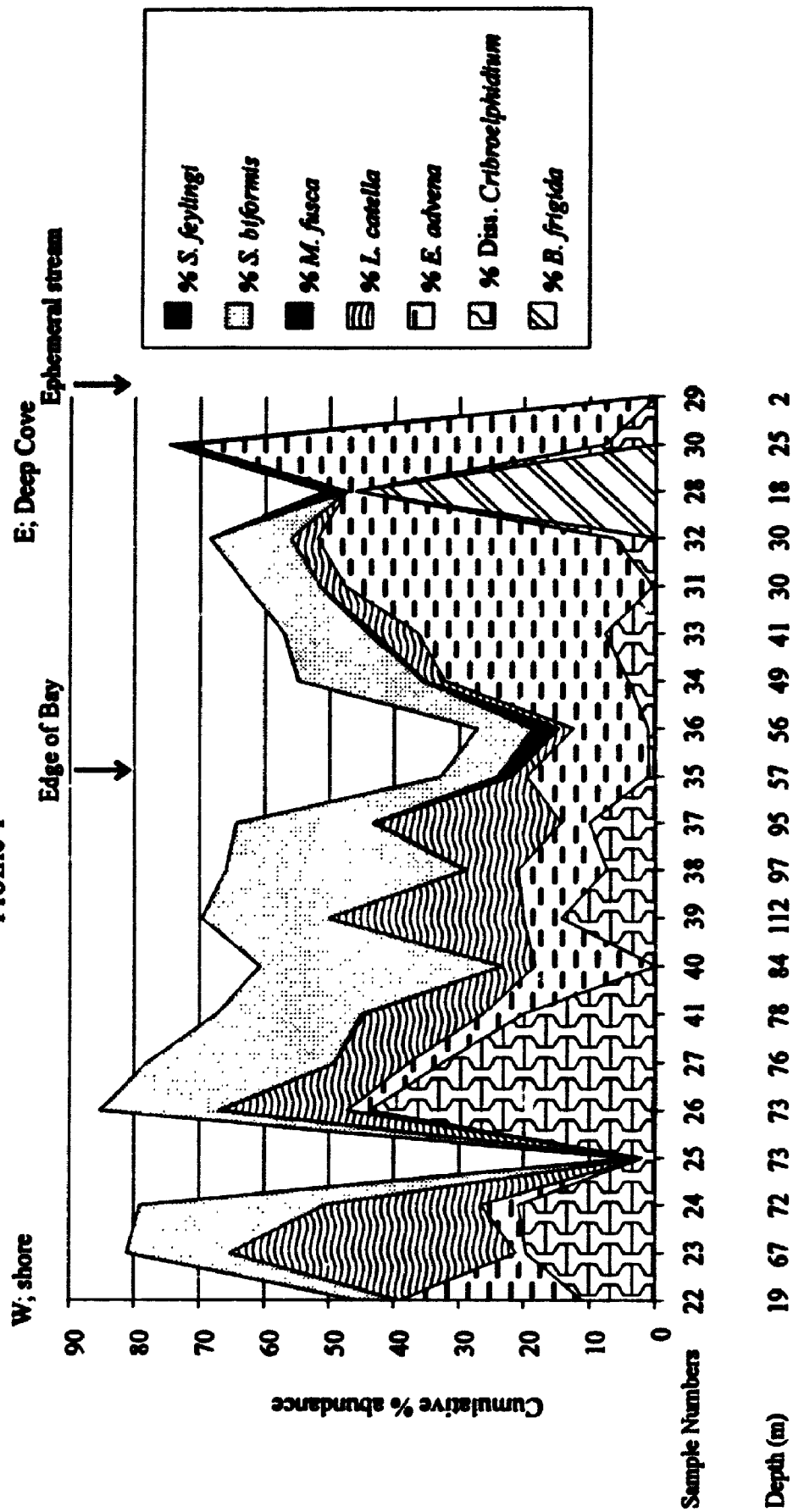


Figure 2-10. Profile 2: Cumulative percent abundance of the dominant foraminiferal species plotted against sample depth. See Fig. 2-13 for location of profile.

Profile 2

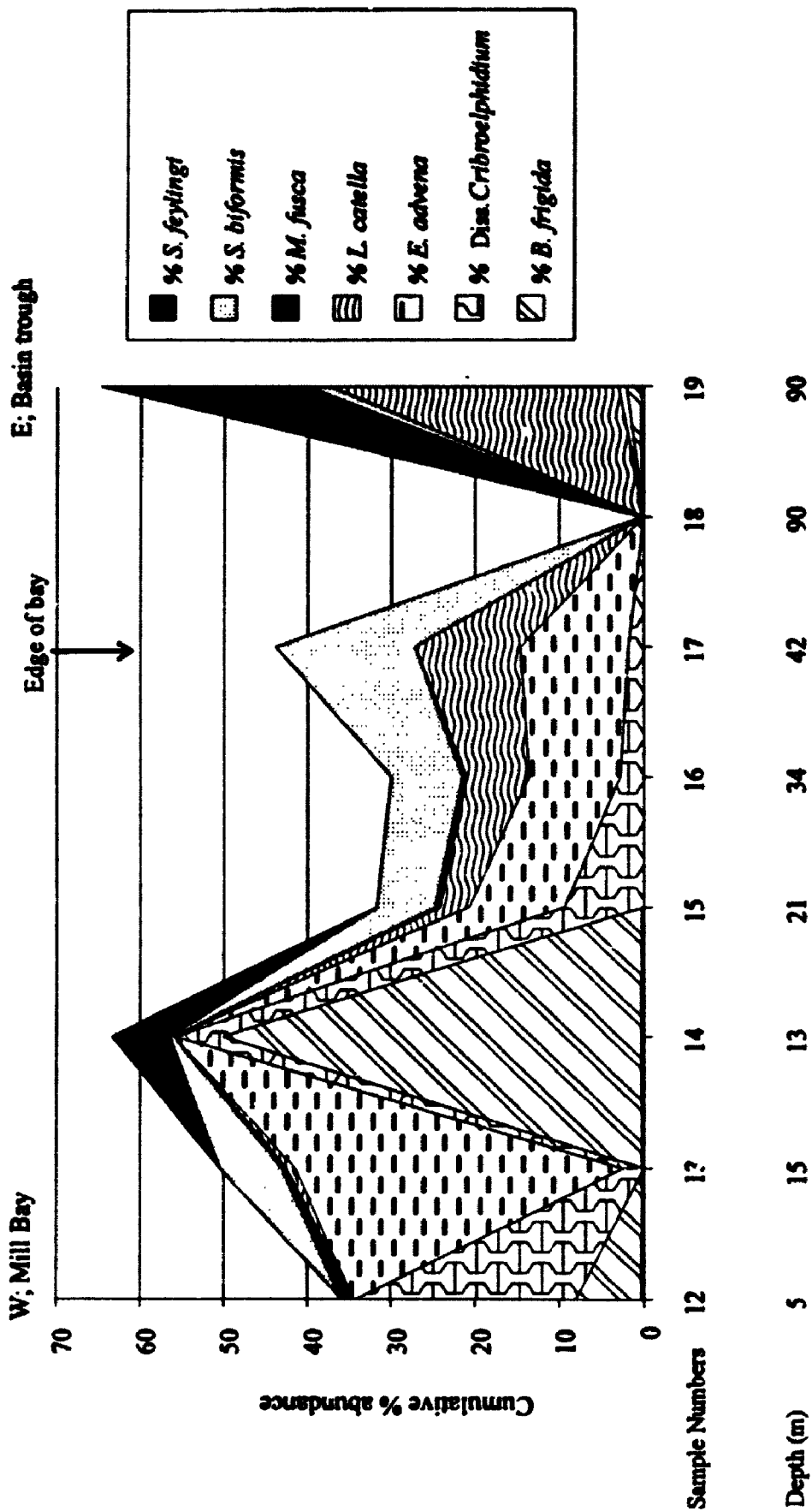


Fig. 2-11) within Patricia Bay, at depths shallower than 12 m, closer to the mouth of an ephemeral stream (Fig. 2-13).

In samples dominated by agglutinated species, Leptohalysis catella is absent at depths shallower than 20 m and Spiroplectammina biformis is present only in trace abundances (all profiles; Figs. 2-9, 2-10, 2-11, and 2-12).

In samples consisting mainly of calcareous foraminifera, Buccella frigida characterizes the assemblages at shallow depths (<20 m; Profiles 1, 2, and 4; Figs. 2-9, 2-10, and 2-12, respectively). At depths of 20-50 m, Buccella frigida and Stainforthia feylingi occur in approximately equal abundances (Profile 4; Sample GS-49; Fig. 2-12).

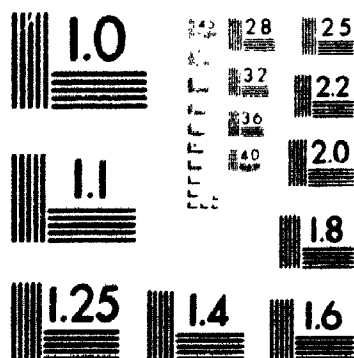
Where dissolved Criboelphidium spp. dominates an assemblage at shallow depths (< 5 m), it represents a substantial abundance of live Criboelphidium spp. that has been dissolved after collection (Appendix 2-1; Samples GS-12 and -50; Profiles 2 and 4; Figs. 2-10 and 2-12, respectively). On the other hand, dissolved Criboelphidium spp. indicating post-mortem dissolution are found in deeper samples (>5 m).

Basin trough

Leptohalysis catella and Spiroplectammina biformis are the most abundant species in dominantly agglutinated assemblages below 57 m (Profile 1; Fig. 2-9; Samples GS-40, 38, and 35). S. biformis is present in most samples from this study and it increases in samples of depths greater than 30 m (all profiles; Figs. 2-9, 2-10, 2-11, and 2-12). At depths >50 m, calcareous assemblages are characterized by

2

PM-1 3½"x4" PHOTOGRAPHIC MICROCOPY TARGET
NBS 1010a ANSI/ISO #2 EQUIVALENT



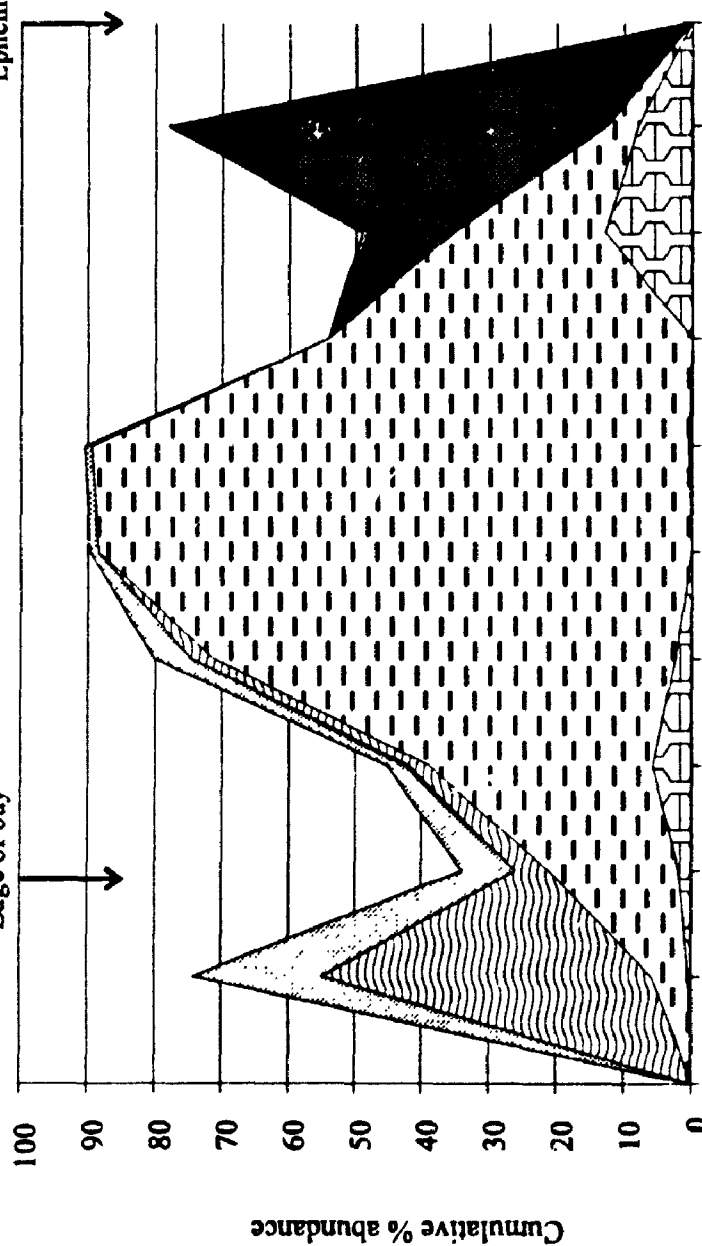
PRECISIONSM RESOLUTION TARGETS

Figure 2-11. Profile 3: Cumulative percent abundance of the dominant foraminiferal species plotted against sample depth. See Fig. 2-13 for location of profile.

Profile 3

W; Patricia Bay
Edge of bay

E; Patricia Bay
Ephemeral stream; sewage outfall

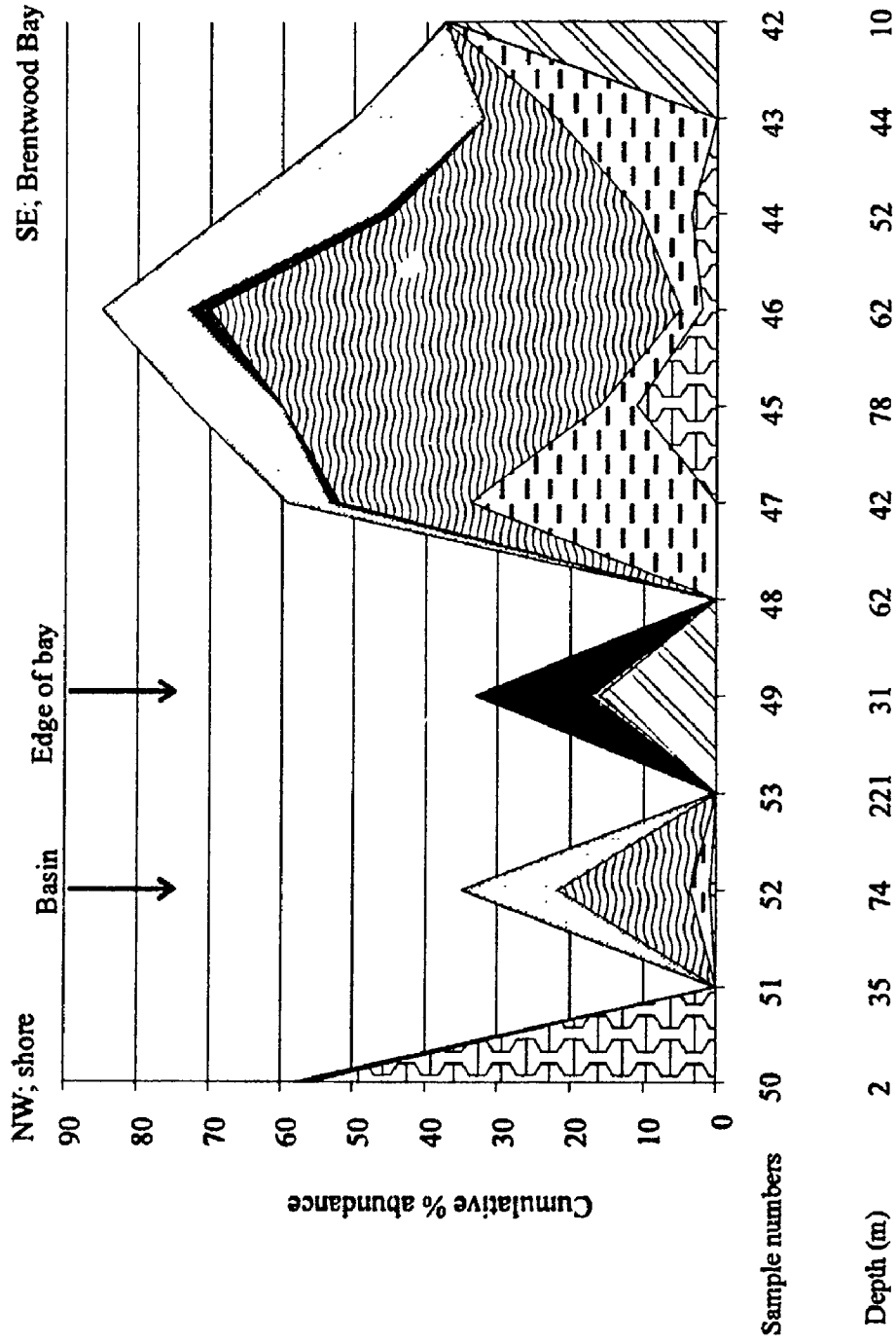


Sample numbers

Depth (m)

Figure 2-12. Profile 4: Cumulative percent abundance of the dominant foraminiferal species plotted against sample depth. See Fig. 2-13 for location of profile.

Profile 4



an abundance of Stainforthia feylingi (Profile 2; Fig. 2-10; sample GS-54, not included in the profiles; Appendix 2-1).

Dissolved Criboelphidium spp. increases with depth, with the exception of sample GS-40 (depth 84 m; Profile 1; Fig. 2-9) which does not contain any.

Although it is a significant component of deeper water assemblages, it dominates only in samples GS-26 and -27 at 73 m and 76 m depth, respectively (Profile 1; Fig. 2-9).

Biofacies

Five biofacies (as defined by Bates and Jackson, 1987; p. 232) are defined on the basis of cluster analysis and faunal distribution profiles. Table 2-2 summarizes the biofacies, their assemblages, the dominant species, the depth range, and the environment in which they are found.

Biofacies 1: Eggerella advena Biofacies

This biofacies, which is also represented by Cluster 1 (Fig. 2-8), is characterized by Eggerella advena, with a relative abundances ranging from 64.3% to 89% among the four samples of the group (Profiles 1 and 3; Figs. 2-9 and 2-11, respectively). The foraminiferal diversity of this biofacies is low. Samples which represent the biofacies range in depth from 15 to 26 m, are grey sands, and are located in Patricia Bay and in Deep Cove on the eastern shore of Saanich Inlet near a highly populated area.

Biofacies 2: Eggerella advena-Spiroplectammina biformis Biofacies

Biofacies 2, which is represented by Cluster 2 (excluding sample GS-52), is dominated by Eggerella advena and Spiroplectammina biformis. Biofacies 2 had

Figure 2-13. Distribution of foraminiferal biofacies in Saanich Inlet defined by Q-mode cluster analysis and the distribution profiles of the dominant species (P-1 to P-4; Figs. 2-9 to 2-12). The triangle (Δ) indicates that there were not enough specimens in the sample to assign it to a biofacies. The question mark (?) indicates that the sample was anomalously clustered in the dendrogram and could not conclusively be assigned to a biofacies based on other criteria, including, dominant fauna, depth of sample, sediment texture.

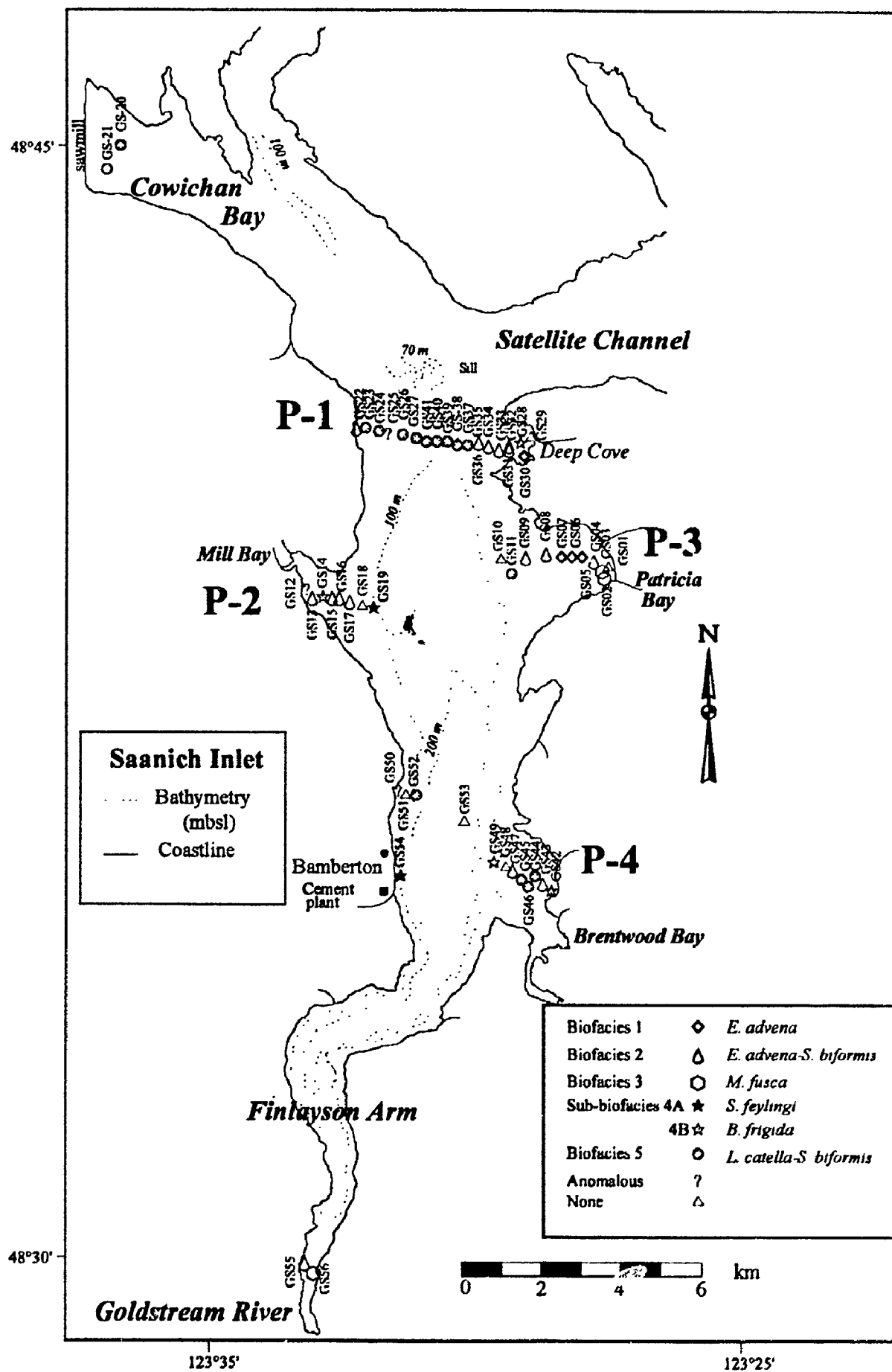


Table 2-2. List of biofacies and their assemblage, sediment texture, depth range, and the environment in which they are found.

Biofacies	Assemblage	Sediment texture	Depth range (m)	Environment
Biofacies 1	<i>Eggerella advena</i> * <i>Trochammina pacifica</i> <i>Trochammina rotaliformis</i>	Grey coarse sand	15-26	Bay/sewage outfall
Biofacies 2	<i>Eggerella advena</i> *- <i>Spiroplectammina biformis</i> * <i>Reophax scoriurus</i> ; <i>Trochammina pacifica</i> <i>Trochammina rotaliformis</i>	Olive coarse sand	12-57	Bay
Biofacies 3	<i>Miliammina fusca</i> * <i>Eggerella advena</i> ; <i>Saccammina cf. atlantica</i>	Coarse sand high organics	3-14	Bay/ephemeral stream outlet
Biofacies 4	<i>Lobatula fletcheri</i> *			
Subiofacies 4a	<i>Stainforthia feylingi</i> * <i>Leptohalysis catella</i> ; <i>Lobatula fletcheri</i>	Mud and Sand	88-90	Basin trough
Subiofacies 4b	<i>Bucella frigida</i> * <i>Criboelphidium excavatum</i> <i>Lobatula fletcheri</i> ; <i>Valvulineria arctica</i>	Coarse sand	10-31	Bay
Biofacies 5	<i>Leptohalysis catella</i> *- <i>Spiroplectammina biformis</i> * <i>Eggerella advena</i> <i>Haplophragmoides columbiensis</i> <i>Trochammina rotaliformis</i>	Olive mud + medium sand; some with abundant organics	40-112	Basin trough Bay/high organics

Note: The asterisk indicates the most characteristic species.

a slightly greater foraminiferal diversity than Biofacies 1 (Appendix 2-1). Samples of the biofacies consist of olive coarse sand, are found at depths ranging from 12 to 57 m, and are located in the bays (Profiles 1 to 4; Figs. 2-9, 2-10, 2-11, and 2-12, respectively).

Sample GS-52 is excluded from Biofacies 2 even though it falls within Cluster 2 (Fig. 2-8). The abundance of Leptohalysis catella in this sample and its greater depth (74 m; Profile 4; Fig. 2-12) reflect conditions of Biofacies 5 as discussed below.

Biofacies 3: Miliammina fusca Biofacies

Biofacies 3, which is represented by Cluster 3 (excluding sample GS-25; Fig. 2-8), is characterized by relatively high abundances (12.8% to 65 %) of Miliammina fusca. Samples from Biofacies 3 are coarse sands with abundant plant debris at depths of 3 to 14 m.

Biofacies 4: Lobatula fletcheri Biofacies

This biofacies, which is represented by Cluster 4 (Fig. 2-8) is dominated by a calcareous fauna; Lobatula fletcheri is the only species present in all samples. The biofacies is subdivided into two sub-biofacies, 4A and 4B, on the basis of depth and sediment texture.

Sub-biofacies 4A: Stainforthia feylingi Sub-biofacies

Sub-biofacies 4A, which is also represented by Sub-cluster 4A, is dominated by Stainforthia feylingi and is found at much greater depths (ca. 90 m) than Sub-biofacies 4B (10-31 m; Fig. 2-8).

Sub-biofacies 4B: Buccella frigida Sub-biofacies

Sub-biofacies 4B, which is represented by sub-cluster 4B (Fig. 2-8), is dominated by Buccella frigida. The samples from this sub-biofacies are sandy and distributed within the bays along the margins of Saanich Inlet (Fig. 2-13; Profiles 1, 2, and 4; Figs. 2-9, 2-10 and 2-12, respectively).

Biofacies 5: Leptohalysis catella-Spiroplectammina biformis Biofacies:

This biofacies includes samples from Clusters 5 and 6 (Fig. 2-8), which have similar foraminiferal content, average depth, and sediment texture. Cluster 5 contains a higher abundance of dissolved Criboelphidium spp. and less plant debris than Cluster 6.

Biofacies 5 is dominated by Leptohalysis catella and Spiroplectammina biformis. Samples are found at depths of 40-112 m, deeper than all other biofacies except 4A (Table 2-2). Samples consist of olive mud with the exception of sample GS-11, which is olive sand. Some samples contain high proportions of plant debris. Most of the samples are from the basin trough distant from shoreline and bays (Fig. 2-13). Those within bays came from depths of 40 m. or more (Figs. 2-9, 2-10, 2-11, and 2-12).

DISCUSSION

% live vs. sample depth

As mentioned above, the percentage of live specimens decreases with depth (Fig. 2-7). Although the percentage of live specimens depends on the percentage of

dead specimens, which in turn, can be affected by other factors, such as production rates, sedimentation rates, and preservation of tests, the lack of living foraminifera at greater depths may also reflect a decrease in dissolved oxygen with depth in the seawater (Fig. 2-3). Furthermore, at greater depths, only trace amounts of live species (*T. pacifica* and *S. biformis*) that can tolerate a wide variety of marine conditions (Murray, 1991) are found. This probably reflects strained living conditions due to low oxygen concentrations.

Biofacies

Biofacies 1: Eggerella advena Biofacies

As mentioned above, Eggerella advena dominates this low-diversity assemblage at shallow depths near a highly populated area. Patricia Bay contains a sewage outfall, and Deep Cove is densely populated with septic systems that may be contaminating the groundwater discharging into the inlet. Furthermore, water quality analyses of Saanich Inlet show that after a period of rainfall, Deep Cove and Pat Bay have the highest fecal coliform sources in the inlet and may exceed the swimming criterion of 200 MPN/100 ml (Aquatic Science Consultants Ltd., 1995).

Although in warm climates, sewage outfall may cause an increase in foraminiferal diversity (Yanko and others, 1994), along the coast of California, sewage reduces the diversity of the foraminiferal biofacies and favours a dramatic increase of agglutinated taxa such as Eggerella advena and Trochammina pacifica (Watkins, 1961; Bandy and others, 1964a, b; Murray, 1991). Similar foraminiferal biofacies are also reported from Atlantic Canada, the Fraser River delta, and

southeast Norway (Schafer and Cole, 1974; Patterson, 1990; Alve 1993, respectively). Schafer and Cole (1974) report foraminiferal diversity decreases and that Eggerella advena, along with Miliammina fusca, dominate assemblages near a pulpmill effluent on the Atlantic coast, Baie des Chaleurs, eastern Québec.

Patterson (1990) observes a dramatic increase in abundance of Trochammina pacifica and low foraminiferal diversity in samples located between two causeways on the Fraser River delta tidal flats containing high levels of organic mud. He attributes the presence of this biofacies to the high levels of organic mud in the area. Alve (1993) reports that one of the most abundant taxa found near sewage outfall is Eggerella advena. This species is also known to tolerate slightly brackish water conditions which are generally found near sewage outfalls (Murray, 1991). Hence, contamination of the water in Saanich Inlet because of sewage outfall and septic system leakage is probably responsible for this low diversity foraminiferal biofacies.

Biofacies 2: Eggerella advena-Spiroplectammina biformis Biofacies

This biofacies is characterized by the abundances of Eggerella advena and Spiroplectammina biformis. Spiroplectammina biformis can tolerate a wide range of marine conditions (Murray, 1991) and increases in abundance with depth along Profiles 1 to 4 (Figs. 2-9, 2-10, 2-11, and 2-12, respectively). The combination of Eggerella advena, which is known to tolerate brackish waters (Murray, 1991), and Spiroplectammina biformis expands the depth range (12-57 m) of Biofacies 1 and becomes Biofacies 2, yet still characterizes shallow waters. Biofacies 2 is found nearshore in bays and near mouths of freshwater streams adjacent to Biofacies 1 (Fig.

2-13). Thus, brackish water conditions and contamination of the water likely play a role in the distribution of Biofacies 2 because of its close association to Biofacies 1.

Biofacies 3: Miliammina fusca Biofacies

Miliammina fusca is characteristic of brackish waters with salinities less than 20‰ (Scott and others, 1980; Alve, 1990) and a high abundance of plant debris at the surface where the sample is collected (Alve, 1990). Biofacies 3 comprises three nearshore samples, two in Patricia Bay and one near the mouth of Goldstream River. These three occur near samples from Biofacies 1 and 2 (Fig. 2-13). This association provides further evidence that the nearshore environments of Patricia Bay and Goldstream River outlet are brackish water environments probably rich in organic debris. Eggerella advena can tolerate brackish waters; however, when the water becomes too brackish, Miliammina fusca will dominate the foraminiferal assemblage close to a zone of freshwater discharge (Scott and others, 1980).

Sample GS-25 grouped within Cluster 3, but does not contain Miliammina fusca, therefore is excluded from Biofacies 3. This sample contains abundant Discammina compressa and Saccammina cf. atlantica, which are common to some samples from Cluster 3 and Biofacies 3 (Appendix 2-1). Discammina compressa should not be considered as an indicator of brackish waters because it is identified in a variety of marine environments (Schröder, 1986; Loeblich and Tappan, 1987). Saccammina lives in a temperate to cold inner shelf (0-100 m) setting (Murray, 1991). Since, all samples from this study were collected within a temperate, inner shelf oceanographic setting, Saccammina should not be considered as an indicator of

any particular environment in Saanich Inlet. Thus, sample GS-25 remains anomalously linked to Cluster 3 without representing the environment of Biofacies 3, although it is geographically associated with samples assigned to Biofacies 5 (Fig. 2-13; Table 2-1). One reason for its anomalous clustering could be that the total count is too low for the fractional abundance of many species to be statistically significant (Fishbein and Patterson, 1989).

Biofacies 4: Lobatula fletcheri Biofacies

Sub-biofacies 4A: Stainforthia feylingi Sub-biofacies

The assemblage from sample GS-19 (Profile 2; Fig. 2-10) of Sub-biofacies 4A is characterized by an abundance of Stainforthia feylingi and has low species diversity. The sample comes from a muddy substrate at a depth of approximately 90 m. S. feylingi is a newly named species, which is conspecific in many studies with specimens referred as Fursenkoina fusiformis and is described as normally being found in arctic to cold boreal environments (Knudsen and Seidenkrantz, 1994).

A similar foraminiferal assemblage from Drammensfjord, southeast Norway is described by Alve (1990). Alve reports that an assemblage dominated by S. fusiformis characterizes a low oxygen environment (towards the redox cline), a muddy organic substrate, and salinities exceeding 30‰. S. fusiformis may be conspecific with F. fusiformis (Alve, 1990, p. 681), which would make it conspecific with S. feylingi (Knudsen and Seidenkrantz, 1994). This issue aside, the foraminiferal assemblages from Drammensfjord and Saanich Inlet reflect similar environmental conditions including deep water, low oxygen, salinities close to 30‰,

and a muddy substrate (Figs. 2-3 and 2-6).

Other studies document that S. feylingi (often listed as Furkensoina fusiformis; Knudsen and Seidenkrantz, 1994) is dominant in deep estuarine environments in eastern Canada (Miller and others, 1982) and coastal fiords in northern Europe (Murray, 1985).

Sample GS-54 in Sub-biofacies 4A is not from a muddy substrate but rather a sand and has a relatively high foraminiferal diversity. Nevertheless, the dominance of Stainforthia feylingi in this sample suggests low oxygen conditions like those reported from a similar environment in Norway by Alve (1990). The small number of live foraminifera in this sample (0.2%) is likely the result of low oxygen conditions. The light colour of the sediment and the greater foraminiferal diversity may be related to the proximity of the sample site to a cement plant (also called limestone quarry) which supplements the water and that contributes high amounts of CaCO_3 (Fig. 2-13; Gucluer and Gross, 1964).

Sub-biofacies 4B: Buccella frigida Sub-biofacies

Sub-biofacies 4B is dominated by Buccella frigida which is indicative of normal³, temperate marine waters (Murray, 1991). This calcareous biofacies indicates relatively higher salinity concentrations and is isolated among agglutinated biofacies reflecting brackish waters in shallow nearshore environments. Such heterogeneity in the spatial distribution of species (Buzas, 1968) has been previously observed and is referred to as patchiness. It is the result of daily temporal and spatial fluctuations of

³ Salinity ranges from 32-37‰ (Murray, 1991).

physical environmental parameters, such as salinity, temperature, oxygen concentrations, etc. (Schröder, 1986; Kaminski and others, 1988). Although other scientists describe patchiness on a centimetre-scale, i.e., within a single box core (Schröder, 1986; Kaminski and others, 1988), we extend its definition to a large scale. Patchiness is not unexpected in Saanich Inlet because of its restricted water circulation pattern.

Biofacies 5: Leptohalysis catella-Spiroplectammina biformis Biofacies:

As mentioned above, Spiroplectammina biformis increases with depth along sample profiles. In addition, Leptohalysis catella becomes more common in agglutinated assemblages with increasing depth, except where S. biformis dominates (Profile 1; Fig. 2-9). Therefore, high numbers of L. catella and S. biformis seem to signal low oxygen levels in deeper water.

Differences in sediment texture most likely explain the statistical distinction between Clusters 5 and 6. Although the sediments hosting Clusters 5 and 6 comprise olive mud with some sand, Cluster 6 samples contain a higher proportion of plant debris. However, the results are not clear enough to separate Clusters 5 and 6 into two biofacies.

Samples GS-20 (53 m) and GS-21 (40 m) contain high amounts of plant debris, probably related to a nearby sawmill on the shore of Cowichan Bay (Fig. 2-13). A high proportion of plant debris, a muddy substrate, and low oxygen levels probably create ideal conditions for Leptohalysis catella to flourish.

Samples GS-12 (5 m) and GS-50 (2 m) are anomalously grouped with Cluster

5 and are excluded from Biofacies 5. Both samples are characterized by a high percentage of live dissolved Criboelphidium spp. The clustering of these samples with deep-water samples of Biofacies 5 is due to dissolution of Criboelphidium specimens after collection. The absence of Leptohalysis catella in these shallow-water samples and the predominantly calcareous fauna (Appendix 2-1) clearly differentiate them from true Biofacies 5 samples.

Sample GS-52 is included in Biofacies 5 because it possesses the same texture and falls within the depth range of this biofacies. It groups within Cluster 2 because of the presence of Eggerella advena (2.7%) and Spiroplectammina biformis (13.4%) but it contains more Leptohalysis catella (17.9%).

Environmental control of the biofacies

In Saanich Inlet, water circulation (or lack thereof) is the main environmental control, which is in turn responsible for variations of environmental parameters, such as salinity, oxygen, temperature, etc. Thus, the bathymetry of the fiord (i.e., presence of the sill) controls water circulation in the basin. Other environmental controls are surface land drainage, contamination, and sediment texture, but these are also influenced by the degree of water circulation in the basin. For example, water contamination occurs in two bays of the inlet and define a biofacies; however, if water circulation were not restricted, contamination might not affect foraminiferal assemblages.

Hence, foraminiferal biofacies indicate that, at shallow depths (above the sill), surface waters are oxygenated and brackish with isolated areas of contamination or

higher salinity. At greater depths (below the sill), biofacies reflect a low oxygen and higher salinity environment.

CONCLUSIONS

A reconnaissance distributional analysis of foraminifera from Saanich Inlet, a fiord with restricted water circulation, demonstrate that:

- 1) The percentage of live foraminifera decreases with increasing depth, probably due to decreasing oxygen concentrations.
- 2) The main environmental control is water circulation which is influenced by the shape of the fiord (i.e., presence of the sill). Related to water circulation are different environmental parameters including salinity, oxygen, temperature, which explain most of the clustering and the distribution of the dominant foraminiferal fauna. Other environmental controls are surface land drainage, contamination, and sediment texture, but these are also affected by the degree of water circulation in the basin.
- 3) Certain foraminiferal species are closely linked to specific environmental parameters. Eggerella advena indicates contamination and brackish water conditions. Miliammina fusca probably reflects very brackish water conditions. Leptohalysis catella reflects deep water, low oxygen concentrations, high organic content, and a muddy (with some sand) substrate. Similarly, Stainforthia feylingi indicates deep water and, probably, low oxygen concentrations. Buccella frigida is indicative of normal temperate marine conditions.

4) Using Q-mode cluster analysis and distribution profiles of dominant species, five foraminiferal biofacies of distinct geographic distribution are defined. These are: 1- Eggerella advena Biofacies of shallow nearshore environments near sewage outfalls and septic system drainage; 2- Eggerella advena-Spiroplectammina biformis Biofacies and 3- Miliammina fusca Biofacies, located close to Biofacies 1 at shallow depths in brackish bays. Although there is relatively little freshwater runoff into Saanich Inlet, Biofacies 1, 2, and 3 indicate that localized ephemeral runoff affects the foraminiferal distribution; 4- Lobatula fletcheri Biofacies, subdivided into: 4A- Stainforthia feylingi Sub-biofacies dominant at greater depths where oxygen levels are low; and 4B- Buccella frigida Sub-biofacies at shallow depths within the bays of the inlet, reflecting poor mixing of normal marine seawater because of restricted circulation; 5- Leptohalysis catella-Spiroplectammina biformis Biofacies found at greater depths far from shore.

Plans for the construction of 5000 houses with tertiary sewage treatment (septic systems) are under consideration (Development Services Department of the Cowichan Valley Regional District, oral communication, 1994) in the Bamberton area (Fig. 2-13). The present foraminiferal study indicates that increasing the amount of septic system drainage into Saanich Inlet could have considerable environmental impact on water quality.

FAUNAL REFERENCE LIST

In the abbreviated list of species given below, names enclosed by square brackets indicate the original generic designations. Original references are cited from the Catalogue of Foraminifera (Ellis and Messina, 1940 and supplements). Plate and figure numbers refer to taxa illustrated here.

Order Foraminiferida

Alveolophragmium crassimargo (Norman), 1892. [Haplophragmium crassimargo].

Alveolophragmium jeffreysi (Williamson), 1858. [Nonionina jeffreysi].

Ammodiscus incertus (d'Orbigny), 1839. [Operculina incerta].

Astrononion gallowayi Loeblich and Tappan, 1953.

Atlantiella atlantica (F. L. Parker), 1952. [Trochamminella atlantica], (Pl. 2-2, Fig. 3).

?Bathysiphon sp. 1.

Remarks: Fine-grained agglutinated tube.

?Bathysiphon sp. 2.

Remarks: Coarse-grained agglutinated tube.

Bolivina compacta Sidebottom, 1905.

Bolivina minuta Natland, 1938.

Bolivina vughani Natland, 1938.

Bolivinellina pacifica (Cushman and McCulloch), 1942. [Bolivina acerosa var. pacifica], (Pl. 2-4, Fig. 3).

Buccella frigida (Cushman), 1922. [Pulvinulina frigida], (Pl. 2-4, Figs. 7, 8).

Buccella inusitata Andersen, 1952.

Buliminella elegantissima (d'Orbigny), 1839. [Bulimina elegantissima], (Pl. 2-4, Fig. 2).

Cassidulina limbata Cushman and Hughes, 1925.

Cassidulina reniforme (Nörvang), 1945. [Cassidulina crassa d'Orbigny var.].

Cibicides sp. 1.

Cibicides sp. 2.

Criboelphidium sp.

Remarks: Partially to completely dissolved.

Criboelphidium bartletti (Cushman), 1933. [Elphidium bartletti]

Criboelphidium excavatum (Terquem), 1876. [Polystomella excavata].

Criboelphidium foraminosum (Cushman), 1939. [Elphidium hughesi var. foraminosum].

Criboelphidium frigidum (Cushman), 1933. [Elphidium frigidum], (Pl. 2-5, Fig. 6).

Criboelphidium groenlandica (Cushman), 1933. [Elphidium groenlandica].

Criboelphidium microgranulosum (Galloway and Wissler), 1927. [Themeon microgranulosum], (Pl. 2-5, Fig. 10).

Criboelphidium hallandense (Brotzen), 1943. [Elphidium hallandense].

Criboelphidium tumidum (Natland), 1938. [Elphidium tumidum].

Crirostomoides sp.

Crirostomoides wiesneri (Parr), 1950. [Labrospira wiesneri].

Cuneata arctica (Brady), 1881. [Reophax arctica], (Pl. 2-3, Fig. 5).

Discamina compressa (Goës), 1882. [Lituolina irregularis var. compressa], (Pl. 2-1, Fig. 9).

Discorbis sp.

Dyocibicides biserialis Cushman and Valentine, 1930. (Pl. 2-4, Figs. 4, 5).

Eggerella advena (Cushman), 1922. [Verneuilina advena], (Pl. 2-1, Fig. 3).

Elphidiella hannah Cushman and Grant, 1927.

Elphidium crispum (Linné).

Epistominella pacifica (Cushman), 1927. [Pulvinulina pacifica].

Epistominella vitrea Parker, 1953.

Favulina melo (d'Orbigny), 1839. [Oolina melo], (Pl. 2-4, Fig. 6).

Fissurina lucida (Williamson), 1848. [Entosolenia marginata (Montagu) var. lucida].

Fissurina marginata (Montagu), 1803. [Vermiculum], (Pl. 2-4, Fig. 9).

Fissurina vitreola (Buchner), 1940. [Lagena vitreola].

Haplophragmoides sp.

Haplophragmoides canariensis (d'Orbigny), 1839. [Nonionina canariensis], (Pl. 2-2, Fig. 6).

Haplophragmoides columbiensis Cushman, 1925.

Haplophragmoides tenuum (Cushman), 1927. [Haplophragmoides tenuis].

Homalohedra borealis (Loeblich and Tappan), 1954. [Oolina borealis].

Hyalinonettrion gracile (O.G. Costa), 1856. [Amphorina gracilis].

Hyperammina friabilis Brady, 1884.

Islandiella norcrossi (Cushman), 1933. [Cassidulina norcrossi].

Lagena sp. 1.

Lagena sp. 2.

Remarks: Partially to almost completely dissolved.

Lagena dorseyae McLean, 1956.

Lagena laevis (Montagu), 1803. [Vermiculum laeve].

Lagena sulcata (Walker and Jacob), 1798. [Serpula (lagena) sulcata].

Leptohalysis catella (Höglund), 1947. [Reophax catella], (Pl. 2-1, Fig. 6).

Lobatula fletcheri (Galloway and Wissler), 1927. [Cibicides fletcheri], (Pl. 2-5, Figs. 1, 2).

Lobatula mckannai (Galloway and Wissler), 1927. [Cibicides mckannai], (Pl. 2-5, Fig. 3).

Miliammina fusca (Brady), 1870. [Quinqueloculina fusca], (Pl. 2-1, Figs. 1, 2).

Miliolinella subrotunda (Montagu), 1803. [Vermiculum subrotundum].

Nodosaria emphysaocyta Loeblich and Tappan, 1953.

Nonionella auricula Heron-Allen and Earland, 1930.

Nonionella stella Cushman and Moyer, 1930. (Pl. 2-5, Fig. 5).

Nonionella turgida Williamson, 1858.

Nonionellina labradorica (J.W. Dawson), 1860. [Nonionina scapha var. labradorica].

Procerolagena sp.

Procerolagena wiesneri (Parr), 1950. [Lagena striata].

Pseudononion bassispinata (Cushman and Moyer), 1930. [Nonion pizarrensis var.

basispinata].

Pygmaeoeseistron hispidum (Reuss), 1863. [Lagena hispida].

Quinqueloculina sp. d'Orbigny, 1826.

Remarks: Partially to almost completely dissolved.

Quinqueloculina arctica Cushman, 1933.

Quinqueloculina seminula (Linné). [Serpula seminulum].

Reophax curtus Cushman, 1920. (Pl. 2-2, Fig. 2).

Reophax gracilis (Kiaer), 1900. [Noëulina gracilis]

Reophax scorpiurus de Montfort, 1808. (Pl. 2-2, Fig. 9).

Rosalina columbiensis (Cushman), 1925. [Discorbis columbiensis].

Saccamina atlantica (Cushman), 1944. [Protonina atlantica].

Saccamina cf. atlantica (Pl. 2-3, Fig. 4).

Remarks: Fusiform agglutinated foraminifera with one chamber.

Saccamina sphaerica Brady, 1871.

Siphonaperta stalkeri (Loeblich and Tappan), 1953. [Quinqueloculina stalkeri].

Spirilina arctica Cushman, 1933.

Spiroplectammina biformis (Parker and Jones), 1878. [Textularia biformis], (Pl. 2-1, Figs. 4, 5).

Spirosigmoilina tenuis (Czjzek), 1848. [Quinqueloculina tenuis].

Stainforthia feylingi Knudsen and Seidenkrantz, 1993. (Pl. 2-4, Fig. 1).

Textularia earlandi Parker, 1952. (Pl. 2-2, Fig. 1).

Trochammina charlottensis Cushman, 1925. (Pl. 2-3, Fig. 6).

Trochammina discorbis Earland, 1934. (Pl. 2-1, Figs. 7, 8).

Trochammina inflata (Montagu), 1808. [Nautilus inflatus], (Pl. 2-3, Fig. 9).

Trochammina nana (Brady), 1881. [Haplophragmium nana].

Trochammina pacifica Cushman, 1925. (Pl. 2-2, Figs. 7, 8).

Trochammina rotaliformis Wright, 1911. (Pl. 2-3, Figs. 1, 2, 3).

Remarks: Specimen is abnormally large.

Trochammina cf. squamata Wright in Heron-Allen and Earland, 1911. (Pl. 2-2, Figs. 4, 5).

Trochammina squamata Parker and Jones, 1860. (Pl. 2-3, Figs. 7, 8).

Trochamminopsis pusilla (Höglund), 1947. [Trochammina quadriloba].

Valvulineria sp.

Valvulineria arctica Green, 1960. (Pl. 2-5, Fig. 4).

ACKNOWLEDGEMENTS

This research was funded by the Geological Survey of Canada (J. J. Clague's Project Number 870017) and by Natural Sciences and Engineering Research Council of Canada Operating Grant OGP0041665 to R. T. Patterson. Sampling facilities and some laboratory equipment were provided by Pacific Geoscience Centre (Geological Survey of Canada, GSC) under T. Forbes' supervision. A. Tsai of the GSC Electron Microbeam Laboratory provided technical help with scanning electron micrographs. Plates were produced with the help of the R. Lacroix, G. Wylie, and G. McNeill of the Photo Mechanical Unit and G. Lemieux and R. Kelly of the Photographic Section

at the GSC. Some text figures were generated by Informatics and Scientific Services, Terrain Sciences, GSC. Discussions with Claudia Schröder-Adams, John J. Clague, Bruce S. Hart, and R. W. C. (Bill) Arnott greatly improved the manuscript. Wayne R. Stevens, Melody Taylor, and Emily Keane are thanked for their assistance.

REFERENCES

- Anderson, J. J. and Devol, A. H., 1973, Deep water renewal in Saanich Inlet, an intermittently anoxic basin: *Estuarine and Coastal Marine Science*, v. 1, p. 1-10.
- Alve, E., 1990, Variations in estuarine foraminiferal assemblages with diminishing oxygen conditions in Drammensfjord, SE Norway: *Paleoecology, Biostratigraphy, Paleoceanography and Taxonomy of Agglutinated Foraminifera*, NATO Series, C, Mathematical and Physical Sciences, v. 327, p. 661-694.
- Alve, E., 1993, Benthic foraminiferal responses to estuarine pollution: A review: *Geological Society of America, Abstracts with Programs*, v. 25, p. A-137.
- Aquatic Science Consultants Limited, 1995, Saanich Inlet study synthesis workshop. Information package, April 25-26: hosted by Ministry Lands and Parks of British Columbia, Saanich Native Heritage Society, and Institute of Ocean Sciences, 46 p.
- Bandy, O. L., Ingle, J. C., and Resig, J. M., 1964a, Foraminifera, Los Angeles County outfall area, California: *Limnology and Oceanography*, v. 9, p. 124-137.
- Bandy, O. L., Ingle, J. C., and Resig, J. M., 1964b, Foraminiferal trends, Laguna Beach outfall area, California: *Limnology and Oceanography*, v. 9, p. 112-123.

- Bates, R. L. and Jackson, J. A., 1987, Glossary of geology, Third edition: American Geological Institute, Alexandria, Virginia, 788 p.
- Buzas, M. A., 1968, On spatial distribution of foraminifera: Contributions from the Cushman Foundation for Foraminiferal Research, v. 19, p. 1-11.
- Carter, N. M., 1934, Physiography and oceanography of some British Columbia fiords: Proceedings of the Fifth Pacific Science Congress, Pacific Science Association, Vancouver, B.C., 1933, v. 1, p. 721-733.
- Clague, J. J. and Bobrowsky, P. T., 1994a, Evidence for a large earthquake and tsunami 100-400 years ago on western Vancouver Island, British Columbia: Quaternary Research, v. 41, p. 176-184.
- Clague, J. J. and Bobrowsky, P. T., 1994b, Tsunami deposits beneath tidal marshes on Vancouver Island, British Columbia: Geological Society of America Bulletin, v. 106, p. 1293-1303.
- Cockbain, A. E., 1963, Distribution of foraminifera in Juan de Fuca and Georgia Straits, British Columbia, Canada: Contributions from the Cushman Foundation for Foraminiferal Research, v. 14, p. 37-57.
- Culver, S.J., 1993, Foraminifera (J. E. Lipps, ed.): Fossil prokaryotes and protists , Blackwell Scientific Publications, p. 203-247.
- Cushman, J. A., 1925, Recent foraminifera from British Columbia: Contributions from the Cushman Foundation for Foraminiferal Research, v. 1, p. 38-47.

- Cushman, J. A. and Todd, R., 1947, Foraminifera from the coast of Washington: Contributions from the Cushman Foundation for Foraminiferal Research, Special Publication 21, 23 p.
- Ellis, B. F. and Messina, A., 1940, Catalogue of foraminifera; American Museum of Natural History, New York, with supplements.
- Fishbein, E., and Patterson, R. T., 1993, Error weighted maximum likelihood (EWML): a new statistically based method to cluster quantitative micropaleontological data: *Journal of Paleontology*, v. 67, p. 475-485.
- Gallagher, M. T., 1979, Substrate controlled assemblages: Recent foraminifera from the continental shelf and slope of Vancouver Island, British Columbia: Unpublished Ph. D. thesis, University of Calgary, 232 p.
- Gross, M. G., Gucluer, S. M., Creager, J. S., and Dawson, W. A., 1963, Varved marine sediments in a stagnant fjord: *Science*, v. 141, p. 918-919.
- Gucluer, S. M. and Gross, M. G., 1964, Recent marine sediments in Saanich Inlet, a stagnant marine basin: *Limnology and Oceanography*, v. 9, p. 359-376.
- Herlinveaux, R. H., 1962, Oceanography of Saanich Inlet in Vancouver Island, British Columbia: *Journal of Fisheries Research Board of Canada*, v. 19, no. 1, p. 1-37.
- Jonasson, K., and Patterson, R. T., 1992, Preservation potential of salt marsh foraminifera from the Fraser River Delta, British Columbia: *Micropaleontology*, v. 38, p. 289-301.

- Jones, G. D., and Ross, C. A., 1979, Seasonal distribution of foraminifera in Samish Bay, Washington: *Journal of Paleontology*, v. 53, p. 245-257.
- Kaminski, M. A., Grassle, J. F., and Whitlash, R. B., 1988, Life history and recolonisation among agglutinated foraminifera in the Panama Basin: *Abhandlungen der Geologischen Bundesanstalt*, v. 41, p. 229-243.
- Knudsen, K. L. and Seidenkrantz, M.-S., 1994, Stainforthia feylingi: New species from Arctic to Subarctic environments, previously recorded as Fursenkoina schreibersiana (Czjzek): *Contributions from the Cushman Foundation of Foraminiferal Research*, Special Publication, no. 32, p. 5-13.
- Loeblich, A. R., and Tappan, H., 1987, Foraminiferal genera and their classification [2 volumes]: Van Norstrand Reinhold Company, New York, 2047 p.
- McCulloch, I. A., 1977, Qualitative observations on Recent foraminiferal tests with emphasis on the eastern Pacific [3 pts.]: University of Southern California, Los Angeles, 1078 p.
- Mathewes, R. W. and Clague, J. J., 1994, Detection of large prehistoric earthquakes in the Pacific Northwest using microfossil analysis: *Science*, v. 264, p. 688-691.
- Miller, A. A. L., Mudie, P. J., and Scott, D. B., 1982, Holocene history of Bedford Basin, Nova Scotia: foraminifera, dinoflagellate, and pollen records: *Canadian Journal of Earth Sciences*, v. 19, p. 2342-2367.

- Murray, J. W., 1985, Recent foraminifera from the North Sea (Forties and Ekofisk areas) and the continental shelf west of Scotland: *Journal of Micropaleontology*, v. 4, p. 117-125.
- Murray, J. W., 1991, *Ecology and paleoecology of benthic foraminifera*: John Wiley and Sons Inc., New York, 397 p.
- Patterson, R. T., 1989, Neogene foraminiferal biostratigraphy of the southern Queen Charlotte Basin: *In Contributions to Canadian Paleontology*, Geological Survey of Canada, Bulletin 396, p. 229-265.
- Patterson, R. T., 1990, Intertidal benthic foraminiferal assemblages on the Fraser River Delta, British Columbia: Modern distribution and paleoecological importance: *Micropaleontology*, v. 36, p. 229-244.
- Patterson, R. T., 1991, Three new species of Holocene benthic foraminifera from the Queen Charlotte Basin-Hecate Strait region of coastal British Columbia: *Transactions of the American Microscopical Society*, v. 110, p. 354-360.
- Patterson, R. T., 1993, Late Quaternary benthic foraminiferal assemblages and paleoceanography of Queen Charlotte Sound and southern Hecate Strait, British Columbia: *Journal of Foraminiferal Research*, v. 23, p. 1-18.
- Patterson, R. T., and Cameron, B. E. B., 1991, Foraminiferal biofacies succession in the late Quaternary Fraser River Delta, British Columbia: *Journal of Foraminiferal Research*, v. 21, p. 228-243.

- Patterson, R. T., and Fishbein, E., 1989, Re-examination of the statistical methods used to determine the number of point counts needed for micropaleontological quantitative research: *Journal of Paleontology*, v. 63, p. 245-248.
- Patterson, R. T., and Luternauer, J. L., 1993, Holocene foraminiferal faunas from cores collected on the Fraser River delta, British Columbia: A paleoecological interpretation: *In* *Current Research, Part A*, Geological Survey of Canada, Paper 93-1A, p. 245-254.
- Patterson, R. T., Burbidge, S. M., and Luternauer, J. L., An atlas of common Quaternary shelf benthic foraminiferal species from off the coast of Canada: *Geological Survey of Canada Bulletin*, in press.
- Phleger, F. B., Jr., 1967, Marsh foraminiferal patterns, Pacific coast of North America: *Universidad Nacional Autónoma de México, Instituto de Biología Anales* 38, Ser. Ciencia del Mar y Limnología, v. 1, p. 11-38.
- Pickard, G. L., 1975, Annual and longer term variations of deepwater properties in the coastal waters of southern British Columbia: *Journal of Fisheries Research Board of Canada*, v. 32, p. 1561-1587.
- Sancetta, C., 1989, Processes controlling the accumulation of diatoms in sediments: A model derived from British Columbian fiords: *Paleoceanography*, v. 4, p. 235-251.
- Sancetta, C., and Calvert, S. E., 1988, The annual cycle of sedimentation in Saanich Inlet, British Columbia: Implications for the interpretation of diatom fossil assemblages: *Deep-Sea Research*, v. 35, p. 71-90.

- Schafer, C. T., and Cole, F. E., 1974, Distributions of benthonic foraminifera: their use in delimiting local nearshore environments: In *Offshore Geology of Eastern Canada*, Geological Survey of Canada, (B. R. Pelletier, ed.), v. 1, p. 103-108.
- Schröder, C. J., 1986, Deep-water arenaceous foraminifera in the Northwest Atlantic Ocean: Canada Department of Fisheries and Oceans, Canadian Technical Report of Hydrography and Ocean Sciences, no. 71, 193 p.
- Scott, D. B., 1974, Recent benthonic foraminifera from Samish and Padilla Bays, Washington: Northwest Science, v. 48, p. 211-218.
- Scott, D. B., and Hermelin, J. O. R., 1993, A device for precision splitting of micropaleontological samples in liquid suspension: *Journal of Paleontology*, v. 67, p. 151-154.
- Scott, D. B., Schafer, C. T., and Medioli, F., 1980, Eastern Canadian estuarine foraminifera: A framework for comparison: *Journal of Foraminiferal Research*, v. 10, p. 205-234.
- Snyder, S. W., Hale, W. R., and Kontrovitz, 1990a, Distributional patterns of modern benthic foraminifera of the Washington shelf: *Micropaleontology*, v. 36, p. 245-258.
- Snyder, S. W., Hale, W. R., and Kontrovitz, 1990b, Assessment of postmortem transportation of modern benthic foraminifera of the Washington shelf: *Micropaleontology*, v. 36, p. 259-282.

- Stucchi, D. J. and Giovando, L. F., 1984, Deep water renewal in Saanich Inlet, B. C.: Proceedings of a multidisciplinary symposium on Saanich Inlet, 2nd February, 1983 (S. K. Juniper and R. O. Brinkhurst, eds.), Canadian Technical report of hydrography and Ocean Sciences no. 38, Institute of Ocean Sciences, Department of Fisheries and Oceans, Sidney, B.C., p.7-15.
- Watkins, J. G., 1961, Foraminiferal ecology around the Orange County, California, ocean sewer fall: *Micropaleontology*, v. 7, p. 199-206.
- Williams, H. F. L., 1989, Foraminiferal zonations on the Fraser River Delta and their application to paleoenvironmental interpretations: *Paleogeography, Paleoclimatology, Paleoecology*, v. 73, p. 39-50.
- Yanko, V., Kronfeld, J., and Flexer, A., 1994, Response of benthic foraminifera to various pollution sources: Implications for pollution monitoring, *Journal of Foraminiferal Research*, v. 24, p. 1-17.

PLATE 2-1

1, 2 Miliammina fusca (Brady). 1 Side view of hypotype from station GS-55, X 240. 2 Side view of hypotype from station GS-03, slightly broken, showing quinqueloculine chamber arrangement and part of the apertural opening at the top, X 300. 3 Eggerella advena (Cushman). Side view of hypotype from station GS-04 showing triserial chamber arrangement, X 380. 4, 5 Spiroplectammina biformis (Parker and Jones). 4 Side view of hypotype from station GS-24 showing chambers with initial coiling and later biserial arrangement, X380. 5 side view of hypotype from station GS-46 with chambers anomalously bent in the early biserial arrangement, X 400. 6 Leptohalysis catella (Höglund). Longitudinal section of hypotype from GS-24 showing beaded chamber arrangement gradually increasing in size, X 380. 7, 8 Trochammina discorbis Earland. 7 Dorsal view of hypotype from station GS-05 showing coarsely agglutinated wall, X 320. 8 Ventral view of hypotype from station GS-47 showing deep umbilicus, X 320. 9 Discammina compressa (Goës). Side view of hypotype from station GS-25 showing coarsely agglutinated wall, X 140.

PLATE 2-2

1 Textularia earlandi Parker. side view of hypotype from station GS-23 showing biserial chamber arrangement, X 300. **2** Reophax curtus Cushman. side view of hypotype from station GS-56 showing extended apertural neck and coarsely agglutinated wall, X 220. **3** Atlantiella atlantica (F. L. Parker). Dorsal view of hypotype from station GS-02 showing globular chamber arrangement with protruding final chamber, X 160. **4, 5** Trochammina cf. squamata Parker and Jones. **4** Dorsal view of hypotype from station GS-47 showing numerous chamber arrangement, X 240. **5** Ventral view of hypotype from station GS-24 showing large final chamber and lunate chambers, X 400. **6** Haplophragmoides canariensis (d'Orbigny). Side view of hypotype from station GS-56 showing coarsely agglutinated wall, X 220. **7, 8** Trochammina pacifica Cushman. **7** Dorsal view of hypotype from station GS-30 showing globular chamber arrangement, X 280. **8** Ventral view of hypotype from station GS-30 showing apertural slit, X 300. **9** Reophax scorpiurus de Montfort. Side view of hypotype from station showing distinct uniserial chamber arrangement with chambers increasing dramatically in size, X 150.

PLATE 2-3

1, 2, 3 Trochammina rotaliformis Wright in Heron-Allen and Earland. 1 Dorsal view of hypotype from station GS-36 showing numerous chambers, X 170. 2 Ventral view of hypotype from station GS-36 showing final chamber occupying one-third of the ventral side, X 170. 3 Side view of hypotype from station GS-36 showing trochoid concavo-convex test and slightly broken apertural slit, X 240. 4 Saccammina cf. atlantica (Cushman). Side view of hypotype from station GS-56 showing fusiform shape rather than tear-drop test shape, X 360. 5 Cuneata arctica (Brady). Side view of hypotype from station GS-24 showing coarsely agglutinated test, X 500. 6 Trochammina charlottensis Cushman. Dorsal view of hypotype from station GS-09 showing large final chamber, X 340. 7, 8 Trochammina squamata Parker and Jones. 7 Dorsal view of hypotype from station GS-30 showing multiple chambers, flat trochoid shape, and rounded periphery, X 340. 8 Ventral view of hypotype from station GS-30 showing lunate chambers, X 340. 9 Trochammina inflata (Montagu). Dorsal view of hypotype from GS-56 showing smooth finish on agglutinated test, X 200.

PLATE 2-4

1 Stainforthia feylingi Knudsen and Seidenkrantz. Side view of hypotype from station GS-49 showing porous wall and part of the apertural opening at top, X 550. **2**

Buliminella elegantissima (d'Orbigny). Side view of hypotype from station GS-32 showing apertural opening and porous test, X 400. **3** Bolivinellina pacifica (Cushman and McCulloch). Side view of hypotype from station GS-49 showing slightly broken elongate test, X 130. **4, 5** Dyocibicides biserialis Cushman and Valentine. **4** Dorsal view of hypotype from station GS-42 showing coiling in early chamber arrangement, X 150. **5** Ventral view of holotype from station GS-42 showing coarsely perforate wall, X 160. **6** Favulina melo (d'Orbigny). Side view of hypotype from station GS-24 showing elevated ridges forming polygonal reticulations, X 360. **7, 8** Buccella frigida (Cushman). **7** Dorsal view of hypotype from station GS-14 showing lobulate but rounded periphery, X 320. **8** Ventral view of hypotype from station GS-14 showing numerous pustules concentrated along incised sutures, X 320. **9** Fissurina marginata (Montagu). Side view of hypotype from station GS-49 showing narrow marginal keel, X 340.

PLATE 2-5

1, 2 Lobatula fletcheri (Galloway and Wissler). **1** Dorsal view of hypotype from station GS-49 showing only a few perforations and a slightly etched test, X 360. **2** Ventral (spiral) view of hypotype from station GS-49 showing a coarsely perforate wall, X 380. **3 Lobatula mckannai** (Galloway and Wissler). Dorsal view of hypotype from station GS-49 showing protruding final chamber, X 360. **4 Valvulineria arctica** Green. Ventral view of hypotype from station GS-42 showing apertural flap covering the aperture, X 400. **5 Nonionella stella** Cushman and Moyer. Ventral view of hypotype from station GS-49 showing flap covering umbilical region, X 130. **6 Criboelphidium frigidum** (Cushman). Side view of hypotype from station GS-42 showing inflated final chamber, X 180. **7 Criboelphidium hallandense** (Brotzen). Side view of hypotype from station GS-14 showing pustules concentrated along sutures, X 300. **8, 9 Elphidiella hannai** Cushman and Grant. **8** Side view of hypotype from station GS-42 showing characteristic double rows of pores along sutures, X 220. **9** Apertural view of hypotype from station GS-42 showing concentrated pustules in the apertural region, X 280. **10 Criboelphidium microgranulosum** (Galloway and Wissler). Side view of hypotype from station GS-42 showing numerous pustules, X 400.

Appendix 2-1. List of species for each sample with their total percent abundance (live and dead), percent live specimens, and total percent error. Asterisk indicates that there were no live specimens in the sample. Samples with less than 100 specimens were not included in the list (GS-04 is an exception). Double asterisk indicates that sample is statistically significant (Fishbein and Patterson, 1993).

[illegible]

Sample	GS-02	GS-03	GS-04	GS-05	GS-06	GS-07	GS-08	GS-09	GS-11	GS-12	GS-13	GS-14
<i>F. lucida</i> %	-	-	-	-	-	-	-	-	-	-	-	-
<i>F. lucida</i> live %	-	-	-	-	-	-	-	-	-	-	-	-
% Uncertainty ±	-	-	-	-	-	-	-	-	-	-	-	-
<i>F. marginata</i> %	-	-	-	-	-	-	-	-	-	-	-	-
<i>F. marginata</i> live %	-	-	-	-	-	-	-	-	-	-	-	-
% Uncertainty ±	-	-	-	-	-	-	-	-	-	-	-	-
<i>F. melo</i> %	-	-	-	-	-	-	-	-	-	-	-	0.3
<i>F. melo</i> live %	-	-	-	-	-	-	-	-	-	-	-	-
% Uncertainty ±	-	-	-	-	-	-	-	-	-	-	-	0.4
<i>F. vitreola</i> %	-	-	-	-	-	-	-	-	-	-	-	-
<i>F. vitreola</i> live %	-	-	-	-	-	-	-	-	-	-	-	-
% Uncertainty ±	-	-	-	-	-	-	-	-	-	-	-	-
<i>H. borealis</i> live %	-	-	-	-	-	-	-	-	-	-	-	-
<i>H. borealis</i> %	-	-	-	-	-	-	-	-	-	-	-	-
% Uncertainty ±	-	-	-	-	-	-	-	-	-	-	-	-
<i>H. canariensis</i> % **	-	-	-	0.5	0.5	0.2	5.9	1	-	-	-	-
<i>H. canariensis</i> live %	-	-	-	-	-	-	1.5	-	-	-	-	-
% Uncertainty ±	-	-	-	0.6	0.7	0.4	2.8	2	-	-	-	-
<i>H. columbrensis</i> % **	-	0.3	-	-	0.3	1.3	0.7	1	3	-	-	-
<i>H. columbrensis</i> live %	-	-	-	-	0.3	-	-	-	-	-	-	-
% Uncertainty ±	-	0.02	-	-	0.5	1.1	1.9	2	1.7	-	-	-
<i>H. friabilis</i> %	-	-	-	-	-	-	-	-	-	-	-	-
<i>H. friabilis</i> live %	-	-	-	-	-	-	-	-	-	-	-	-
% Uncertainty ±	-	-	-	-	-	-	-	-	-	-	-	-
<i>H. gracile</i> %	-	-	-	-	-	0.4	-	-	-	-	-	0.1
<i>H. gracile</i> live %	-	-	-	-	-	-	-	-	-	-	-	-
% Uncertainty ±	-	-	-	-	-	0.6	-	-	-	-	-	0.3
<i>H. tenaxum</i> %	-	-	-	-	-	-	-	-	-	0.2	-	-
<i>H. tenaxum</i> live %	-	-	-	-	-	-	-	-	-	-	-	-
% Uncertainty ±	-	-	-	-	-	-	-	-	-	0.4	-	-
<i>Haplophragmoides</i> sp %	-	-	-	-	-	-	-	-	-	-	-	-
<i>Haplophragmoides</i> sp live %	-	-	-	-	-	-	-	-	-	-	-	-
% Uncertainty ±	-	-	-	-	-	-	-	-	-	-	-	-
<i>I. norcrossi</i> %	-	-	-	-	-	-	-	-	-	0.2	-	-
<i>I. norcrossi</i> live %	-	-	-	-	-	-	-	-	-	-	-	-
% Uncertainty ±	-	-	-	-	-	-	-	-	-	0.4	-	-
<i>L. catella</i> % **	-	-	-	-	-	3.3	3	5	48.8	-	-	1
<i>L. catella</i> live %	-	-	-	-	-	-	-	-	-	-	-	-
% Uncertainty ±	-	-	-	-	-	1.7	2	4.3	4.9	-	-	1

[illegible]

Sample	GS-02	GS-03	GS-04	GS-05	GS-06	GS-07	GS-08	GS-09	GS-11	GS-12	GS-13	GS-14
<i>S. atlantica</i> %		-		-	-	-	-	2	-	-	-	-
<i>S. atlantica</i> live %	-				-	-	-	-	-	-	-	-
% Uncertainty ±		-	-	-	-	-	-	27	-	-	-	-
<i>S. biformis</i> % **	-	09	-	1	13	56	26	8	20	-	75	04
<i>S. biformis</i> live %	-	-	-	03	1	09	07	-	-	-	18	-
% Uncertainty ±	-	1	-	08	11	21	19	53	39	-	26	05
<i>S. cf atlantica</i> % **	35	42.2	4	05	03	-	-	3	98	02	115	01
<i>S. cf atlantica</i> live %	15	11	-	05	-	-	-	-	08	-	3	-
% Uncertainty ±	25	52	54	06	05	-	-	33	29	04	31	03
<i>S. feydingeri</i> % **	-	-		-	-	-	-	-	-	-	-	69
<i>S. feydingeri</i> live %	-	-	-	-	-	-	-	-	-	-	-	-
% Uncertainty ±	-	-	-	-	-	-	-	-	-	-	-	19
<i>S. sphaerica</i> %	-	-	-	-	-	-	-	-	-	-	-	-
<i>S. sphaerica</i> live %	-	-	-	-	-	-	-	-	-	-	-	-
% Uncertainty ±	-	-	-	-	-	-	-	-	-	-	-	-
<i>S. stalkeri</i> %	-	-	-	-	-	-	-	-	-	-	-	-
<i>S. stalkeri</i> live %	-	-	-	-	-	-	-	-	-	-	-	-
% Uncertainty ±	-	-	-	-	-	-	-	-	-	-	-	-
<i>S. tenuis</i> %	-	-	-	-	-	-	-	-	-	0.7	-	-
<i>S. tenuis</i> live %	-	-	-	-	-	-	-	-	-	-	-	-
% Uncertainty ±	-	-	-	-	-	-	-	-	-	0.7	-	-
<i>T. charlottensis</i> % **	-	-	-	-	-	-	07	2	03	-	13	-
<i>T. charlottensis</i> live %	-	-	-	-	-	-	-	-	-	-	-	-
% Uncertainty ±	-	-	-	-	-	-	1	27	05	-	12	-
<i>T. discorbis</i> % **	-	-	-	03	-	18	3	-	1	-	-	-
<i>T. discorbis</i> live %	-	-	-	-	-	07	-	-	-	-	-	-
% Uncertainty ±	-	-	-	05	-	12	2	-	1	-	-	-
<i>T. earlandi</i> %	-	-	-	-	-	02	-	-	-	-	05	-
<i>T. earlandi</i> live %	-	-	-	-	-	-	-	-	-	-	-	-
% Uncertainty ±	-	-	-	-	-	04	-	-	-	-	07	-
<i>T. inflata</i> %	-	03	-	-	-	-	-	-	-	-	-	-
<i>T. inflata</i> live %	-	-	-	-	-	-	-	-	-	-	-	-
% Uncertainty ±	-	002	-	-	-	-	-	-	-	-	-	-
<i>T. cf rotaliformis</i> % **	-	03	-	03	-	-	-	-	05	-	08	-
<i>T. cf rotaliformis</i> live %	-	-	-	-	-	-	-	-	-	-	-	-
% Uncertainty ±	-	002	-	05	-	-	-	-	07	-	08	-
<i>T. rotaliformis</i> % **	15	57	-	25	13	62	152	10	25	1	115	25
<i>T. rotaliformis</i> live %	-	11	-	-	-	04	-	-	-	02	13	-
% Uncertainty ±	17	24	-	12	14	22	43	59	15	09	31	12

[illegible]

[illegible]

[illegible]

Sample	GS-15	GS-16	GS-17	GS-19 *	GS-20 *	GS-21 *	GS-22	GS-23 *	GS-24 *	GS-25 *	GS-26
<i>F. lucida</i> %	-	-	-	-	-	-	-	-	-	-	-
<i>F. lucida</i> live %	-	-	-	-	-	-	-	-	-	-	-
% Uncertainty ±	-	-	-	-	-	-	-	-	-	-	-
<i>F. marginata</i> %	-	-	-	-	-	-	-	-	-	-	-
<i>F. marginata</i> live %	-	-	-	-	-	-	-	-	-	-	-
% Uncertainty ±	-	-	-	-	-	-	-	-	-	-	-
<i>F. melo</i> %	-	-	-	-	-	-	-	-	-	-	-
<i>F. melo</i> live %	-	-	-	-	-	-	-	-	-	-	-
% Uncertainty ±	-	-	-	-	-	-	-	-	-	-	-
<i>F. vitreola</i> %	-	-	-	-	-	-	-	-	-	-	-
<i>F. vitreola</i> live %	-	-	-	-	-	-	-	-	-	-	-
% Uncertainty ±	-	-	-	-	-	-	-	-	-	-	-
<i>H. borealis</i> live %	-	-	-	-	-	-	-	-	-	-	-
<i>H. borealis</i> %	-	-	-	-	-	-	-	-	-	-	-
% Uncertainty ±	-	-	-	-	-	-	-	-	-	-	-
<i>H. canariensis</i> % **	-	-	-	-	-	-	0.3	-	-	-	0.2
<i>H. canariensis</i> live %	-	-	-	-	-	-	-	-	-	-	-
% Uncertainty ±	-	-	-	-	-	-	0.7	-	-	-	0.4
<i>H. columbiensis</i> % **	6	2.2	4	-	12	4.7	0.3	12	3	-	0.6
<i>H. columbiensis</i> live %	-	0.2	-	-	-	-	-	-	-	-	-
% Uncertainty ±	2.1	1.3	1.9	-	1.3	4	0.7	1	1.7	-	0.7
<i>H. friabilis</i> %	-	0.4	-	-	-	-	-	-	-	-	-
<i>H. friabilis</i> live %	-	-	-	-	-	-	-	-	-	-	-
% Uncertainty ±	-	0.6	-	-	-	-	-	-	-	-	-
<i>H. gracile</i> %	-	-	-	-	-	-	-	-	-	-	-
<i>H. gracile</i> live %	-	-	-	-	-	-	-	-	-	-	-
% Uncertainty ±	-	-	-	-	-	-	-	-	-	-	-
<i>H. tenue</i> %	-	-	-	-	-	-	-	-	-	-	-
<i>H. tenue</i> live %	-	-	-	-	-	-	-	-	-	-	-
% Uncertainty ±	-	-	-	-	-	-	-	-	-	-	-
<i>Haplophragmoides</i> sp %	-	-	-	-	-	-	-	-	-	-	-
<i>Haplophragmoides</i> sp live %	-	-	-	-	-	-	-	-	-	-	-
% Uncertainty ±	-	-	-	-	-	-	-	-	-	-	-
<i>I. norcrossi</i> %	-	-	-	2.9	-	-	-	-	-	-	-
<i>I. norcrossi</i> live %	-	-	-	-	-	-	-	-	-	-	-
% Uncertainty ±	-	-	-	3.3	-	-	-	-	-	-	-
<i>L. castella</i> % **	3.4	7.4	12.5	34.3	39.2	24.3	-	4.4	2.4	-	19.4
<i>L. castella</i> live %	-	-	-	-	-	-	-	-	-	-	-
% Uncertainty ±	1.6	2.3	3.2	9.2	6.1	8.1	-	4.4	4.2	-	3.5

Sample	GS-15	GS-16	GS-17	GS-19 *	GS-20 *	GS-21 *	GS-22	GS-23 *	GS-24 *	GS-25 *	GS-26
<i>N. turgida</i> %	-	-	-	-	-	-	-	-	-	-	-
<i>N. turgida</i> live %	-	-	-	-	-	-	-	-	-	-	-
% Uncertainty ±	-	-	-	-	-	-	-	-	-	-	-
<i>P. bassispinata</i> %	-	-	-	-	-	-	-	-	-	-	-
<i>P. bassispinata</i> live %	-	-	-	-	-	-	-	-	-	-	-
% Uncertainty ±	-	-	-	-	-	-	-	-	-	-	-
<i>P. hispidum</i> %	-	-	-	-	-	-	-	-	-	-	-
<i>P. hispidum</i> live %	-	-	-	-	-	-	-	-	-	-	-
% Uncertainty ±	-	-	-	-	-	-	-	-	-	-	-
<i>P. wiesneri</i> %	-	-	-	-	-	-	-	-	-	-	-
<i>P. wiesneri</i> live %	-	-	-	-	-	-	-	-	-	-	-
% Uncertainty ±	-	-	-	-	-	-	-	-	-	-	-
<i>Procerolagena</i> sp %	-	-	-	1	-	-	-	-	-	-	-
<i>Procerolagena</i> sp live %	-	-	-	-	-	-	-	-	-	-	-
% Uncertainty ±	-	-	-	19	-	-	-	-	-	-	-
<i>Q. artica</i> %	-	-	-	-	-	-	-	-	-	-	-
<i>Q. artica</i> live %	-	-	-	-	-	-	-	-	-	-	-
% Uncertainty ±	-	-	-	-	-	-	-	-	-	-	-
<i>Q. semirula</i> %	-	-	-	-	-	-	-	-	-	-	-
<i>Q. semirula</i> live %	-	-	-	-	-	-	-	-	-	-	-
% Uncertainty ±	-	-	-	-	-	-	-	-	-	-	-
<i>Quinqueloculina</i> sp % **	-	-	-	-	-	-	-	-	-	-	-
<i>Quinqueloculina</i> sp live %	-	-	-	-	-	-	-	-	-	-	-
% Uncertainty ±	-	-	-	-	-	-	-	-	-	-	-
<i>R. columbiensis</i> %	-	-	-	-	-	-	-	-	-	-	-
<i>R. columbiensis</i> live %	-	-	-	-	-	-	-	-	-	-	-
% Uncertainty ±	-	-	-	-	-	-	-	-	-	-	-
<i>R. curtus</i> %	-	14	-	-	-	19	-	-	08	79	06
<i>R. curtus</i> live %	-	-	-	-	-	-	-	-	-	-	-
% Uncertainty ±	-	1	-	-	-	26	-	-	08	53	07
<i>R. gracile</i> %	-	-	-	-	-	-	-	-	-	4	-
<i>R. gracile</i> live %	-	-	-	-	-	-	-	-	-	-	-
% Uncertainty ±	-	-	-	-	-	-	-	-	-	38	-
<i>R. scorpiurus</i> % **	68	126	6	-	04	09	16	2	2	144	-
<i>R. scorpiurus</i> live %	-	62	3	-	-	-	13	-	-	-	-
% Uncertainty ±	22	29	23	-	08	18	41	12	14	69	-
<i>S. arctica</i> live %	-	-	-	-	-	-	-	-	-	-	-
<i>S. arctica</i> %	02	06	-	-	-	-	03	-	-	-	02
% Uncertainty ±	04	07	-	-	-	-	07	-	-	-	04

Sample	GS-15	GS-16	GS-17	GS-19 *	GS-20 *	GS-21 *	GS-22	GS-23 *	GS-24 *	GS-25 *	GS-26
<i>S. atlantica</i> %	-	-	-	-	-	-	-	-	-	7.9	-
<i>S. atlantica</i> live %	-	-	-	-	-	-	-	-	-	-	-
% Uncertainty ±	-	-	-	-	-	-	-	-	-	5.3	-
<i>S. biformis</i> % **	7	8.6	16.8	2.9	35.6	40.2	6.7	16	28.5	2	18.4
<i>S. biformis</i> live %	-	-	1	-	-	-	2.3	-	-	-	0.2
% Uncertainty ±	2.2	2.5	3.7	3.3	5.9	9.3	2.8	3.2	4.4	2.7	3.4
<i>S. cf atlantica</i> % **	4	4.4	8	-	1.6	2.8	0.3	2	2.5	13.9	0.6
<i>S. cf atlantica</i> live %	-	-	3.3	-	-	-	-	-	-	-	-
% Uncertainty ±	1.7	1.8	2.7	-	1.6	3.1	0.7	1.2	1.5	6.7	0.7
<i>S. feylingi</i> % **	-	-	-	24.5	-	-	-	-	-	-	-
<i>S. feylingi</i> live %	-	-	-	-	-	-	-	-	-	-	-
% Uncertainty ±	-	-	-	8.3	-	-	-	-	-	-	-
<i>S. sphaerica</i> %	-	-	-	-	-	-	-	-	-	-	-
<i>S. sphaerica</i> live %	-	-	-	-	-	-	-	-	-	-	-
% Uncertainty ±	-	-	-	-	-	-	-	-	-	-	-
<i>S. stalkeri</i> %	-	-	-	-	-	-	-	-	-	-	-
<i>S. stalkeri</i> live %	-	-	-	-	-	-	-	-	-	-	-
% Uncertainty ±	-	-	-	-	-	-	-	-	-	-	-
<i>S. tenuis</i> %	-	-	-	-	-	-	-	-	-	-	-
<i>S. tenuis</i> live %	-	-	-	-	-	-	-	-	-	-	-
% Uncertainty ±	-	-	-	-	-	-	-	-	-	-	-
<i>T. charlottensis</i> % **	1	4.2	-	-	-	-	1	-	-	-	-
<i>T. charlottensis</i> live %	-	-	-	-	-	-	-	-	-	-	-
% Uncertainty ±	0.9	1.8	-	-	-	-	1.1	-	-	-	-
<i>T. discorhis</i> % **	1	3.6	0.5	-	-	-	1.7	-	-	-	-
<i>T. discorhis</i> live %	-	0.6	-	-	-	-	1	-	-	-	-
% Uncertainty ±	0.9	1.5	0.7	-	-	-	1.4	-	-	-	-
<i>T. earlandi</i> %	0.9	0.2	-	-	-	-	0.7	0.8	1	-	0.4
<i>T. earlandi</i> live %	-	-	-	-	-	-	0.3	-	-	-	-
% Uncertainty ±	1.2	0.4	-	-	-	-	0.9	0.8	1	-	0.6
<i>T. inflata</i> %	-	-	-	-	-	-	-	-	-	-	-
<i>T. inflata</i> live %	-	-	-	-	-	-	-	-	-	-	-
% Uncertainty ±	-	-	-	-	-	-	-	-	-	-	-
<i>T. cf rotaliformis</i> % **	-	0.2	-	-	-	1.9	0.7	-	-	-	0.4
<i>T. cf rotaliformis</i> live %	-	-	-	-	-	-	0.7	-	-	-	-
% Uncertainty ±	-	0.4	-	-	-	2.6	0.9	-	-	-	0.6
<i>T. rotaliformis</i> % **	22.2	15.4	11.5	-	1.2	4.7	8.7	3.4	2	-	4.6
<i>T. rotaliformis</i> live %	0.6	1	0.3	-	-	-	1.7	-	-	-	-
% Uncertainty ±	3.6	3.2	3.1	-	1.3	4	3.2	1.6	1.4	-	1.8

[illegible]

Sample	GS-27	GS-28 *	GS-30	GS-31	GS-32	GS-33	GS-34	GS-35	GS-36	GS 37 *	GS 38	GS 39 *
<i>F lucida</i> %	-	-	-	-	-	-	-	-	-			
<i>F lucida</i> live %	-	-	-	-	-	-	-	-	-			
% Uncertainty ±	-	-	-	-	-	-	-	-	-			
<i>F marginata</i> %	-	-	-	-	-	-	-	-	-			
<i>F marginata</i> live %	-	-	-	-	-	-	-	-	-		11	
% Uncertainty ±	-	-	-	-	-	-	-	-	-			
<i>F melo</i> %	-	14	-	-	-	-	-	-	-			
<i>F melo</i> live %	-	-	-	-	-	-	-	-	-			
% Uncertainty ±	-	1	-	-	-	-	-	-	-			
<i>F vitreola</i> %	-	-	-	-	-	-	-	-	-			
<i>F vitreola</i> live %	-	-	-	-	-	-	-	-	-			
% Uncertainty ±	-	-	-	-	-	-	-	-	-			
<i>H borealis</i> live %	-	-	-	-	-	-	-	-	-			
<i>H borealis</i> %	-	-	-	-	-	-	-	-	-			
% Uncertainty ±	-	-	-	-	-	-	-	-	-			
<i>H canariensis</i> % **	-	02	15	-	1	03	-	35	1			
<i>H canariensis</i> live %	-	-	02	-	-	-	-	-	-			
% Uncertainty ±	-	04	12	-	14	07	-	18	1			
<i>H columbiensis</i> % **	13	-	-	2	2	2	06	07	1	28	34	27
<i>H columbiensis</i> live %	-	-	-	-	-	-	-	-	-			
% Uncertainty ±	11	-	-	19	10	16	08	08	1	2	10	18
<i>H friabilis</i> %	-	-	-	-	-	-	-	-	-			
<i>H friabilis</i> live %	-	-	-	-	-	-	-	-	-			
% Uncertainty ±	-	-	-	-	-	-	-	-	-			
<i>H gracile</i> %	-	-	-	-	-	-	-	-	-			
<i>H gracile</i> live %	-	-	-	-	-	-	-	-	-			
% Uncertainty ±	-	-	-	-	-	-	-	-	-			
<i>H tenuum</i> %	-	-	-	-	-	-	-	-	-			
<i>H tenuum</i> live %	-	-	-	-	-	-	-	-	-			
% Uncertainty ±	-	-	-	-	-	-	-	-	-			
<i>Haplophragmoides</i> sp %	-	-	-	-	-	-	-	-	-			
<i>Haplophragmoides</i> sp live %	-	-	-	-	-	-	-	-	-			
% Uncertainty ±	-	-	-	-	-	-	-	-	-			
<i>I norcrossi</i> %	-	-	-	-	-	-	-	-	-			
<i>I norcrossi</i> live %	-	-	-	-	-	-	-	-	-			
% Uncertainty ±	-	-	-	-	-	-	-	-	-			
<i>L. catella</i> % **	113	-	02	39	4	67	3	22	22	284	8	30
<i>L. catella</i> live %	-	-	-	-	-	-	-	-	-			
% Uncertainty ±	31	-	05	27	27	28	18	14	14	56	28	52

Sample	GS-27	GS-28 *	GS-30	GS-31	GS-32	GS-33	GS-34	GS-35	GS-36	GS-37	GS-38	GS-39 *
<i>N. turgida</i> %	-	-	-	-	-	-	-	-	-	-	-	-
<i>N. turgida</i> live %	-	-	-	-	-	-	-	-	-	-	-	-
% Uncertainty ±	-	-	-	-	-	-	-	-	-	-	-	-
<i>P. bassispinata</i> %	-	-	-	-	-	-	-	-	-	-	-	-
<i>P. bassispinata</i> live %	-	-	-	-	-	-	-	-	-	-	-	-
% Uncertainty ±	-	-	-	-	-	-	-	-	-	-	-	-
<i>P. hispidum</i> %	-	-	-	-	-	-	-	-	-	-	-	-
<i>P. hispidum</i> live %	-	-	-	-	-	-	-	-	-	-	-	-
% Uncertainty ±	-	-	-	-	-	-	-	-	-	-	-	-
<i>P. wegmersi</i> %	-	0.6	-	-	-	-	-	-	-	-	-	-
<i>P. wegmersi</i> live %	-	-	-	-	-	-	-	-	-	-	-	-
% Uncertainty ±	-	0.7	-	-	-	-	-	-	-	-	-	-
<i>Procerolagena</i> sp. %	-	-	-	-	-	-	-	-	-	-	-	-
<i>Procerolagena</i> sp. live %	-	-	-	-	-	-	-	-	-	-	-	-
% Uncertainty ±	-	-	-	-	-	-	-	-	-	-	-	-
<i>Q. artica</i> %	-	-	-	-	-	-	-	-	-	-	-	-
<i>Q. artica</i> live %	-	-	-	-	-	-	-	-	-	-	-	-
% Uncertainty ±	-	-	-	-	-	-	-	-	-	-	-	-
<i>Q. semirula</i> %	-	-	-	-	-	-	-	-	-	-	-	-
<i>Q. semirula</i> live %	-	-	-	-	-	-	-	-	-	-	-	-
% Uncertainty ±	-	-	-	-	-	-	-	-	-	-	-	-
<i>Quinqueloculina</i> sp. %, **	-	-	-	-	-	-	-	-	-	-	-	-
<i>Quinqueloculina</i> sp. live %	-	-	-	-	-	-	-	-	-	-	-	-
% Uncertainty ±	-	-	-	-	-	-	-	-	-	-	-	-
<i>R. columbiensis</i> %	-	-	-	-	-	-	-	-	-	-	-	-
<i>R. columbiensis</i> live %	-	-	-	-	-	-	-	-	-	-	-	-
% Uncertainty ±	-	-	-	-	-	-	-	-	-	-	-	-
<i>R. curtus</i> %	-	-	-	-	-	0.3	-	-	-	-	-	-
<i>R. curtus</i> live %	-	-	-	-	-	-	-	-	-	-	-	-
% Uncertainty ±	-	-	-	-	-	0.7	-	-	-	-	-	-
<i>R. gracile</i> %	-	-	-	-	-	-	-	-	-	-	-	-
<i>R. gracile</i> live %	-	-	-	-	-	-	-	-	-	-	-	-
% Uncertainty ±	-	-	-	-	-	-	-	-	-	-	-	-
<i>R. scorpiurus</i> %, **	2.5	-	3	3.9	9	5	4.5	12.4	21	9.4	0.6	-
<i>R. scorpiurus</i> live %	0.3	-	1	0.5	0.5	-	-	0.2	0.5	-	-	-
% Uncertainty ±	1.5	-	1.7	2.7	4	2.5	2.2	3.2	4	0.8	0.8	-
<i>S. arctica</i> live %	-	-	-	-	-	-	-	-	-	-	-	-
<i>S. arctica</i> %	-	-	-	1.5	1	-	-	-	0.2	1.2	-	-
% Uncertainty ±	-	-	-	1.7	1.4	-	-	-	0.5	1.4	-	-

Sample	GS-27	GS-28 *	GS-30	GS-31	GS-32	GS-33	GS-34	GS-35	GS-36	GS-37	GS-38	GS-39 *
<i>S. atlantica</i> %	03					2						
<i>S. atlantica</i> live %						03						
% Uncertainty ±	05					16						
<i>S. biformis</i> % **	29		25	113	125	13	193	99	87	212	369	197
<i>S. biformis</i> live %			05	34	25	23	33		02			
% Uncertainty ±	44		15	43	46	38	43	28	28	51	51	45
<i>S. cf atlantica</i> % **	03	04	27	25	25	57	3	42	25	96	23	
<i>S. cf atlantica</i> live %			15		05	3			02			
% Uncertainty ±	05	06	16	21	22	26	18	2	15	36	16	
<i>S. fedingsi</i> % **		34										
<i>S. fedingsi</i> live %												
% Uncertainty ±		16										
<i>S. sphaerica</i> %											11	
<i>S. sphaerica</i> live %												
% Uncertainty ±											11	
<i>S. stalkeri</i> %												
<i>S. stalkeri</i> live %												
% Uncertainty ±												
<i>S. temus</i> %												
<i>S. temus</i> live %												
% Uncertainty ±												
<i>T. charlottensis</i> % **	2	02	25	2	25		57	5	17	08		
<i>T. charlottensis</i> live %			02									
% Uncertainty ±	14	04	15	19	22		25	21	37	11		
<i>T. discorbis</i> % **	03		12	39	25	67	73	97	14			1
<i>T. discorbis</i> live %			05	34		2	51	12	12			
% Uncertainty ±	05		11	27	22	28	28	29	34			11
<i>T. earlandi</i> %	08			05						16	09	13
<i>T. earlandi</i> live %												
% Uncertainty ±	08			1						16	1	13
<i>T. inflata</i> %												
<i>T. inflata</i> live %												
% Uncertainty ±												
<i>T. cf rotaliformis</i> % **	05						12		25		14	
<i>T. cf rotaliformis</i> live %												
% Uncertainty ±	07						12		15		12	
<i>T. rotaliformis</i> % **	58	04	05	74	65	53	66	15	17	8	131	127
<i>T. rotaliformis</i> live %												
% Uncertainty ±	23	06	07	36	34	25	27	12	13	34	35	38

[illegible]

Sample	GS-40	GS-41	GS-42	GS-43	GS-44	GS-45	GS-46 *	GS-47	GS-48	GS-50	GS-52	GS-54	GS-55	GS-56
<i>Bathysiphon</i> sp. 1 %	1	0.6	-	-	-	-	-	-	-	2	0.9			
<i>Bathysiphon</i> sp. 1 live %	-	-	-	-	-	-	-	-	-					
% Uncertainty ±	1	0.7	-	-	-	-	-	-	-	1.9	1.1			
<i>Bathysiphon</i> sp. 2 %	-	-	-	-	-	-	-	-	-					
<i>Bathysiphon</i> sp. 2 live %	-	-	-	-	-	-	-	-	-					
% Uncertainty ±	-	-	-	-	-	-	-	-	-					
<i>C. arctica</i> % **	12.3	12.6	-	-	2.9	-	-	0.5	1			0.2	2.8	0.9
<i>C. arctica</i> live %	-	-	-	-	-	-	-	-	-					
% Uncertainty ±	3.2	2.9	-	-	2.5	-	-	0.7	1			0.4	1.8	1.0
<i>C. bariletti</i> % **	-	-	5.3	-	-	-	-	-	0.3			0.2		
<i>C. bariletti</i> live %	-	-	0.2	-	-	-	-	-						
% Uncertainty ±	-	-	1.8	-	-	-	-	-	0.5			0.4		
<i>C. excavatum</i> % **	-	-	7.5	-	-	-	-	-				1.6		
<i>C. excavatum</i> live %	-	-	-	-	-	-	-	-						
% Uncertainty ±	-	-	2.1	-	-	-	-	-				1.1		
<i>C. foraminosum</i> %	-	-	-	-	-	-	-	-						
<i>C. foraminosum</i> live %	-	-	-	-	-	-	-	-						
% Uncertainty ±	-	-	-	-	-	-	-	-						
<i>C. frigidum</i> % **	-	-	6.7	-	-	-	-	-	3.3			5.2		
<i>C. frigidum</i> live %	-	-	0.3	-	-	-	-	-						
% Uncertainty ±	-	-	2	-	-	-	-	-	1.7			1.9		
<i>C. groenlandica</i> %	-	-	-	-	-	-	-	-						
<i>C. groenlandica</i> live %	-	-	-	-	-	-	-	-						
% Uncertainty ±	-	-	-	-	-	-	-	-						
<i>C. limbata</i> %	-	-	-	-	-	-	-	-	0.3			0.4		
<i>C. limbata</i> live %	-	-	-	-	-	-	-	-						
% Uncertainty ±	-	-	-	-	-	-	-	-	0.5			0.6		
<i>C. microgranulosum</i> %	-	-	1.8	-	-	-	-	-	0.8					
<i>C. microgranulosum</i> live %	-	-	-	-	-	-	-	-						
% Uncertainty ±	-	-	1.1	-	-	-	-	-	0.8					
<i>C. reniforme</i> %	-	-	-	-	-	-	-	-	3.3			2.6		
<i>C. reniforme</i> live %	-	-	-	-	-	-	-	-						
% Uncertainty ±	-	-	-	-	-	-	-	-	1.7			1.4		
<i>C. hallandense</i> % **	-	-	-	-	-	-	-	-						
<i>C. hallandense</i> live %	-	-	-	-	-	-	-	-						
% Uncertainty ±	-	-	-	-	-	-	-	-						
<i>C. tumidum</i> %	-	-	-	-	-	-	-	-						
<i>C. tumidum</i> live %	-	-	-	-	-	-	-	-						
% Uncertainty ±	-	-	-	-	-	-	-	-						

Sample	GS-40	GS-41	GS-42	GS-43	GS-44	GS-45	GS-46 *	GS-47	GS-49	GS-50	GS-52	GS-54	GS-55	GS-56
<i>C. wisnerti</i> %		-	-	-	-	-	-	-	-	-	-	-	-	36
<i>C. wisnerti</i> live %	-	-	-	-	-	-	-	-	-	-	-	-	-	-
% Uncertainty ±		-	-	-	-	-	-	-	-	-	-	-	-	35
<i>Cibicides</i> sp. 1 % **	-	-	-	-	-	-	-	-	-	-	-	-	-	-
<i>Cibicides</i> sp. 1 live %	-	-	-	-	-	-	-	-	-	-	-	-	-	-
% Uncertainty ±	-	-	-	-	-	-	-	-	-	-	-	-	-	-
<i>Cibicides</i> sp. 2 %		-	-	-	-	-	-	0.3	-	-	0.6	-	-	-
<i>Cibicides</i> sp. 2 live %	-	-	-	-	-	-	-	-	-	-	-	-	-	-
% Uncertainty ±	-	-	-	-	-	-	-	0.5	-	-	0.7	-	-	-
<i>Cribrostomoides</i> sp. live %	-	-	-	-	-	-	-	-	-	-	-	-	-	-
<i>Cribrostomoides</i> sp. %	-	-	-	-	-	-	-	-	0.5	-	-	-	-	-
% Uncertainty ±	-	-	-	-	-	-	-	-	1	-	-	-	-	-
<i>D. biserialis</i> % **	-	-	4	-	-	-	-	0.8	-	-	0.8	-	-	-
<i>D. biserialis</i> live %	-	-	0.3	-	-	-	-	-	-	-	-	-	-	-
% Uncertainty ±	-	-	1.6	-	-	-	-	0.8	-	-	0.8	-	-	-
<i>D. compressa</i> % **	-	-	-	2	-	-	-	4	-	-	1.8	-	11.7	38.2
<i>D. compressa</i> live %	-	-	-	-	-	-	-	-	-	-	-	-	0.6	-
% Uncertainty ±	-	-	-	2.2	-	-	-	1.9	-	-	2.5	-	3.5	9.1
<i>Discorbis</i> sp. %	-	-	-	-	-	-	-	-	-	-	-	-	-	-
<i>Discorbis</i> sp. live %	-	-	-	-	-	-	-	-	-	-	-	-	-	-
% Uncertainty ±	-	-	-	-	-	-	-	-	-	-	-	-	-	-
<i>Diss. Criboelphidium</i> % **	-	20	0.2	-	3.5	11	2	-	-	55.7	0.9	-	0.6	-
<i>Diss. Criboelphidium</i> live %	-	3	-	-	-	-	-	-	-	53.2	-	-	-	-
% Uncertainty ±	-	3.5	0.3	-	2.8	6.1	2.7	-	-	6.9	1.7	-	0.9	-
<i>E. advena</i> % **	18.3	6.2	0.2	2.2	7.1	5	3	33.8	0.3	1	2.7	-	43.2	5.5
<i>E. advena</i> live %	-	0.4	-	6.7	0.6	-	-	7	-	0.5	-	-	2.78	-
% Uncertainty ±	3.8	2.1	0.3	6.6	3.9	4.3	3.3	4.6	0.5	1.4	3	-	5.4	4.2
<i>E. crispum</i> %	-	-	0.3	-	-	-	-	-	-	-	-	-	-	-
<i>E. crispum</i> live %	-	-	-	-	-	-	-	-	-	-	-	-	-	-
% Uncertainty ±	-	-	0.5	-	-	-	-	-	-	-	-	-	-	-
<i>E. haruai</i> %	-	-	1.3	-	-	-	-	-	-	-	-	-	-	-
<i>E. haruai</i> live %	-	-	-	-	-	-	-	-	-	-	-	-	-	-
% Uncertainty ±	-	-	0.9	-	-	-	-	-	-	-	-	-	-	-
<i>E. pacifica</i> % **	-	-	4	-	-	-	-	-	1	-	-	0.2	-	-
<i>E. pacifica</i> live %	-	-	-	-	-	-	-	-	-	-	-	-	-	-
% Uncertainty ±	-	-	1.6	-	-	-	-	-	1	-	-	0.4	-	-
<i>E. vitrea</i> % **	-	-	4.7	-	-	-	-	-	0.8	-	-	2.8	-	-
<i>E. vitrea</i> live %	-	-	-	-	-	-	-	-	-	-	-	-	-	-
% Uncertainty ±	-	-	1.7	-	-	-	-	-	0.8	-	-	1.4	-	-

Sample	GS-40	GS-41	GS-42	GS-43	GS-44	GS-45	GS-46 *	47	GS-49	GS-50	GS-52	GS-54	GS-55	GS-56
<i>F lucida</i> %	-	-	-	-	-	-	-	-	0.8					
<i>F lucida</i> live %	-	-	-	-	-	-	-	-						
% Uncertainty ±	-	-	-	-	-	-	-	-	0.8					
<i>F marginata</i> %	-	-	-	-	-	-	-	-	0.3					
<i>F marginata</i> live %	-	-	-	-	-	-	-	-						
% Uncertainty ±	-	-	-	-	-	-	-	-	0.5					
<i>F melo</i> %	-	-	1.2	-	-	-	-	-						
<i>F melo</i> live %	-	-	-	-	-	-	-	-						
% Uncertainty ±	-	-	0.9	-	-	-	-	-						
<i>F vitreola</i> %	-	-	-	-	-	-	-	-	3.3					
<i>F vitreola</i> live %	-	-	-	-	-	-	-	-						
% Uncertainty ±	-	-	-	-	-	-	-	-	1.7					
<i>H borealis</i> live %	-	-	-	-	-	-	-	-						
<i>H borealis</i> %	-	-	-	-	-	-	-	-						
% Uncertainty ±	-	-	-	-	-	-	-	-						
<i>H canariensis</i> % **	-	-	-	-	-	-	-	-			0.9		0.9	0.9
<i>H canariensis</i> live %	-	-	-	-	-	-	-	-						
% Uncertainty ±	-	-	-	-	-	-	-	-			1.7		1	1.8
<i>H columbiensis</i> % **	5.8	1.2	-	2	1.2	4	2	6.7			5.4	0.4		
<i>H columbiensis</i> live %	-	-	-	2	-	-	-	-						
% Uncertainty ±	2.3	1	-	2.2	1.6	3.8	2.7	2.4			4.2	0.6		
<i>H friabilis</i> %	-	-	-	-	-	-	-	-						
<i>H friabilis</i> live %	-	-	-	-	-	-	-	-						
% Uncertainty ±	-	-	-	-	-	-	-	-						
<i>H gracile</i> %	-	-	-	-	-	-	-	-						
<i>H gracile</i> live %	-	-	-	-	-	-	-	-						
% Uncertainty ±	-	-	-	-	-	-	-	-						
<i>H tenuum</i> %	-	-	-	-	-	-	-	-						
<i>H tenuum</i> live %	-	-	-	-	-	-	-	-						
% Uncertainty ±	-	-	-	-	-	-	-	-						
<i>Haplophragmoides</i> sp %	4.8	-	-	-	-	-	-	-						
<i>Haplophragmoides</i> sp live %	-	-	-	-	-	-	-	-						
% Uncertainty ±	2.1	-	-	-	-	-	-	-						
<i>I norcrossi</i> %	-	-	-	-	-	-	-	-						
<i>I norcrossi</i> live %	-	-	-	-	-	-	-	-						
% Uncertainty ±	-	-	-	-	-	-	-	-						
<i>L. castella</i> % **	5	18.2	-	10	34.1	44	65	18.2	0.8		17.9	5	2.5	
<i>L. castella</i> live %	-	-	-	-	0.6	-	-	-						
% Uncertainty ±	2.1	3.4	-	4.8	7.1	9.7	9.3	3.8	0.8		7.1	1.9	1.7	

Sample	GS-40	GS-41	GS-42	GS-43	GS-44	GS-45	GS-46 *	GS-47	GS-49	GS-50	GS-52	GS-54	GS-55	GS-56
<i>L. dorseyae</i> %	-	-	-	-	-	-	-	-	-	-	-	-	-	-
<i>L. dorseyae</i> live %	-	-	-	-	-	-	-	-	-	-	-	-	-	-
% Uncertainty ±	-	-	-	-	-	-	-	-	-	-	-	-	-	-
<i>L. fletcheri</i> % **	-	-	52	-	-	-	-	-	138	-	-	08	-	-
<i>L. fletcheri</i> live %	-	-	-	-	-	-	-	-	-	-	-	-	-	-
% Uncertainty ±	-	-	18	-	-	-	-	-	34	-	-	08	-	-
<i>L. laevis</i> %	-	-	-	-	-	-	-	-	-	-	-	-	-	-
<i>L. laevis</i> live %	-	-	-	-	-	-	-	-	-	-	-	-	-	-
% Uncertainty ±	-	-	-	-	-	-	-	-	-	-	-	-	-	-
<i>L. mckannai</i> %	-	-	08	-	-	-	-	-	-	-	-	06	-	-
<i>L. mckannai</i> live %	-	-	-	-	-	-	-	-	-	-	-	-	-	-
% Uncertainty ±	-	-	07	-	-	-	-	-	-	-	-	07	-	-
<i>L. sulcata</i> %	-	-	-	-	-	-	-	-	-	-	-	-	-	-
<i>L. sulcata</i> live %	-	-	-	-	-	-	-	-	-	-	-	-	-	-
% Uncertainty ±	-	-	-	-	-	-	-	-	-	-	-	-	-	-
<i>Lagena</i> sp 1 %	-	-	03	-	-	-	-	-	-	-	-	-	-	-
<i>Lagena</i> sp 1 live %	-	-	-	-	-	-	-	-	-	-	-	-	-	-
% Uncertainty ±	-	-	05	-	-	-	-	-	-	-	-	-	-	-
<i>Lagena</i> sp 2 live %	-	-	-	-	-	-	-	-	-	-	-	-	-	-
<i>Lagena</i> sp 2 %	-	-	03	-	-	-	-	-	-	-	-	-	-	-
% Uncertainty ±	-	-	05	-	-	-	-	-	-	-	-	-	-	-
<i>M. fusca</i> % **	-	06	-	-	18	-	3	12	-	1	-	02	136	327
<i>M. fusca</i> live %	-	02	-	-	-	-	-	-	-	-	-	-	-	-
% Uncertainty ±	-	07	-	-	2	-	33	11	-	14	-	04	37	88
<i>M. subrotunda</i> %	-	-	-	-	-	-	-	-	05	-	-	1	-	-
<i>M. subrotunda</i> live %	-	-	-	-	-	-	-	-	-	-	-	-	-	-
% Uncertainty ±	-	-	-	-	-	-	-	-	07	-	-	09	-	-
<i>N. auricula</i> % **	-	-	58	-	-	-	-	-	-	-	-	12	-	-
<i>N. auricula</i> live %	-	-	-	-	-	-	-	-	-	-	-	-	-	-
% Uncertainty ±	-	-	10	-	-	-	-	-	-	-	-	1	-	-
<i>N. emphysoecista</i> live %	-	-	-	-	-	-	-	-	-	-	-	-	-	-
<i>N. emphysoecista</i> %	-	-	-	-	-	-	-	-	1	-	-	-	-	-
% Uncertainty ±	-	-	-	-	-	-	-	-	1	-	-	-	-	-
<i>N. labradorica</i> %	-	-	-	-	-	-	-	-	05	-	-	02	-	-
<i>N. labradorica</i> live %	-	-	-	-	-	-	-	-	-	-	-	-	-	-
% Uncertainty ±	-	-	-	-	-	-	-	-	07	-	-	04	-	-
<i>N. stella</i> %	-	-	-	-	-	-	-	-	08	-	-	26	-	-
<i>N. stella</i> live %	-	-	-	-	-	-	-	-	-	-	-	-	-	-
% Uncertainty ±	-	-	-	-	-	-	-	-	08	-	-	14	-	-

Sample	GS-40	GS-41	GS-42	GS-43	GS-44	GS-45	GS-46*	GS-47	GS-49	GS-50	GS-52	GS-54	GS-55	GS-56
<i>N. turgida</i> %	-	-	1.7	-	-	-	-	-	-	-	-	-	-	-
<i>N. turgida</i> live %	-	-	-	-	-	-	-	-	-	-	-	-	-	-
% Uncertainty ±	-	-	1	-	-	-	-	-	-	-	-	-	-	-
<i>P. bassispinata</i> %	-	-	-	-	-	-	-	-	-	-	-	-	-	-
<i>P. bassispinata</i> live %	-	-	-	-	-	-	-	-	-	-	-	-	-	-
% Uncertainty ±	-	-	-	-	-	-	-	-	-	-	-	-	-	-
<i>P. hispidum</i> %	-	-	-	-	-	-	-	-	0.8	-	-	0.2	-	-
<i>P. hispidum</i> live %	-	-	-	-	-	-	-	-	-	-	-	-	-	-
% Uncertainty ±	-	-	-	-	-	-	-	-	0.8	-	-	0.4	-	-
<i>P. wiesneri</i> %	-	-	-	-	-	-	-	-	1.5	-	-	-	-	-
<i>P. wiesneri</i> live %	-	-	-	-	-	-	-	-	-	-	-	-	-	-
% Uncertainty ±	-	-	-	-	-	-	-	-	1.2	-	-	-	-	-
<i>Procerolagena</i> sp. %	-	-	-	-	-	-	-	-	0.5	-	-	-	-	-
<i>Procerolagena</i> sp. live %	-	-	-	-	-	-	-	-	-	-	-	-	-	-
% Uncertainty ±	-	-	-	-	-	-	-	-	0.7	-	-	-	-	-
<i>Q. artica</i> %	-	-	0.3	-	-	-	-	-	-	-	-	-	-	-
<i>Q. artica</i> live %	-	-	-	-	-	-	-	-	-	-	-	-	-	-
% Uncertainty ±	-	-	0.5	-	-	-	-	-	-	-	-	-	-	-
<i>Q. semirula</i> %	-	-	0.3	-	-	-	-	-	0.3	-	-	0.6	-	-
<i>Q. semirula</i> live %	-	-	-	-	-	-	-	-	-	-	-	-	-	-
% Uncertainty ±	-	-	0.5	-	-	-	-	-	0.5	-	-	0.7	-	-
<i>Quinqueloculina</i> sp. %**	-	-	1.2	-	-	-	-	-	-	23.9	-	4.2	-	-
<i>Quinqueloculina</i> sp. live %	-	-	0.3	-	-	-	-	-	-	20	-	-	-	-
% Uncertainty ±	-	-	0.9	-	-	-	-	-	-	5.9	-	1.8	-	-
<i>R. columbiensis</i> %	-	-	-	-	-	-	-	-	1	-	-	-	-	-
<i>R. columbiensis</i> live %	-	-	-	-	-	-	-	-	-	-	-	-	-	-
% Uncertainty ±	-	-	-	-	-	-	-	-	1	-	-	-	-	-
<i>R. curtus</i> %	-	0.4	-	-	-	-	-	-	-	-	-	-	0.9	1.8
<i>R. curtus</i> live %	-	-	-	-	-	-	-	-	-	-	-	-	-	-
% Uncertainty ±	-	0.6	-	-	-	-	-	-	-	-	-	-	1	2.5
<i>R. gracile</i> %	-	-	-	-	-	-	-	-	-	-	-	-	-	-
<i>R. gracile</i> live %	-	-	-	-	-	-	-	-	-	-	-	-	-	-
% Uncertainty ±	-	-	-	-	-	-	-	-	-	-	-	-	-	-
<i>R. scorpiurus</i> %**	0.3	0.2	-	2	-	-	-	-	1	-	5.4	0.4	2.2	1.8
<i>R. scorpiurus</i> live %	-	0.2	-	-	-	-	-	-	-	-	-	-	-	-
% Uncertainty ±	0.5	0.4	-	2.2	-	-	-	-	1	-	4.2	0.6	1.6	2.5
<i>S. arctica</i> live %	-	-	-	-	-	-	-	-	-	-	-	-	-	-
<i>S. arctica</i> %	0.3	0.2	-	1.3	-	-	-	-	0.7	0.5	-	0.2	-	-
% Uncertainty ±	0.5	0.4	-	1.8	-	-	-	-	0.8	1	-	0.4	-	-

Sample	GS-40	GS-41	GS-42	GS-43	GS-44	GS-45	GS-46 *	GS-47	GS-49	GS-50	GS-52	GS-54	GS-55	GS-56
<i>S. atlantica</i> %	-	-	-	-	-	-	-	-	-	-	-	-	-	-
<i>S. atlantica</i> live %	-	-	-	-	-	-	-	-	-	-	-	-	-	-
% Uncertainty ±	-	-	-	-	-	-	-	-	-	-	-	-	-	-
<i>S. biformis</i> % **	37.5	22.4	-	18	21.2	13	12	62	0.3	-	13.4	18	12	4.5
<i>S. biformis</i> live %	-	0.6	-	5.3	-	-	-	-	-	-	3.6	-	0.9	-
% Uncertainty ±	4.7	3.7	-	6.1	6.1	6.6	6.4	2.4	0.5	-	6.3	1.2	3.5	3.9
<i>S. cf atlantica</i> % **	2	0.4	-	-	0.6	-	1	3	-	-	0.9	0.2	-	4.5
<i>S. cf atlantica</i> live %	-	-	-	-	-	-	-	-	-	-	-	-	-	0.9
% Uncertainty ±	1.4	0.6	-	-	1.1	-	2	1.7	-	-	1.7	0.4	-	3.9
<i>S. feylingsi</i> % **	-	-	-	-	-	-	-	-	15.8	-	-	25.1	-	-
<i>S. feylingsi</i> live %	-	-	-	-	-	-	-	-	-	-	-	-	-	-
% Uncertainty ±	-	-	-	-	-	-	-	-	3.6	-	-	3.8	-	-
<i>S. sphaerica</i> %	-	-	-	-	-	-	-	-	-	-	-	-	-	-
<i>S. sphaerica</i> live %	-	-	-	-	-	-	-	-	-	-	-	-	-	-
% Uncertainty ±	-	-	-	-	-	-	-	-	-	-	-	-	-	-
<i>S. stalkeri</i> %	-	-	-	-	-	-	-	-	-	-	-	1.6	-	-
<i>S. stalkeri</i> live %	-	-	-	-	-	-	-	-	-	-	-	-	-	-
% Uncertainty ±	-	-	-	-	-	-	-	-	-	-	-	1.1	-	-
<i>S. tenuis</i> %	-	-	-	-	-	-	-	-	-	-	-	-	-	-
<i>S. tenuis</i> live %	-	-	-	-	-	-	-	-	-	-	-	-	-	-
% Uncertainty ±	-	-	-	-	-	-	-	-	-	-	-	-	-	-
<i>T. charlottensis</i> % **	1.5	-	-	-	-	-	2	1.5	-	-	8	-	-	-
<i>T. charlottensis</i> live %	-	-	-	-	-	-	-	-	-	-	-	-	-	-
% Uncertainty ±	1.2	-	-	-	-	-	2.7	1.2	-	-	5	-	-	-
<i>T. discobis</i> % **	-	0.6	-	2	0.6	-	-	2	-	-	7.1	0.8	0.3	-
<i>T. discobis</i> live %	-	0.6	-	2	-	-	-	-	-	-	2.7	-	-	-
% Uncertainty ±	-	0.7	-	2.2	1.1	-	-	1.4	-	-	4.8	0.8	0.6	-
<i>T. earlandi</i> %	-	1.2	0.2	1.3	1.8	-	-	0.2	-	-	-	0.4	0.6	-
<i>T. earlandi</i> live %	-	-	-	-	-	-	-	-	-	-	-	-	-	-
% Uncertainty ±	-	1	0.3	1.8	2	-	-	0.5	-	-	-	0.6	0.9	-
<i>T. inflata</i> %	-	-	-	-	-	-	-	-	-	-	-	-	0.3	5.5
<i>T. inflata</i> live %	-	-	-	-	-	-	-	-	-	-	-	-	-	-
% Uncertainty ±	-	-	-	-	-	-	-	-	-	-	-	-	0.6	4.2
<i>T. cf rotalisformis</i> % **	-	1.6	-	-	2.4	3	-	1	-	-	7.1	-	0.9	-
<i>T. cf rotalisformis</i> live %	-	-	-	-	-	-	-	-	-	-	-	-	-	-
% Uncertainty ±	-	1.1	-	-	2.3	3.3	-	1	-	-	4.8	-	1	-
<i>T. rotalisformis</i> % **	7.3	9.2	0.8	12.7	14.1	18	5	13.4	1.5	3.5	5.4	1.8	3.1	-
<i>T. rotalisformis</i> live %	-	-	-	1.3	-	-	-	-	-	2.5	-	-	-	-
% Uncertainty ±	2.5	2.5	0.7	5.3	5.2	7.5	4.3	3.3	1.2	2.5	4.2	1.2	1.9	-

[illegible]

CHAPTER 3. Paleoseismic evidence in late Holocene sediments, Saanich Inlet, British Columbia.

ABSTRACT

Eight piston cores of sediment spanning the last 1500 years were collected from Saanich Inlet, an intermittently anoxic fiord on southern Vancouver Island, to obtain information on sedimentation and prehistoric earthquake activity. The cores consist mainly of fine-grained varved sediments and massive beds deposited by subaqueous debris flows. The debris flows may have been triggered by earthquakes or by the build-up of fine sediment on the walls of the inlet. Cesium-137 and ^{210}Pb data, ^{14}C ages, and varve counts were used to date and correlate massive layers in the eight cores. The uppermost massive layer in two cores may record a magnitude 7.2 earthquake in 1946 near Comox, B.C., 200 km north-northwest of Saanich Inlet. Five older layers are found in two or more cores and are about 200, 550, 800-850, 1050-1100, 1100-1150 years old. Two or three of these can be correlated with previously documented earthquakes in the region. There is an average of one massive layer per 116 varves (range of 15-336) in the core with the greatest number of such layers. This is broadly consistent with the expected periodicity of moderate to large earthquakes in the region (on average, one earthquake of local Modified Mercalli Intensity VII or VIII per 100 years). Saanich Inlet may contain a proxy record of all moderate and large earthquakes that have affected southwestern British Columbia during Holocene time, but the set of massive layers likely includes both seismically and nonseismically generated deposits.

INTRODUCTION

Southwestern British Columbia is one of the most tectonically active areas in Canada, and as a result, there is concern that a moderate to large earthquake may extensively damage the cities and economic infrastructure of the region. Seismic activity is related to subduction of the oceanic Juan de Fuca plate beneath the continental North America plate along the Cascadia subduction zone (Riddihough and Hyndman, 1976; Fig. 3-1). The Juan de Fuca and Explorer plates are young (6-9 Ma and <6 Ma, respectively), thin (<30 km), hot, and buoyant (Rogers, 1988). Geodetic evidence (Savage and others, 1991; Dragert and others, 1994) and heat-flow modelling (Hyndman and Wang, 1993) indicate that the boundary between these oceanic plates and the North America plate is presently locked and is accumulating strain. Eventually the boundary may rupture, releasing the accumulated strain energy in a megathrust earthquake ($M_w \geq 8$)¹, with potentially catastrophic consequences (Clague and Bobrowsky, 1993).

Two other types of earthquakes also occur in southwestern British Columbia. The most common are earthquakes originating within the North America plate, generally at depths of 10-30 km (Rogers, 1992). At the leading edge of the North America plate, heat flow through the upper crust is low because the subducting oceanic plate absorbs much of the heat flowing upward from the Earth's interior. As a consequence, there is a thickened section of crust cool enough to permit brittle fracture causing earthquakes (Rogers, 1992). Four large crustal earthquakes have

¹ Also referred to as a plate-boundary or subduction earthquake.

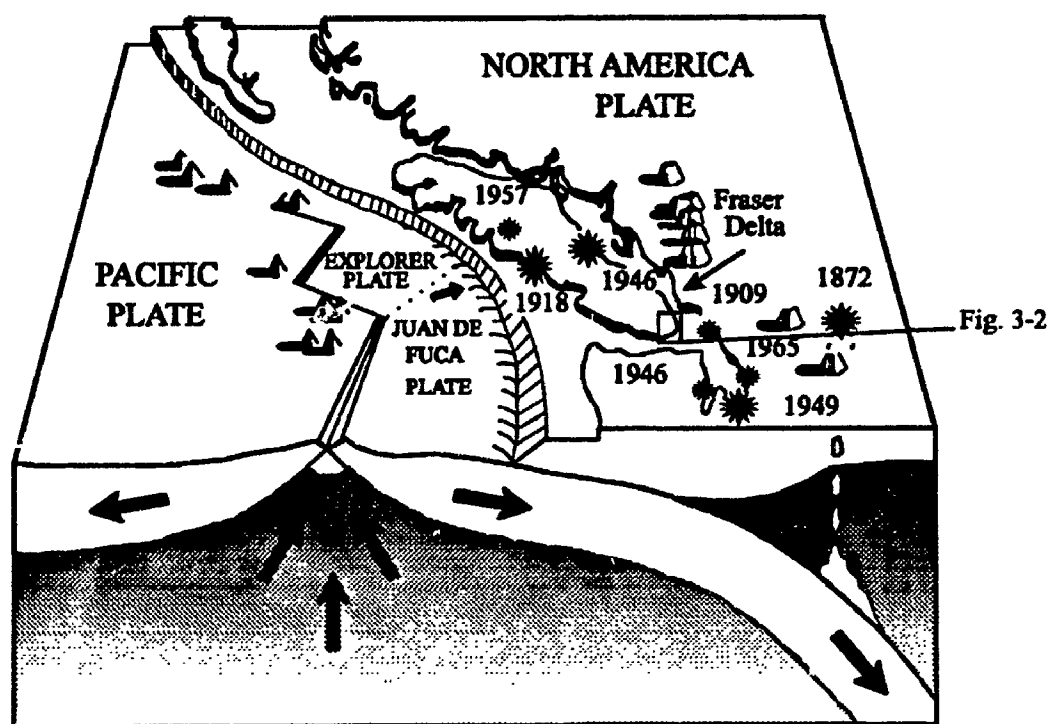


Figure 3-1. Schematic diagram showing subduction of the oceanic Juan de Fuca plate beneath North America, and epicentres of large historic earthquakes that have affected southwestern British Columbia and northwestern Washington. The two plates are locked and accumulating strain, which will eventually be released in a large earthquake (modified from an Energy, Mines and Resources Canada illustration).

affected the region in historic time, in 1918 ($M=7$) and 1946 ($M=7.2$) on Vancouver Island, in 1872 ($M=7.4$) probably near Lake Chelan in northern Washington, and near Seattle and Tacoma ($M \sim 7.0$; Rogers, 1994). Three of the four earthquakes occurred away from the southern Strait of Georgia-Puget Sound area, where most small and moderate earthquakes are concentrated.

Earthquakes also occur at depths of up to about 80 km within the Juan de Fuca plate. These subcrustal earthquakes are concentrated in two regions -beneath Vancouver Island where the descending plate bends from horizontal to $10-20^\circ$, and beneath the Strait of Georgia where the plate bends further to about 30° . The seismicity is also concentrated between latitudes 47° N and 49.5° N, continuing at a much lower rate to the north and south. This is likely due to arching of the subducting plate to accommodate the bend in the coastline in this region (Crosson and Owens, 1987).

A major problem in assessing seismic risk in southwestern British Columbia is that the historical period, during which earthquakes have been instrumentally recorded, is very short (ca. 100 years; Rogers, 1988). Geologic studies can be useful in extending this short record and thus may provide better estimates of earthquake recurrence and magnitude. Several different types of geologic evidence have been found for past large earthquakes in southwestern British Columbia and northern Washington. These include: (1) stratigraphic indicators of sudden land-level changes and tsunamis, i.e. buried marsh soils capped, in some cases, by sheets of sand and gravel (Atwater, 1987, 1992; Darienzo and Peterson, 1990; Atwater and Moore,

1992; Clague and Bobrowsky 1994a, b; Clague and others, 1994; Mathewes and Clague, 1994); (2) sand dykes and sand blows produced by coseismic liquefaction (Clague and others, 1992; Obermeier, in press); and (3) seismically triggered landslides (Adams, 1990; Jacoby and others, 1992; Karlin and Abella, 1992; Schuster and others, 1992).

A limitation of most paleoseismological studies is that the timing of events cannot be precisely established because of reliance on radiocarbon dating. Even using well constrained, high resolution radiocarbon ages, temporal resolution is at best ± 20 years. In some cases, however, sediments with high temporal resolution, such as varves, can be used to more precisely date past events, including earthquakes. Varves are annual deposits which are best preserved in anoxic marine basins and inlets, and in some glacial and nonglacial lakes.

Saanich Inlet on southern Vancouver Island (Fig. 3-2) was chosen as a site for a paleoseismicity study because the thick Holocene sediments in the central part of the fiord are varved and thus have the potential for providing annual resolution for events such as earthquakes. In addition, massive silty clay layers, which may have been emplaced by sediment gravity flows triggered by earthquakes are present within the varved sequence (Bobrowsky and Clague, 1990; Blais, 1992; Blais and others, 1993).

The objectives of this study were fourfold: (1) to determine the source and age of the sediments in the central part of Saanich Inlet; (2) to ascertain whether the massive silty clay layers are indeed sediment gravity flow deposits; (3) to determine whether the massive layers are products of earthquakes, and (4) to attempt to use

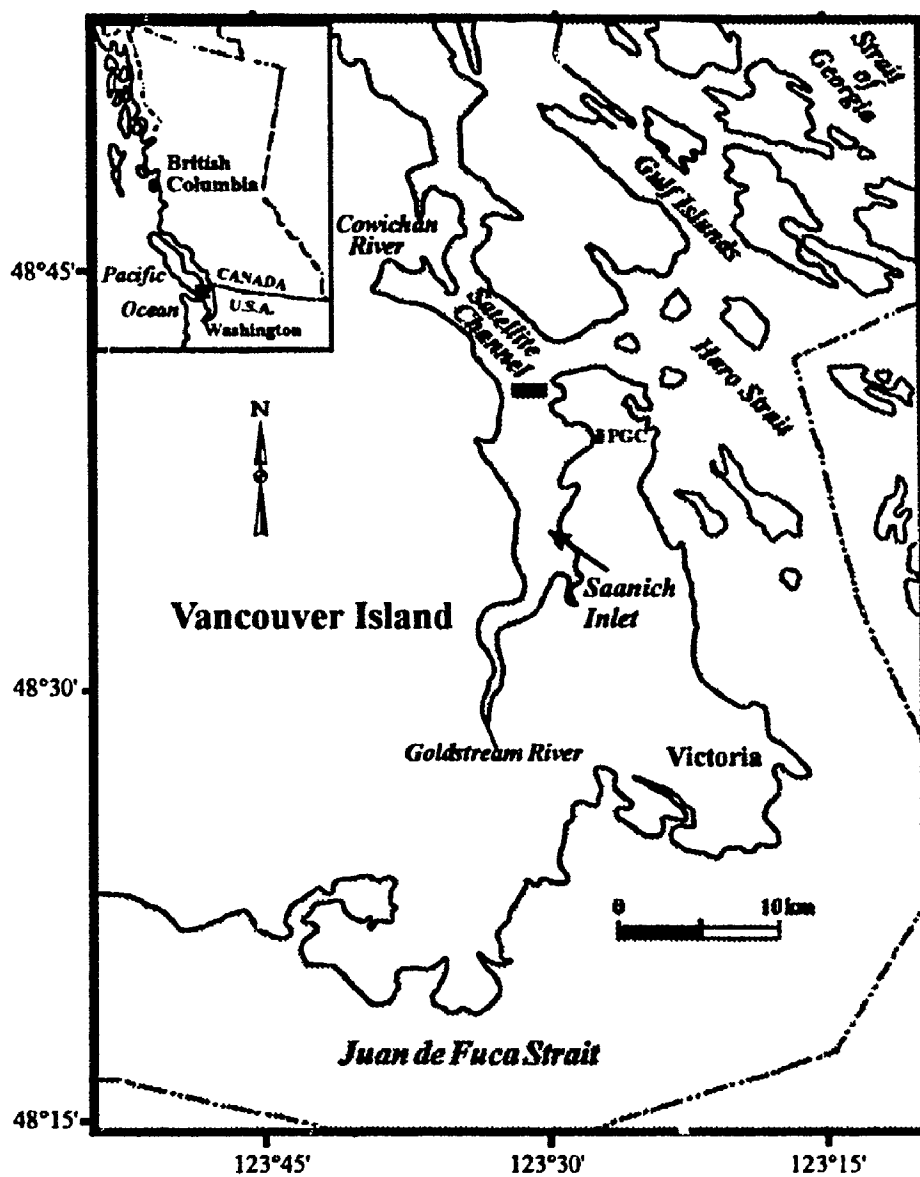


Figure 3-2. Location map, Saanich Inlet, British Columbia. The shaded box locates the bedrock sill at the north end of the inlet. PGC=Pacific Geoscience Centre.

varves as a precise dating tool.

STUDY AREA

Saanich Inlet (Fig. 3-2) is 26 km long, up to 8 km wide, and has average and maximum depths of 120 m and 236 m, respectively. It is indented by five bays into which small ephemeral streams flow. The only significant stream is Goldstream River at the south end of the inlet, and it contributes only a small percentage of the 9×10^4 tonnes of sediment that accumulates in Saanich Inlet each year (Gross and others, 1963). In this respect, Saanich Inlet differs from most other fiords in British Columbia which have large inputs of freshwater and sediment at their heads (Herlinveaux, 1962).

Plumes of clay- and silt-size sediment from Cowichan River enter Saanich Inlet from the northwest (Fig. 3-2) during periods of high discharge, commonly in the fall and winter (Herlinveaux, 1962). Another possible source of terrigenous sediment is Fraser River, which is the largest river in the region. Although it has not been proven that Fraser River sediment enters Saanich Inlet, some satellite images show a turbid plume extending westward from the mouth of the river across the Strait of Georgia towards the Gulf Islands (e.g., RadarSat Images 02020-212, 02020-5538, 02020-7575; May 13, July 16, and August 17, 1992, respectively).

A bedrock sill at 70 m depth at the mouth of the inlet (Figs. 3-2 and 3-3) restricts water circulation, creating anoxic conditions below depths of 70-150 m (Carter, 1934; Gross and others, 1963). In late summer or fall, dense cold water

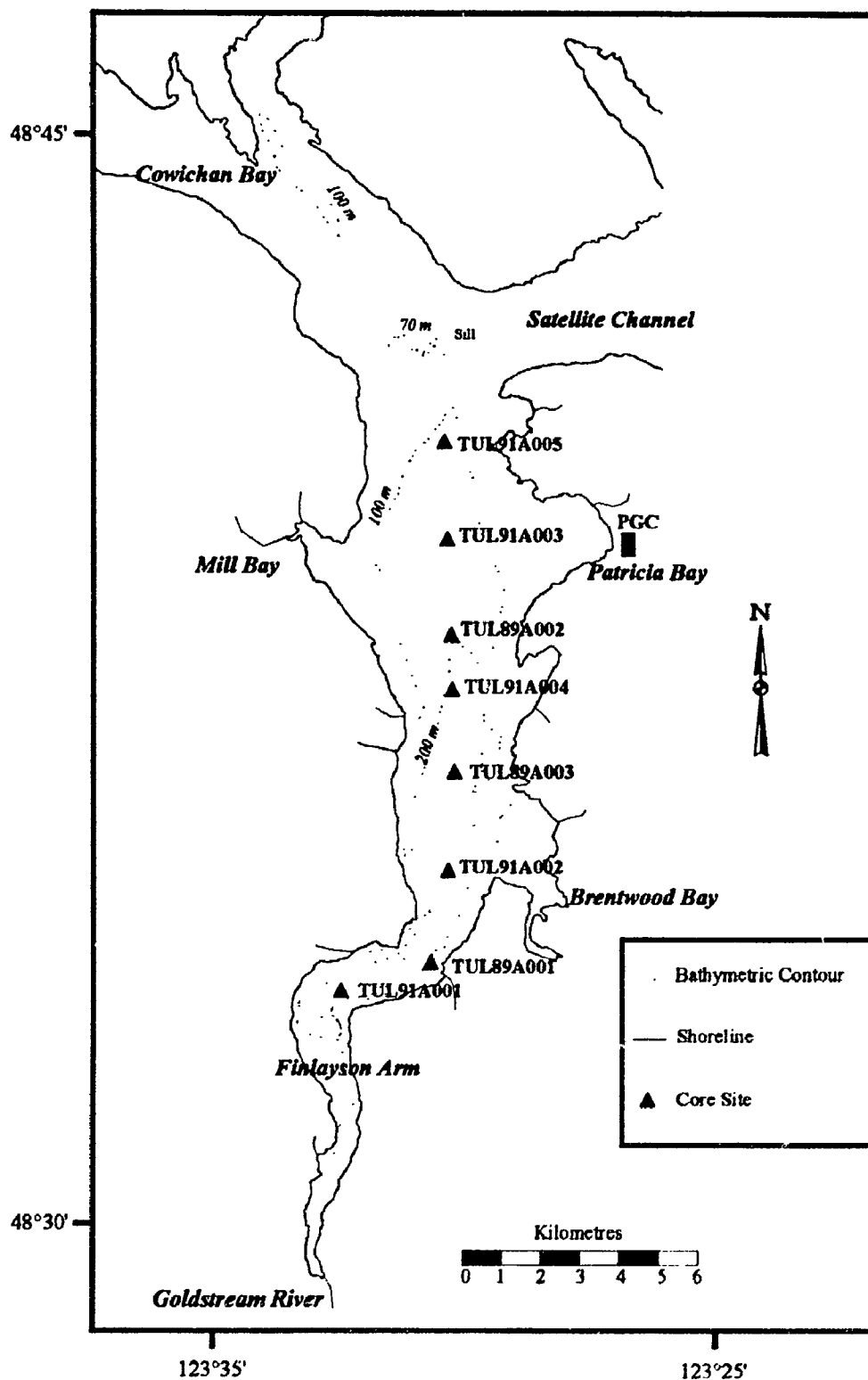


Figure 3-3. Map of Saanich Inlet showing core sites.

enters the inlet from Haro Strait. This water flushes the upper part of the anoxic zone and increases the amount of dissolved oxygen in the inlet (Herlinveaux, 1962; Anderson and Devol, 1973; Stucchi and Giovando, 1984). The amount of flushing differs from year to year, and, as a result, the thickness of the anoxic layer is highly variable (Anderson and Devol, 1973) and sometimes does not take place (Stucchi and Giovando, 1984). Flushing rates are thought to be high and residence times short (Stucchi and Giovando, 1984; EnviroEd Consultants Ltd., 1995). Due to the short residence time and low concentrations of oxygen (Herlinveaux, 1962), conditions below 150 m depth are considered anoxic.

There are three main types of sediment in Saanich Inlet (Fig. 3-4; Gucluer and Gross, 1964): (1) silt on the sill at the mouth of the inlet; (2) poorly- to moderately-sorted fine sand in nearshore environments; and (3) diatomaceous silty clay in deep water. The last group of sediments, which is of particular interest in this study, consists primarily of alternating laminae of terrigenous silty clay deposited during fall and spring freshets and diatoms deposited during spring and summer blooms. Individual couplets have been shown to be annual deposits and thus may be termed varves (Sancetta and Calvert, 1988; Sancetta, 1989). Because anoxic conditions exist at the sediment-water interface in deep water in the central part of the inlet, epifauna and infauna are absent, and there is no bioturbation that would otherwise destroy stratification.

The sill not only inhibits water circulation but also "prevents the introduction of any coarse-grained sediments that might enter as turbidity currents along the

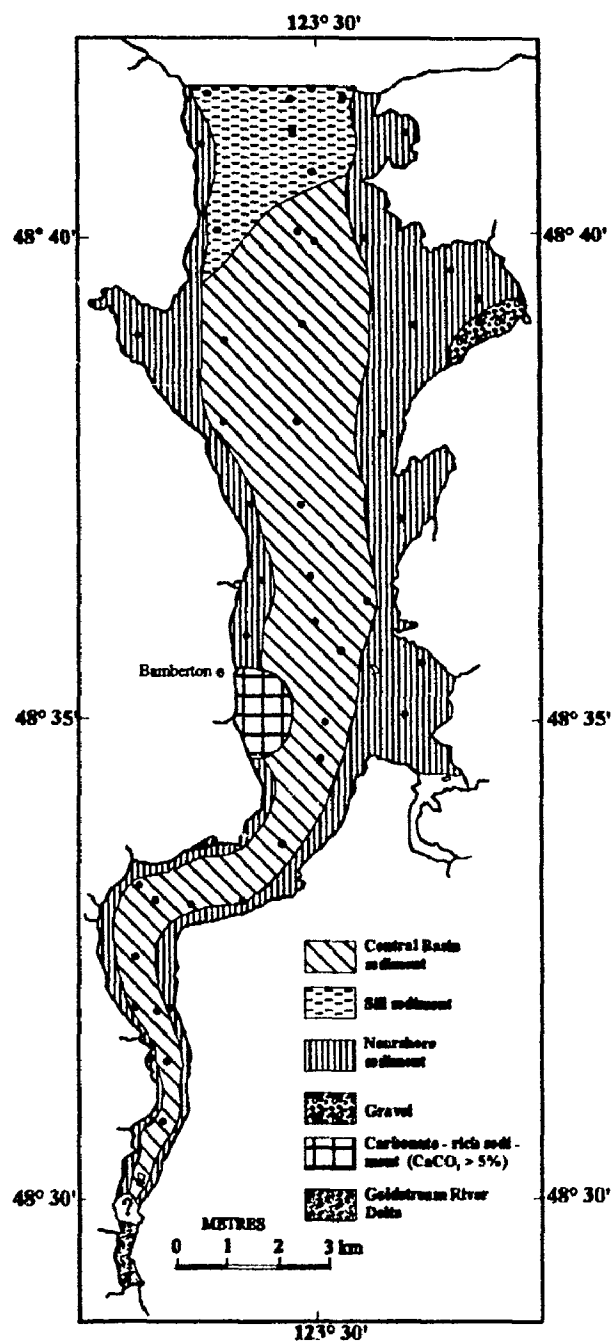


Figure 3-4. Surface sediment samples (black dots) and distribution of sediment types in Saanich Inlet. Central Basin sediment= silt and clay with abundant diatom frustules. Sill sediment= silt. Nearshore sediment= poorly sorted, fine sand and some gravel. Carbonate-rich sediment= near limestone quarry in Bamerton. (Modified from G. J. J. J. and Gross, 1964).

bottom of Satellite Channel" from Cowichan River or possibly Fraser River (Gucluer and Gross, 1964, p. 373). Suspension, therefore, is the main mode of sediment transport in the inlet. This explains why sediments along the axis of the basin are finer than those along bordering slopes and on the sill (Fig. 3-4; Gucluer and Gross, 1964). However, if suspension is the main mode of sediment transport, what is the origin of the massive layers observed in the varved sequence?

PREVIOUS WORK

Previous oceanographic, geochemical, and sedimentological work in Saanich Inlet provided a foundation and a point of departure for this study. The first baseline oceanographic data were presented by Herlinveaux (1962). Anderson and Devol (1973) extended this work by documenting and explaining the flushing events that affect the fiord.

Numerous geochemical studies have been conducted on Saanich Inlet waters (e.g., Brown and others, 1972; Devol and others, 1984; Hamilton and Hedges, 1988; Kuivila and others, 1990) and sediments (e.g., Matsumoto and Wong, 1977; Bornhold, 1978; Carpenter and Beasley, 1981; Devol and Ahmed, 1981; Powys, 1987; François, 1988; Anderson and others, 1989; Cowie and others, 1992). Most of these studies address issues beyond the scope of this paper, with the exception of those in which ^{210}Pb data were used to date the upper parts of sediment cores. For example, from ^{210}Pb analyses on sediment cores collected in the central part of the

basin, Matsumoto and Wong (1977) established that sedimentation fluxes² were higher at the north end of the inlet ($0.27 \text{ g cm}^{-2} \text{ y}^{-1}$) than at the south end ($0.093 \text{ g cm}^{-2} \text{ y}^{-1}$).

Gucluer (1962), Gross and others (1963), Gucluer and Gross (1964), Buddemeier (1969), and Powys (1987) studied the physical properties of Saanich Inlet sediments and postulated that the rhythmically laminated deposits in the deeper parts of the fiord were varves. Sancetta and Calvert (1988) and Sancetta (1989) confirmed this by documenting seasonal changes in diatom assemblages within individual couplets.

Heusser (1983) conducted a palynological study of sediment cores from Saanich Inlet. The resulting climatic and vegetation reconstructions complemented those made elsewhere in southwestern British Columbia (Mathewes, 1985).

Most attempts to obtain good seismic images of the subbottom in Saanich Inlet have been thwarted by the presence of interstitial gas in the sediments: -The gas scatters and attenuates the seismic energy from penetrating into the sediment column. Lister (1967), however, obtained seismic records that showed the Holocene fill in the central part of the fiord to be more than 55 m thick.

Heightened awareness of the earthquake hazard in southwestern British Columbia in the 1980s stimulated stratigraphic and sedimentological studies in Saanich Inlet that were aimed at providing paleoseismic information. Bobrowsky and Clague (1990), for example, suggested that massive layers within the varved succession were deposited by sediment gravity flows triggered by large earthquakes. Blais (1992),

²Called sedimentation rates in Matsumoto and Wong (1977).

Blais and others (1993), and this paper expand on this early work.

METHODS AND MATERIALS

Eight 10-cm diameter cores, ranging in length from 8.85 m to 11.91 m, were collected in 1989 and 1991 aboard the CSS Tully with a piston corer (Fig. 3-3). The cores were collected along the axis of Saanich Inlet at water depths ranging from 168 to 227 m (Table 3-1) using a Magnavox MX1102 GPS (Global Positioning System) for navigation. The amount of freefall of the trigger (pilot) core was reduced during the 1991 coring operation in an effort to recover the uppermost water-rich sediments that appear to have been lost during 1989. Cores were collected in standard CAB (cellulose acetate butyrate) tubes which fit inside the metal core barrel. Some disturbance of the cores occurred as they were recovered due to the escape of gas from the sediments. Expansion of the gas upon core retrieval resulted in the formation of horizontal and subhorizontal cracks between laminae.

Each core was cut into approximately 1.5 m lengths and later split and stored in a cold room at the Pacific Geoscience Centre (PGC). The split cores were photographed and described in detail (colour, unit thickness, contacts, structures, fossils).

Subsamples were analyzed for particle-size distribution and clay mineralogy to detect possible textural and compositional differences between varved and massive units. Grain size analyses were performed at PGC using a Micromeritic SediGraph 5100. Clay mineral analyses were conducted on the $<2\mu\text{m}$ fraction of subsamples.

Table 3-1. Location, depth, and length of piston cores

Core	Latitude N	Longitude W	Core depth (m)	Core length (cm)
TUL89A001	48° 33.73'	123° 30.45'	227	885
TUL89A002	48° 38.41'	123° 30.17'	198	1178
TUL89A003	48° 36.10'	123° 30.00'	227	1180
TUL91A001	48° 33.21'	123° 32.07'	220	1191
TUL91A002	48° 34.94'	123° 30.23'	228	1155
TUL91A003	48° 39.63'	123° 30.19'	176	1161
TUL91A004	48° 37.21'	123° 30.11'	214	1030
TUL91A005	48° 40.74'	123° 30.22'	168	945

Clay extractions were carried out at PGC according to the method outlined by Holtzapffel (1985). Dried clay pastes were analyzed with a Phillips 1710 X-ray diffractometer at the Geological Survey of Canada in Ottawa (GSC). The relative abundance of each clay mineral species was determined from peak heights on diffractograms.

Subsamples were also collected for foraminiferal analysis. Each subsample was washed on a 63 μm screen; residues were transferred to vials, immersed in a formalin solution, and examined with an Olympus (Model 219142) binocular microscope (see Chapter 2 or Blais and Patterson, in press, for identification keys). All foraminifera in each sample were counted; no sample contained more than 14 specimens. A cellulose tape peel of a freeze core containing a massive layer and over 40 varves (collected by C. Sancetta in 1989) also was examined for foraminifera.

Shells, wood fragments, and other plant material extracted from the cores were radiocarbon dated at IsoTrace Laboratory (University of Toronto). Approximate calendric ages were calculated from the radiocarbon ages using the calibration method of Stuiver and Reimer (1993). A reservoir age correction of 801 ± 23 years was applied to marine shell age determinations (Robinson and Thomson, 1981; Stuiver and Braziunas, 1993).

The uppermost sediments in each core were analyzed for ^{210}Pb and ^{137}Cs . Cesium-137 is a short-lived artificial radioisotope (half-life=30 years) produced by atmospheric nuclear testing in the 1950s and 1960s. It first appeared in the atmosphere in 1954, and concentrations peaked in 1963. The technique thus can be

used to date sediments that are less than 40 years old (Ritchie and others, 1975; Ashley and Moritz, 1979). However, ^{137}Cs is not completely immobile in some sediments; it can be transported by molecular diffusion through pore water (Santschi and others, 1983; Geyh and Schleicher, 1990). Nevertheless, the technique was used on subsamples from the tops of each piston core; the results are discussed in the error analysis section. Each sample was freeze-dried, weighed, and transferred to a Marinelli beaker. Cesium-137 concentrations were then determined with an APTEC gamma ray spectrometer at PGC.

Subsamples of the upper parts of all cores were analyzed for ^{210}Pb at Flett Research Ltd. (Winnipeg) using a 4000 channel Canberra Model 8180 Multichannel Analyzer connected to a 300 mm² surface barrier detector following the method outlined by Eakins and Morrison (1978). Lead-210, a member of the ^{238}U decay series, has a half-life of 22 years and can be used to date sediments that are up to 150 years old (Robbins, 1978). In this decay series, ^{222}Ra is formed as gas and diffuses in the atmosphere where it decays through a series of short-lived intermediates to ^{210}Pb . Lead-210 is deposited in sediments at the earth's surface in rain or by dry fallout (Beasley, 1969; Feely and Seitz, 1970). This atmospherically derived ^{210}Pb is termed "excess ^{210}Pb ". Lead-210 is also produced from ^{222}Ra in sediments; this component is called "supported or background ^{210}Pb ". Dating is done by measuring excess ^{210}Pb concentrations as a function of depth in a sequence of sediments. The technique is applied assuming that excess ^{210}Pb has a constant rate of input and is not mobile in the sediments (Macdonald and others, 1984). Analyzed sediments should not have been

disturbed by bioturbation or physical mixing. A complete sediment profile without hiatuses is preferable (Geyh and Schleicher, 1990). If only part of the sediment profile is sampled, a regression line can be calculated to extrapolate values (R. Flett, oral communication, 1994). This procedure was used in this study.

RESULTS

Sedimentology

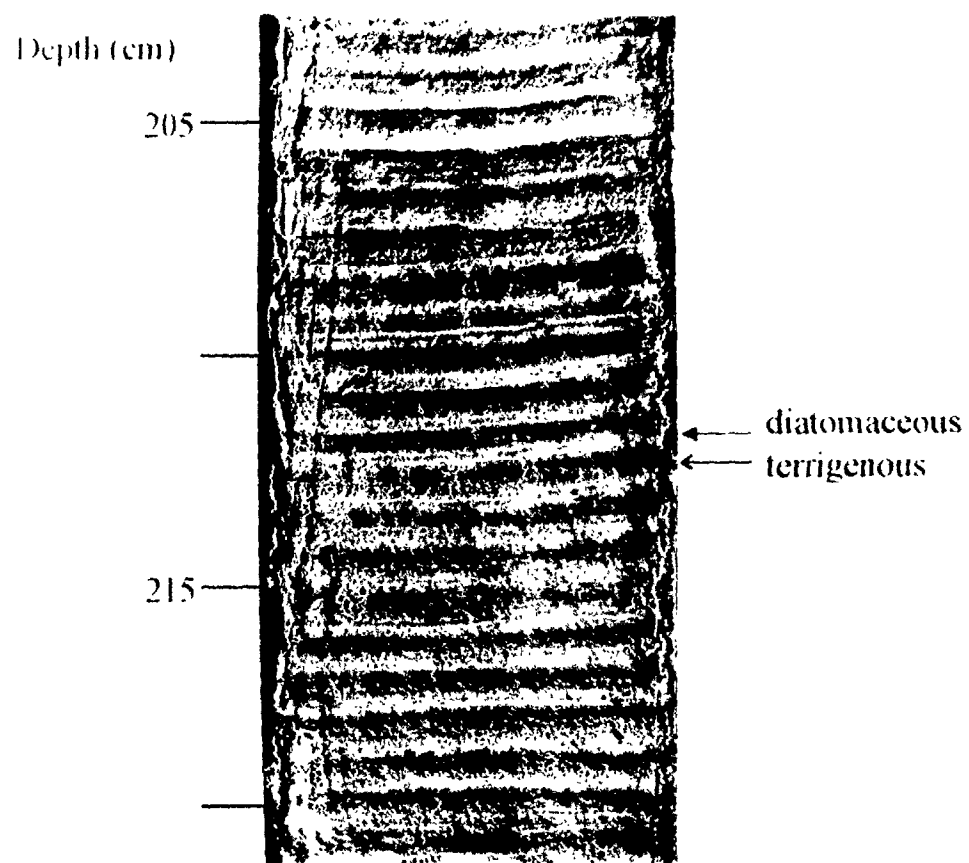
Varved sediments

The varved sediments consist of alternating, light-coloured (olive to olive brown; 5Y4/3, 2.5Y4/3) diatom-rich laminae and darker (dark olive grey to very dark greyish brown; 5Y3/2, 2.5Y3/2) silt and clay laminae. Most laminae are horizontal and undisturbed (Plate 3-1), but laminae in the upper parts of cores are commonly contorted, probably due to disturbance during coring. The terrigenous lamina of many couplets commonly consists of a lower, lighter, clay-rich zone and an upper, darker, more silty zone (Plate 3-1).

Couplets range from 1 to 25 mm in thickness, generally with gradational contacts between light- and dark-coloured laminae. There are no obvious variations in varve thickness (Fig. 3-5) and therefore no change in the sedimentation rate during the period spanned by the cored sediments. In addition, varve thicknesses do not appear to change at depths corresponding to the period of reservoir construction and water diversion in the Goldstream River watershed (ca. 1892-1900 AD).

In order to estimate sedimentation rates at core sites, average varve thicknesses

Plate 3-1. Typical varved sediments from Saanich Inlet (core TUL89A-002). Each couplet comprises a dark silty clay (terrigenous) lamina and a light diatom-rich lamina (arrows).



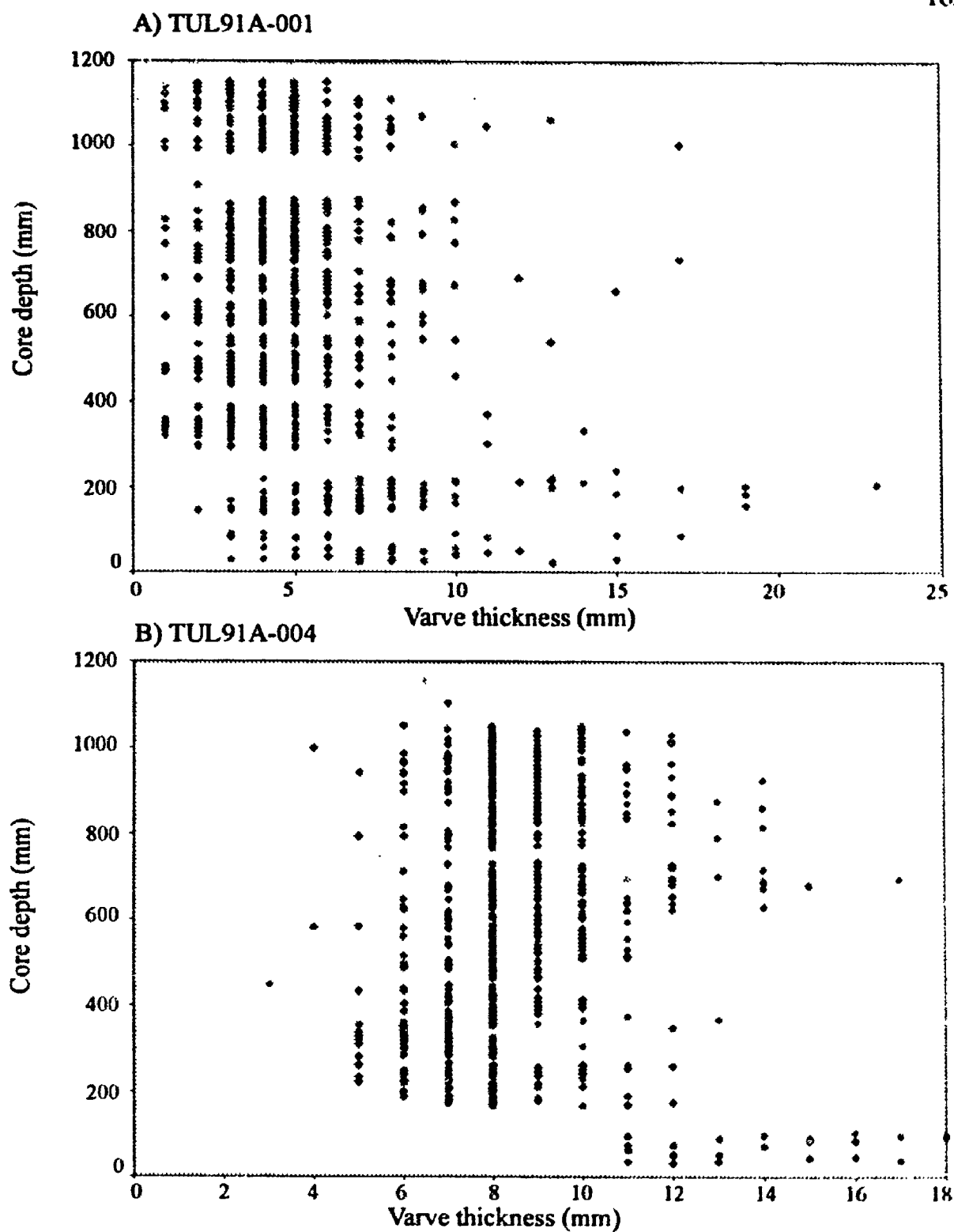
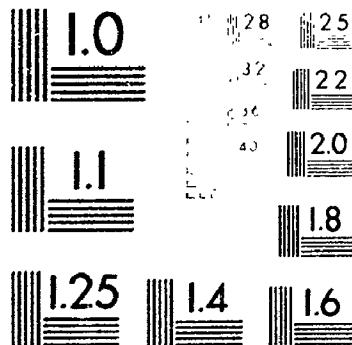


Figure 3-5. Scattergram of varve thickness versus core depth for cores A) TUL91A-001 and B) TUL91A-004. Correlation coefficients are $r = -0.1924$ and $r = 0.0167$, respectively.

3

PM-1 3 1/2" x 4" PHOTOGRAPHIC MICROCOPY TARGET
NBS 1010a ANSI/ISO #2 EQUIVALENT



PRECISIONSM RESOLUTION TARGETS

were calculated using two methods. The first method ignores the compaction that resulted from brief upright storage of the cores prior to splitting. However, all the cores were subjected to the same amount of compaction, therefore data from one core should be comparable with those from another. Average varve thicknesses for four of the five cores collected in 1991, are given in Table 3-2. The second method compensates for compaction of the varves. Thus, for each core, the total thicknesses of the massive layers were subtracted from the length of core, and the remainder divided by the total number of varves. This gives the average varve thickness and, therefore the sedimentation rate. With both methods, sedimentation rates generally decrease from north to south with the exception of core TUL89A-003 (Table 3-2). The concentrations of points in Figure 3-5 also shows that sedimentation rates are higher (varves are thicker) in the north (TUL91A-004) than in the south (TUL91A-001).

Massive layers

Massive layers comprise dark olive grey (5Y3/2), homogeneous silty clay with no obvious sedimentary structures (Plate 3-2). Commonly, these layers erosively overlie varved sediments. Above most basal contacts, there is a 2-10 cm zone of diffuse, brecciated, horizontal to nearly horizontal fine laminae with similar colour variations observed in the varved winter and summer layers (Plate 3-3). Varve intraclasts with no apparent fabric are present in the lower parts of some massive beds, indicating that varved sediments have been eroded and incorporated into some of the massive layers. In places, varves are overturned, truncated, and erosionally

Table 3-2. Average varve thicknesses (sedimentation rates in mm/y) of compacted and uncompacted varves.

	South				North			
	Cores: TUL91A-001 TUL89A-001 TUL91A-002 TUL89A-002 TUL91A-003 TUL89A-003 TUL91A-004 TUL89A-002 TUL91A-003							
Average varve thickness of uncompacted varves (mm)	4.65	6.51	6.92	5.7	9.57	10.39	12.71	
Average varve thickness of compacted varves (mm)	4.44		4.68	8.35			9.08	

Plate 3-2. Massive silty clay layer underlain and overlain by varved sediments (core TUL89A-002).

Depth (cm)

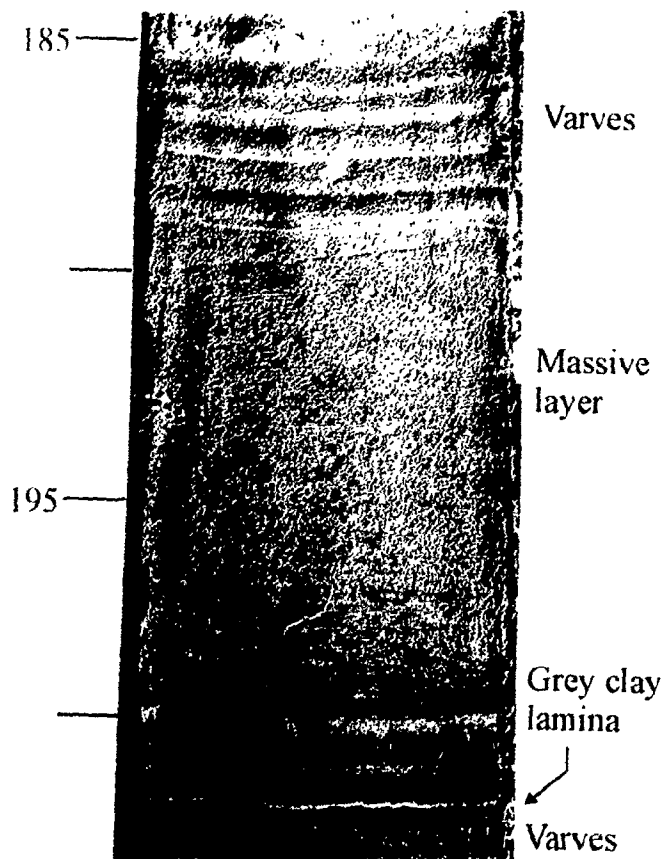
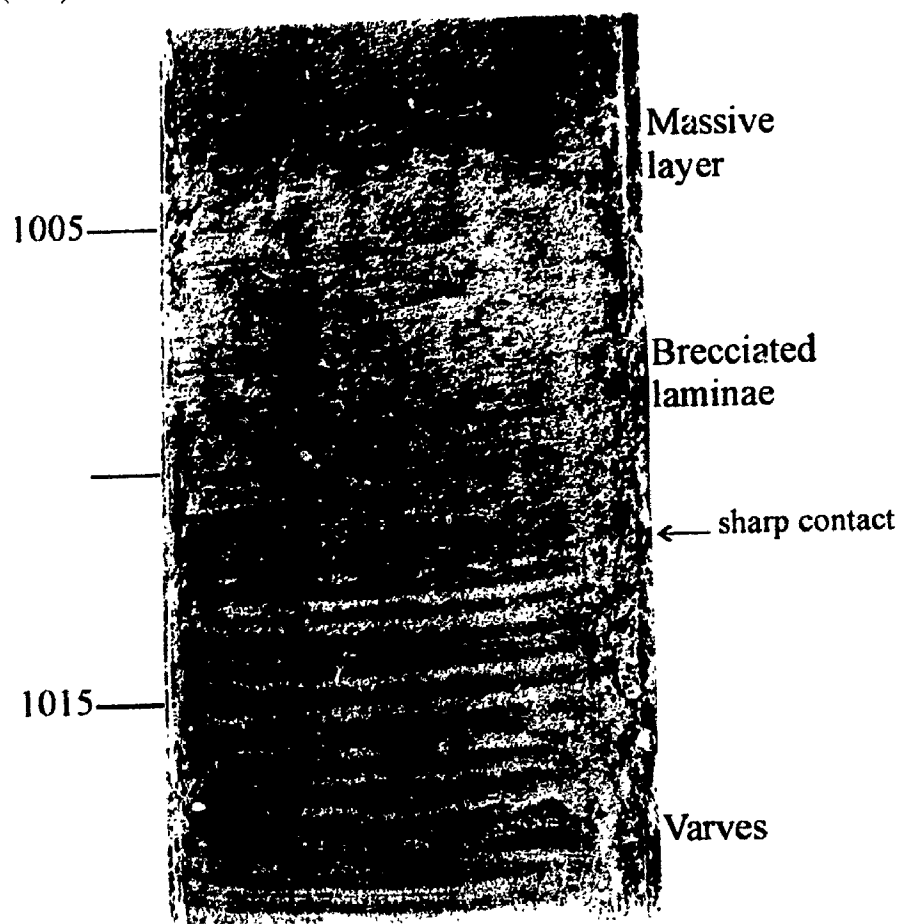




Plate 3-3. Brecciated laminae at the base of a massive layer (core TUL89A-003).

Depth (cm)



overlain by massive layers (Plate 3-4).

A total of 53 massive layers are found in seven of the eight cores (Fig. 3-6; Table 3-3). They range in thickness from 2 to 110 cm (average thickness = 16.5 cm; Table 3-3). There are no systematic trends in the thickness of massive layers within any core, but the layers appear to be slightly thicker in southern Saanich Inlet (TUL89A-001, TUL89A-003, TUL91A-001, and TUL91A-002; Fig. 3-6). Massive layers are more abundant in the narrow, steeply-inclined, southern part of the inlet (TUL89A-001, TUL89A-003, TUL91A-001, and, TUL91A-002, Fig. 3-3) than in the wide, gently-sloping, northern part of the inlet (TUL89A-002, TUL91A-003, and TUL91A-004).

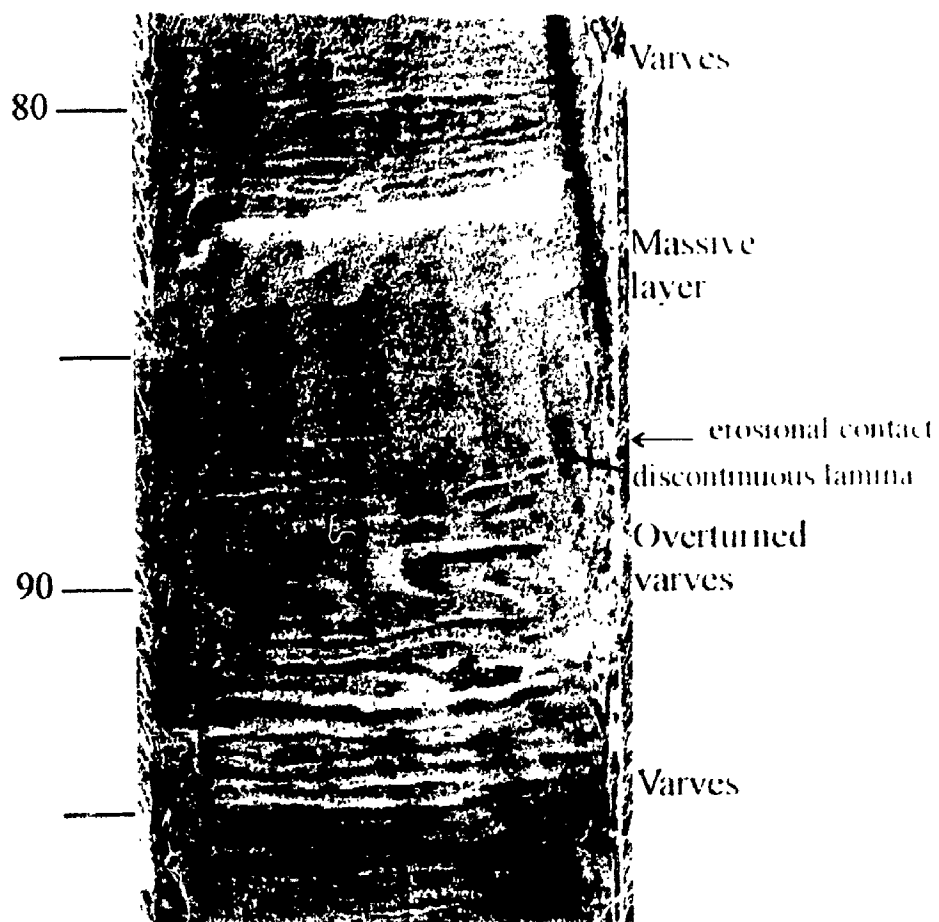
Particle-size analysis

Cored sediments are generally fine-grained silty clay; a notable exception is the gravelly base (granule-sized clasts) of one massive layer (TUL91A-001 at 9.86-9.88 m depth). Particle-size analytical data show that most sediments consist of silty clay with less than 5% fine sand (Fig. 3-7; Appendix 3-1). Many massive layers are coarser than the varves that bound them (see also Bobrowsky and Clague, 1990), but otherwise there is little difference in texture between the varved and massive sediments (Fig. 3-8).

In order to test whether there are grain size differences between the massive layers and the varves, a Student t-test was performed on the percent sand in the two types of sediment. In this test (Davis, 1986), the mean percent values of fine sand are compared and hypothesized to be equal. In other words, the null hypothesis, H_0 :

Plate 3-4. Discontinuous lamina and deformed overturned varves below massive layer. Base of massive layer is showing erosional contact overlying truncated and overturned varves (core TUL89A-001).

Depth (cm)



[illegible]

Figure 3-6. Summary of core stratigraphy and radiometric age data.

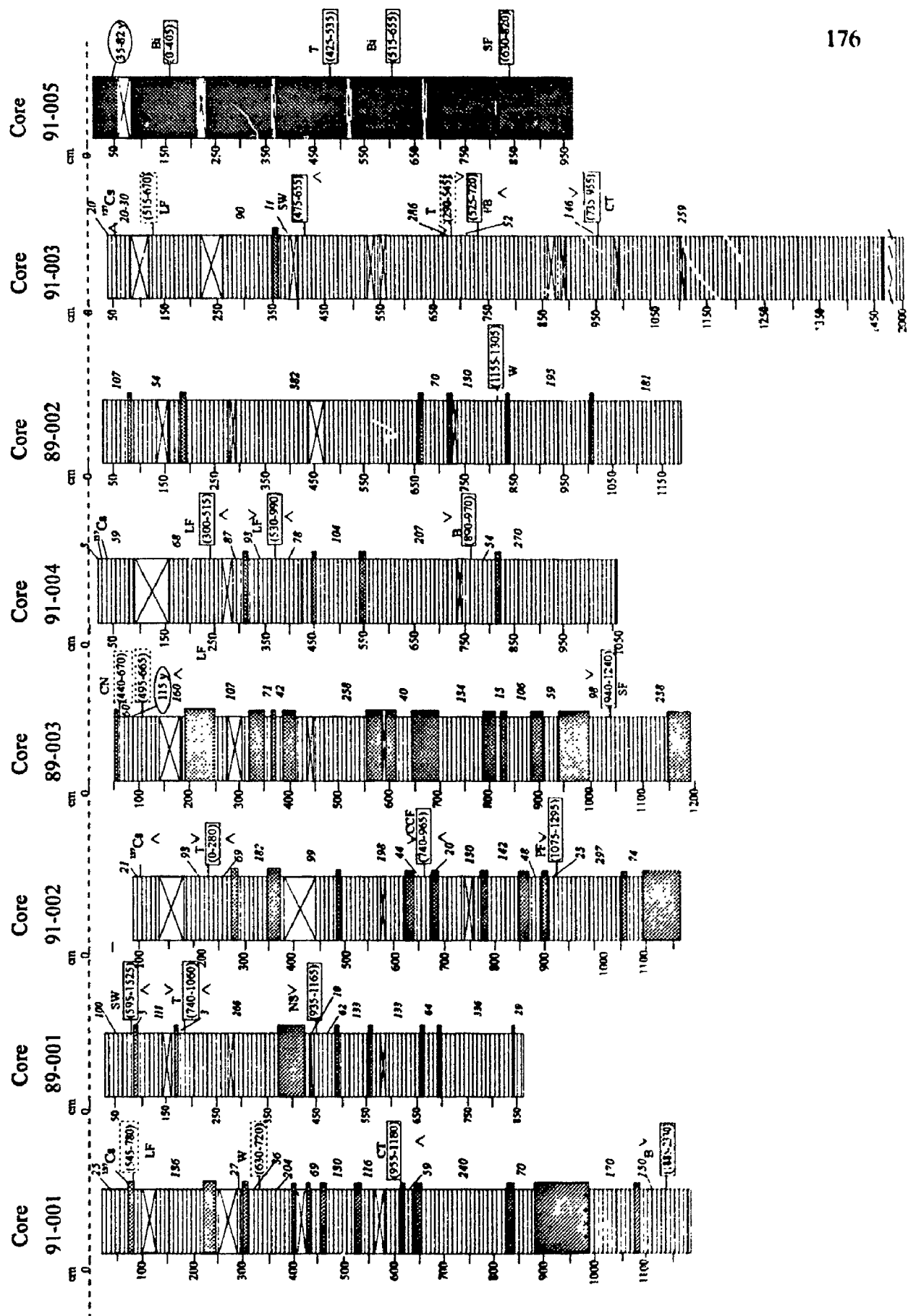


Table 3-3. Distribution of massive layers within the cores

South		North						
TUL91A-001	TUL89A-001	TUL91A-002	TUL89A-003	TUL91A-004	TUL89A-002	TUL91A-003	TUL89A-002	TUL91A-003
63-78	F 82-87	NS 277-282	F 46-53	NS 306-316	NS 73-75	NS 306-316	F 73-75	NS 350-356
223-247	F 166-169	NS 356-374	NS 199-247	NS 448-461	F 185-196	NS 448-461	NS 185-196	NS 350-356
302-308	F 371-418	F 482-486	NS 318-343	NS 547-552	F 656-660	NS 547-552	F 656-660	NS 350-356
397-401	F 476-479	NF 610-639	F 365-367	F 810-814	NS 725-729	F 810-814	NS 725-729	NS 350-356
428-439	F 559-562	F 676-683	NS 384-403	F 384-403	F 840-843	F 384-403	F 840-843	NS 350-356
462-468	F 656-660	NS 777-782	NS 556-619	F 556-619	1006-1008	F 556-619	1006-1008	NS 350-356
521-528	F 694-698	F 868-871	F 644-698	F 644-698		F 644-698		
607-612	F 848-850	F 899-905	NS 777-809	F 777-809		F 777-809		
638-651		1058-1063	NS 816-824	F 816-824		F 816-824		
831-841		1098-1170	F 885-907	NS 885-907		NS 885-907		
877-987			937-997	NF 937-997		NF 937-997		
1073-1082			1149-1177	NF 1149-1177		NF 1149-1177		

Note: Numbers are depths of layers in centimetres. F, foraminifera present; NF, no foraminifera; NS, no sample collected for foraminiferal analysis.

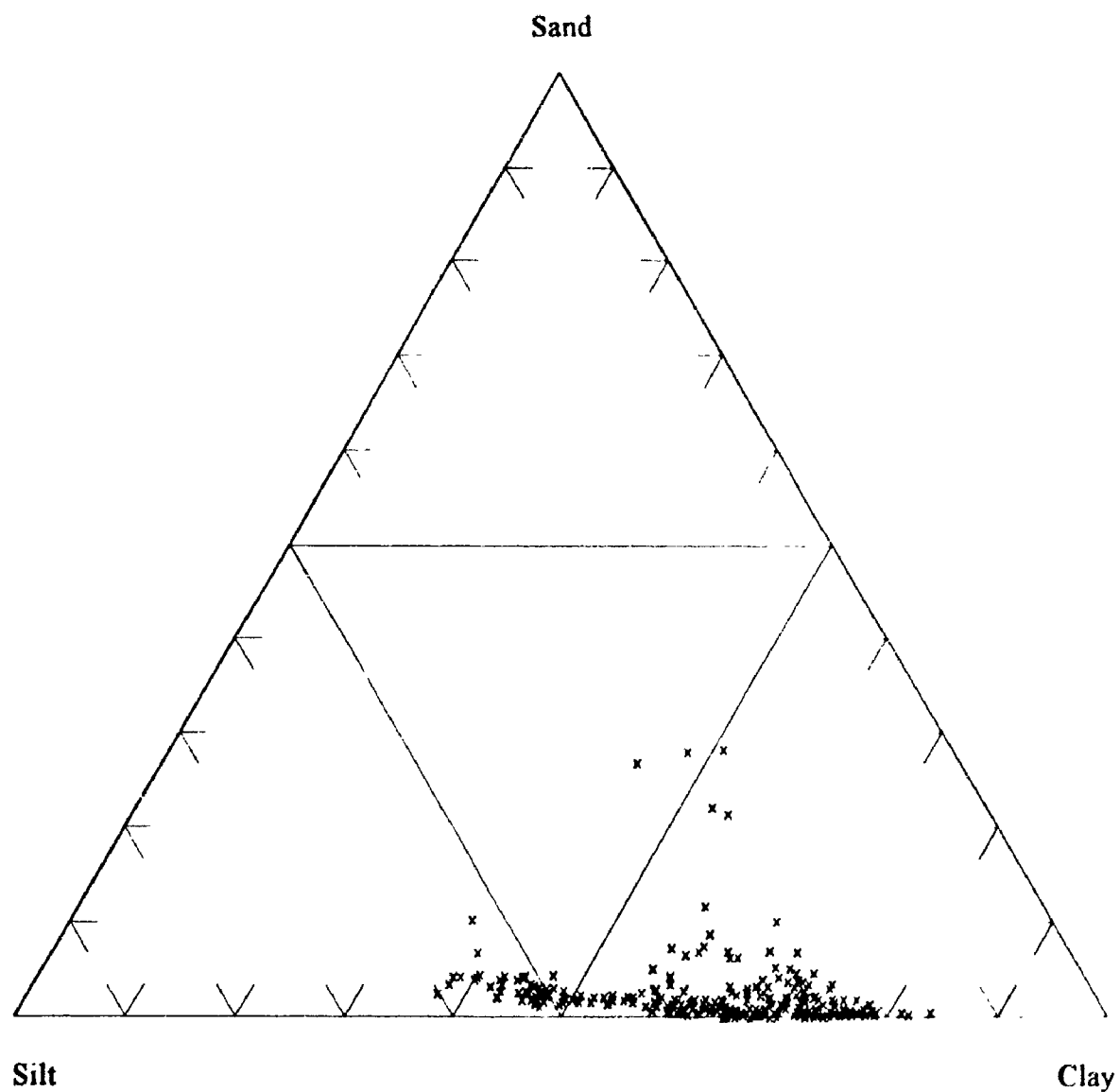


Figure 3-7. Particle-size distribution of all samples (varves, massive layers, and massive clayey silt from core TUL91A-005). Sand apex fraction is fine sand (<0.25 mm)

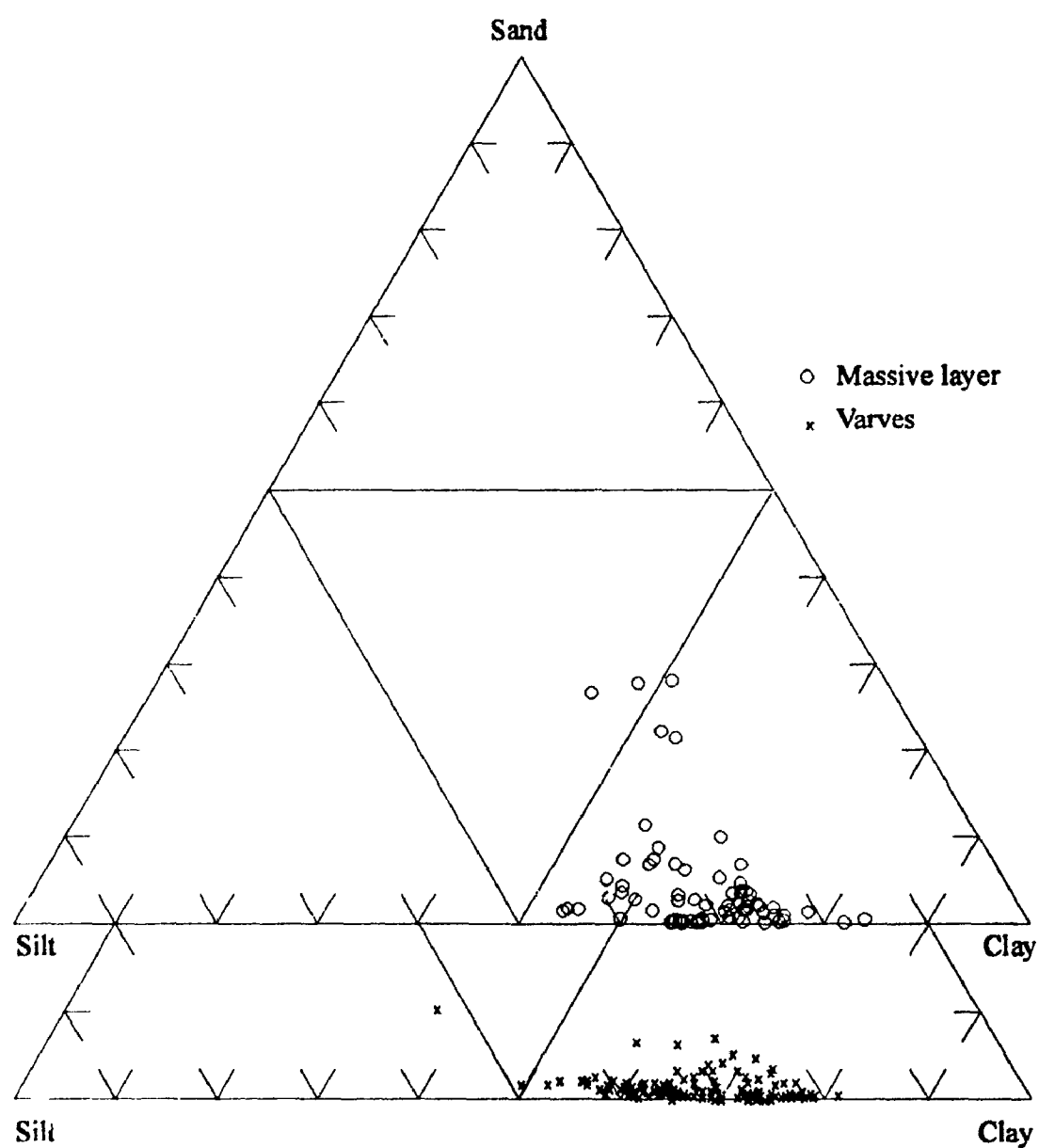


Figure 3-8. Particle-size distribution of samples of varves and massive layers. Sand apex fraction is fine sand (<0.25 mm).

$\mu_1 = \mu_2$, where μ_1 is the hypothetical mean percent fine sand for the varves and μ_2 is the hypothetical mean of percent fine sand for the massive layers (see Appendix 3-2 for details).

The result ($t = -3.22$ for a two-tailed distribution) is that there is one chance in a thousand that the mean sand contents the varves and the massive layers are equal. Therefore, we can reject the hypothesis that the means are the same (Davis, 1986). The significance of this result is discussed in the section entitled "Debris flow deposits".

There appears to be no normal or inverse grading in the massive layers (Fig. 3-9; Appendix 3-3). However, in some cases, there are not enough data to draw this conclusion.

Particle-size data for varve samples were plotted on ternary diagrams (Appendix 3-4a) to compare particle size and sedimentation rates (Table 3-2). As an example, core TUL91A-001 (farthest south) has the lowest calculated sedimentation rate and some of the coarsest varves. In contrast, core TUL89A-001 (second farthest south) has some of the finest varves and second lowest calculated sedimentation rate (Fig. 3-10; Table 3-2; Appendix 3-4a). Overall, there is no discernable trend in particle size towards the south corresponding to the decreasing sedimentation rate in this direction.

Particle-size data for massive layers were also plotted on ternary diagrams (Appendix 3-4b) to determine whether or not there are areal trends. Overall, grain size variations vary randomly from one core to the next.

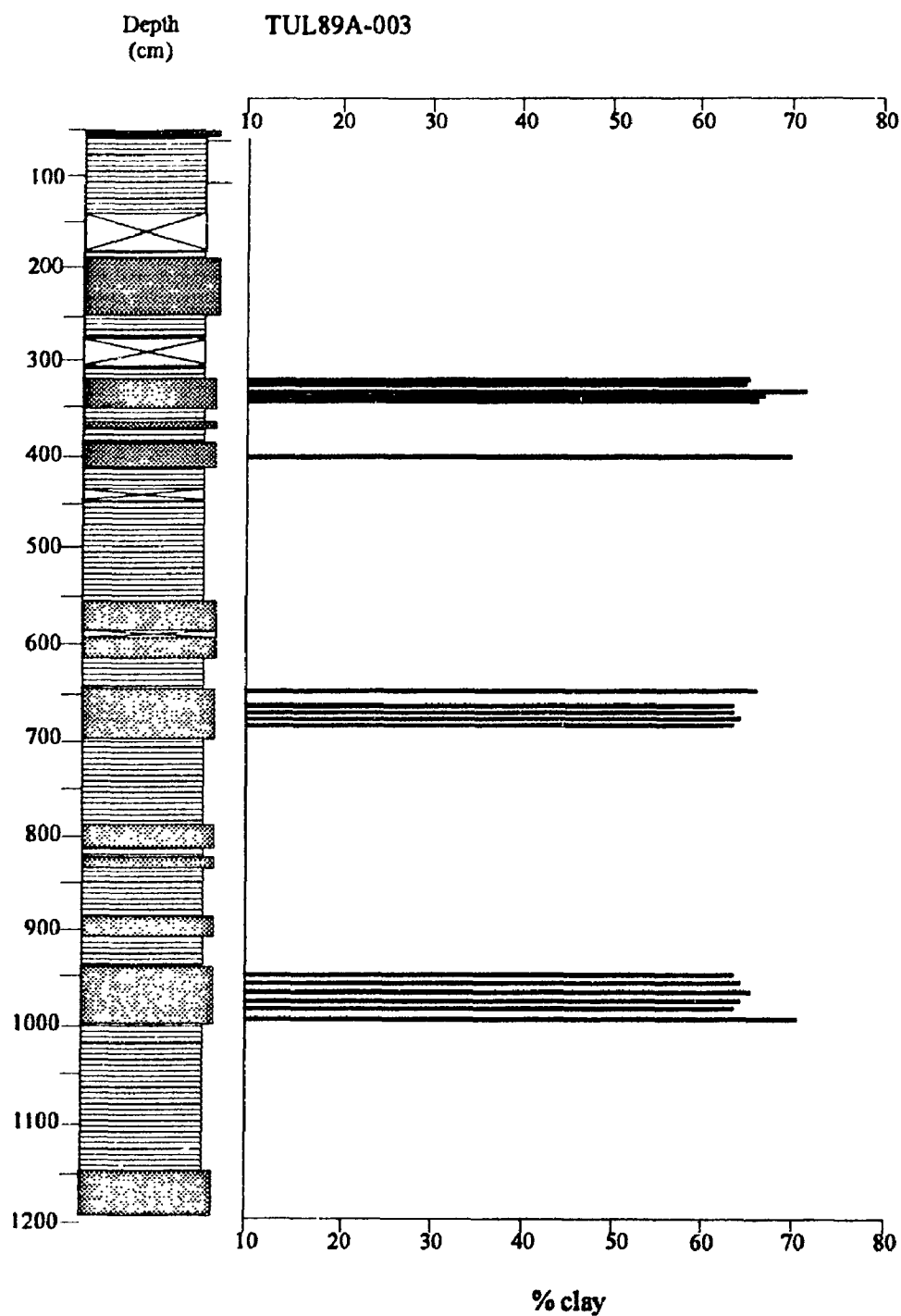


Figure 3-9. Percent clay in massive layers showing lack of normal and reverse grading.

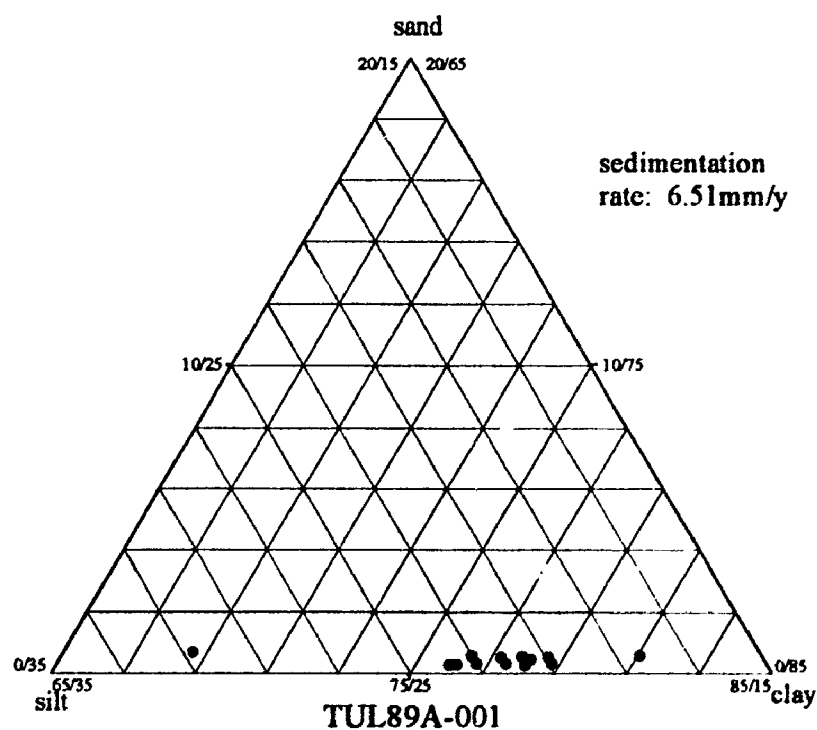
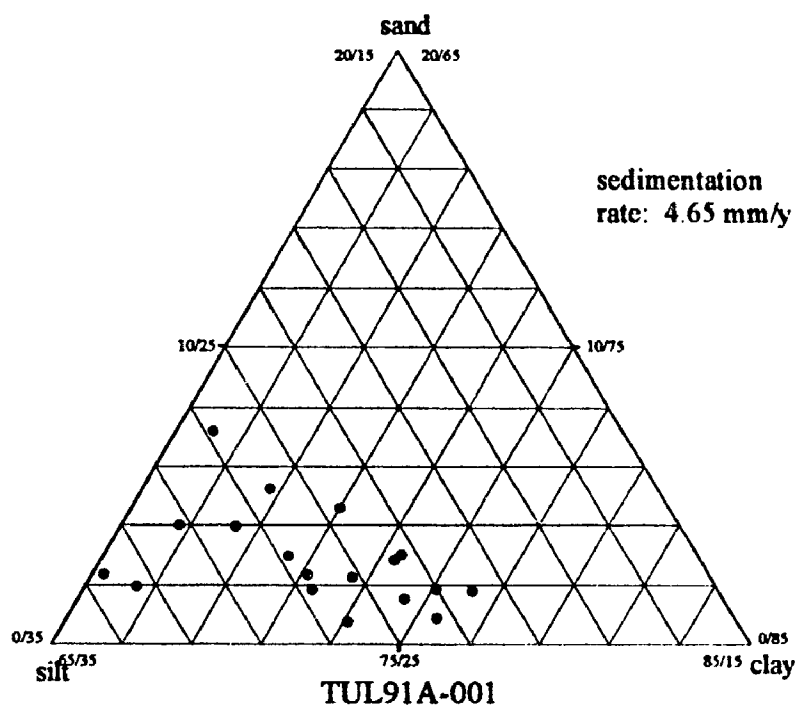


Figure 3-10. Comparison of varve size fractions of varved sediments and sedimentation rates for cores TUL91A-001, the farthest south, and TUL89A-001, the second farthest south. Sand apex represents fine sand.

The northernmost, shallowest core (TUL91A-005) lacks distinctive massive layers or varves. The entire core is composed of weakly stratified clayey silt with scattered shell fragments and whole shells and no obvious trace fossils (Plate 3-5). Silty-clay laminae similar to the ones observed in the varves are randomly distributed throughout the core. Foraminifera are also present throughout the sediments. Particle-size data indicate that the sediments in this core are more silty than varved and massive sediments in the other seven cores (Fig. 3-11).

The sedimentation rate for core TUL91A-005 was calculated from mean calibrated ^{14}C ages. Values range from 12.55 to 25.7 mm/a. These values also indicate that the sedimentation rate is higher in the north than in the south.

Clay mineralogy

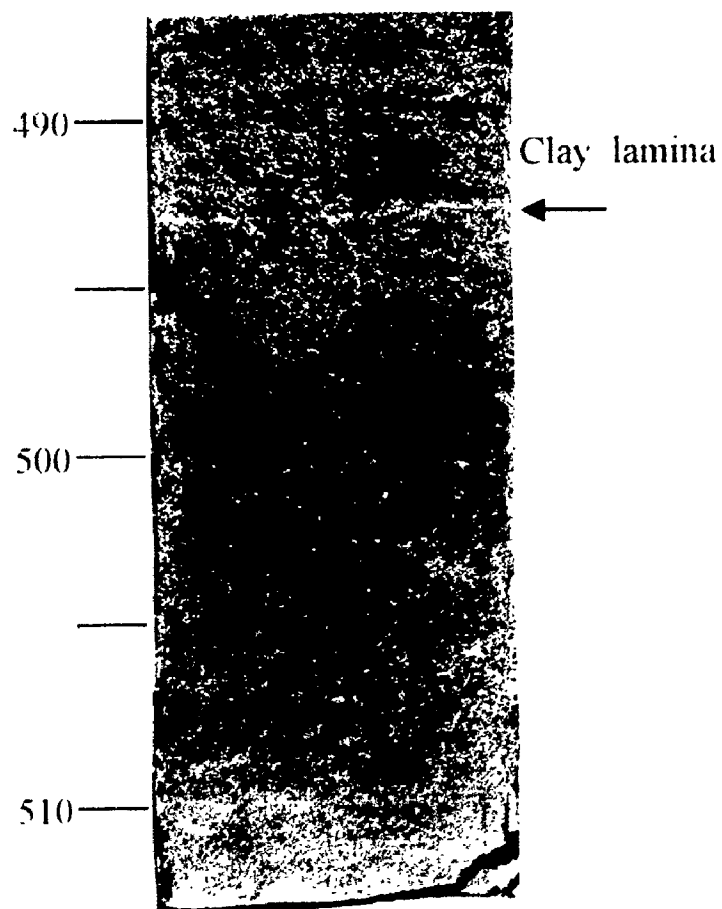
Clay mineral analyses were performed on massive layers and on light and dark layers of couplets in an effort to determine the provenance of the sediments. Samples of possible source sediments (Cowichan, Goldstream, and Fraser River deposits) were also analyzed. It was theorized that sediments from the Fraser River would have higher percentages of muscovite-illite (Mackintosh and Gardner, 1966) because of an S-type pluton (two mica granite) provenance (Roddick, 1965). The X-ray diffraction analyses, however, are inconclusive because there are no significant differences in clay mineralogy among the various types of sediment (Appendix 3-5).

Micropaleontology

The varved sediments contain diatoms (siliceous tests) but lack foraminifera; this is confirmed with observations made on the cellulose tape peel. This is expected

Plate 3-5. Clayey silt containing scattered shells and shell fragments (core TUL91A-005). The sediment in this core appears massive, but includes some poorly-defined laminae.

Depth (cm)



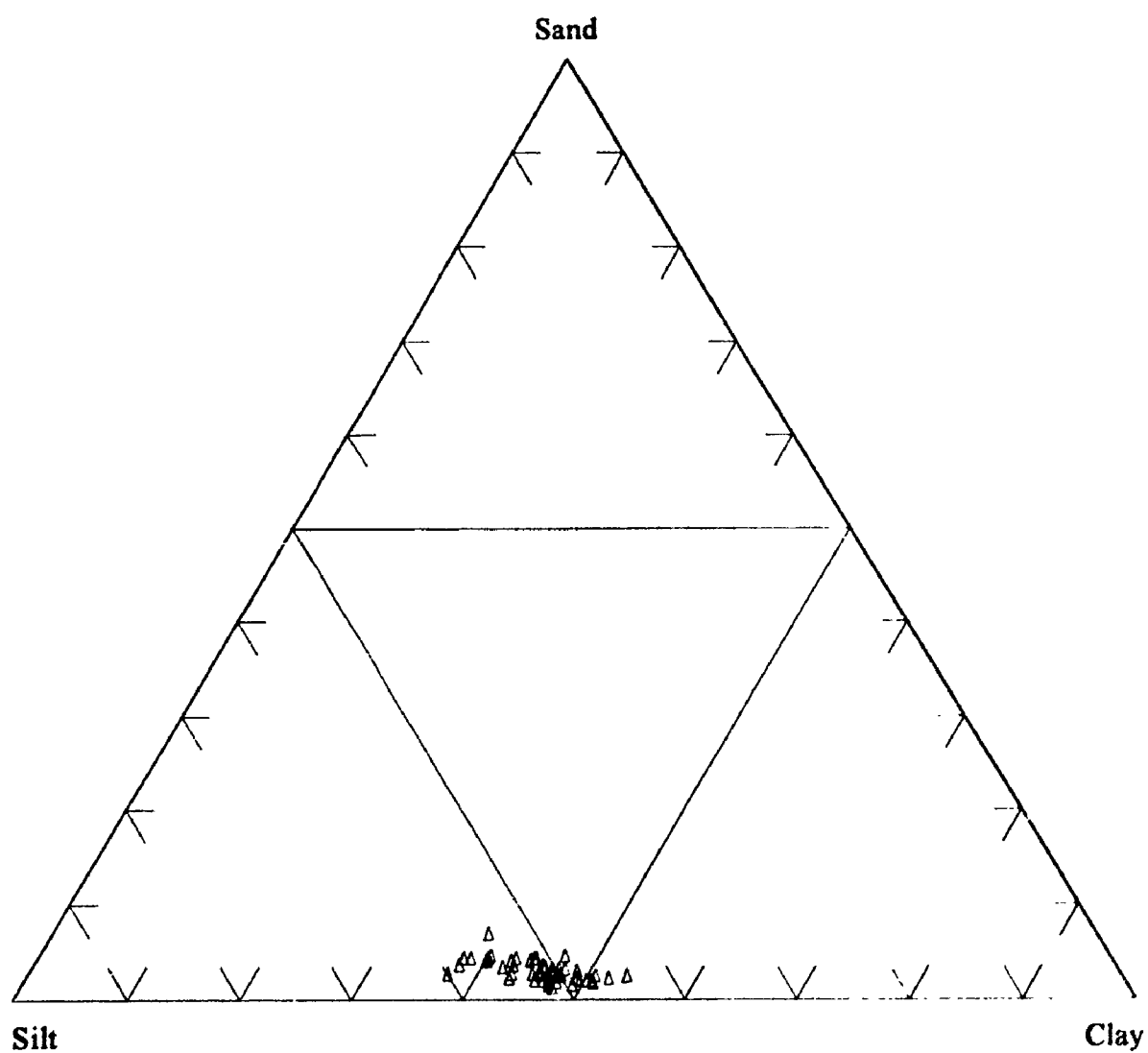


Figure 3-11. Particle-size distribution of samples of massive clayey silt from core TUL91A-005. Sand apex is fine sand fraction (<0.25 mm).

because calcareous foraminifera dissolve in a reducing environment. The massive layers, however, contain both diatoms and calcareous and agglutinated benthic foraminifera (Tables 3-3 and 3-4; Appendix 3-6). This implies that the foraminifera were transported from above the anoxic zone (< 150 m depth), deposited, and buried rapidly within the sediments to inhibit dissolution of the tests.

The most abundant types of foraminifera found in the massive layers are *Trochammina* spp. (*T. nana*= 18, *T. pacifica*= 16, *T. squamata*= 10; Appendix 3-6). This genus is common in a variety of marine environments. The second most abundant foraminiferal taxa are *Spiroplectammina biformis* and *Eggerella advena* (17 and 13, respectively). These two species dominate foraminiferal assemblages of shallow waters in Saanich Inlet (Blais and Patterson, in press, Chapter 2).

Dating

Cesium-137

The uppermost sediments in four of the eight cores (TUL91A-001, TUL91A-002, TUL91A-003, and TUL91A-004) contain trace amounts of ^{137}Cs . Concentrations are too low to identify the expected 1963 peak (Ashley and Moritz, 1979). Furthermore, as mentioned above, there is slight possibility that ^{137}Cs is mobile within the sediments after deposition (Santschi and others, 1983). However, it does not appear to be the case in Saanich Inlet varves (A. Collins, oral communication, 1995). From a study carried out by Ms. Collins (M.Sc. thesis at University of Victoria, B. C.), a layer of wood chips resulting from saw mill activity at Mill Bay between 1863 and 1878 was found in Saanich Inlet sediments. The

- Bolivinellina pacifica* (Cushman and McCulloch), 1942. [*Bolivina acerosa* var. *pacifica*]
Buccella frigida (Cushman), 1922. [*Pulvinulina frigida*]*
Buliminella elegantissima (d'Orbigny), 1839. [*Bulimina elegantissima*]*
Cassidulina limbata Cushman and Hughes, 1925
Cibicides sp. 1.
Criboelphidium sp.
Criboelphidium bartletti (Cushman), 1933. [*Elphidium bartletti*]
Criboelphidium frigidum (Cushman), 1933. [*Elphidium frigidum*]*
Criboelphidium hallandense (Brotzen), 1943. [*Elphidium subarcticum*]
Cuneata arctica (Brady), 1881. [*Reophax arctica*]*
Eggerella advena (Cushman), 1922. [*Verneuilina advena*]*
Elphidiella hannai Cushman and Grant, 1927
Epistominella pacifica (Cushman), 1927. [*Pulvinulina pacifica*].
Favulina melo (d'Orbigny), 1839. [*Oolina melo*]*
Globigerina sp.
Haplophragmoides canariensis (d'Orbigny), 1839. [*Nonionina canariensis*]*
Leptohalysis catella (Höglund), 1947. [*Reophax catella*]*
Lobatula fletcheri (Galloway and Wissler), 1927. [*Cibicides fletcheri*]*
Lobatula mckannai (Galloway and Wissler), 1927. [*Cibicides mckannai*]*
Miliammina fusca (Brady), 1870. [*Quinqueloculina fusca*]*
Nonionella stella Cushman and Moyer, 1930*
Procerolagena wiesneri (Parr), 1950. [*Lagena striata*]
Quinqueloculina sp. d'Orbigny, 1826
Reophax gracilis (Kiaer) 1900. [*Nodulina gracilis*]
Rosalina columbiensis (Cushman), 1925. [*Discorbis columbiensis*]
Spiroplectammina biformis (Parker and Jones), 1878. [*Textularia biformis*]*
Stainforthia feylingi Knudsen and Seidenkrantz, 1993*
Trochammina charlottensis Cushman, 1925*
Trochammina discorbis Earland, 1934*
Trochammina nana (Brady), 1881. [*Haplophragmium nana*]
Trochammina pacifica Cushman, 1925*
Trochammina rotaliformis Wright, 1911*
Trochammina squamata Parker and Jones, 1860*

Note: Species identified with an asterisk are illustrated in Blais and Patterson (in press, Chapter 2).

number of varves between the marker horizon and the lowest occurrence of ^{137}Cs concentrations shows that ^{137}Cs is not mobile in the Saanich Inlet sediments. Hence, a datum of 1954 (beginning of nuclear testing in the atmosphere) is assigned to the deepest sediments containing ^{137}Cs .

Due to the soupy nature of the uppermost sediments at the core sites, there was concern that the sediment-water interface was not recovered during coring. This appears to be true for most of the 1989 cores, but the presence of ^{137}Cs in four of the five 1991 cores indicates that they are nearly complete.

Lead-210

Two cores (TUL89A-003 and TUL91A-005) contain sediments with excess ^{210}Pb concentrations (Fig. 3-12). Because of a lack of data points, it is not possible to estimate the background concentrations of ^{210}Pb , which are required to accurately calculate the ages of the sediments. Nevertheless, age estimates were obtained using a least squares method for calculating a best-fit regression line with background as a variable (Appendix 3-7). A best-fit line was calculated by varying the background value, with the available data points providing constraints. The best-fit line was then used to estimate the accumulation rate and, hence, the age of the sediments at a specific depth.

In core TUL89A-003, sediments at 83-85 cm depth are approximately 115 years old. Two age estimates were made for core TUL91A-005 using different data points. Using all the data, sediments at 50-51 cm depth are estimated to be 35 years old. If only the lowest three data points are used (the uppermost sediments may be

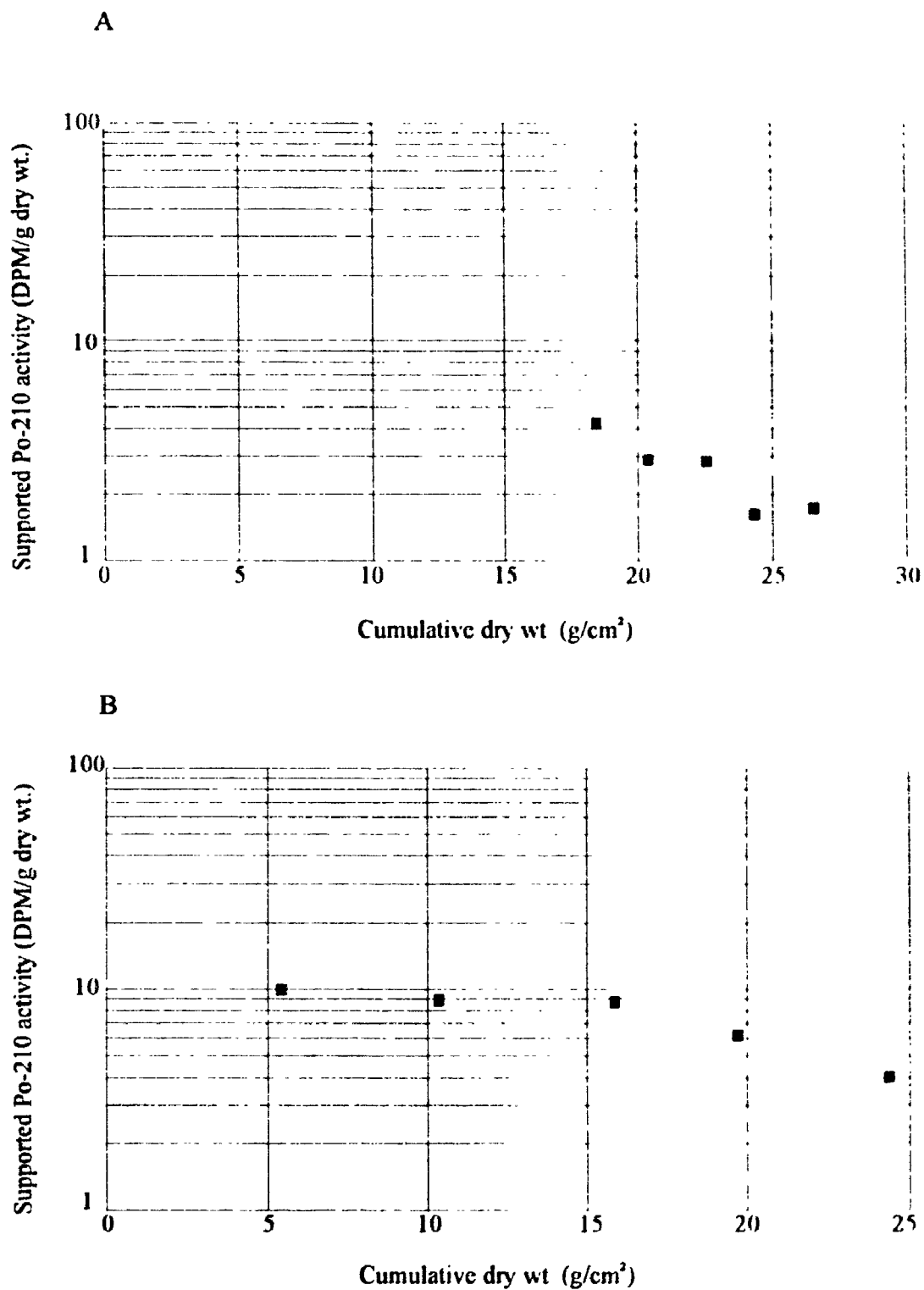


Figure 3-12. Semi-log plots of ²¹⁰Pb data from (A) core TUL89A-003 and (B) TUL91A-005.

mixed), the calculated age at 50-51 cm depth is 82 years. Even with this uncertainty, the analyses show that sediments near the sediment-water interface were recovered in both cores.

Carbon-14

Mean calibrated ^{14}C ages range from 115 (0-155)³ cal y BP (calendar years before AD 1950) to 2110 (1885-2330)² cal y BP (Table 3-5; Fig. 3-6). Five of the 26 ^{14}C ages are considered anomalous, based on stratigraphic position, calculated sedimentation rates, varve counts, and other radiometric ages (Fig. 3-6). Four of the five appear to be too old; in these cases, the dated material may have been reworked from older Holocene sediments. One ^{14}C age from core TUL91A-003 may be too young. Its stratigraphic position within the core and its relation to other radiometric ages are discussed below.

Varve chronology

Varves are counted and tabulated on the core logs (Fig. 3-6). Cumulative numbers of varves down to each massive layer are also tabulated (Table 3-6). Sediments at the top of each core are loose and water-saturated, making it difficult to count the varves. Only the visible varves were counted and no estimate was made of the number of varves in uppermost sediments that were completely disturbed. In addition, there was some disturbance of the sediments due to sectioning of the cores. Sediment disturbance was only a few cm's thick when it was observed and generally varves were still visible. Because some erosion occurred during the emplacement of

³ Values in parentheses are 2σ age ranges.

Table 3-5 Radiocarbon ages from the study area

Radiocarbon age (¹⁴ C yr B.P.) ^a	Calibrated age range (cal yr before A.D. 1950) ^b	Core TUL	Laboratory No. ^c	Location		Depth (cm) ^d	Dated material
				Latitude (°N)	Longitude (°W)		
110±50	mod.-280	91A-002	TO-3535	48°34.9'	123°30.2'	229-230	twig
370±50	300-515	91A-004	TO-3539	48°37.2'	123°30.1'	248.5-249.5	leaf fragments
400±80	290-545	91A-003	TO-4050	48°39.6'	123°30.2'	680.5	twig
430±50	425-535	91A-005	TO-3687	48°40.7'	123°30.2'	478.5	deciduous twig
560±100	440-670	89A-003	TO-3533	48°36.1'	123°30.0'	53	conifer needle
580±80	495-665	89A-003	TO-3632	48°36.1'	123°30.0'	81	leaf fragments
620±70	515-670	91A-003	TO-3536	48°39.6'	123°30.2'	115	plant remains
710±50	630-720	91A-001	TO-3703	48°33.2'	123°32.1'	329.5-330	wood fragments
720±80	545-780	91A-001	TO-3534	48°33.2'	123°32.1'	66-68	deciduous leaf
820±150	530-990	91A-004	TO-3686	48°37.2'	123°30.1'	365	leaf fragments
960±50	735-955	91A-003	TO-3685	48°39.6'	123°30.2'	952.5	conifer twig
970±50	740-965	91A-002	TO-3684	48°34.9'	123°30.2'	662	conifer cone
970±80	mod.-405	91A-005	TO-2904	48°40.7'	123°30.2'	158	bivalve shell
1000±40	890-970	91A-004	TO-2903	48°37.2'	123°30.1'	759.5	bark
1010±70	740-1060	89A-001	TO-3531	48°33.7'	123°30.4'	172	conifer twig
1130±50	935-1165	89A-001	TO-3530	48°33.7'	123°30.4'	448	nut shell
1170±50	955-1180	91A-001	TO-2900	48°33.2'	123°32.1'	606.5	conifer twig
1300±50	1075-1295	91A-002	TO-2901	48°34.9'	123°30.2'	921	plant fragments
1320±50	1155-1305	89A-002	TO-3537	48°38.4'	123°30.2'	826	wood fragments
1370±60	475-655	91A-003	TO-3705	48°39.6'	123°30.2'	411.5	seaweed
1410±40	515-655	91A-005	TO-2905	48°40.7'	123°30.2'	602.5	bivalve shell
1460±60	525-720	91A-003	TO-2902	48°39.6'	123°30.2'	738	fish bone
1560±50	630-820	91A-005	TO-2906	48°40.7'	123°30.2'	846	shell fragments
1880±240	595-1525	89A-001	TO-3532	48°33.7'	123°30.4'	76	seaweed
1940±60	940-1240	89A-003	TO-1553	48°36.1'	123°30.0'	1041	shell fragments
2120±80	1885-2330	91A-001	TO-3683	48°33.2'	123°32.1'	1138	bark

^aLaboratory reported error terms are 1σ. Ages corrected to δ¹³C = -25.0‰ PDB.

^bDetermined from dendrocalibrated data of Linick and others (1986), Kromer and Becker (1993), Pearson and Stuiver (1993), Stuiver and Braziunas (1993), Stuiver and Reimer (1993), and Stuiver and Pearson (1993). The range represents the 95% confidence interval (±2σ) using an error multiplier of 1.

^cTO, IsoTrace (University of Toronto).

^dDepth below sediment-water interface.

Table 3-6. Cumulative number of varves from top of core to massive layer (ml)

South			North			
TUL91A-001*	TUL89A-001	TUL91A-002*	TUL89A-003*	TUL91A-004*	TUL89A-002	TUL91A-003*
40	105	202	59	254	107	155
ml	ml	ml	ml	ml	ml	ml
176	216	384	334	425	161	
ml	ml	ml	ml	ml	ml	
203	485	483	441	529	543	
ml	ml	ml	ml	ml	ml	
443	557	681	512	790	613	
ml	ml	ml	ml		ml	
512	690	745	554		743	
ml	ml	ml	ml		ml	
642	823	875	810		938	
ml	ml	ml	ml			
758	887	1017	850			
ml	ml	ml	ml			
828	1223	1065	921			
ml		ml	ml			
1057		1387	936			
ml		ml	ml			
1127		1461	1042			
ml			ml			
1297			1101			
			ml			
			1435			
Total number	1447	1252	1461	1435	1119	909
of varves						

Note: Asterisk indicates presence of ^{137}Cs or ^{210}Pb .

the massive layers, the total number of varves in each core represents the minimum time spanned by that core.

DISCUSSION

Debris flow deposits

When the massive layers in Saanich Inlet were first studied by Bobrowsky and Clague (1990), it was not clear whether they were products of in situ liquefaction of varves or sediment gravity flows. Bobrowsky and Clague (1990) favoured the latter mainly because most of the massive layers they studied were coarser than the bounding varved sediments, which is usually incompatible with in situ liquefaction. Particle-size analyses in this study (Fig. 3-8) show that many massive layers are coarser than the bounding varves, supporting an allogenic origin. Furthermore, the Student t-test on the percentage of sand in samples of the varves and massive sediment indicates that the means are not the same, therefore implying different depositional mechanisms.

Other evidence also supports a sediment gravity flow origin: (1) basal contacts of massive layers are sharp, and some are clearly erosional (Plates 3-3 and 3-4); (2) in core TUL91A-001, one massive layer contained a 2 cm granule sized gravel base erosionally overlying varves (Blais, 1992); (3) massive layers contain brecciated varves and varve intraclasts indicating that varves have been eroded and incorporated into the flow; (4) most massive layers exhibit a lower brecciated zone of varves underlying massive mud; (5) most massive layers contain benthic foraminifera (Table

3-2), which implies that the sediment was transported from above the anoxic zone (< 150 m depth).

The above characteristics are consistent with deposition by submarine sediment gravity flows. Sedimentary structures and textures of the massive layers point towards two possible mechanisms for forming them; either turbidity flows or debris flows. Some of the massive layers were possibly deposited by turbidity flows. They could represent the E unit (pelagic mud) of the Bouma sequence. However, most massive layers are products of debris flows: (1) none of the massive layers exhibits sedimentary structures and textures of a classic turbidite, i.e., Bouma sequence, formed by a turbidity flow; (2) there is no normal or inverse grading in the massive layers; (3) most massive layers contain a basal zone of brecciated varves which is interpreted as a shear zone at the base of a debris flow in the zone of laminar flow (Middleton and Hampton, 1976; Johnson and Rodine, 1984); (4) massive mud overlying the brecciated zone is possibly the plug or raft in the debris flow (Middleton and Hampton, 1976; Johnson and Rodine, 1984); and (5) varve intraclasts show no apparent fabric (Arnott and Hand, 1989).

Correlation of the cores

Correlations are based on ^{137}Cs and ^{210}Pb analyses, ^{14}C ages, and varve counts. The presence of ^{137}Cs or ^{210}Pb in six of the eight cores indicates that the top or near top of the sediment column had been recovered during coring. This provides a datum (AD 1994) for correlating the uppermost part of these cores. Radiocarbon ages help determine the stratigraphic position of the two cores lacking ^{137}Cs and ^{210}Pb .

(TUL89A-001 and 002). Finally, varve counts provide cross-checks on accuracy of ^{14}C and ^{210}Pb ages.

Generally, there is a good correlation between the varve counts and the ^{14}C ages (see vertical arrows on Fig. 3-6). However, correlations are less certain in the upper part of the cores above the highest ^{14}C ages and below the ^{137}Cs and ^{210}Pb zones. The core with the largest number of massive layers (TUL89A-003) has a ^{210}Pb age near the top. There is also good agreement between a ^{14}C age on shell fragments at 10.4 m depth in the core, and the total number of varves down to that depth. The calibrated mean age on the shell fragments at 10.4 m depth is 1080 cal y BP (2σ range=940-1240 cal y BP). The ^{210}Pb age and varve counts give an age of 1205 years (from the 1994 datum) at the same depth. Comparison of these two data sets suggests that there are no more than 79 missing and uncounted varves in core TUL89A-003. The age estimates for the massive layers in this core, based on varve counts are thus considered to be accurate to within 6% (Table 3-7).

One ^{14}C age (age range: 290-545 cal y BP, TO-4050) from the upper part of core TUL91A-003 may be too young, although it is consistent with the age of the top of the core inferred from ^{137}Cs data and the calculated sedimentation rate. If it is valid, the two ^{14}C ages from the top of this core are too old. In either case, the correlation of this core with the others remains unchanged because of the presence of ^{137}Cs as a datum.

Regional correlations

The number of varves separating successive massive layers ranges from 15

Table 3-7. Age of massive layers for core TUL89A-003

Massive layer	Age of massive layer (years)
1	59
2	334
3	441
4	512
5	554
6	810
7	850
8	921
9	936
10	1042
11	1101
12	1435

Note: Age is determined by cumulative number of varves from top of core to massive layer (1994 datum).

(TUL89A-003) to > 754 (TUL91A-003). For the core with the largest number of massive layers (TUL89A-003), there are, on average, 116 varves per layer (range=15-336).

It is difficult to positively correlate massive layers between the cores because of the lack of unique markers, inherent imprecision of radiocarbon ages, and the possibility of sediment loss due to stripping of varves by debris flows. However, some massive layers in two or more cores appear to correlate, based on varve counts below the surface datum established from ^{137}Cs and ^{210}Pb data (Fig. 3-6; Table 3-6). The correlations become less certain with depth because of the increasing likelihood that varves have been lost due to erosion by debris flows.

Inspection of Table 3-6 suggests that there are possible correlations of massive layers dating about 200, 400-500, 750-850, 1000-1150, and 1450 years ago. We attempted to refine the correlations by adjusting the ages of successively older massive layers to account for missing varves using the following procedure. The youngest massive layers of approximately the same age were assumed to correlate; of the two or more correlated layers, that with the fewest number of varves above it was assigned the same age as the layer with the largest number of varves (Table 3-8). When the age of a massive layer was increased, all the other massive layers below it in that core were similarly adjusted. Correlations and related age adjustments were carried out in a step-wise fashion down the cores until there were no further matches (Table 3-8).

Three scenarios were considered. In one scenario, we correlated the third

Table 3-8. Scenario (a) Possible correlations based on adjusted cumulative number of varves (Table 3-6)

South		North				
TUL91A-001*	TUL89A-001	TUL91A-002*	TUL89A-003*	TUL91A-004*	TUL89A-002	TUL91A-003*
40	105	203 202 I	59	254	107	155
ml	ml	ml	ml	ml	ml	ml
176	216	385 384	334	443 425 II	161	
ml	ml	ml	ml	ml	ml	
203 I	485	484 483	443 441 II	556 547 529 IV	543	
ml	ml	ml	ml	ml	ml	
443 II	557	682 681	514 512 III	830 817 808 790 V	613	
ml	ml	ml	ml		ml	
514 512 III	690	746 745	556 554 IV		743	
ml	ml	ml	ml		ml	
644 642	823	876 875 VI	830 812 810 V		938	
ml	ml	ml	ml			
760 758	887	1018 1017	876 870 852 850 VI			
ml	ml	ml	ml			
830 828 V	1223	1068 1066 1065 VII	947 941 923 921			
ml		ml	ml			
1068 1059 1057 VII		1390 1388 1387	962 956 938 936			
ml		ml	ml			
1138 1129 1127 VIII	1472 1464 1462 1461 IX		1068 1062 1044 1042 VII			
ml			ml			
1308 1299 1297		1138 1127 1121 1103 1101 VIII	ml			
			ml			
		1472 1461 1455 1437 1435 IX				

Note: Asterisk indicates presence of ^{137}Cs or ^{210}Pb . The massive layers of the two cores that lack ^{137}Cs and ^{210}Pb have not been correlated. See text for explanation of the adjustment method.

massive layer in core TUL91A-001 with the first massive layer in core TUL91A-002 (scenario (a); Table 3-8). This produced correlations at 203, 443, 514, 556, 830, 876, 1068, 1138, and 1472 years. The second and third scenarios assume that the first massive layers of cores TUL89A-003 and TUL91A-001 correlate; in one case both are considered to be 40 years old and in the other case, 59 years old (scenarios (b) and (c), respectively; Appendix 3-8). All three scenarios yield similar correlations in the upper parts of the cores, massive layers that are 202-203, 441-443, and 545-556 years old. In the lower parts of the cores, the correlations are less certain, although there appear to be correlative layers with ages of approximately 800-850, 1050-1100, 1100-1150, and 1450-1500 years (Table 3-9).

Style and pattern of sedimentation

The eight cores collected from Saanich Inlet provide a sediment record spanning 1500 years (Fig. 3-6; Table 3-6). During fall and winter, terrigenous sediment (clay, silt, and some fine sand) with few diatoms is deposited from suspension. During spring and summer, diatom-rich sediment rains out onto the floor of the inlet. Sedimentation rates decrease from north to south demonstrating that the main source of sediment is the Cowichan River. Seven of the eight cores show regular deposition of rhythmites under anoxic conditions, interrupted sporadically by high-energy debris flows that erode varves along their path (Fig. 3-13).

Particle-size distribution in the varves shows no relation to sedimentation rate. For example, comparison of varves from cores TUL91A-001 and TUL89A-001 (Fig. 3-10; Appendix 3-4), the two most southerly cores, indicates that coarseness of the

Table 3-9. Summary of correlations based on scenarios a), b), and c)

a)	b)	c)
	I=59	I=40
I=203	II=202	II=203
II=443	III=441	III=443
III=514		IV=514
IV=556	IV=545	V=556
		VI=760
V=830	V=810	VII=830
VI=876	VI=880	
VII=1068	VII=1042	VIII=1080
VIII=1138	VIII=1109	IX=1150
IX=1472	IX=1443	X=1484

Note: Roman numeral indicates correlation number; arabic number indicates years (1994 datum).

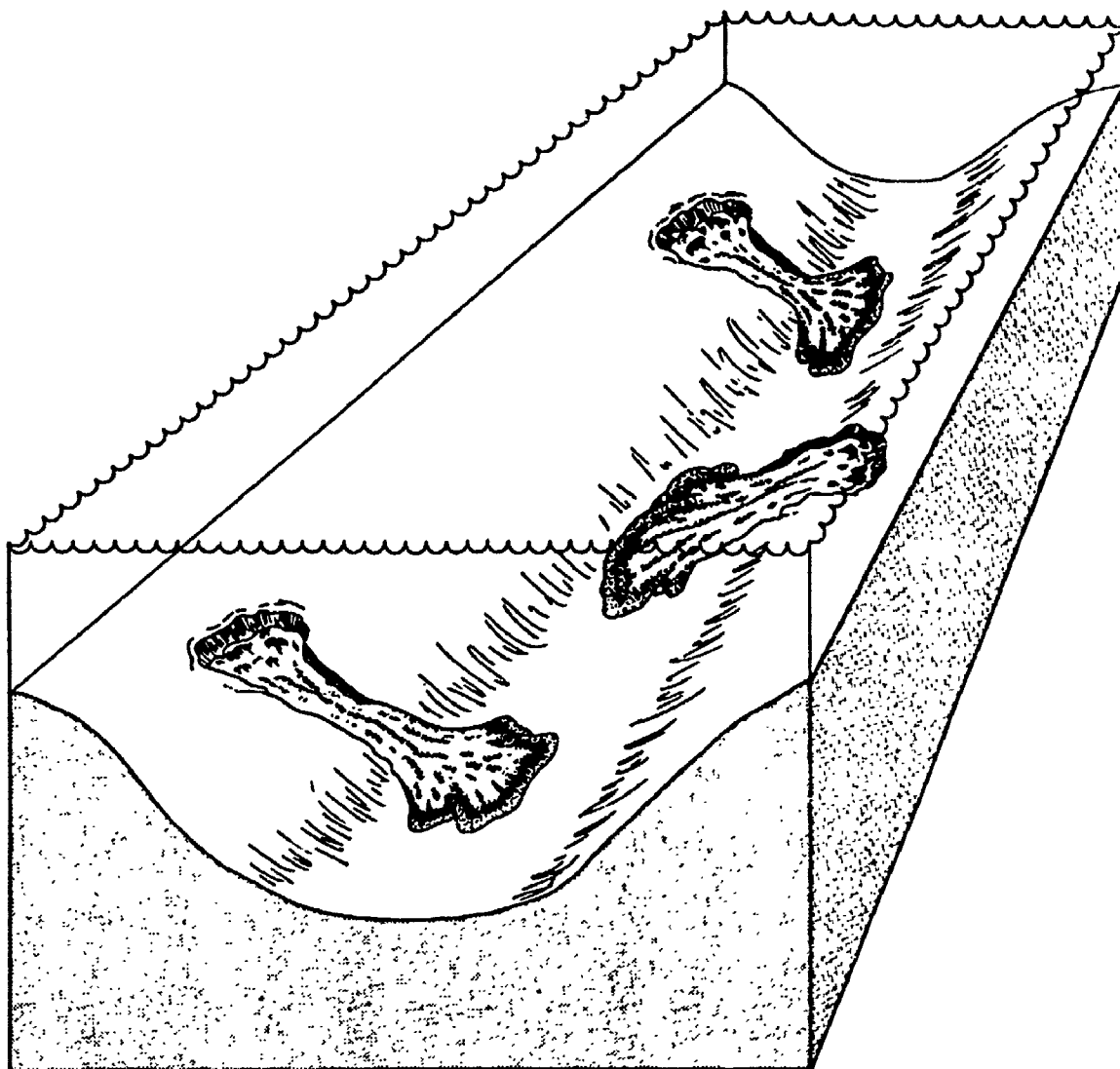


Figure 3-13. Schematic diagram showing the inferred origin of massive layers within the varved sequence in Saanich Inlet.

varves does not depend on the sedimentation rate. This implies that the coarser material (fine sand) has been deposited from sources additional to Cowichan River, such as ephemeral streams and, perhaps, Goldstream River.

The possibility that turbidity currents could originate from the Cowichan River delta and carry sediments into Saanich Inlet was considered. However, there are arguments against this hypothesis: (1) Given the bathymetry (Plate 1-1), the size of the sediment failure and turbidity flow would have to be extremely large. The flow would have to start at Cowichan Bay, follow the bathymetry down to 154 m, take a right turn, climb over the sill at 70 m, and travel down Saanich Inlet; (2) there are no classic Bouma-sequence turbidites in the cores; (3) the massive layers do not show grading or imbrication of clasts typical of turbidites; (4) if south flowing turbidity currents deposited the massive layers, the layers would be thicker and coarser (proximal to source) in the north and thinner and finer (distal to source) in the south. On the contrary, the massive layers show no such trends in thickness (Appendices 3-3, 3-4, and 3-8).

The northernmost core (TUL91A-005) lacks the rhythmic lamination of the other seven cores. It was first hypothesized that the sediments in this core were deposited by one large debris flow. However, this interpretation is discounted because of the presence of (1) undisturbed clay laminae throughout the core (Plate 3-5) similar to the ones found in the varves, (2) faint layering reflecting subtle colour and probably textural variations, and (3) paired bivalve shells that lived in situ, within the mud.

The sediments of core TUL91A-005 possess more silt than the varves and massive layers in the other cores (Fig. 3-11). This leads us to conclude that the sediments in this core were deposited from suspension like the varves, but closer to the main source of terrigenous sediment (Cowichan River).

There are at least two possible explanations for the absence of rhythmic lamination at the northernmost core site. The site is adjacent to the sill at the north end of the inlet, nearest the Cowichan River. As a consequence, the high influx of terrigenous sediment throughout the year may overwhelm the seasonal diatom blooms that produce the light-coloured laminae farther south. This explanation was proposed earlier by Sancetta (1989, p. 509), who commented that the north end of the basin near the sill "receives a large component of lithic particles all year round". A second possible explanation is that bottom waters at this site may be oxygenated. This would allow bivalves and other infauna to bioturbate the sediments, obscuring or destroying stratification. The presence of calcareous foraminifera within the sediments indicates that there is some oxygen at the sediment-water interface, for otherwise these foraminifera would be dissolved in reducing anoxic conditions. This suggests that, at least near the sill, the depth to which oxic conditions occur is deeper than 150 m in the northern part of the basin than in the central part of the basin.

As mentioned previously, there are more massive layers in the southern part of the inlet where the sedimentation rate is lower compared to the northern part where the sedimentation rate is higher. Assuming that sediment accumulates on steep as well as shallow basin walls in the inlet, more frequent failures would be expected

where the slopes are steeper, which is consistent with the core data.

Causes of the debris flows

In Saanich Inlet, potential causes of slope failures such as current scour, surface water waves, and tidal water level changes (Prior and Coleman, 1984) are not likely to occur because of the quiet nature of the basin waters. However, there are two other mechanisms for potentially triggering sediment gravity flows in Saanich Inlet. The first is oversteepening of slopes, i.e., accumulating sediments exceed their critical angle of repose. This could result from progressive deposition of sediment from suspension on the walls of the inlet or from the growth of deltas, such as the Goldstream River delta or ephemeral streams.

The second mechanism is seismic shaking. Whether or not an earthquake would trigger debris flows in Saanich Inlet depends on many factors, including (1) the amount of sediment on the walls of the inlet, (2) the strength of the sediments being shaken, (3) the acceleration and period of the seismic waves, and (4) the duration of shaking. From the core data, it is not possible to assess these factors. Nevertheless, some alternative scenarios can be proposed.

Model 1: None of the debris flows were triggered by earthquakes

Many of the massive layers do not appear to correlate from one core to the next, and it is possible that the debris flows were independently triggered at different times. The lack of correlation of many of the massive layers could be explained by random failure of slopes on which sediment is gradually accumulating. However, this triggering mechanism cannot easily explain massive layers that can be correlated over

large areas, i.e., at over two or more core sites. If massive layers correlate at two different core sites, and these sites are separated by one at which massive layers do not correlate, it is implied that two separate debris flow events occurred simultaneously. Separate simultaneous debris flows are harder to explain in a setting where slope failure occurs due to gradual build-up of sediment than in one where the trigger is earthquakes.

Model 2: All of the debris flows were triggered by earthquakes

Exposed sections of rhythmically stratified, Pleistocene glaciolacustrine varves in the Puget Lowland of Washington, approximately 120 km southeast of Saanich Inlet, contain deformational structures similar to those produced by simulated seismic shaking (Sims, 1975). Sims estimated that in a section of 1804 varves, 14 of 21 exposed deformed zones were the result of seismic shaking, giving an average of 129 varves between each seismic event. Successive deformed zones were separated by 60 to 276 varves. By including additional deformational structures that could potentially be products of earthquakes, the range becomes 23 to 276 varves. Sims (1975) concluded from this study that varves could be used to determine the age of these deformational structures and, hence, seismic activity assuming the presence of a datum.

Sims' results coincide roughly with ours. As mentioned above, the number of varves separating massive layers in Saanich Inlet ranges from 15 to >754, with an average of 116. This average is near Sim's estimate of the average number of years separating deformed zones caused by seismic shaking.

The recurrence interval of earthquakes of Modified Mercalli Intensity VII or VIII in the Victoria area is about one every hundred years (Rogers and Hasewaga, 1978; Rogers, 1980; G. C. Rogers, written communication, 1994). Assuming that such an earthquake could trigger failures of sediments on the walls of Saanich Inlet, it is possible that all the massive layers in the cores are products of earthquakes. Core TUL89A-003, for example, contains 10 massive layers that are younger than 1000 years, and it is possible that each corresponds to an earthquake (ages summarized in Table 3-7). If this is correct, cores from the southern part of the inlet contain a more complete record of earthquakes than cores farther north, probably because it requires less seismic energy to produce slope failures where the side walls are steeper. The earthquakes responsible for these slope failures might include all three types: crustal and subcrustal events, and rarer, larger plate-boundary events.

Four massive layers in Saanich Inlet may be contemporaneous with moderate to large earthquakes that have been documented elsewhere in southwestern British Columbia and Washington state. The uppermost massive layers in core TUL89A-003 and, possibly, core TUL91A-001 may be products of the 1946 Vancouver Island earthquake, centered near Comox, 200 km north-northwest of Saanich Inlet (Rogers and Hasewaga, 1978; Rogers, 1980). The uppermost massive layer in TUL89A-003 gave an age of about 59 years (1935 AD), based on ^{210}Pb data and varve counts. There are uncertainties in calculating ^{210}Pb ages using best-fit regression lines that could introduce errors of a few tens of years. This might account for an apparent date of 1935 AD for an event that actually occurred in 1946. The presence of ^{137}Cs

within the uppermost massive layer in core TUL91A-001 suggests a slightly younger age (post-1954), but if coring has disturbed the uppermost soupy sediments, the debris flow deposit may be slightly older than the ^{137}Cs data suggest.

A massive layer dating to about 200 years ago may have been emplaced during a strong earthquake recorded by Spanish explorers wintering on the west coast of Vancouver Island in 1793 (Clague, 1995). Another layer about 550 years old or one 800-850 years old may date to an earthquake that occurred sometime between 500 and 800 cal y BP (Clague and Bobrowsky, 1994b), although this link is tenuous.

Another large earthquake, centered near Seattle, approximately 140 km south-southeast of Saanich Inlet, occurred about 1000-1100 years ago and may be responsible for a widespread massive layer in Saanich Inlet that dates to about 1050-1150 years ago. This earthquake produced surface rupture, numerous large landslides and subaqueous slope failures, and a tsunami in Puget Sound (Atwater and Moore, 1992; Bucknam and others, 1992; Jacoby and others, 1992; Karlin and Abella, 1992; Schuster and others, 1992). Although the earthquake was a considerable distance from Saanich Inlet, it apparently was very large and may have caused sufficiently strong ground motion on southern Vancouver Island to trigger debris flows in Saanich Inlet. There is also evidence that a Cascadia megaquake may have occurred about 1000 years ago (Darienzo and Petersen, 1990; 900-1300 years ago, Atwater, 1992), perhaps related to the Seattle event.

The last great earthquake or series of closely spaced earthquakes on the Cascadia subduction zone occurred about 300 years ago. There is abundant evidence

for this event in coastal wetlands from northern California to central Vancouver Island (Atwater, 1987, 1992; Darienzo and Peterson, 1990; Atwater and Yamaguchi, 1991; Clarke and Carver, 1992; Nelson, 1992; Obermeier and others, 1993; Clague and Bobrowsky, 1994a, b). The area affected by this earthquake was very large and should have included southern Vancouver Island. Although Saanich Inlet should have been severely shaken, only one massive layer in core TUL89A-003 was found that might coincide with this event.

In summary, given that moderate to large earthquakes capable of generating debris flows in Saanich Inlet are fairly frequent and that at least two historic earthquakes appear to have produced such failures, one could conclude that all of the massive layers record earthquakes. If correct, an earthquake strong enough to trigger failures in Saanich Inlet occurs, on average, once every 100 years. Intervals of earthquakes, however, are probably highly variable (a few tens to hundreds of years, judging by the record of massive layers in core TUL89A-003; Table 3-7).

Model 3: Some, but not all of the debris flows, were triggered by earthquakes

It is likely that the widespread massive layers that are about 200, 550-850, and 1050-1150 years old are products of earthquakes. Several other massive layers probably are present in two or more cores, and they too may have been emplaced by earthquakes. For example, massive layers at about 440, 550, 800-850, and 1450-1500 years old may represent as yet unreported seismic events. On the other hand, some massive layers appear to be present in only one core. The flows that deposited

them just as likely were caused by the slope failures due to gradual progressive buildup of sediment on the walls of the inlet or earthquakes. Nevertheless, given the presence of potentially unstable accumulations of sediment on these slopes, it might be expected that every strong earthquake that has struck the area would trigger debris flows. Thus, Saanich Inlet probably contains a proxy record of moderate to large earthquakes during Holocene time, but the set of massive layers includes nonseismically triggered debris flows in addition to those caused by earthquakes (Fig. 3-14).

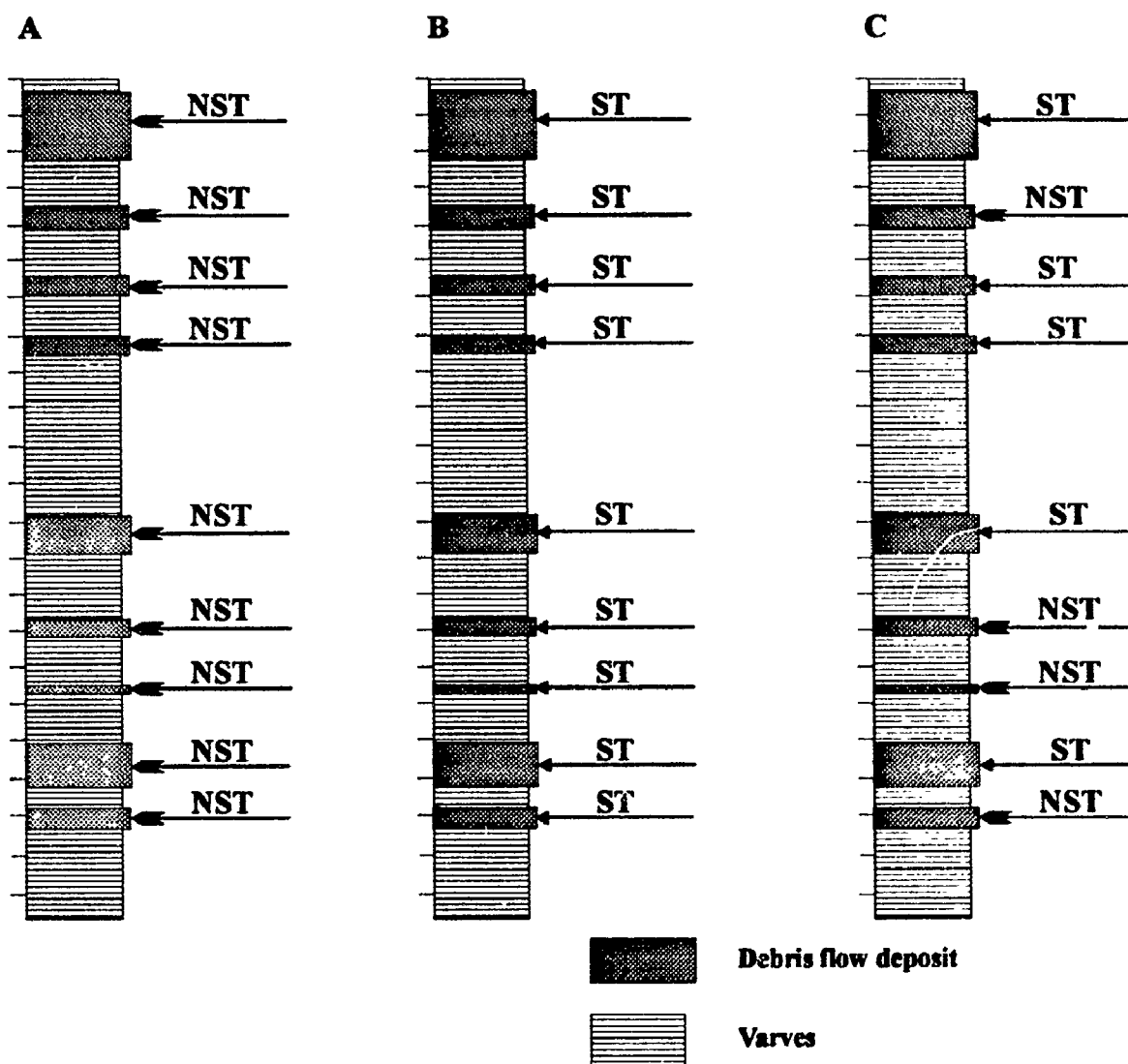
Error analysis

Lack of a precise datum

There are potentially many sources of error in estimating the ages of the massive layers. The most important is probably the lack of a datum in the cores. This potential error stems from the possibility that the uppermost sediments, directly below the seafloor, were lost during coring. When using ^{210}Pb as a dating tool, it is important to collect the uppermost sediments in order to measure the initial activity concentration of excess ^{210}Pb at a specific site. When it is not certain if the uppermost sediments are in a core, the initial activity concentration can be extrapolated using a statistical regression line method (R. Flett, oral communication, 1994) to calculate the age of the sediments. The calculated age, however, is subject to uncertainties.

A complete profile of concentrations ^{137}Cs provides precise age estimates; i.e., the peak concentration in radiocesium should correspond to 1964. The mere presence

Figure 3-14. Three interpretations of a hypothetical sequence of massive layers deposited by debris flows in Saanich Inlet. A. No debris flow deposits were seismically triggered (NST). B. All the debris flow deposits were seismically triggered (ST). C. Some debris flow deposits were seismically triggered. (A, B, and C correspond to models 1, 2, and 3, respectively, in the text).



of radiocesium shows the sediments are younger than 1954, but does not give a precise age.

Carbon-14 dating provides ages that are accurate to, at best, 20 years, and more commonly 100 to several hundred years. Therefore ^{14}C dating is not very helpful in establishing the ages of the massive layers in our cores which are less than 1500 years old. In addition, there is an uncertain reservoir age correction that must be applied to marine fossils when they are dated (Robinson and Thomson, 1981; Stuiver and Braziunas, 1993). The reservoir age correction of 801 ± 23 years calculated for marine organisms from coastal Washington, Oregon and adjacent British Columbia may not be appropriate for Saanich Inlet. It is possible that the reservoir age for organisms from Saanich Inlet may be different.

Missing varves

Another possible source of error in estimating the ages of massive layers is that some varves may be missing. The reasons for missing varves are that: (1) erosion during deposition of the massive layers (the cumulative total of missing varves increases downcore) and (2) disturbance during coring or sectioning. Our attempts at correlation, however, indicate that only 6% of the varves are missing in the core with the greatest number of massive layers.

Contamination

When using radioisotopes to date sediments, there is always the possibility that the material being dated is contaminated or reworked. Precautions are taken to prevent contamination, but the possibility can rarely be completely ruled out. By

submitting a large number of samples, as in this study, and by using different methods of dating, one can minimize these sources of error.

Dating using varves

The use of varves to precisely date massive layers was met with some problems mainly because of uncertainties in the ages of the tops of the cores (see above discussion). These uncertainties led us to refine our correlations using the method outlined earlier in the chapter (Table 3-6; Appendix 3-8). Ages of the massive layers that were similar in all three scenarios provided the age ranges of that we cite. The age ranges increase downcore because of the increase in number of missing varves due to erosion by debris flows (Table 3-9). Hence, in our study, taking into account the sources of error, an error estimate using varves is in the order of 10-20 years for massive layers correlations younger than 550 years and 20-100 years for those older than 550 years.

CONCLUSIONS

1. Deep-water sediments in Saanich Inlet consist mainly of silty clay varves and intercalated massive beds of silty clay. The varved sediments consist of alternating layers of terrigenous detritus, derived primarily from Cowichan River, and diatoms produced during spring and summer blooms. The varves thus record the quiet progressive deposition of sediment from suspension.
2. Sedimentation rates decrease from north to south confirming Cowichan River as the main source of sediment. However, particle-size variations in the varves indicate

that there are additional sediment sources, likely including ephemeral streams and perhaps Goldstream River.

3. Several types of evidence indicate that the massive layers were deposited by sediment gravity flows: (a) a Student t-test on the contents of sand in varves and massive layers indicates that the massive layers are allogenic; (b) basal contacts of massive layers are sharp, and some are clearly erosional; (3) one massive layer in core TUL91A-001 has a 2 cm thick granule base that erosionally overlies varves; (d) most massive layers contain brecciated varves and varve intraclasts indicating that varves have been eroded and incorporated into the flow; (e) most massive layers exhibit a lower brecciated zone of varves underlying massive mud; (f) most massive layers contain benthic foraminifera, which implies that the sediment was transported from above the anoxic zone (< 150 m depth). Massive layers are more common in the southern part of Saanich Inlet, where the side walls are steep, than in the northern part where slopes are gentler.
4. Massive layers are products of small failures of sediments from the side walls of Saanich Inlet, rather than large turbidity flows that travel the length of the fiord.
5. The sediment gravity flows are more precisely defined as debris flow deposits rather than turbidites because: (a) none of the massive layers exhibit sedimentary structures and textures of a classic turbidite, i.e., Bouma-sequence; (b) there is no normal or inverse grading in the massive layers; (c) most massive layers contain a zone of brecciated varves thought the result from shearing at the base of a debris flow in the zone of laminar flow; (d) massive mud overlying the brecciated zone is

interpreted as the plug or raft of the debris flow; and (e) varve intraclasts show no apparent directional fabric.

6. Most, but probably not all of the massive layers were emplaced during earthquakes. These earthquakes include both distant great plate-boundary events and smaller local crustal and subcrustal quakes. Massive layers at the top of cores TUL89A-003 and TUL91A-001 may have been deposited during the 1946 Vancouver Island earthquake (M7.2; Modified Mercalli Intensity VI at Saanich Inlet). A massive layer, dating to about 200 years ago and found in cores TUL91A-001 and TUL91A-002, may have been emplaced during a strong earthquake in February 1793, reported by Spanish explorers wintering on the west coast of Vancouver Island. Another widespread massive layer, about 1050-1150 years old, may record a large crustal earthquake centered near Seattle, 140 km south-southeast of Saanich Inlet. This earthquake may be linked to plate-boundary failure farther west. Some of the other massive layers probably record other prehistoric earthquakes as yet undocumented elsewhere. Still other massive layers may be products of nonseismically triggered failures of metastable sediments that have gradually accumulated on the side slopes of the inlet.

7. The number of varves separating adjacent massive layers in the eight cores ranges from 15 to >754. The average value of 116 is broadly consistent with the expected periodicity of moderate to large earthquakes in the region.

8. There are several sources of error that introduce uncertainty into the age estimates for the massive layers in Saanich Inlet. These include uncertainties in the ages of the

uppermost sediments in the cores and loss of varves due to erosion by debris flows.

ACKNOWLEDGEMENTS

This research was funded by the Geological Survey of Canada (GSC; J. J. Clague's Project No. 870017) and by the Natural Sciences and Engineering Research Council of Canada (Operating Grant OGP0041665 to R. T. Patterson). Cores were collected by R. McDonald and G. Jewsbury (Pacific Geoscience Centre; PGC). B. Hart (New Mexico Bureau of Mines and Mineral Resources) supplied a sample from Fraser River for clay mineral analysis. T. Forbes (PGC) did the particle-size analyses and provided assistance in the laboratory. W. Bentkowski and T. Hamilton (PGC) made the ^{137}Cs determinations. Carbon-14 age dating and calibrations were done by R. P. Beukens at IsoTrace Laboratory, and ^{210}Pb determinations were made R. J. Flett of Flett Research Ltd. Clay-mineral analyses were performed by R. Delabio (GSC). D. Everett of the GSC Cartography Division drafted Figure 3-13. A. Collins is thanked for sharing some of the results of her study. Discussions with B.S. Hart, R.W.C. Arnott, and P.T. Bobrowsky have greatly improved the manuscript. M. Taylor and E. Keane (students) assisted for one summer in data processing. W. R. Stevens provided technical assistance throughout the project.

REFERENCES

- Adams, J., 1990, Paleoseismicity of the Cascadia subduction zone -evidence from turbidites off the Oregon-Washington margin: *Tectonics*, vol. 9, p. 569-583.
- Anderson, J. J. and Devol, A. H., 1973, Deep water renewal in Saanich Inlet, an intermittently anoxic basin: *Estuarine and Coastal Marine Science*, vol. 1, p. 1-10.
- Anderson, R. F., LeHuray, A. P., Fleisher, M. Q., and Murray, J. W., 1989, Uranium deposition in Saanich Inlet sediments, Vancouver Island: *Geochimica et Cosmochimica Acta*, vol. 53, p. 2205-2213.
- Arnott, R.W.C. and Hand, B.M., 1989, Bedforms, primary structures and grain fabric in the presence of suspended sediment rain: *Journal of Sedimentary Petrology*, vol. 59, p. 1062-1069.
- Ashley, G. M. and Moritz, L. E., 1979, Determination of lacustrine sedimentation rates by radioactive fallout (^{137}Cs), Pitt Lake, British Columbia: *Canadian Journal of Earth Sciences*, vol. 16, p. 965-970.
- Atwater, B. F., 1987, Evidence for great Holocene earthquakes along the outer coast of Washington State: *Science*, vol. 236, p. 942-944.
- Atwater, B. F., 1992, Geologic evidence for earthquakes during the past 2000 years along the Copalis River, southern coastal Washington: *Journal of Geophysical Research*, vol. 97, p. 1901-1919.
- Atwater, B. F. and Moore, A. L., 1992, A tsunami about 1000 years ago in Puget Sound, Washington: *Science*, vol. 258, p. 1614-1616.

- Atwater, B. F. and Yamaguchi, D. K., 1991, Sudden, probably coseismic submergence of Holocene trees and grass in coastal Washington state: *Geology*, v. 19, p. 706-709.
- Beasley, T. M., 1969, Lead-210 production by nuclear devices 1946-1958: *Nature*, vol. 224, p. 573.
- Blais, A., 1992, Holocene sediments from Saanich Inlet, British Columbia and their neotectonic implications: Current Research, Part A; Geological Survey of Canada, Paper 92-1A, p. 195-198.
- Blais, A. and Patterson, R. T., Foraminiferal biofacies of Saanich Inlet, Vancouver Island, British Columbia: Valuable environmental indicators: *Journal of Foraminiferal Research*, in press.
- Blais, A., Clague, J. J., and Bobrowsky, P. T., 1993, Marine geological studies of coastal areas: Saanich Inlet to the Fraser River delta: Canadian Quaternary Association, Program with Abstracts and Field Guide, p. G19-G23.
- Bobrowsky, P. T. and Clague, J. J., 1990, Holocene sediments from Saanich Inlet, British Columbia, and their neotectonic implications: Current Research, Part E, Geological Survey of Canada, Paper 90-1E, p. 251-256.
- Bornhold, B. D., 1978, Carbon/nitrogen (C/N) ratios in surficial marine sediments of British Columbia: Current Research, Part C, Geological Survey of Canada, Paper 78-1C, p. 108-112.

- Brown, F. S., Baedeker, M. J., Nissenbaum, A., and Kaplan, I. R., 1972, Early diagenesis in a reducing fjord, Saanich Inlet, British Columbia-III. Changes in organic constituents of sediment: *Geochimica et Cosmochimica Acta*, vol. 36, p. 1185-1203.
- Bucknam, R. C., Hemphill-Haley, E., and Leopold, E. B., 1992, Abrupt uplift within the past 1700 years at southern Puget Sound, Washington: *Science*, vol. 258, p. 1611-1613.
- Buddemeier, R. W., 1969, A radiocarbon study of varved marine sediments of Saanich Inlet, British Columbia: Ph. D. thesis, University of Washington, Seattle, Washington, 126 p.
- Carpenter, R. and Beasley, T. M., 1981, Plutonium and americium in anoxic marine sediments: Evidence against remobilization: *Geochimica et Cosmochimica Acta*, vol. 45, p. 1917-1930.
- Carter, N. M., 1934, Physiography and oceanography of some British Columbia fiords: *Proceedings of the Fifth Pacific Science Congress, Pacific Science Association, Vancouver, B.C., 1933*, vol. 1, p. 721-733.
- Clague, J. J., 1995, Early historical and ethnographical accounts of large earthquakes and tsunamis on western Vancouver Island, British Columbia: *Current Research 1995-A*, Geological Survey of Canada, p. 47-50.
- Clague J. J. and Bobrowsky, P. T., 1993: Implications of a large earthquake in British Columbia: *Canadian Quaternary Association, Program with Abstracts and Field Guide*, p. A9.

- Clague J. J. and Bobrowsky, P. T., 1994a, Evidence for a large earthquake and tsunami 100-400 years ago on western Vancouver Island, British Columbia: *Quaternary Research*, vol. 41, p. 176-184.
- Clague J. J. and Bobrowsky, P. T., 1994b, Tsunami deposits beneath tidal marshes on Vancouver Island, British Columbia: *Geological Society of America Bulletin*, vol. 106, p. 1293-1303.
- Clague, J. J., Bobrowsky, P. T., Hamilton, T. S., 1994, A sand sheet deposited by the 1964 Alaska tsunami at Port Alberni, British Columbia: *Estuarine Coastal and Shelf Science*, vol. 38, p. 413-421.
- Clague, J. J., Naesgaard, E., and Sy, A., 1992, Liquefaction features on the Fraser delta: evidence for prehistoric earthquakes?: *Canadian Journal of Earth Sciences*, vol. 29, p. 1734-1745.
- Clarke, S., H., Jr., and Carver, G. A., 1992, Late Holocene tectonics and paleoseismicity, southern Cascadia subduction zone: *Science*, vol., 255, p. 188-192.
- Cowie, G. L., Hedges, J. I., and Calvert, S. E., 1992, Sources and relative reactivities of amino acids, neutral sugars, and lignin in an intermittently anoxic marine environment: *Geochimica et Cosmochimica Acta*, vol. 56, p. 1963-1978.
- Crosson, R. S. and Owens, T. J., 1987, Slab geometry of the Cascadia subduction zone beneath Washington from earthquake hypocenters and teleseismic converted waves: *Geophysical Research Letters*, vol. 14, p. 824-827.

- Darlenzo, M. E. and Peterson, C. D., 1990, Episodic tectonic subsidence of late Holocene salt marshes, northern Oregon, central Cascadia margin: *Tectonics*, vol. 9, p. 1-22.
- Davis, J. C., 1986, *Statistics and data analysis in geology*, second edition, John Wiley and Sons, Toronto, 646 p.
- Devol, A. H. and Ahmed, S. I., 1981, Are high rates of sulphate reduction associated with anaerobic oxidation of methane?: *Nature*, vol. 291, p. 407-408.
- Devol, A. H., Anderson, J. J., Kuivila, K., and Murray, J. W., 1984, A model for coupled sulphate reduction and methane oxidation in the sediments of Saanich Inlet: *Geochimica et Cosmochimica Acta*, vol. 48, p. 993-1004.
- Dragert, H., Hyndman, R. D., Rogers, G. C., and Wang, K., 1994, Current deformation and the width of the seismogenic zone of the northern Cascadia subduction thrust: *Journal of Geophysical Research*, vol. 99, p. 653-668.
- Eakins, J. D. and Morrison, R. T., 1978, A new procedure for determination of ^{210}Pb in lake marine sediments: *International Journal of Applied Radiation and Isotopes*, vol. 29, p. 531-536.
- EnviroEd Consultants Limited, 1995, Saanich Inlet study synthesis workshop, Information package, April 25-26: hosted by Ministry Lands and Parks of British Columbia, Saanich Native Heritage Society, and Institute of Ocean Sciences, 46 p.
- Feely, H. W. and Seitz, H., 1970, Use of lead-210 as a tracer of transport processes in the stratosphere: *Journal of Geophysical Research*, vol. 75, p. 2885-2894.

- François, R., 1988, A study on the regulation of the concentrations of some trace metals (Rb, Sr, Zn, Pb, Cu, V, Cr, Ni, Mn, and Mo) in Saanich Inlet sediments, British Columbia, Canada: *Marine Geology*, vol. 83, p. 285-308.
- Geyh, M. A. and Schleicher, H., 1990, Absolute age determination, physical and chemical dating methods and their application, Springer-Verlag, New York, 503 p.
- Gross, M. G., Gucluer, S. M., Creager, J. S., and Dawson, W. A., 1963, Varved marine sediments in a stagnant fjord: *Science*, vol. 141, p. 918-919.
- Gucluer, S. M., 1962, Recent sediments in Saanich Inlet, British Columbia: M.Sc. thesis, University of Washington, Seattle, Washington, 119 p.
- Gucluer, S. M. and Gross, M. G., 1964, Recent marine sediments in Saanich Inlet, a stagnant marine basin: *Limnology and Oceanography*, vol. 9, p. 359-376.
- Hamilton, S. E. and Hedges, J. I., 1988, The comparative geochemistries of lignins and carbohydrates in an anoxic fjord: *Geochimica et Cosmochimica Acta*, vol. 52, p. 129-142.
- Herlinveaux, R. H., 1962, Oceanography of Saanich Inlet in Vancouver Island, British Columbia: *Fisheries Research Board of Canada Journal*, vol. 19, no. 1, p. 1-37.
- Heusser, L. E., 1983, Palynology and paleoecology of postglacial sediments in an anoxic basin, Saanich Inlet, British Columbia: *Canadian Journal of Earth Sciences*, vol. 20, p. 873-885.

- Holtzapffel, T., 1985, Les minéraux argileux: Préparation: Analyse diffractométrique et détermination: Société Géologique du Nord, Publication no 12, p. 1-136.
- Hyndman, R. D. and Wang, K., 1993, Thermal constraints on the zone of major thrust earthquake failure: the Cascadia subduction zone: Journal of Geophysical Research, vol. 98, p. 2039-2060.
- Jacoby, G. C., Williams, P. L., and Buckley, B. M., 1992, Tree ring correlation between prehistoric landslides and abrupt tectonic events in Seattle, Washington: Science, vol. 258, p. 1621-1623.
- Johnson, A. M. and Rodine, J. R., 1984, Debris flow: Slope instability (D. Brunsten and D. B. Prior, eds.), John Wiley and Sons, New York, p. 257-361.
- Karlin, R. E. and Abella, S. E. B., 1992, Paleoearthquakes in the Puget Sound region recorded in sediments from Lake Washington, U.S.A.: Science, vol. 258, p. 1617-1619.
- Kromer, B. and Becker, B., 1993, German oak and pine ^{14}C calibration, 7200-9439 B.C.: Radiocarbon, vol. 35, p. 125-135.
- Kuivila, K. M., Murray, J. W., and Devol, A. H., 1990, Methane production in the sulphate-depleted sediments of two marine basins: Geochimica et Cosmochimica Acta, vol. 54, p. 403-411.

- Linick, T. W., Long, A., Damon, P. E., and Ferguson, C. W., 1986, High-precision radiocarbon dating of bristlecone pine from 6554 to 5350 B.C.: *Radiocarbon*, vol. 28 (2B), p. 943-953.
- Lister, C. R. B., 1967, Shallow seismic profiling in Saanich Inlet: *Northwest Science*, vol. 41, p. 80-83.
- Macdonald, R. W., Macdonald, D. M., and Wong, C. S., 1984, A manual for the determination of ^{210}Pb at Ocean Chemistry: Canada Department of Fisheries and Oceans, Institute of Ocean Sciences, Sidney, B. C., 37 p.
- Mackintosh, E. E. and Gardner, E. H., 1966, A mineralogical and chemical study of lower Fraser River alluvial sediments: *Canadian Journal of Soil Science*, vol. 46, p.37-46.
- Mathewes, R. W., 1985, Paleobotanical evidence for climatic change in southern British Columbia during late-glacial and Holocene time: *Climatic Change in Canada 5, Critical Periods in the Quaternary Climatic History of Northern North America*, (C. R. Harington, ed.): National Museums of Canada, National Museum of Natural Sciences, Syllogeus Series, no. 55, p. 397-422.
- Mathewes, R. W. and Clague, J. J., 1994, Detection of large prehistoric earthquakes in the Pacific Northwest by microfossil analysis: *Science*, vol. 264, p. 688-691.
- Matsumoto, E. and Wong, C. S., 1977, Heavy metal sedimentation in Saanich Inlet measured with ^{210}Pb technique: *Journal of Geophysical Research*, vol. 82, p. 5477-5482.

- Middleton, G. V. and Hampton, M. A., 1976, Subaqueous sediment transport and deposition of sediment gravity flows: Marine transport and environmental management (D.J. Stanley, D.J.P. Swift, eds.), John Wiley and Sons, Toronto, p. 197-218.
- Nelson, A. R., 1992, Holocene tidal-marsh stratigraphy in south-central Oregon - evidence for localized sudden submergence in the Cascadia subduction zone: Quaternary Coasts of the United States: Marine and Lacustrine Systems (C. H. Fletcher, III, and J. F. Wehmiller, eds.): Society of Economic Paleontologists and Mineralogists, Special Publication no. 48, p. 288-301.
- Obermeier, S. F., Preliminary limits for the strength of shaking for the Columbia River valley and the southern half of coastal Washington for the Cascadia subduction zone earthquake of about 300 years ago: U.S. Geological Survey Open-File Report, in press.
- Obermeier, S. F., Atwater, B. F., Benson, B. E., Peterson, C. D., Moses, L. J., Pringle, P. T., and Palmer, S. P., 1993, Liquefaction about 300 years ago along tidal reaches of the Columbia River, Oregon and Washington: Eos, vol. 74, p. 198-199.
- Pearson, G.W. and Stuiver, M., 1993, High-precision bidecal calibration of the radiocarbon time scale, 500-2500 B.C.: Radiocarbon, vol. 35, p. 25-33.
- Powys, R. I. L., 1987, The geochemistry and diatom assemblages of varved sediments from Saanich Inlet, B. C.: M.Sc. thesis, University of British Columbia, Vancouver, B.C., 200 p.

- Prior, D.B. and Coleman, J. M., 1984, Submarine slope instability (D. Brunsden and D. B. Prior, eds.): Slope instability, John Wiley and Sons, Toronto, p. 419-455.
- Riddihough, R. P. and Hyndman, R. W., 1976, Canada's active western margin- The case for subduction: Geoscience Canada, vol. 3, p. 269-278.
- Ritchie, J. C., Hawks, P. H., and McHenry, J. R., 1975, Deposition rates using fallout cesium-137: Geological Society of America Bulletin, vol. 86, p. 1128-1130.
- Robbins, J. A., 1978, Geochemical and geophysical application of radioactive lead: Biochemistry of lead in the environment (J. O. Nriagu, ed.), Elsevier, Amsterdam, p. 285-393.
- Robinson, S. W. and Thompson, G., 1981, Radiocarbon corrections for marine shell dates with application to southern Pacific Northwest Coast prehistory: Syesis, vol. 14, p. 45-57.
- Roddick, J.A., 1965, Vancouver North, Coquitlam and Pitt Lake map areas, with special emphasis on the evolution of the plutonic rocks: Geological Survey of Canada, Memoir, no. 335, 276 p.
- Rogers, G. C., 1980, A documentation of soil failure during the British Columbia earthquake of 23 June, 1946: Canadian Geotechnical Journal, vol. 17, p. 122-127.

- Rogers, G. C., 1988, An assessment of the megathrust earthquake potential of the Cascadia subduction zone: *Canadian Journal of Earth Sciences*, vol. 25, p. 844-852.
- Rogers, G. C., 1992, The earthquake threat in southwest British Columbia, *Geotechnique and Natural Hazards*: BiTech Publishers, Vancouver, B.C., p. 63-69.
- Rogers, G. C., 1994, Earthquakes in Vancouver (J.W.H. Monger, ed): *Geology and geological hazards of the Vancouver region, southwestern British Columbia*, Geological Survey of Canada Bulletin, no. 481, p. 221-229.
- Rogers, G.C. and Hasewaga, H. S., 1978, A second look at the British Columbia earthquake of 23 June 1946: *Seismological Society of America Bulletin*, vol. 68, p. 653-675.
- Sancetta, C., 1989, Spatial and temporal trends of diatom flux in British Columbian fjords: *Journal of Plankton Research*, vol. 11, p. 503-520.
- Sancetta, C. and Calvert, S. E., 1988, The annual cycle of sedimentation in Saanich Inlet, British Columbia: Implications for the interpretation of diatom fossil assemblages: *Deep-Sea Research*, vol. 35, p. 71-90.
- Santschi, P. H., Li, Y.-H., Alder, D. M., Amdurer, M., Bell, J., and Nyfeller, U. P., 1983, The relative mobility of natural (Th, Pb, Po) and fallout (Pu, Am, Cs) radionuclides in the coastal marine environment: result from model ecosystems (MERL) and Narragasset Bay: *Geochimica Cosmochimica Acta*, vol. 47, p. 201-210.

- Savage, J. C., Lisowski, M, and Prescott, W. H., 1991, Strain accumulation in western Washington: *Journal of Geophysical Research*, vol. 96, p. 14,493-14,507.
- Schuster, R. L., Logan, R. L., and Pringle, P. T., 1992, Prehistoric rock avalanches in the Olympic Mountains, Washington: *Science*, vol. 258, p. 1620-1621.
- Sims, J.D., 1975, Determining earthquake recurrence intervals from deformational structures in young lacustrine sediments: *Tectonophysics*, v. 29, p. 141-152.
- Stucchi, D. J. and Giovando, L. F., 1984, Deep water renewal in Saanich Inlet, B. C.: Proceedings of a multidisciplinary symposium on Saanich Inlet, 2nd February, 1983 (S. K. Juniper and R. O. Brinkhurst, eds.), Canadian Technical report of hydrography and Ocean Sciences no. 38, Institute of Ocean Sciences, Department of Fisheries and Oceans, Sidney, B.C., p.7-15.
- Stuiver, M. and Braziunas, T. F., 1993, Modelling atmospheric ^{14}C influences and ^{14}C ages of marine samples to 10,000 BC: *Radiocarbon*, vol. 35, p. 137-189.
- Stuiver, M. and Pearson, G. W., 1993, High-precision bidecal calibration of the radiocarbon time scale, A.D. 1950-500 B.C. and 2500-6000 B.C., *Radiocarbon*, vol. 35, p. 1-23.
- Stuiver, M. and Reimer, P. J., 1993, Extended ^{14}C data base and revised CALIB 3.0 ^{14}C age calibration program: *Radiocarbon*, vol. 35, p. 215-230.

TUL89A-001

Varves				Massive layers			
Depth (cm)	Sand %	Silt %	Clay %	Depth (cm)	Sand%	Silt %	Clay %
363-367	0.36	23.53	76.11	373-377	0.12	17.95	81.93
367-371	0.3	20.91	78.79	383-387	0.14	25.68	74.18
418.5-422.5	0.42	20.98	78.6	393-397	0.26	24.25	75.5
422.5-426.5	0.62	21.89	77.49	403-407	1.54	26.71	71.75
467-471	0.67	30.73	68.6	413-417	0.3	23.74	75.95
543-547	0.29	23.09	76.62	849.5-852	0.47	15.78	83.75
639-643	0.31	18.47	81.22				
644-648	0.32	22.13	77.55				
670-674	0.22	23.12	76.66				
709-713	0.4	23.07	76.53				
741-745	0.25	21.87	77.89				
831-835	0.35	22.32	77.33				
845.5-849.5	0.19	22.34	77.47				
852-856	0.24	23.87	75.88				

TUL89A-002

Varves				Massive layer			
Depth (cm)	Sand %	Silt %	Clay %	Depth (cm)	Sand%	Silt %	Clay %
50-54	0.15	34.87	64.98	655.5-659.5	0.27	31.67	68.05
54-58	0.14	31.89	67.97				
246-250	0.18	29.97	69.85				
554-560	0.31	27.75	71.95				
651.5-655.5	0.13	30.99	68.88				
665.5-669.5	0.2	28.4	71.41				
685-689	0.21	27.35	72.44				
725-729	0.29	34.83	64.88				
799-803	0.1	26.5	73.4				
1053-1057	0.08	30.76	69.16				
1168-1172	0.21	30.01	69.78				

TUL89A-003

Varves				Massive layers			
Depth (cm)	Sand %	Silt %	Clay %	Depth (cm)	Sand%	Silt %	Clay %
314-318	0.25	27.17	72.58	318-322	0.21	32.06	67.73
343-347	0.13	25.58	74.28	322-326	0.16	32.34	67.49
348-353	0.48	24.84	74.68	328-333	0.22	27.75	72.03
382-384	0.19	26.83	72.98	333-325.5	0.37	30.83	68.8
393-398	0.3	30.1	69.6	335.5-338	0.45	31.65	67.9
403-407	0.23	26.37	73.4	644.5-648.5	0.14	33.77	66.09
418-423	0.3	22.69	77.01	658.5-662.5	0.18	33.87	65.95
638.5-642.5	0.35	26.13	73.53	668.5-672.5	0.25	33.98	65.77
698.5-702.5	0.29	26.9	72.81	678.5-682.5	0.18	33.78	66.04
931.5-935.5	0.14	23.52	76.34	688.5-692.5	0.35	34.34	65.3
1001.5-1005.5	0.37	21.07	78.56	941.5-945.5	0.13	34.89	64.97
1009.5-1013.5	0.19	26.25	73.56	951.5-955.5	0.23	33.65	66.12

TUL89A-003

231

Varves				Massive layers			
Depth (cm)	Sand %	Silt %	Clay %	Depth (cm)	Sand%	Silt %	Clay %
1011.5-1013	0.23	25.29	74.48	961.5-965.5	0.24	32.9	66.86
1014.5-1019.5	0.16	24.96	74.88	971.5-975.5	0.18	33.72	66.1
				981.5-985.5	0.19	34.69	65.12
				991.5-995.5	0.72	28.87	70.42

TUL91A-001

Varves				Massive layers			
Depth (cm)	Sand %	Silt %	Clay %	Depth (cm)	Sand%	Silt %	Clay %
58-60	1.53	24.04	74.43	64-66	3.54	26.33	70.13
152-154	1.81	23.13	75.07	69-71	0.95	24.34	74.71
184-186	2.33	26.38	71.29	76-78	3.69	25.73	70.58
209-211	2.36	32.41	65.23	226-228	4.59	25.83	69.58
298-300	4.49	24.31	71.2	230-232	6.86	31.16	61.99
352-354	3.95	29.33	66.72	234-236	1.83	23.98	74.18
394-396	1.98	31.71	66.32	302-304	7.4	33.01	59.59
486-488	0.89	23.41	75.7	305-307	9.98	25.07	64.95
512-514	4.05	27.72	68.24	399-401	3.36	25.5	71.14
535-537	1.73	26.59	71.68	428-430	11.68	30.84	57.47
589-591	5.05	26.29	68.66	432-434	22.17	24.9	52.93
607.5-609.5	3.26	23.32	73.42	454-456	5.21	27.58	67.21
624.5-626.5	2.97	23.58	73.45	462-464	3.24	30.26	66.49
665-667	2.34	25.24	72.42	465.5-467.5	6.8	33.76	59.44
751-753	1.72	21.92	76.36	521-523	2.05	28.29	69.66
805-807	3.18	26.72	70.1	526-528	1.53	27	71.48
992-994	7.01	27.28	65.7	610-612	1.32	20.82	77.85
1027-1029	0.76	26.05	73.19	639-641	3.74	26.18	70.08
1117-1119	6.41	35.2	58.39	648-650	2.54	26.06	71.4
				831-833	1.93	26.4	71.67
				834-836	2.26	27.03	70.71
				837-839	3.49	27.19	69.32
				847-849	1.56	28.29	70.15
				881.5-883.5	5.09	38.82	56.09
				904-906	2.09	30.43	67.48
				942-944	8.73	31.87	59.4
				926-928	2.73	31.3	65.97
				951-953	27.8	24.38	47.79
				969-971	19.86	22.18	50.83
				980-982	6.8	24.68	68.51
				985.5-987.5	8.02	5.96	14.55
				1073-1075	26.67	29.59	43.74
				1079-1081	7.37	36.05	56.58

TUL91A-002

Varves				Massive layers			
Depth (cm)	Sand %	Silt %	Clay %	Depth (cm)	Sand%	Silt %	Clay %
200.5-202.5	2.11	29.53	68.36	277-279	0.49	31.62	67.9
246.5-248.5	1.21	29.87	68.92	279-281	2.16	25.38	72.46
272.5-274.5	0.93	31.46	67.62	484-486	1.98	25.26	72.77
285.5-287	3.24	29.22	67.54	611-613	3.28	32.64	64.08
463-465	6.25	31.23	62.52	618-620	4.31	37.63	58.06
538-540	2.56	31.33	66.1	636-638	2.58	32.96	64.46
660-662	3.14	32.64	64.22	681-683	6.19	30.49	63.32
974-976	0.63	33.14	66.23	899-901	1.23	25.23	73.54
1058-1060	1.11	27.44	71.44	903-905	0.68	27.	71.4
1082-1084	0.45	24.62	74.93	1060-1062	1.32	28.98	69.7
				1101-1103	2.93	39.71	57.36
				1124-1126	1.46	36.05	62.49
				1145-1147	3.55	38.09	58.37
				1161-1163	2.76	37.16	60.07

TUL91A-003

Varves				Massive layers			
Depth (cm)	Sand %	Silt %	Clay %	Depth (cm)	Sand%	Silt %	Clay %
82-84	1.45	49.16	49.38	350-352	1.45	44.89	53.66
191.5-193.5	2.33	41.3	56.37	353-355	1.7	44.29	54.01
319-321	1.71	35.77	62.53				
434.5-436.5	1.22	35.23	63.56				
471.5-473.5	0.78	35.76	63.47				
540.5-542.5	1.58	38.6	59.82				
672.5-674.5	0.57	37.9	61.52				
720.5-722.5	1.05	34.14	64.81				
755.5-757.5	1.05	34.68	64.26				
828.5-830.5	2.12	44.88	53.01				
872-874	1.97	42.67	55.36				
888-890	1.11	39.57	59.32				
925.5-927.5	1.73	42.43	55.85				
936.5-938.5	9.92	53.16	36.92				
1031-1033	1.91	39.59	58.5				
1076-1078	0.78	41.04	58.18				
1120-1122	1.67	46.26	52.07				
1144-1146	0.94	37.38	61.68				
1192-1194	1.49	40.62	57.88				

TUL91A-004

Varves				Massive layers			
Depth (cm)	Sand %	Silt %	Clay %	Depth (cm)	Sand%	Silt %	Clay %
97-99	2.12	42.11	55.77	448.5-450.5	0.54	39.69	59.77
183.5-185.5	0.36	38.3	61.34	810.5-812.5	1.65	43.27	55.08
199.5-201.5	0.75	34.86	64.39				
214.5-216.5	0.25	38.01	61.74				
233.5-235.5	0.59	38.37	61.04				

TUL91A-004

Depth (cm)	Varves		
	Sand %	Silt %	Clay %
294.5-296.5	0.54	34.14	65.32
315.5-317.5	0.7	38.92	60.38
388.5-390.5	1.14	40.42	58.44
418.5-420.5	1.27	37.22	61.5
455.5-457.5	0.88	36.12	62.99
501.5-503.5	0.87	32.05	67.08
557.5-559.5	1.82	34.21	63.97
603.5-605.5	0.58	32.93	66.49
648.5-650.5	0.6	32.25	67.15
680.5-682.5	1.35	38.91	59.74
728.5-730.5	1.56	34.98	63.45
762.5-764.5	0.73	35.04	64.23
800.5-802.5	1.55	36.85	61.6
856.5-858.5	1.27	38.04	60.69
898.5-900.5	1.11	41.52	57.37
944.5-946.5	1.03	37.31	61.66
968.5-970.5	0.98	33.78	65.25
984.5-986.5	0.62	35.12	64.26
1038-1040	0.48	36.95	62.57

TUL91A-005

Depth (cm)	Massive clayey silt			Depth (cm)	Massive clayey silt		
	Sand %	Silt %	Clay %		Sand %	Silt %	Clay %
42-44	2.82	59.95	37.23	444.5-446.5	4.56	48.42	47.02
89-91	2.11	51.66	46.23	464.5-466.5	2.87	49.65	47.48
102-104	1.98	52.56	45.46	494.5-496.5	2.71	51.33	45.96
109-111	1.66	49.26	49.07	502.5-504.5	1.95	48.01	50.04
129-131	1.97	48.54	49.49	508.5-510.5	2.58	50.64	46.77
140-142	2.2	54.59	43.21	541.5-543.5	2.57	49.98	47.45
147-149	3.94	53.65	42.41	563.5-565.5	3.17	49.65	47.18
159-161	2.75	52.42	44.83	567.5-569.5	3.48	54.71	41.8
169-171	2.76	50.27	46.97	571.5-573.5	4.27	51.35	44.38
179-181	4.38	57.72	37.9	575.5-577.5	3.01	51.43	45.56
192-194	4.29	55.41	40.3	579.5-581.5	2.35	51.1	46.56
199-201	6.96	54.18	38.86	608.5-610.5	2.38	44.12	53.5
241.5-243.5	3.73	58.37	37.9	611.5-613.5	2.29	45.69	52.02
261.5-263.5	4.37	57.03	38.6	615.5-617.5	2.34	48.61	49.06
281.5-283.5	4.09	55.7	40.2	640-641.5	2.51	46.81	50.68
291.5-293.5	3.66	53.55	42.79	641.5-643.5	3.14	49.13	47.73
311.5-313.5	2.93	51.64	45.44	661.5-663.5	4.42	55.2	40.38
341.5-343.5	1.62	51.46	46.92	687-689	2.51	54.37	43.12
384.5-386.5	4.24	51.44	44.32	697-699	3.98	51.86	44.16
394.5-396.5	3.33	51	45.67	712-714	2.69	51.64	45.67
408.5-410.5	3.53	50.94	45.54	727-729	2.87	50.01	47.12
414.5-416.5	2.52	51.02	46.46	737-739	2.56	49.92	47.52
422.5-424.5	4.26	52.98	42.75				

TUL91A-005

234

Depth (cm)	Massive clayey silt		
	Sand %	Silt %	Clay %
747-749	3.12	50.38	46.5
757-759	1.81	50.65	47.54
767-769	1.39	51.25	47.36
787-789	1.9	51.21	46.89
797-799	2.03	47.44	50.53
851-853	2.22	48.63	49.15
855-857	1.88	47.28	50.84
881-883	2.85	51.72	45.43
898-900	2.39	50.06	47.55
905-907	1.78	51.54	46.68
910-912	2.79	48.33	48.88

A null hypothesis (H_0) is put forward to find out whether the mean % sand fractions of the varves (μ_1) vs. massive layers (μ_2) are the same. $H_0: \mu_1 = \mu_2$.

The formula for the t-test is:

$$t = \frac{\bar{X}_1 - \bar{X}_2}{S_e}$$

where the mean % sand of varves (\bar{X}_1) and the mean % sand of the massive layers (\bar{X}_2) are subtracted and divided by the standard error.

The standard error (S_e) is calculated:

$$S_e = S_p \sqrt{\frac{1}{n_1} + \frac{1}{n_2}}$$

where S_p = a pooled estimate of the standard deviation,

n_1 = number varve samples

n_2 = number of massive layer samples

S_p^2 is calculated by combining the sample variances of two data sets (1 = varve samples; 2 = massive layer samples):

$$S_p^2 = \frac{[n_1 - 1] S_1^2 + [n_2 - 1] S_2^2}{n_1 + n_2 - 2}$$

Therefore in a two-tailed distribution:

Varves:

$n_1 = 116$

$\bar{X}_1 = -0.0931$

$S_1^2 = 0.218$

$S_1 = 0.467$

Massive layers:

$n_2 = 73$

$\bar{X}_2 = 0.166$

$S_2^2 = 0.402$

$S_2 = 0.634$

¹ The % values of sand are converted to log normal values in order to make values follow a normal distribution.

$$S_p^2 = \frac{[116-1] S_1^2 + [73-1] S_2^2}{n_1 + n_2 - 2}$$

$$S_p^2 = \frac{25.07 + 28.94}{187}$$

$$S_p = 0.538$$

$$\therefore S_e = S_p \sqrt{\frac{1}{116} + \frac{1}{73}}$$

$$= 0.0804$$

$$\therefore t = \frac{\bar{X}_1 - \bar{X}_2}{S_e}$$

$$t = \frac{-0.931 - 0.166}{0.0804}$$

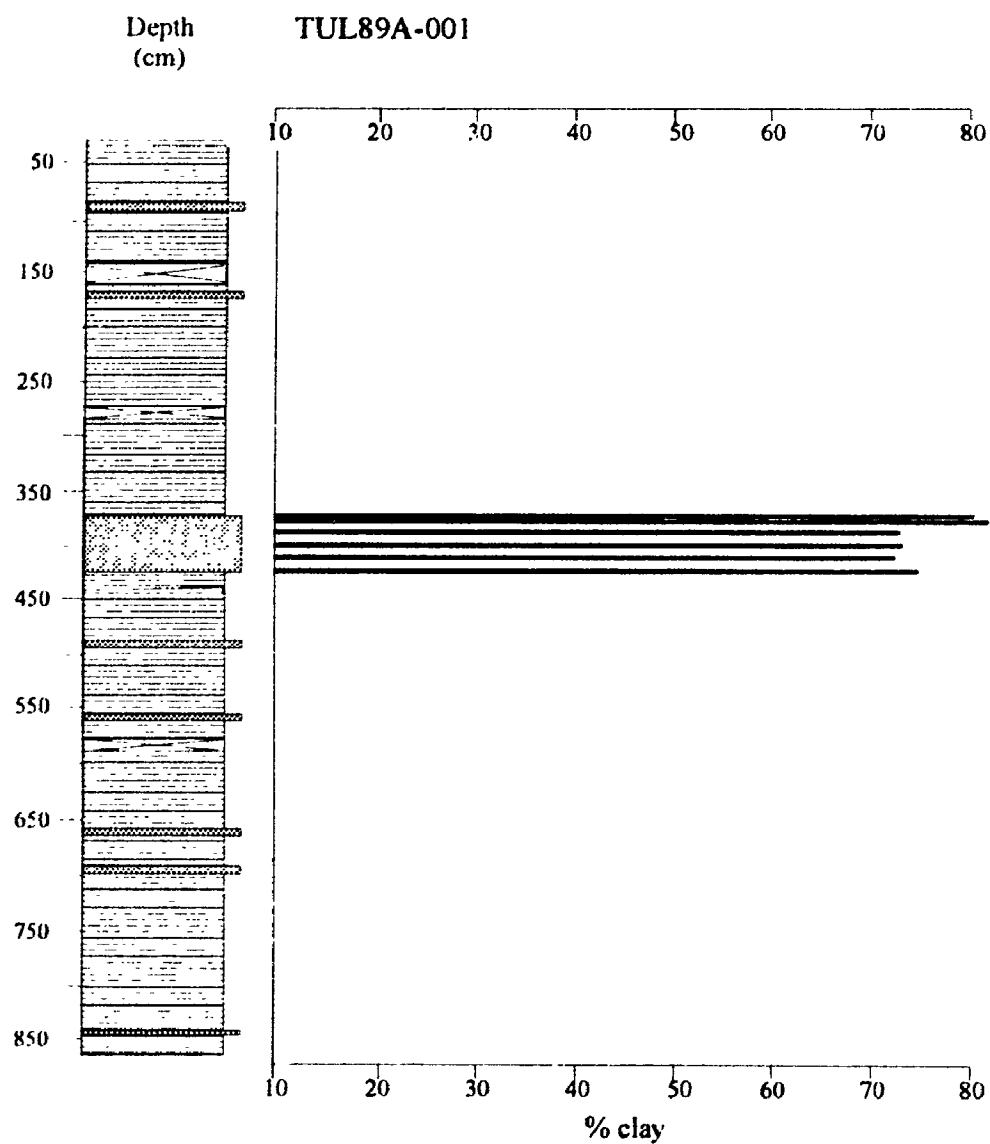
$$= -3.22$$

The value of t is reported to Table 2.11 (p. 62) in Davis, 1986 to find the level of significance of the null hypothesis.

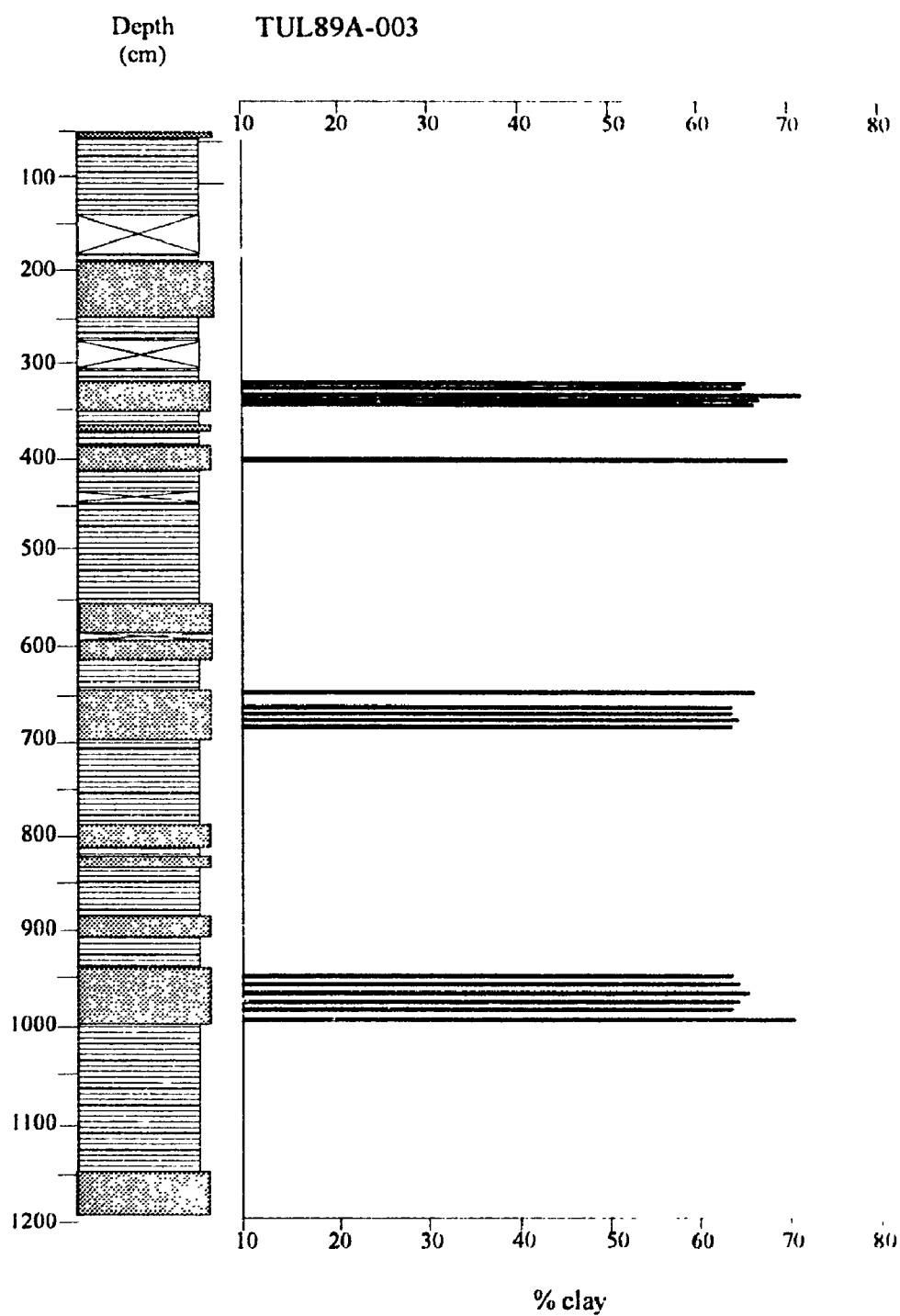
To use the table, the degrees of freedom (ν) are needed: $n_1 + n_2 - 2 = 187$ and the value of t .

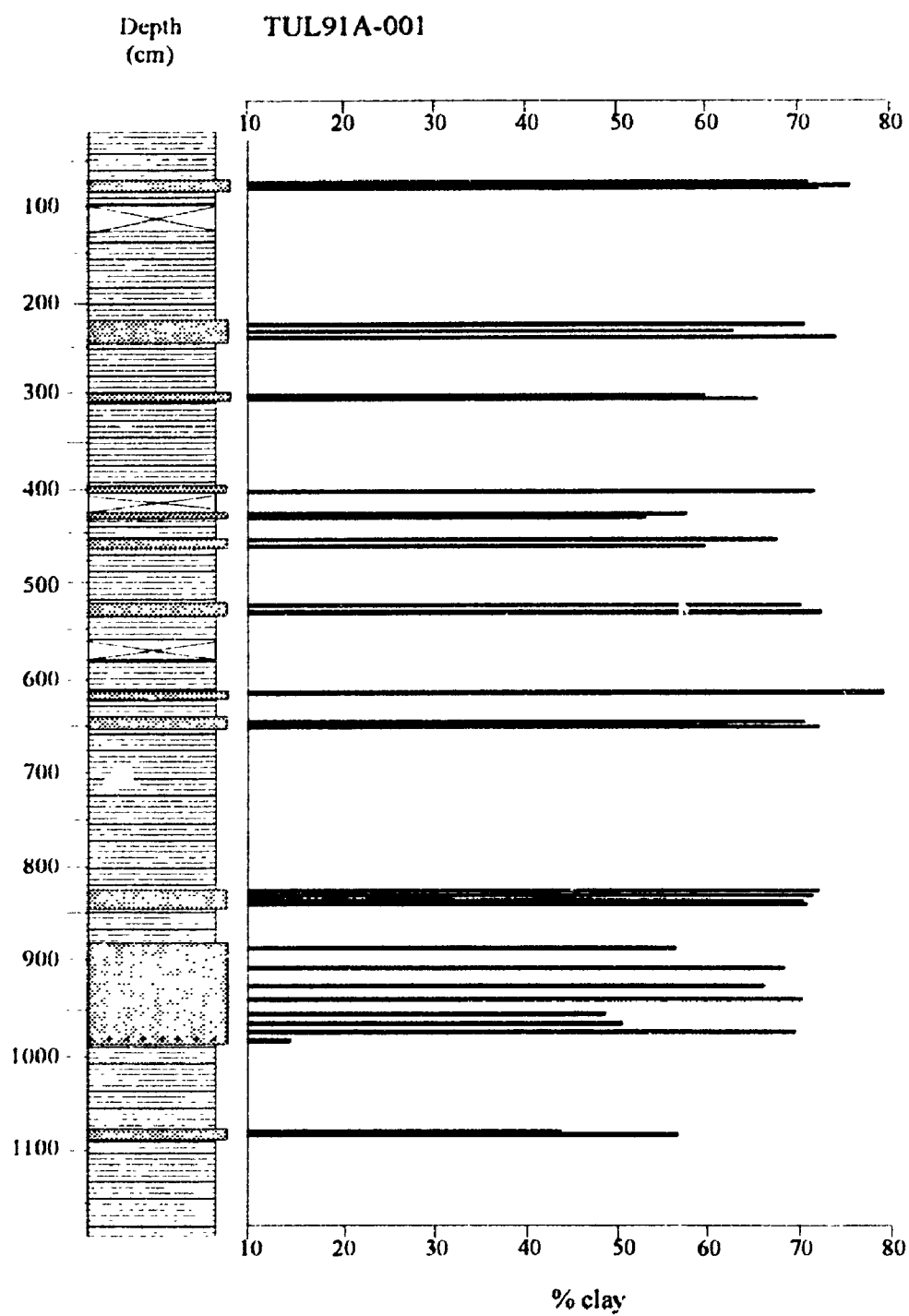
The level of significance is 0.1 %, which means that there is 1 chance in a 1000 that the means for % sand fraction of the varves and the massive layers are equal. Therefore, the null hypothesis $H_0: \mu_1 = \mu_2$ is rejected.

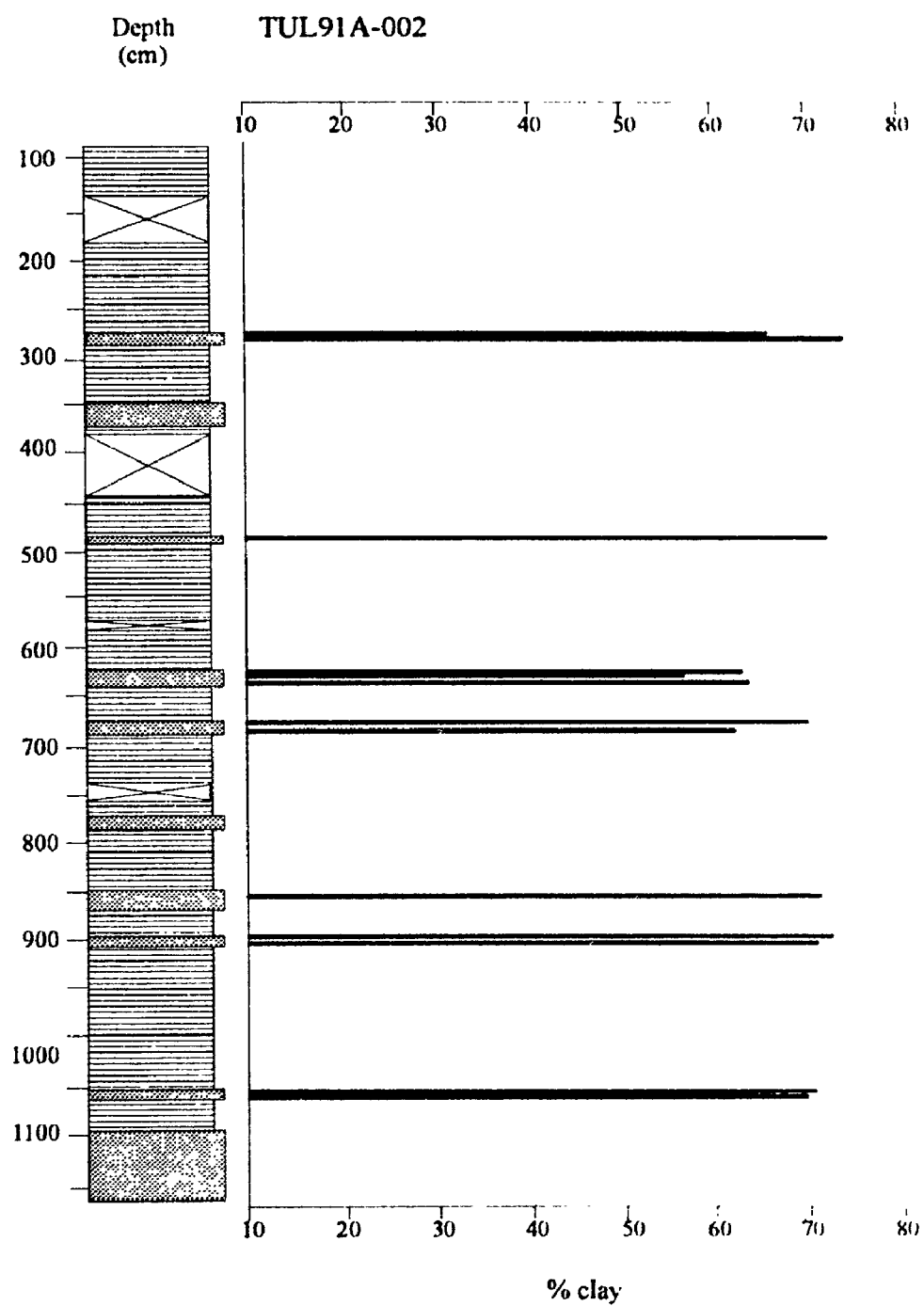
Appendix 3-3. Percent clay fractions in massive layers

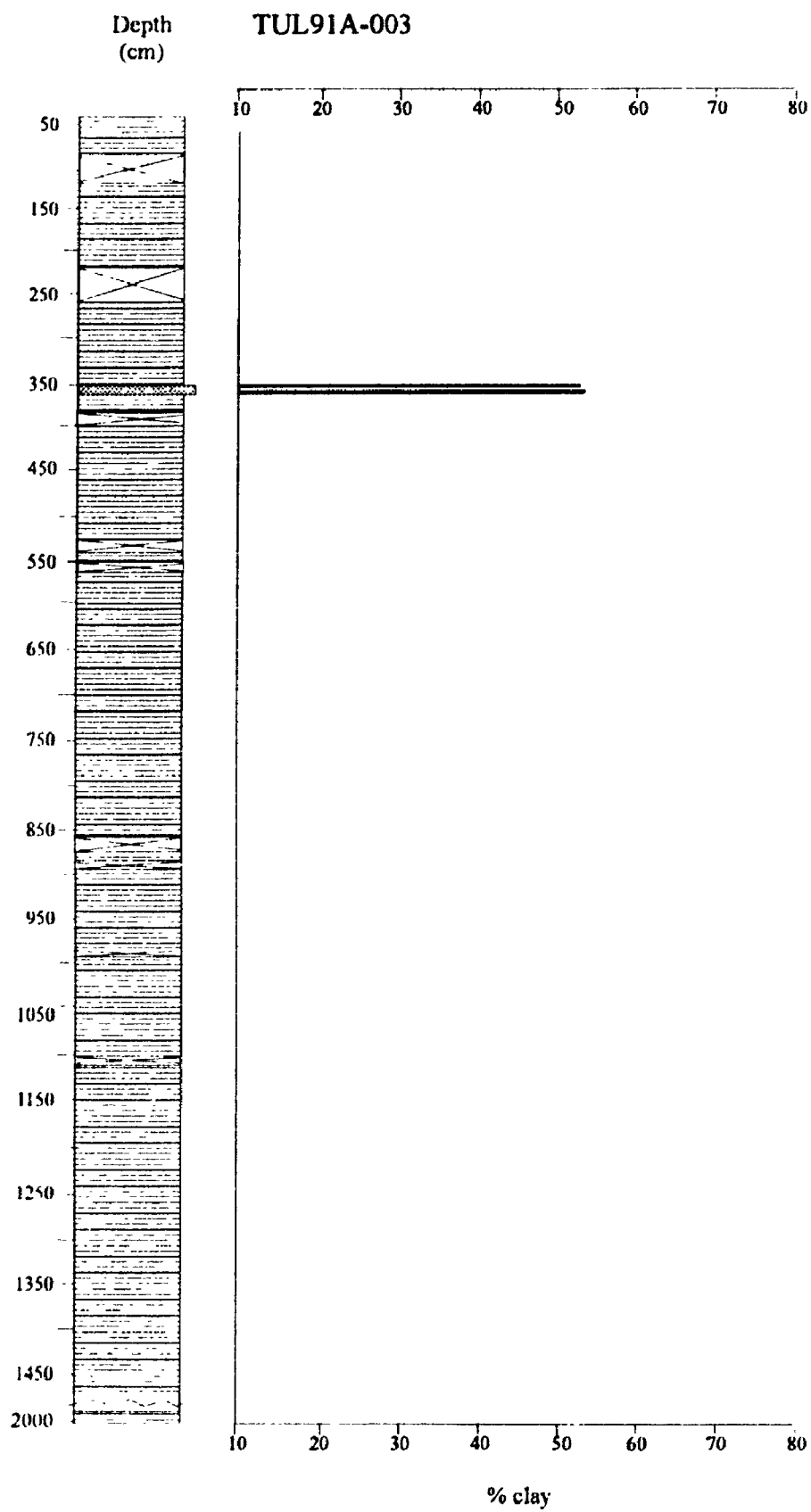


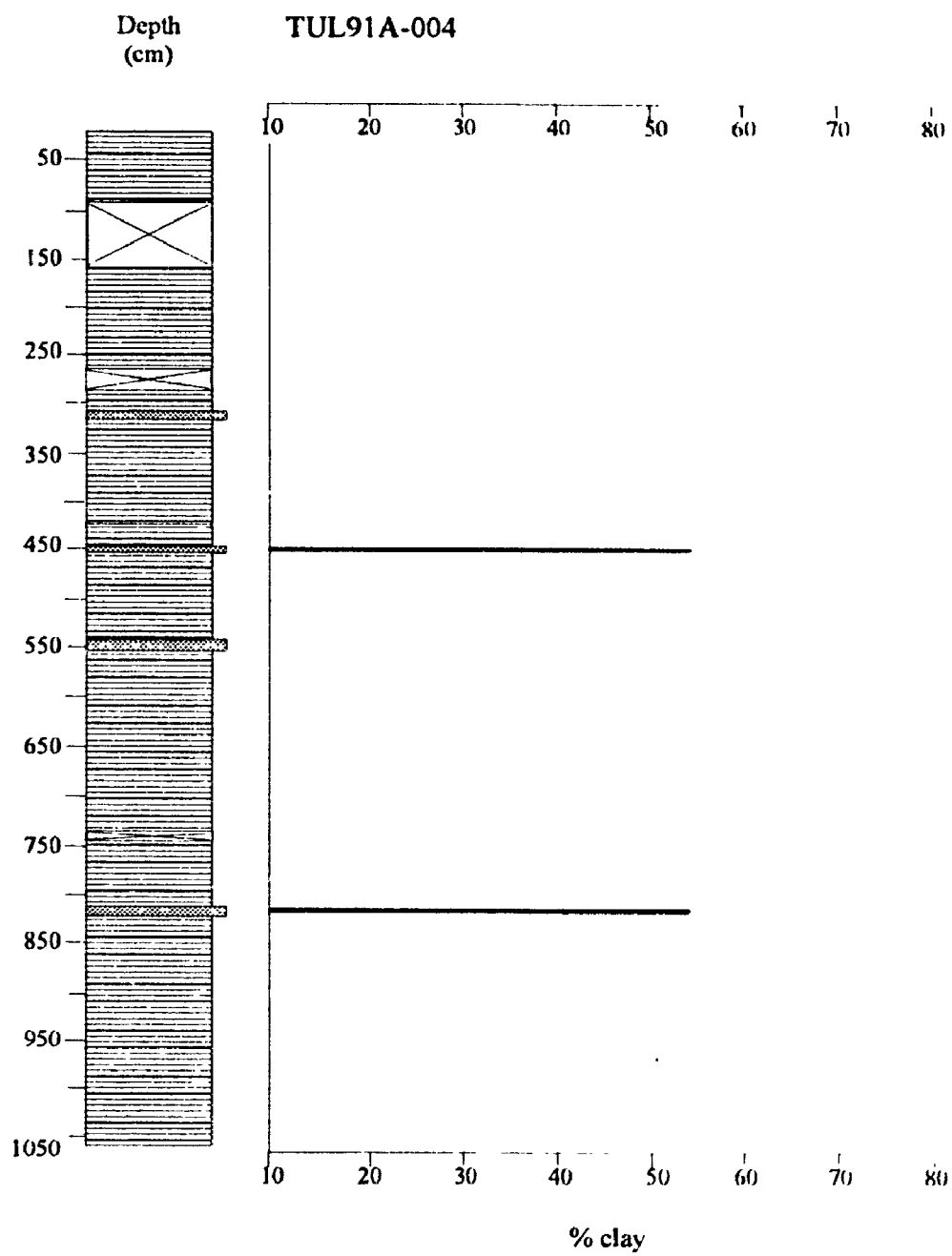
Note. No compilation is made for core TUL89A-002 because there is only one data point.



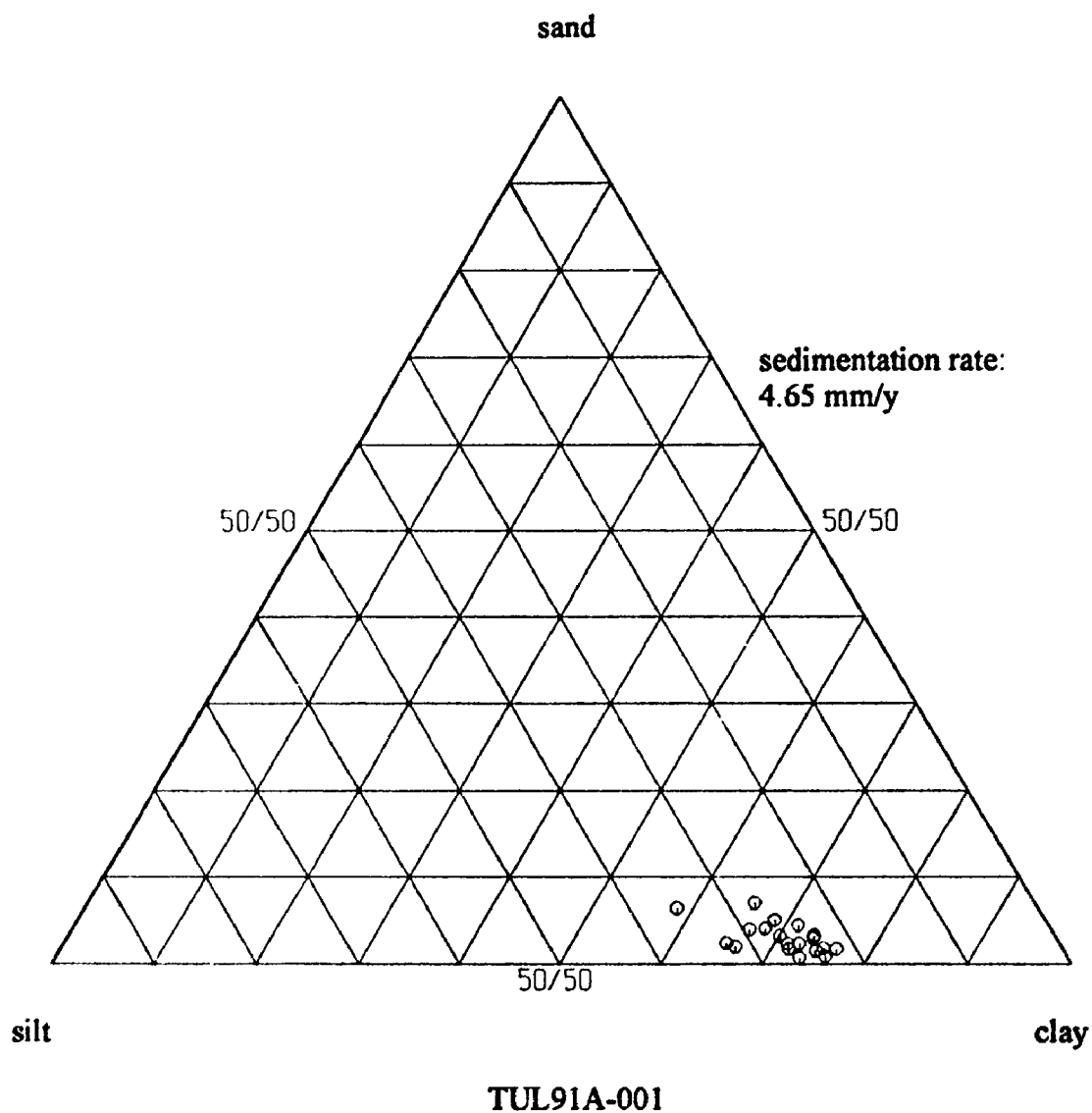




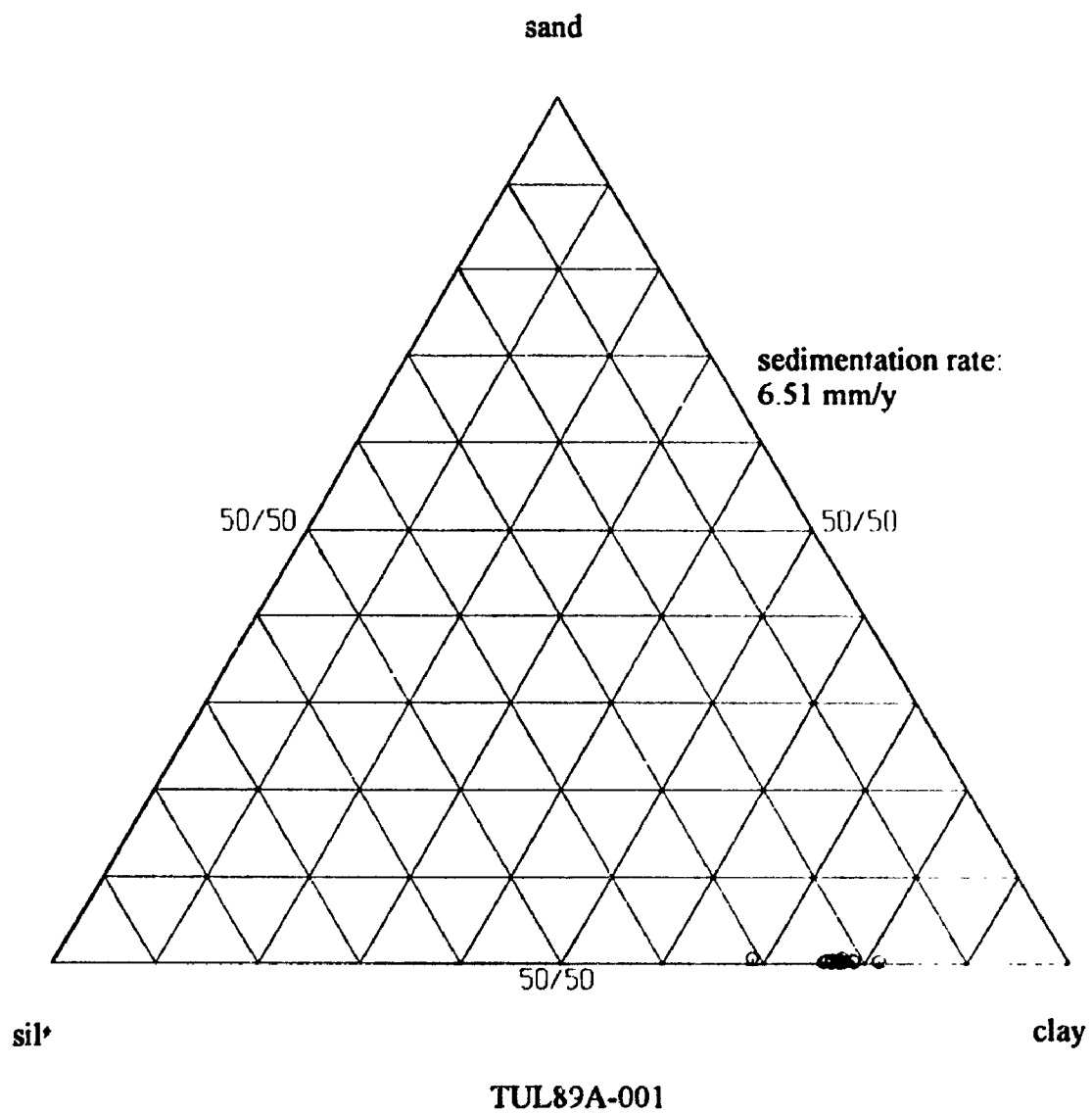


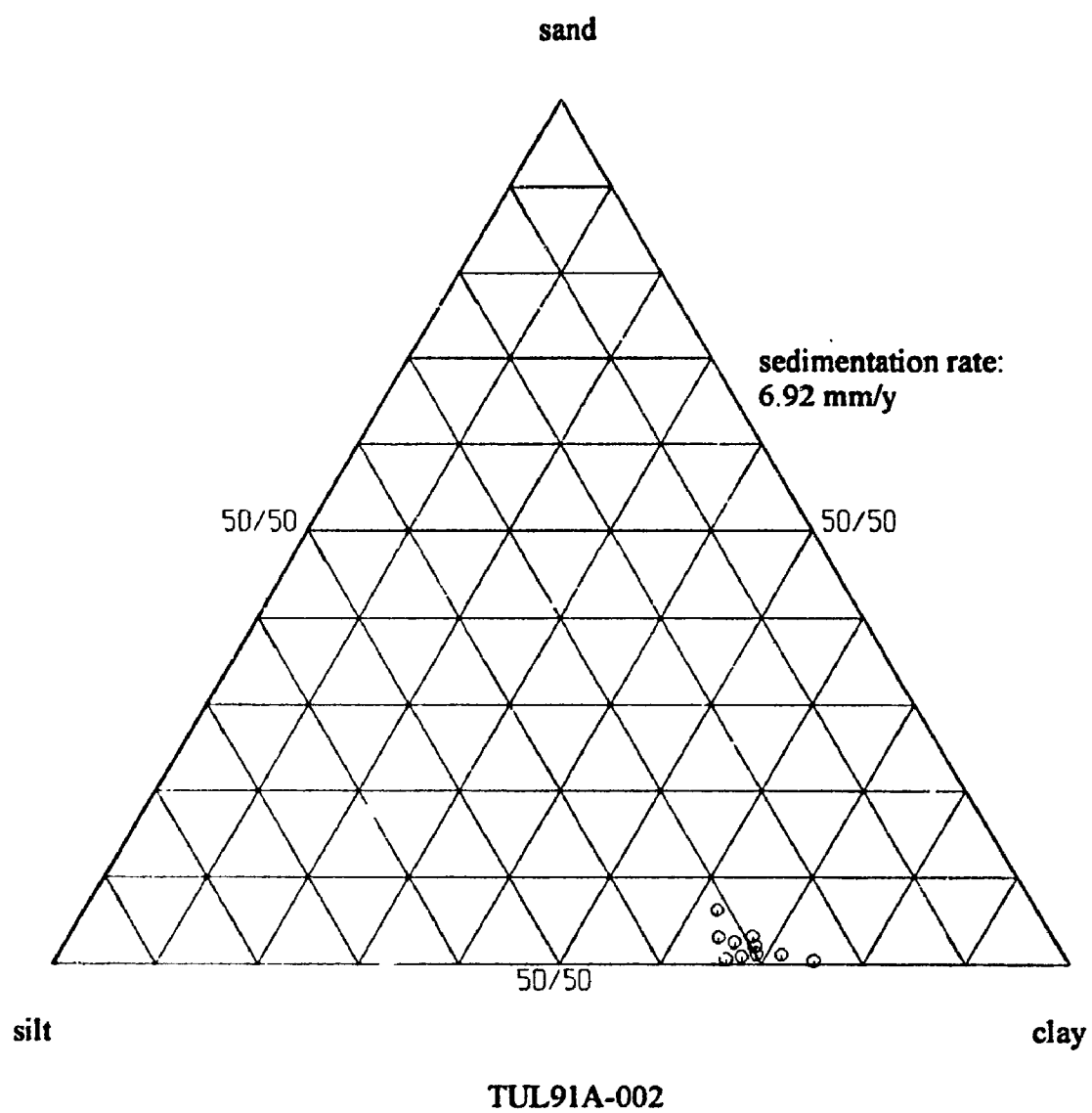


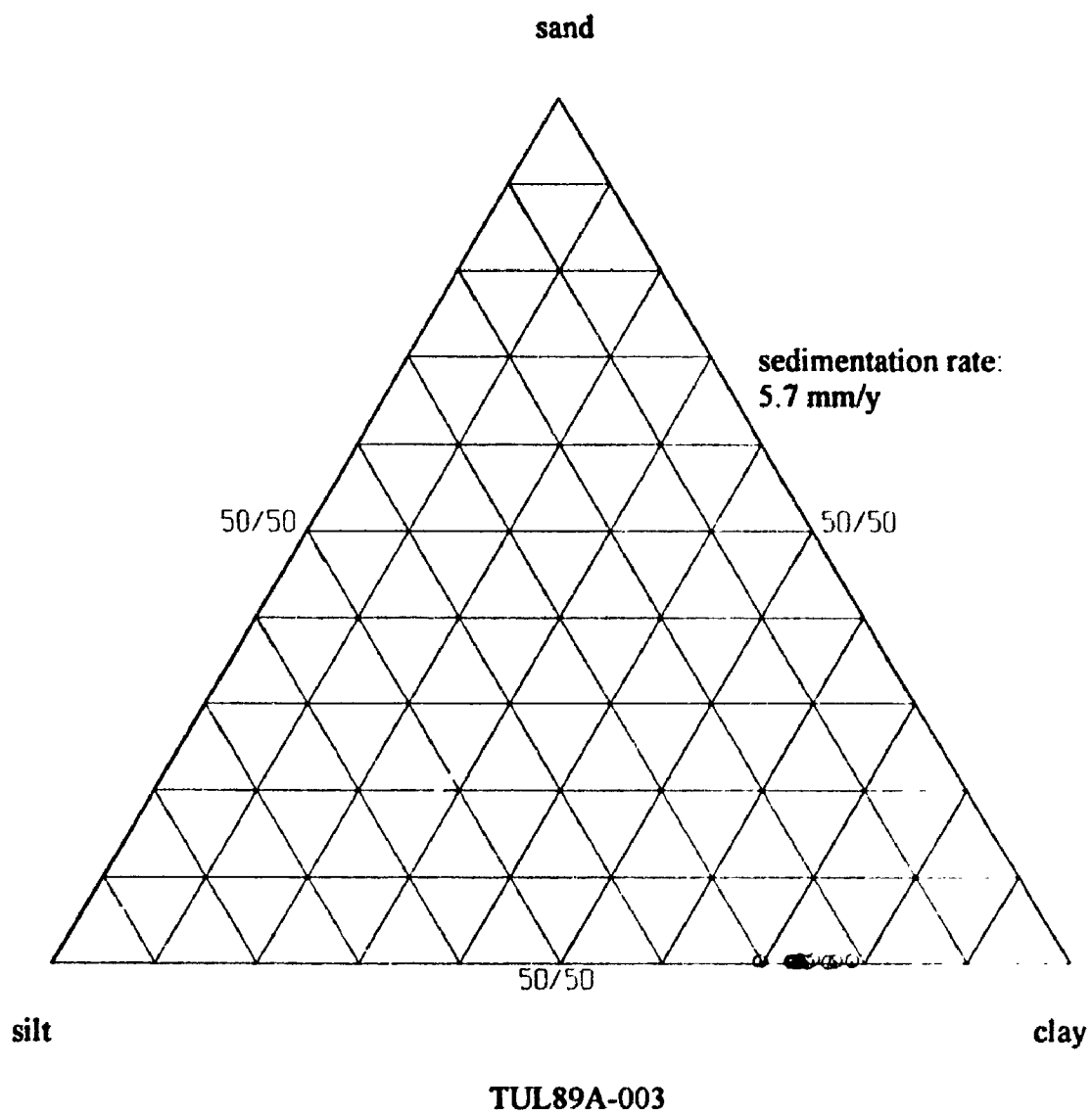
Appendix 3-4a Particle-size fractions (%) of varves per core.

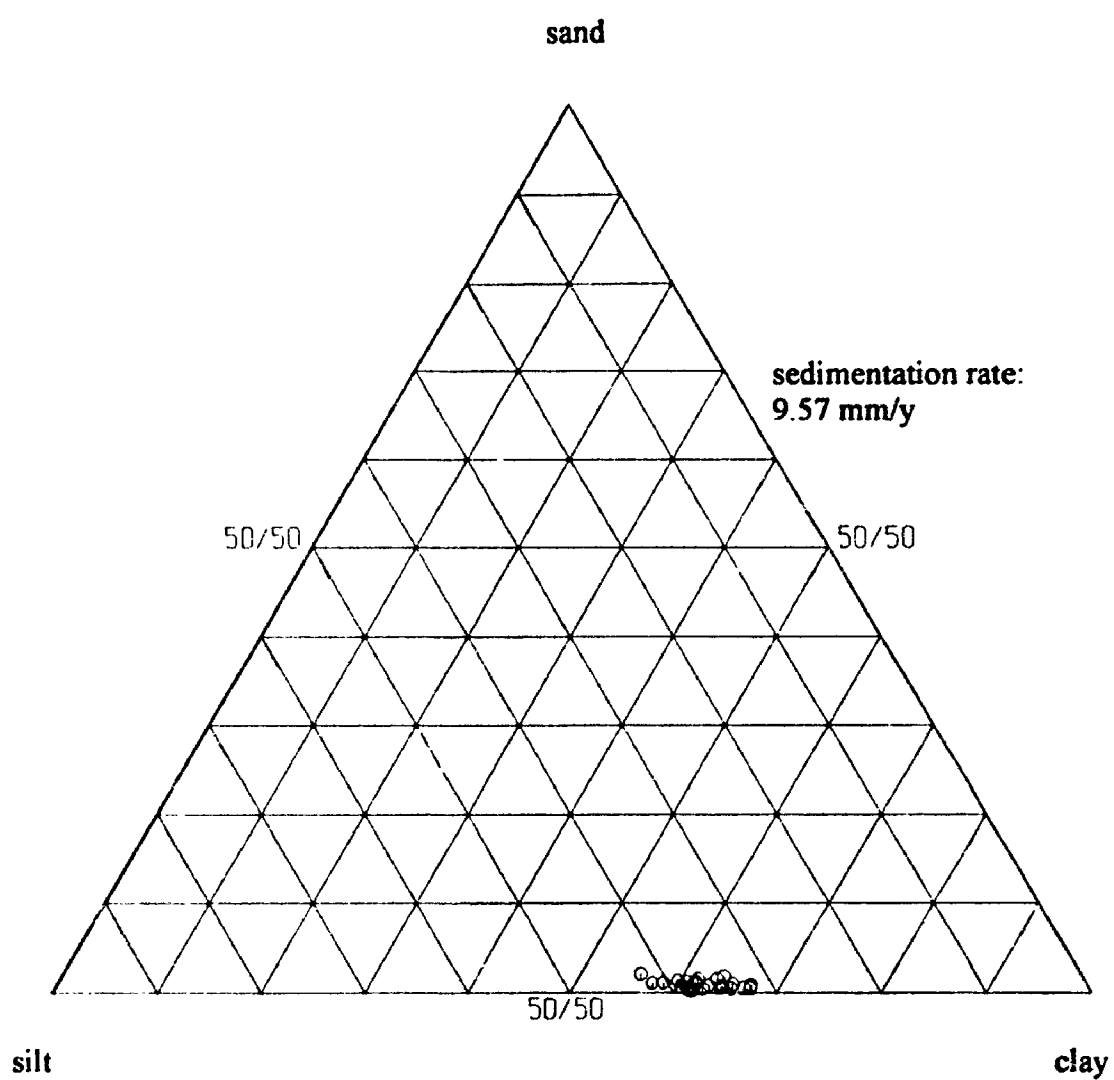


Note. Sand apex fraction is fine sand. Ternary diagrams are arranged in geographic order from south to north.

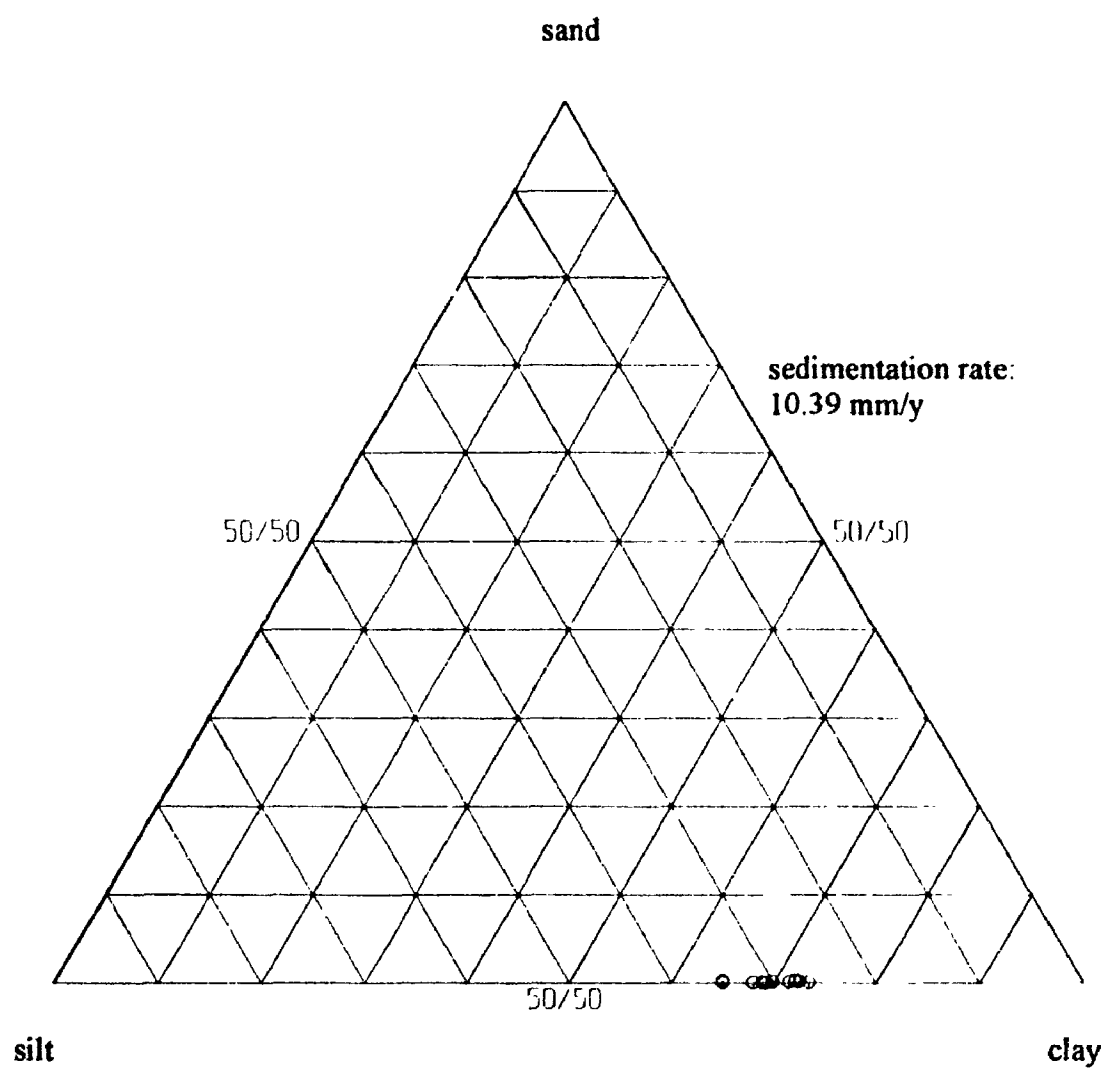




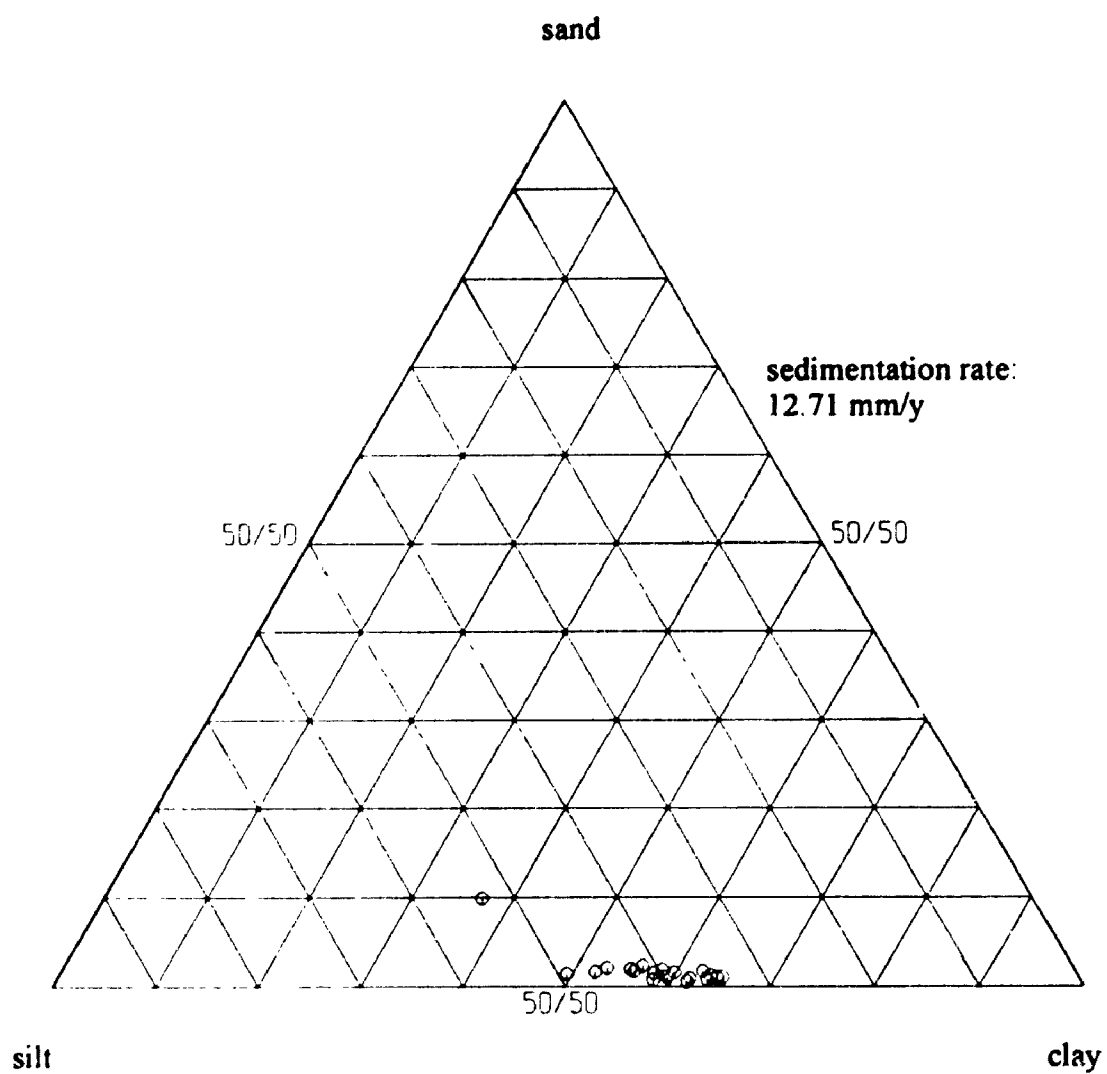




TUL91A-004

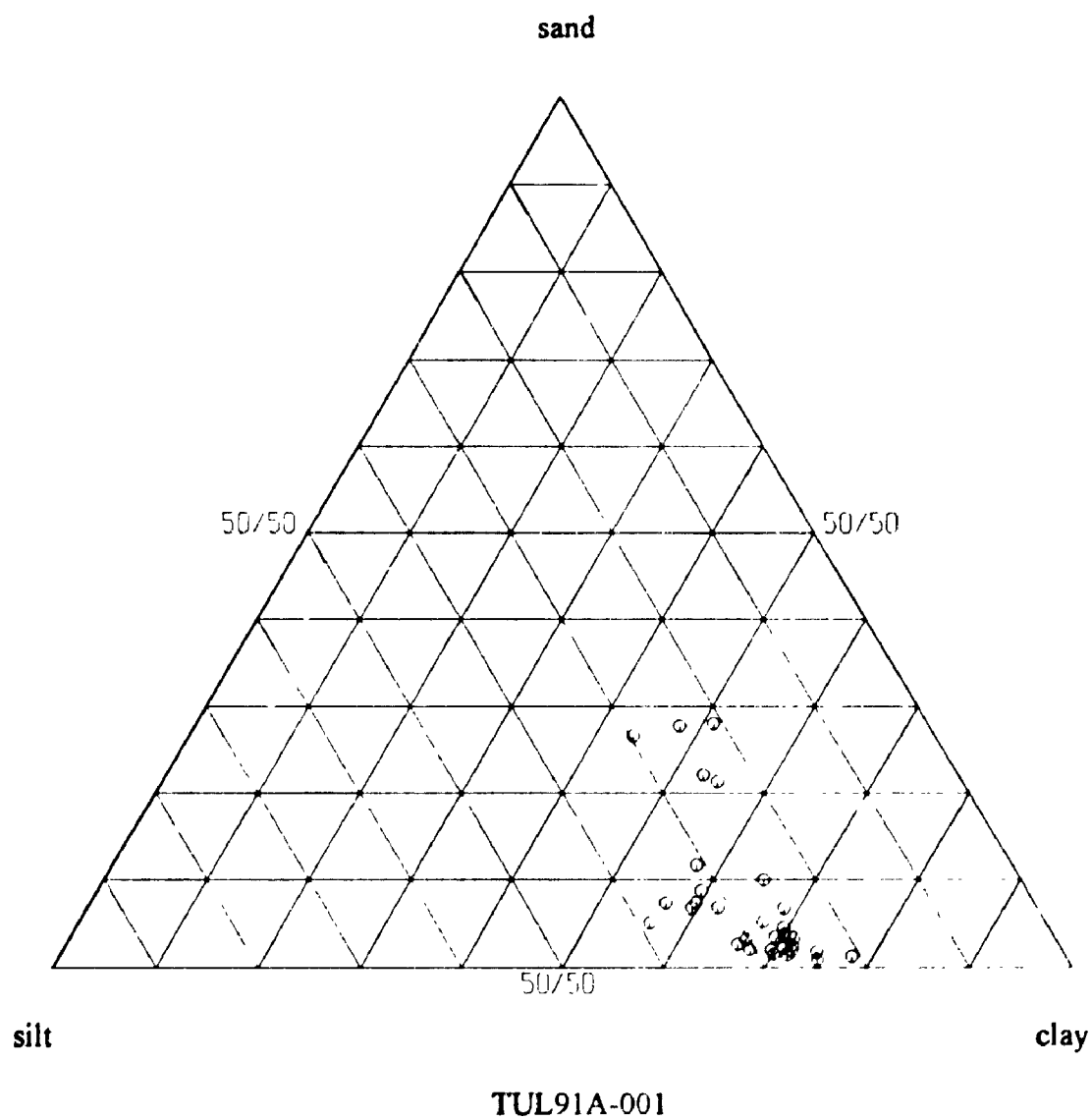


TUL89A-002

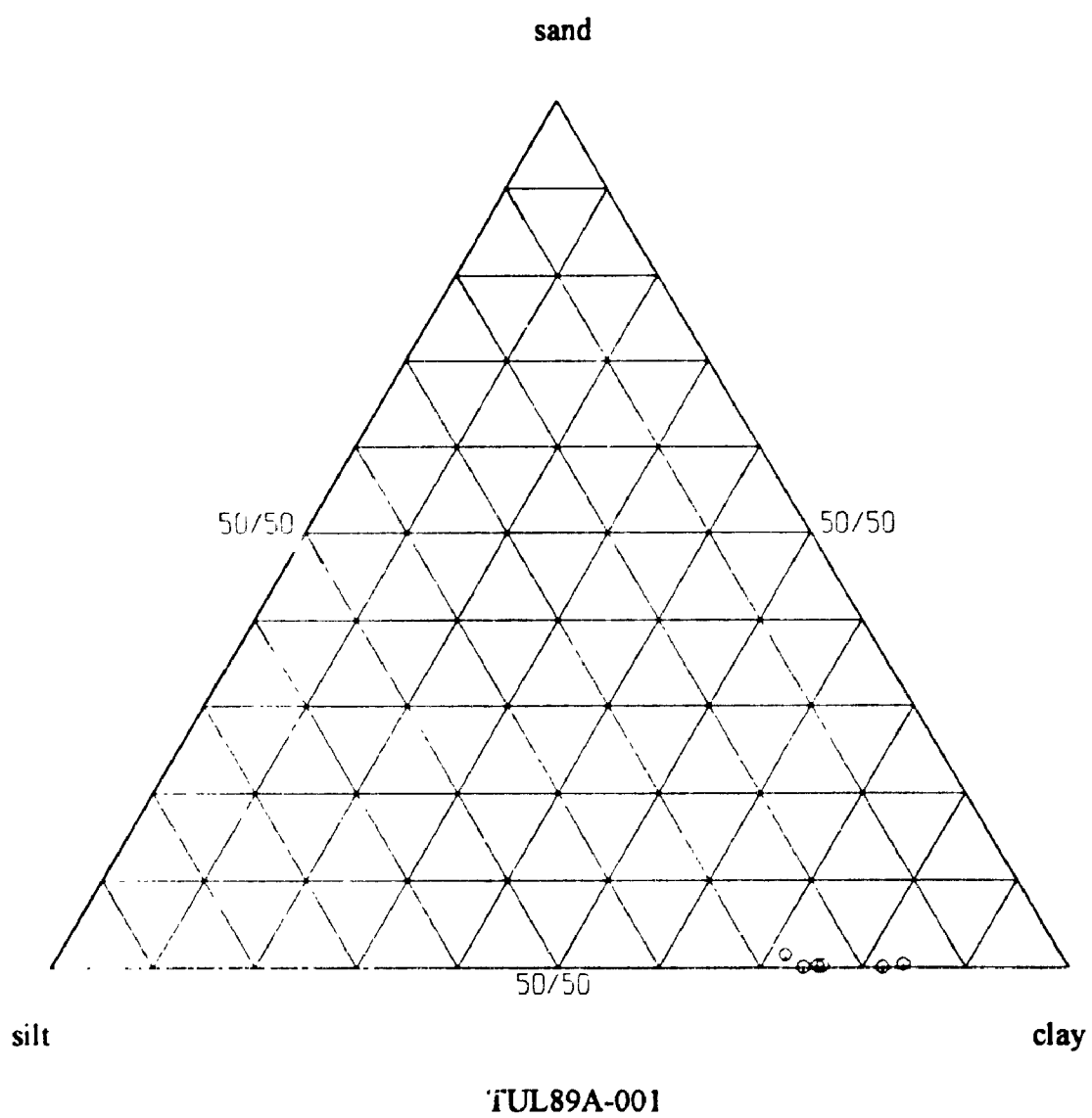


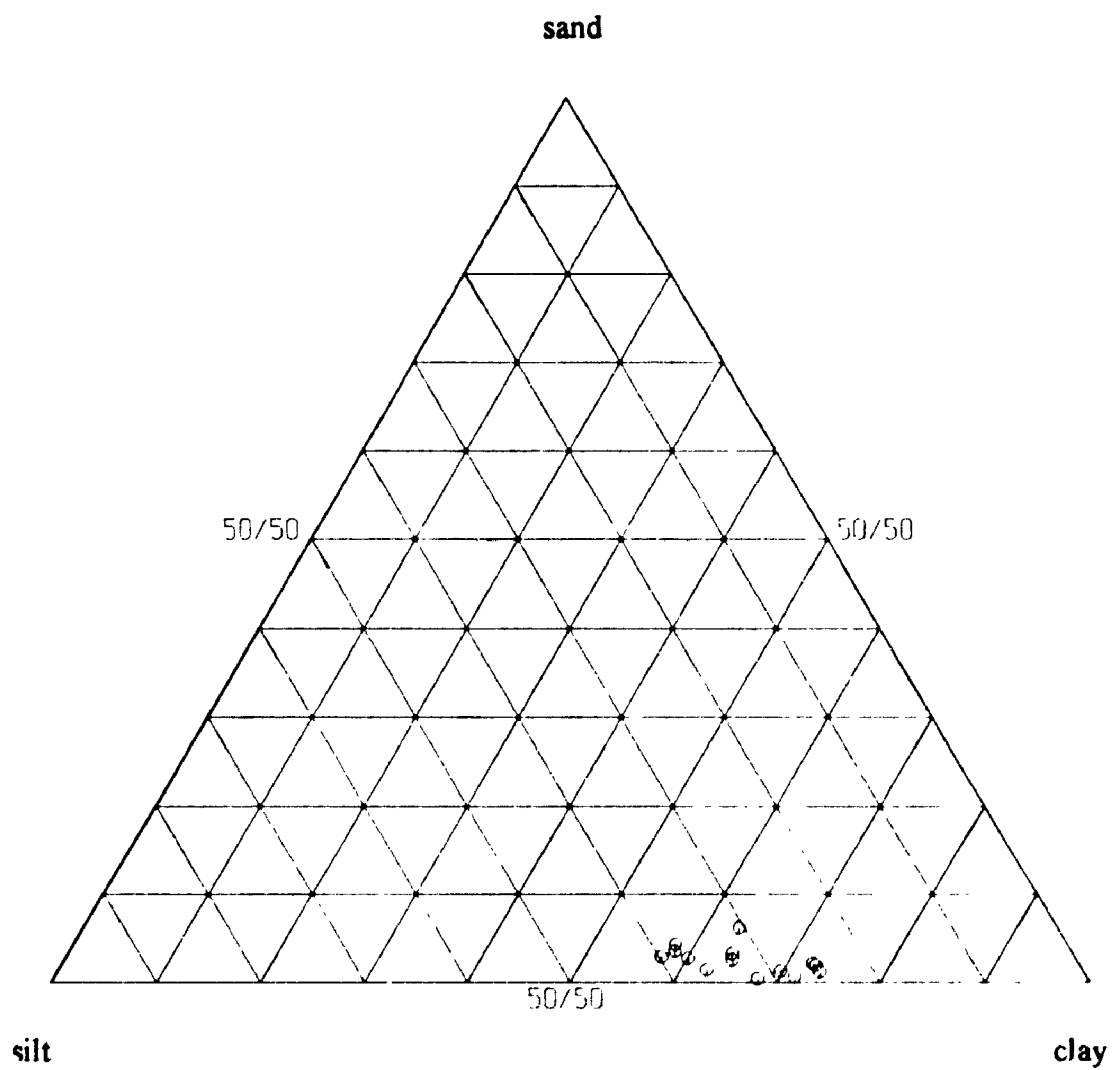
TUL91A-003

Appendix 3-4b. Particle-size fractions (%) of massive layers per core. ---

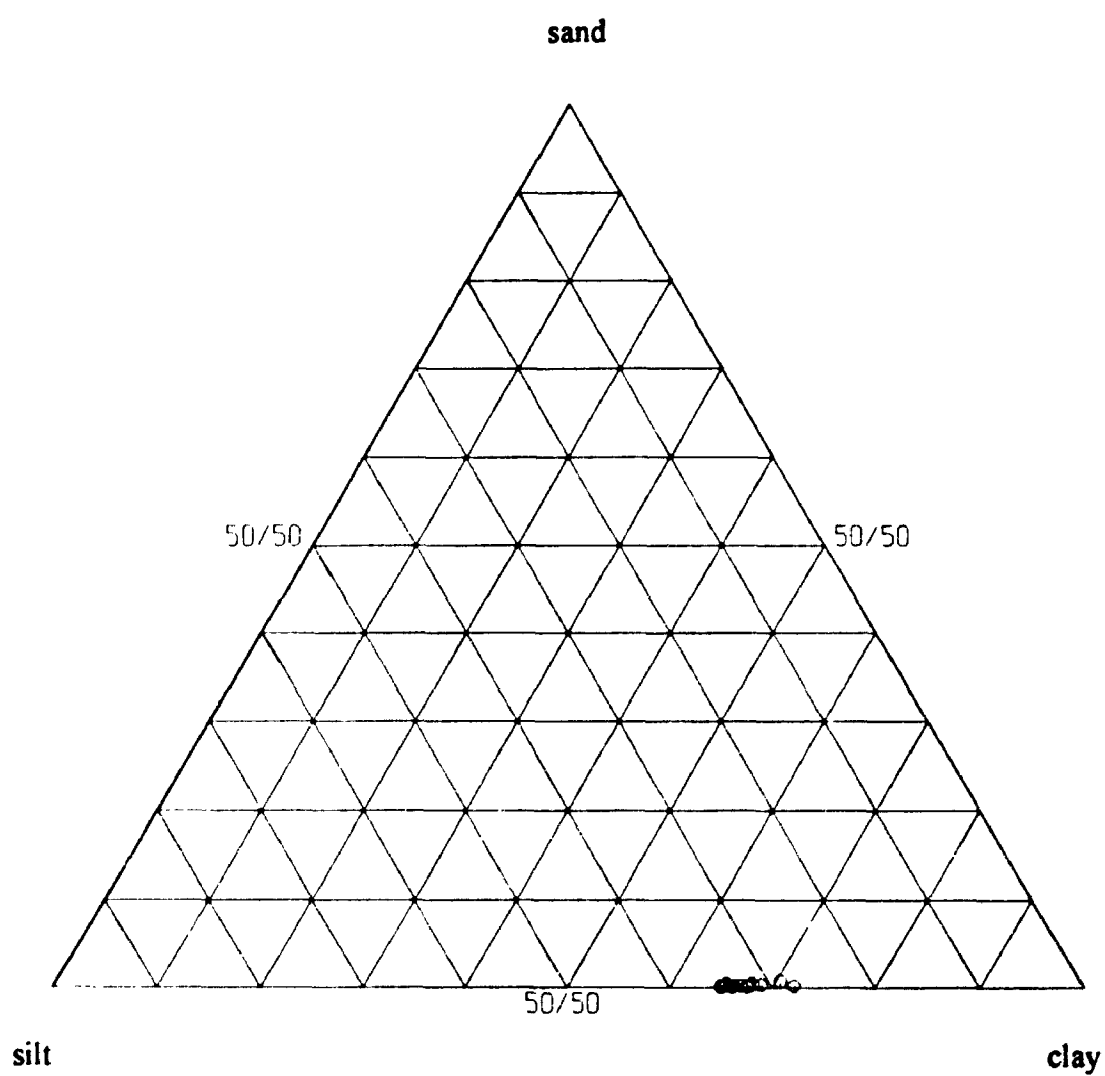


Note. Sand apex fraction is fine sand. Ternary diagrams are arranged in geographic order from south to north.

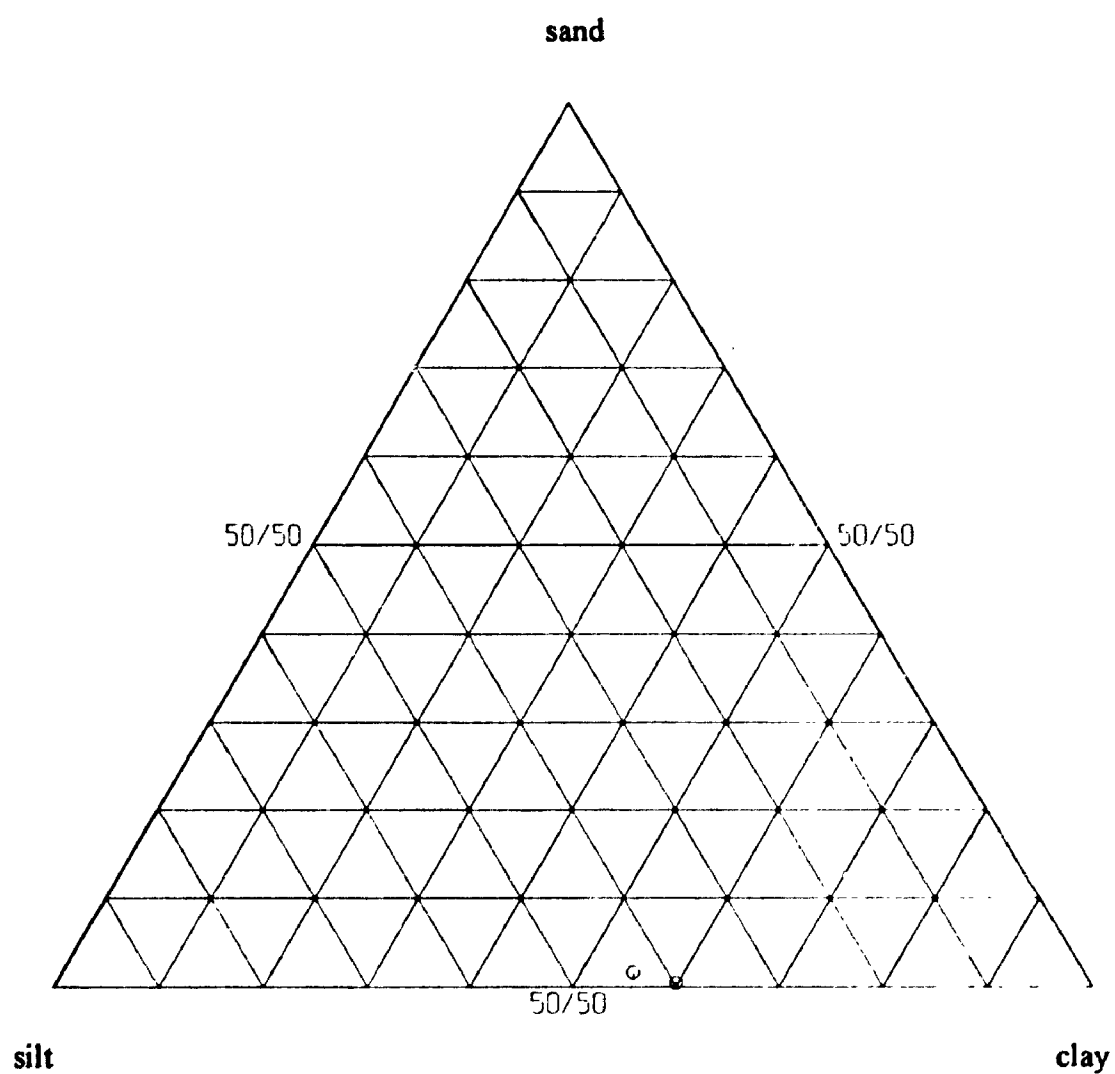




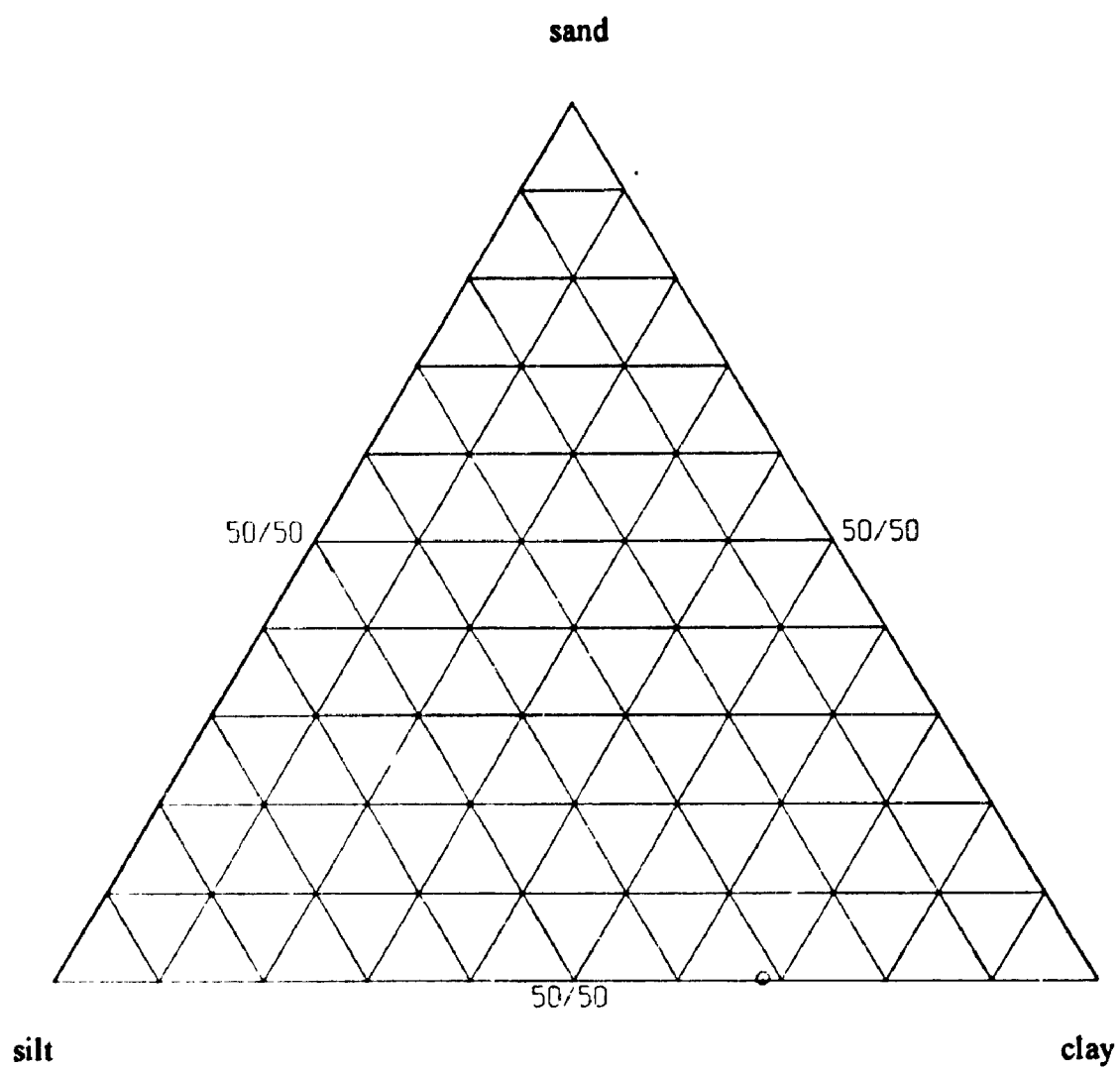
TUL91A-002



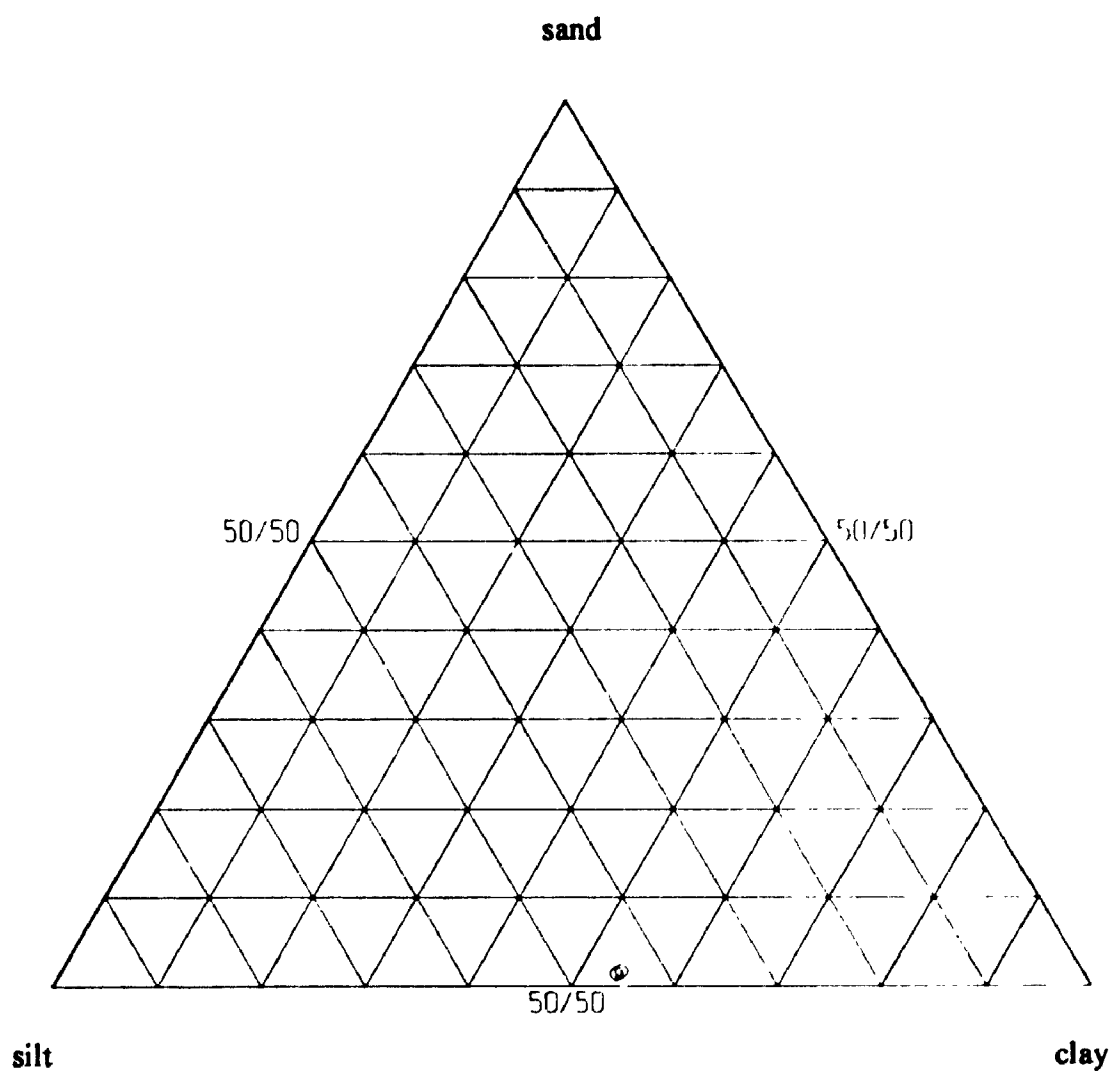
TUL89A-003



TUL91A-004



TUL89A-002



TUL91A-003

Sample No	Sediment type	Quartz	Feldspar (Na + K)	Chlorite	Illite	Smectite	Calcite
89-001-320-322	massive layer	minor	minor (Na)	minor	trace		
89-001-550-552	massive layer	minor	minor (Na)	minor	trace		
89-001-558-560	varves	minor	minor (Na)	minor	trace		
89-001-596-598	massive layer	minor	minor (Na)	minor	trace		
89-001-683	grey layer in varve	minor	minor (Na)	minor	trace		
89-001-727-728	massive layer	minor	minor (Na)	minor	trace		
89-002-199	varve	minor	minor (Na)	major	minor	trace	
89-002-203-205	massive layer	minor	minor (Na)	minor	trace		
89-002-217	grey layer in varve	minor	minor (Na)	minor	trace		
89-002-632	grey layer in varve	minor	minor (Na)	minor	trace		
89-002-733-735	massive layer	minor	minor (Na)	major	trace		
89-002-917	grey layer in varve	minor	minor (Na)	major	trace		
89-002-959	varve	minor	minor (Na)	minor	trace		
89-003-210-212	massive layer	minor	minor (Na)	minor	trace		
89-003-230-232	massive layer	minor	minor (Na)	minor	trace		
89-003-501	grey layer in varve	minor	minor (Na)	minor	trace		
89-003-539	grey layer in varve	minor	minor (Na)	major	trace		
89-003-568-570	massive layer	minor	minor (Na)	minor	trace	trace	
89-003-608-610	massive layer	minor	minor (Na)	minor	trace	trace	
89-003-690-692	massive layer	major	minor (Na)	minor	trace		
89-003-704	varve	minor	minor (Na)	minor	trace	trace	
89-003-760	grey layer in varve	minor	trace (Na)	minor	trace		
89-003-825-827	massive layer	minor	minor (Na)	minor	trace		
89-003-897-899	massive layer	minor	minor (Na)	minor	trace		
89-003-998-1000	massive layer	minor	minor (Na)	minor	trace		
89-003-1152	grey layer in varve	trace	trace (Na)	minor	trace		
89-003-1168-1170	massive layer	minor	minor (Na)	minor	trace		
91-001-23-28	varves	minor	minor (Na)	minor	trace	trace	
91-001-49	grey layer in varve	minor	minor (Na)	minor	trace		
91-001-59	grey layer in varve	minor	minor (Na)	minor	trace	trace	
91-001-69-70	massive layer	minor	minor (Na)	major	trace		
91-001-80	grey layer in varve	minor	minor (Na)	minor	trace		
91-001-238-240	massive layer	minor	minor (Na)	minor	trace		trace
91-001-430-432	massive layer	trace	trace (Na)	minor	trace	trace	
91-001-463-465	massive layer	minor	minor (Na)	minor	trace	trace	
91-001-609-610	massive layer	minor	minor (Na)	minor	trace		
91-001-638-640	massive layer	minor	minor (Na)	minor	trace	trace	
91-001-655	grey layer in varve	trace	trace (Na)	minor	trace		
91-001-823	grey layer in varve	minor	trace (Na)	major	trace		
91-001-833-835	massive layer	minor	minor (Na)	minor	trace		
91-001-842-844	varves	minor	minor (Na)	minor	trace		
91-001-886-888	massive layer	minor	minor (Na)	minor	trace		
91-001-1016	grey layer in varve	minor	minor (Na)	minor	trace		
91-001-1073-1075	massive layer	major	minor (Na)	minor	trace		
91-002-229-231	varves	minor	trace (Na)	minor	trace		
91-002-286	grey layer in varve	minor	minor (Na)	minor	trace		
91-002-358-360	massive layer	minor	minor (Na)	minor	trace		
91-002-533	grey layer in varve	minor	minor (Na)	minor	trace		
91-002-549	grey layer in varve	minor	minor (Na)	minor	trace		
91-002-648	grey layer in varve	minor	minor (Na)	minor	trace		
91-002-676-678	massive layer	minor	minor (Na)	minor	trace		
91-002-689	varve	minor	minor (Na)	minor	trace	trace	
91-002-899-905	massive layer	major	minor (Na)	minor	trace		
91-002-1038-1040	varves	minor	minor (Na)	minor	trace		

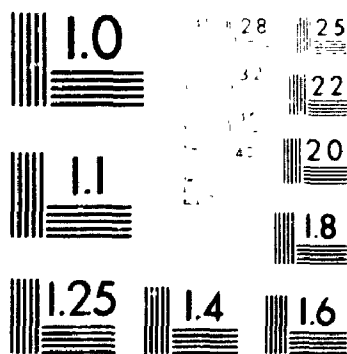
Sample No.	Sediment type	Quartz	Feldspar (Na + K)	Chlorite	Illite	Smectite	Calc	Amph
91-002-1059-1061	massive layer	minor	minor (Na)	minor	trace		258	
91-003-181	grey layer in varve	minor	minor (Na)	major	trace	trace		trace amph
91-003-310	varve	major	minor (Na)	minor	trace			
91-003-352-354	massive layer	major	minor (Na)	minor	trace			
91-003-356	grey layer in varve	minor	minor (Na)	major	trace	trace amph		
91-003-357	grey layer in varve	minor	trace (Na)	major	trace			
91-003-1154	varve	major	minor (Na)	minor	trace			
91-003-1183	grey layer in varve	minor	minor (Na)	minor	trace	trace		
91-004-38-39	grey layer in varve	minor	trace (Na)	major	trace			
91-004-43	grey layer in varve	minor	trace (Na)	major	trace			
91-004-55	varve	minor	minor (Na)	minor	trace	trace		
91-004-502	varve	minor	minor (Na)	minor	trace			
91-004-554	varve	minor	minor (Na)	major	trace	trace		
91-004-594	grey layer in varve	minor	trace (Na)	major	trace			
91-004-601	varve	minor	minor (Na)	minor	trace	trace		
91-004-787	grey layer in varve	minor	minor (Na)	minor	trace			
91-004-810-812	massive layer	major	minor (Na)	minor	trace			
91-004-817	grey layer in varve	minor	minor (Na)	minor	trace			
91-005-25-27	clayey silt	minor	minor (Na)	minor	trace			
91-005-30	grey layer	minor	minor (Na)	major	minor			
91-005-278-280	clayey silt	minor	minor (Na)	minor	trace			
91-005-404-405	clayey silt	major	minor (Na)	minor	trace			
91-005-493	grey layer	minor	minor (Na)	major	trace	trace		
91-005-583-584	clayey silt	minor	minor (Na)	minor	trace	trace		
91-005-640-642	clayey silt	minor	minor (Na)	minor	trace	trace		
91-005-676	clayey silt	major	minor (Na)	minor	trace			
91-005-850	grey layer	minor	trace (Na)	major	trace			
91-005-870-872	clayey silt	major	minor (Na)	minor	trace			
92-gs-21	grab sample	major	minor (Na)	minor	trace	trace amph		
92-gs-54	grab sample	minor		trace				major
92-gs-55	grab sample	minor	minor (Na)	major	minor	trace amph		
92-gs-56	grab sample	minor	minor (Na)	major	trace	trace amph		
VEC92A-59	grab sample	trace	trace (Na)	major	minor	minor		

Note Sample 92-gs-21 was collected near the mouth of the Cowichan River, sample 92-gs-54 is a sample from the west side of Saanich Inlet opposite Brentwood Bay, samples 92-gs-55 and 92-gs-56 are from the mouth of Goldstream River, and sample VEC92A-59 was collected near the mouth of Fraser River

Values are semi-quantitative, e.g., if a sample contains three clay minerals with minor amounts, it means that the minerals are present in equal proportions (X-ray lab, GSC)

4 OF 4

PM-1 3 1/2 x 4" PHOTOGRAPHIC MICROCOPY TARGET
NBS 1010a ANSI/ISO #2 EQUIVALENT

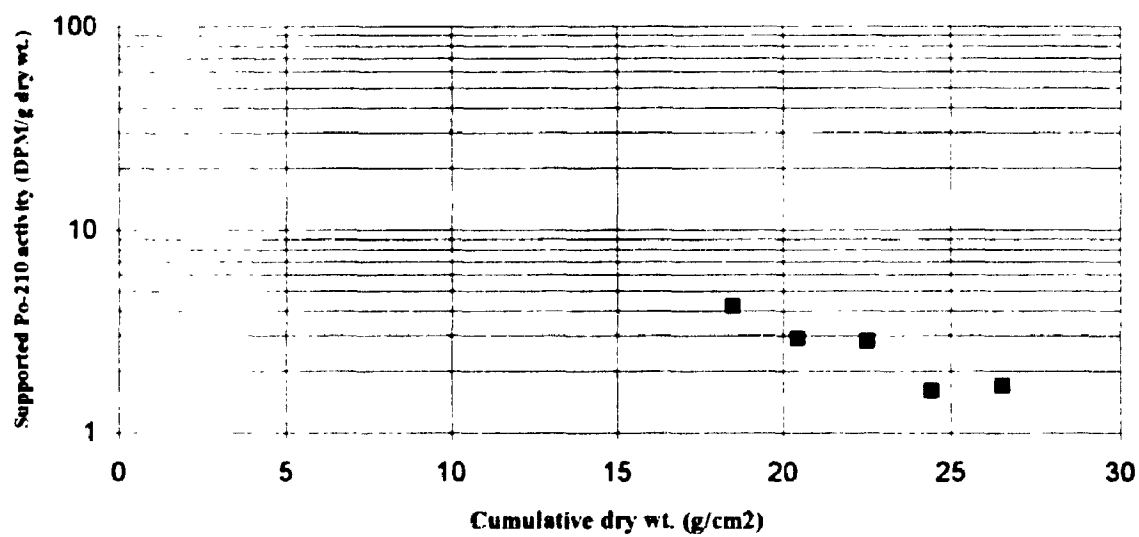


PRECISIONSM RESOLUTION TARGETS

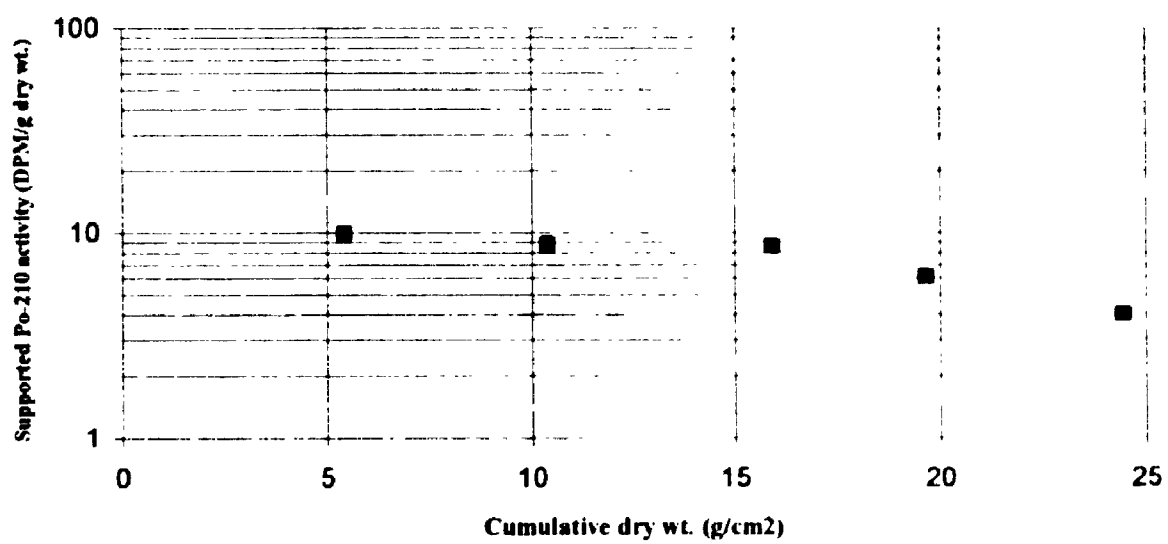
Core TUL89A-003	Cumulative dry wt. mid point (g/cm ²)	Specific activity (DPM/g) ^a	Error (DPM/g) ± 1σ
Depth (cm)			
55-56	18.5	4.2	0.5
61-62	20.44	2.9	0.4
68-69	22.55	2.8	0.4
75-76	24.43	1.6	0.3
83-84	26.52	1.7	0.3

Core TUL91A-005	Cumulative dry wt. mid point (g/cm ²)	Specific activity (DPM/g)	Error (DPM/g) ± 1σ
Depth (cm)			
10-11	5.43	9.9	0.7
20-21	10.4	8.8	0.7
32-33	15.93	8.6	0.7
40-41	19.68	6.1	0.6
50-51	24.45	4	0.5

^a DPM=Desintegrations per minute

Core TUL89A-003

Core TUL91A-005



Determination of accumulation rates based on least square, best-fit method with background as a variable

Y1=4.2 DPM/g Y2=1 762 DPM/g	X1=18.5g/cm ² X2=24.431g/cm ²	R ² = 0.885 Bkg=0.00 ^a Accum=211.5 mg/cm ² /yr
Y1=4.1 DPM/g Y2=1.683 DPM/g	X1=18.5g/cm ² X2=24.431g/cm ²	R ² = 0.884 Bkg=0.08 Accum=204.8 mg/cm ² /yr
Y1=4.1 DPM/g Y2=1.604 DPM/g	X1=18.5g/cm ² X2=24.431g/cm ²	R ² = 0.882 Bkg=0.16 Accum=198.0 mg/cm ² /yr
Y1=4.0 DPM/g Y2=1.524 DPM/g	X1=18.5g/cm ² X2=24.431g/cm ²	R ² = 0.881 Bkg=0.24 Accum=191.2 mg/cm ² /yr
Y1=3.9 DPM/g Y2=1.445 DPM/g	X1=18.5g/cm ² X2=24.431g/cm ²	R ² = 0.879 Bkg=0.32 Accum=184.4 mg/cm ² /yr
Y1=3.9 DPM/g Y2=1.366 DPM/g	X1=18.5g/cm ² X2=24.431g/cm ²	R ² = 0.877 Bkg=0.40 Accum=177.5 mg/cm ² /yr
Y1=3.8 DPM/g Y2=1.286 DPM/g	X1=18.5g/cm ² X2=24.431g/cm ²	R ² = 0.875 Bkg=0.48 Accum=170.6 mg/cm ² /yr
Y1=3.7 DPM/g Y2=1.207 DPM/g	X1=18.5g/cm ² X2=24.431g/cm ²	R ² = 0.872 Bkg=0.56 Accum=163.5mg/cm ² /yr
Y1=3.7 DPM/g Y2=1.127 DPM/g	X1=18.5g/cm ² X2=24.431g/cm ²	R ² = 0.870 Bkg=0.64 Accum=156.4 mg/cm ² /yr
Y1=3.6 DPM/g Y2=1.047 DPM/g	X1=18.5g/cm ² X2=24.431g/cm ²	R ² = 0.866 Bkg=0.71 Accum=149.3 mg/cm ² /yr
Y1=3.5 DPM/g Y2=0.967 DPM/g	X1=18.5g/cm ² X2=24.431g/cm ²	R ² = 0.863 Bkg=0.79 Accum=142.0mg/cm ² /yr
Y1=3.5 DPM/g Y2=0.886 DPM/g	X1=18.5g/cm ² X2=24.431g/cm ²	R ² = 0.859 Bkg=0.87 Accum=134.5 mg/cm ² /yr

^a The accumulation rate (Accum) is determined for the best-fit line with the highest coefficient of determination (R²)

Y1=3.4 DPM/g Y2=0.804 DPM/g	X1=18.5g/cm ² X2=24.431g/cm ²	R ² = 0.854 Bkg=0.95 Accum=126.9 mg/cm ² /yr
Y1=3.4 DPM/g Y2=0.722 DPM/g	X1=18.5g/cm ² X2=24.431g/cm ²	R ² = 0.848 Bkg=1.03 Accum=119.1 mg/cm ² /yr
Y1=3.4 DPM/g Y2=0.639 DPM/g	X1=18.5g/cm ² X2=24.431g/cm ²	R ² = 0.841 Bkg=1.11 Accum=111.1 mg/cm ² /yr
Y1=3.3 DPM/g Y2=0.554 DPM/g	X1=18.5g/cm ² X2=24.431g/cm ²	R ² = 0.832 Bkg=1.19 Accum=102.7 mg/cm ² /yr
Y1=3.3 DPM/g Y2=0.468 DPM/g	X1=18.5g/cm ² X2=24.431g/cm ²	R ² = 0.822 Bkg=1.27 Accum=93.9 mg/cm ² /yr
Y1=3.4 DPM/g Y2=0.378 DPM/g	X1=18.5g/cm ² X2=24.431g/cm ²	R ² = 0.808 Bkg=1.35 Accum=84.3 mg/cm ² /yr
Y1=3.5 DPM/g Y2=0.283 DPM/g	X1=18.5g/cm ² X2=24.431g/cm ²	R ² = 0.790 Bkg=1.43 Accum=73.7 mg/cm ² /yr
Y1=3.7 DPM/g Y2=0.178 DPM/g	X1=18.5g/cm ² X2=24.431g/cm ²	R ² = 0.763 Bkg=1.51 Accum=60.6 mg/cm ² /yr
Y1=5.4 DPM/g Y2=0.038 DPM/g	X1=18.5g/cm ² X2=24.431g/cm ²	R ² = 0.700 Bkg=1.59 Accum=37.2 mg/cm ² /yr

Calculation of age of sediment.

Cumulative dry wt. (g/cm²) ÷ accumulation rate (g/cm²/yr) = age of sediment (yr)

24.43g/cm² ÷ 0.211g/cm²/yr = 115 yrs.

Therefore, at 75-76 cm depth, the sediment is 115 yrs old.

Determination of accumulation rates based on the least square, best-fit method for all data points with background as a variable

Y1=11.1 DPM/g Y2=4.693 DPM/g	X1=5.432g/cm ² X2=24.452g/cm ²	R ² = 0.839 Bkg=0.00 ^a Accum=690.3 mg/cm ² /yr
Y1=10.9 DPM/g Y2=4.490 DPM/g	X1=5.432g/cm ² X2=24.452g/cm ²	R ² = 0.837 Bkg=0.20 Accum=668.3mg/cm ² /yr
Y1=10.7 DPM/g Y2=4.287 DPM/g	X1=5.432g/cm ² X2=24.452g/cm ²	R ² = 0.835 Bkg=0.40 Accum=646.1mg/cm ² /yr
Y1=10.5 DPM/g Y2=4.084 DPM/g	X1=5.432g/cm ² X2=24.452g/cm ²	R ² = 0.833 Bkg=0.60 Accum=623.8mg/cm ² /yr
Y1=10.4DPM/g Y2=3.880 DPM/g	X1=5.432g/cm ² X2=24.452g/cm ²	R ² = 0.830 Bkg=0.80 Accum=601.4 mg/cm ² /yr
Y1=10.2 DPM/g Y2=3.676 DPM/g	X1=5.432g/cm ² X2=24.452g/cm ²	R ² = 0.828 Bkg=1.00 Accum=578.8mg/cm ² /yr
Y1=10.1 DPM/g Y2=3.471 DPM/g	X1=5.432g/cm ² X2=24.452g/cm ²	R ² = 0.825 Bkg=1.20 Accum=556.1mg/cm ² /yr
Y1=9.1 DPM/g Y2=3.266 DPM/g	X1=5.432g/cm ² X2=24.452g/cm ²	R ² = 0.822 Bkg=1.40 Accum=533.2mg/cm ² /yr
Y1=9.8 DPM/g Y2=3.060 DPM/g	X1=5.432g/cm ² X2=24.452g/cm ²	R ² = 0.818 Bkg=1.60 Accum=510.1mg/cm ² /yr
Y1=9.6 DPM/g Y2=2.853 DPM/g	X1=5.432g/cm ² X2=24.452g/cm ²	R ² = 0.815 Bkg=1.80 Accum=486.6mg/cm ² /yr
Y1=9.5 DPM/g Y2=2.645 DPM/g	X1=5.432g/cm ² X2=24.452g/cm ²	R ² = 0.810 Bkg=2.01 Accum=462.9mg/cm ² /yr
Y1=9.4 DPM/g Y2=2.435 DPM/g	X1=5.432g/cm ² X2=24.452g/cm ²	R ² = 0.805 Bkg=2.21 Accum=438.8mg/cm ² /yr
Y1=9.3 DPM/g Y2=2.224 DPM/g	X1=5.432g/cm ² X2=24.452g/cm ²	R ² = 0.800 Bkg=2.41 Accum=414.2mg/cm ² /yr

Y1=9.2 DPM/g Y2=2.010 DPM/g	X1=5.432g/cm ² X2=24.452g/cm ²	R ² = 0.793 Bkg=2.0 Accum=389.0mg/cm ² /yr
Y1=9.1 DPM/g Y2=1.792 DPM/g	X1=5.432g/cm ² X2=24.452g/cm ²	R ² = 0.785 Bkg=2.81 Accum=363.1mg/cm ² /yr
Y1=9.1 DPM/g Y2=1.570 DPM/g	X1=5.432g/cm ² X2=24.452g/cm ²	R ² = 0.776 Bkg=3.01 Accum=336.1mg/cm ² /yr
Y1=9.2 DPM/g Y2=1.342 DPM/g	X1=5.432g/cm ² X2=24.452g/cm ²	R ² = 0.764 Bkg=3.21 Accum=307.6mg/cm ² /yr
Y1=9.3 DPM/g Y2=1.103 DPM/g	X1=5.432g/cm ² X2=24.452g/cm ²	R ² = 0.749 Bkg=3.41 Accum=276.9mg/cm ² /yr
Y1=9.7 DPM/g Y2=0.847 DPM/g	X1=5.432g/cm ² X2=24.452g/cm ²	R ² = 0.727 Bkg=3.61 Accum=242.5mg/cm ² /yr
Y1=10.6 DPM/g Y2=0.553 DPM/g	X1=5.432g/cm ² X2=24.452g/cm ²	R ² = 0.695 Bkg=3.81 Accum=200.1mg/cm ² /yr
Y1=18.8 DPM/g Y2=0.090 DPM/g	X1=5.432g/cm ² X2=24.452g/cm ²	R ² = 0.601 Bkg=4.01 Accum=110.7mg/cm ² /yr

* The accumulation rate (Accum) is determined for the best-fit line with the highest coefficient of determination (R²)

Calculation of age of sediment

Cumulative dry wt. (g/cm²) ÷ accumulation rate (g/cm²/yr) = age of sediment (yr)

24.45g/cm² ÷ 0.690g/cm²/yr = 35 yrs at 40-41 cm depth

Determination of accumulation rates based on the least square, best-fit method for the lowest three^a data points with background as a variable

Y1=8.6 DPM/g Y2=4.002 DPM/g	X1=15.935g/cm ² X2=24.452g/cm ²	R ² = 0.999 Bkg=0.00 Accum=347.8 mg/cm ² /yr
Y1=8.4 DPM/g Y2=3.805 DPM/g	X1=15.935g/cm ² X2=24.452g/cm ²	R ² = 1.000 Bkg=0.20 Accum=335.6 mg/cm ² /yr
Y1=8.2 DPM/g Y2=3.608 DPM/g	X1=15.935g/cm ² X2=24.452g/cm ²	R ² = 1.000 Bkg=0.40 Accum=323.3 mg/cm ² /yr
Y1=8.0 DPM/g Y2=3.411 DPM/g	X1=15.935g/cm ² X2=24.452g/cm ²	R ² = 1.000 Bkg=0.60 Accum=311.0 mg/cm ² /yr
Y1=7.8 DPM/g Y2=3.214 DPM/g	X1=15.935g/cm ² X2=24.452g/cm ²	R ² = 1.000 Bkg=0.80 ^b Accum=298.6 mg/cm ² /yr
Y1=7.6 DPM/g Y2=3.017 DPM/g	X1=15.935g/cm ² X2=24.452g/cm ²	R ² = 1.000 Bkg=1.00 Accum=286.1 mg/cm ² /yr
Y1=7.4 DPM/g Y2=2.821 DPM/g	X1=15.935g/cm ² X2=24.452g/cm ²	R ² = 1.000 Bkg=1.20 Accum=273.5 mg/cm ² /yr
Y1=7.2 DPM/g Y2=2.624 DPM/g	X1=15.935g/cm ² X2=24.452g/cm ²	R ² = 1.000 Bkg=1.40 Accum=260.9 mg/cm ² /yr
Y1=7.1 DPM/g Y2=2.428 DPM/g	X1=15.935g/cm ² X2=24.452g/cm ²	R ² = 1.000 Bkg=1.60 Accum=248.2 mg/cm ² /yr
Y1=6.9 DPM/g Y2=2.232 DPM/g	X1=15.935g/cm ² X2=24.452g/cm ²	R ² = 0.999 Bkg=1.80 Accum=235.3 mg/cm ² /yr
Y1=6.7 DPM/g Y2=2.036 DPM/g	X1=15.935g/cm ² X2=24.452g/cm ²	R ² = 0.999 Bkg=2.01 Accum=222.3 mg/cm ² /yr
Y1=6.5 DPM/g Y2=1.840 DPM/g	X1=15.935g/cm ² X2=24.452g/cm ²	R ² = 0.998 Bkg=2.21 Accum=209.1 mg/cm ² /yr
Y1=6.4 DPM/g Y2=1.645 DPM/g	X1=15.935g/cm ² X2=24.452g/cm ²	R ² = 0.997 Bkg=2.410 Accum=195.8 mg/cm ² /yr

Y1=6.2 DPM/g Y2=1.449 DPM/g	X1=15.935g/cm ² X2=24.452g/cm ²	R ² = 0.996 Bkg=2.61 Accum=182.1 mg/cm ² /yr
Y1=6.1 DPM/g Y2=1.253 DPM/g	X1=15.935g/cm ² X2=24.452g/cm ²	R ² = 0.994 Bkg=2.81 Accum=168.1 mg/cm ² /yr
Y1=5.9 DPM/g Y2=1.057 DPM/g	X1=15.935g/cm ² X2=24.452g/cm ²	R ² = 0.991 Bkg=3.01 Accum=153.6 mg/cm ² /yr
Y1=5.8 DPM/g Y2=0.860 DPM/g	X1=15.935g/cm ² X2=24.452g/cm ²	R ² = 0.986 Bkg=3.21 Accum=138.5 mg/cm ² /yr
Y1=5.8 DPM/g Y2=0.662 DPM/g	X1=15.935g/cm ² X2=24.452g/cm ²	R ² =0.980 Bkg=3.41 Accum=122.4 mg/cm ² /yr
Y1=5.8 DPM/g Y2=0.460 DPM/g	X1=15.935g/cm ² X2=24.452g/cm ²	R ² = 0.970 Bkg=3.61 Accum=104.6 mg/cm ² /yr
Y1=6.1 DPM/g Y2=0.252 DPM/g	X1=15.935g/cm ² X2=24.452g/cm ²	R ² = 0.952 Bkg=3.81 Accum=83.3 mg/cm ² /yr
Y1=9.3 DPM/g Y2=0.017 DPM/g	X1=15.935g/cm ² X2=24.452g/cm ²	R ² = 0.893 Bkg=4.01 Accum=42.1mg/cm ² /yr

^a Higher data may be unreliable because of sediment mixing during coring

^b The background value (0.800 DPM) is the average of all values that have a coefficient of determination (R²) of 1.00.

Calculation of age of sediment:

Cumulative dry wt. (g/cm²) ÷ accumulation rate (g/cm²/yr) = age of sediment (yr)

24.45g/cm² ÷ 0.2986g/cm²/yr = 82 yrs at 40-41 cm depth

Appendix 3-8 Scenario (b) Possible correlations based on adjusted cumulative number of varves (Table 3-6)

South		TUL 91A-001*	TUL 89A-001	TUL 91A-002*	TUL 89A-003*	TUL 91A-004*	TUL 89A-002	North	
40	I	40	I	40	59	I	107	TUL 91A-003*	155
ml		ml		ml	ml		ml		ml
176		105		203 242	315 224	443 425	161		
ml		ml		385 284	ml	III			
203	II	216		ml	443 422 444	ml	ml		
ml		ml		484 48*	III	V	543		
443	III	485		ml	514 493 512	ml	ml		
ml		ml		682 684	IV		613		
514 512	IV	557		ml	556 535 554	V	ml		
ml		ml		760 746 745	VI		743		
644 642		690		ml			ml		
ml		ml		890 876 875			938		
760 758	VI	823		ml	830 812 794 810	VII			
ml		ml		1032 1018 1017	ml				
830 828	VII	887		ml	870 852 834 850				
ml		ml		1080 1066 1065	941 923 902 921				
1080 1059 1057	VIII	1223		ml	ml				
ml				1402 1388 1387	956 938 917 936				
1150 1129 1127	IX			ml	ml				
ml				1484 1476 1462 1461	1080 1062 1044 1023 1042	VIII			
1320 1299 1297					ml				
					1150 1139 1121 1103 1082 1101	IX			
					ml				
					1484 1473 1455 1437 1416 1435	X			

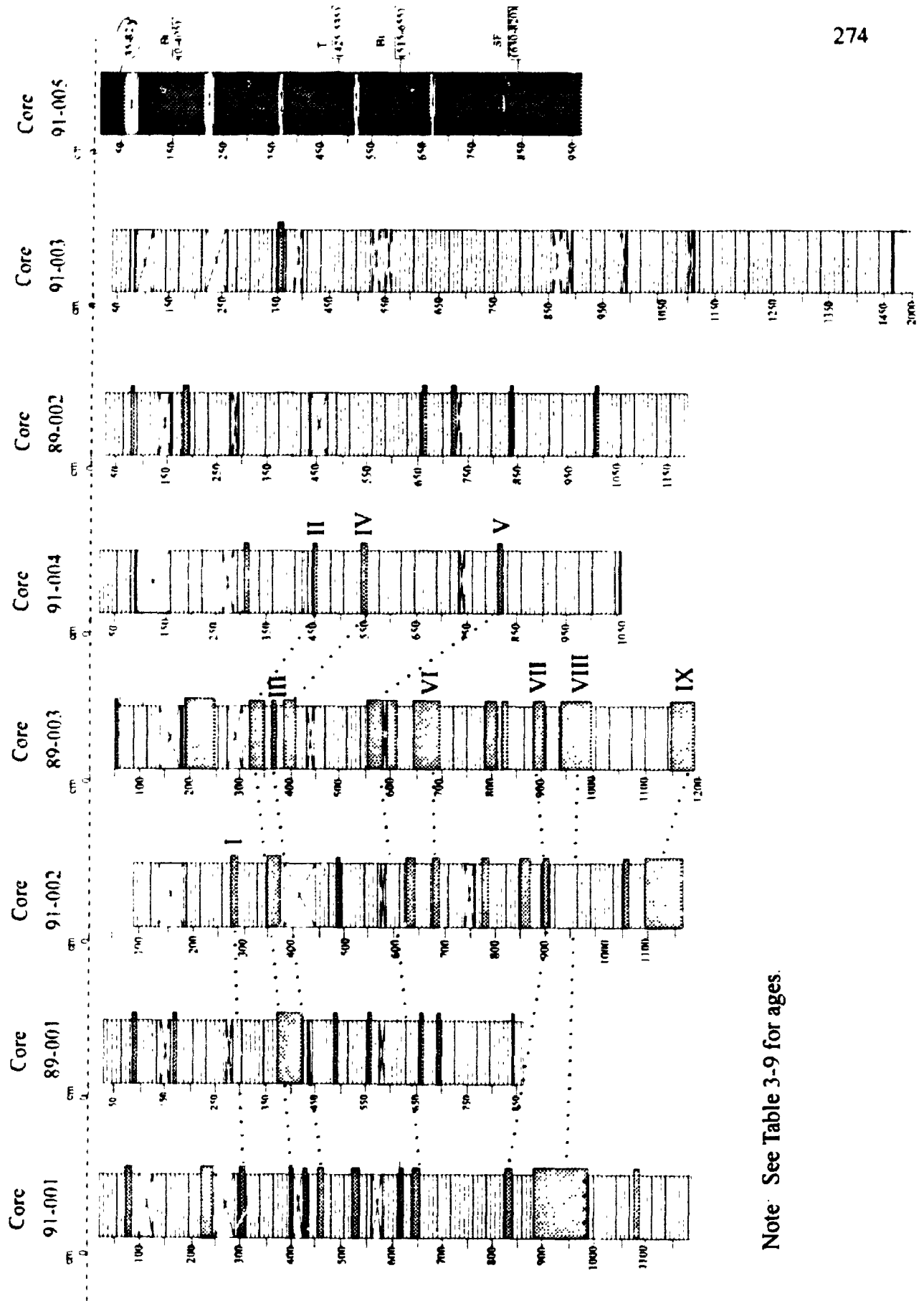
Note: Asterisk indicates presence of ^{137}Cs or ^{210}Pb . The massive layers of the two cores that lack ^{137}Cs and ^{210}Pb have not been correlated. Scenario (b) assumes layer 1 in TUL 91A-001 and TUL 89A-003 is 40 years old. See text for explanation of the adjustment method.

Appendix 3-8 Scenario (c) Possible correlations based on adjusted cumulative number of varves (Table 3-6)

South	TUL91A-001*	TUL89A-001	TUL91A-002*	TUL89A-003*	TUL91A-004*	TUL89A-002	North TUL91A-003*
	59 40 I		202 II	59 I	254	107	155
	ml	105	ml	ml	ml	ml	ml
	202 195 176 II	ml	384	334	441 425 III	161	
	ml	216	ml	ml	ml	ml	
	229 222 203	ml	483	441 III	545 529 IV	543	
	ml	485	ml	ml	ml	ml	
	469 462 443	ml	681	512	810 806 790 V	613	
	ml	557	ml	ml		ml	
	545 538 521 512 IV	ml	745	554		743	
	ml	690	ml	ml		ml	
	675 668 661 642	ml	880 875 VI	810 V		938	
	ml	823	ml	ml			
	810 791 784 772 758 V	ml	1042 1022 1012 VII	850			
	ml	887	ml	ml			
	880 861 854 842 828 VI	ml	1109 1090 1070 1065 VIII	921			
	ml	1223	ml	ml			
	1109 1090 1082 1076 1052 VIII		1443 1431 1412 1392 1382 IX	936			
	ml		ml	ml			
	1179 1160 1153 1146 1127		1517 1505 1486 1466 1461	1042 VII			
	ml			ml			
	1349 1320 1323 1316 1297			1109 1101 VIII			
				ml			
				1443 1425 IX			

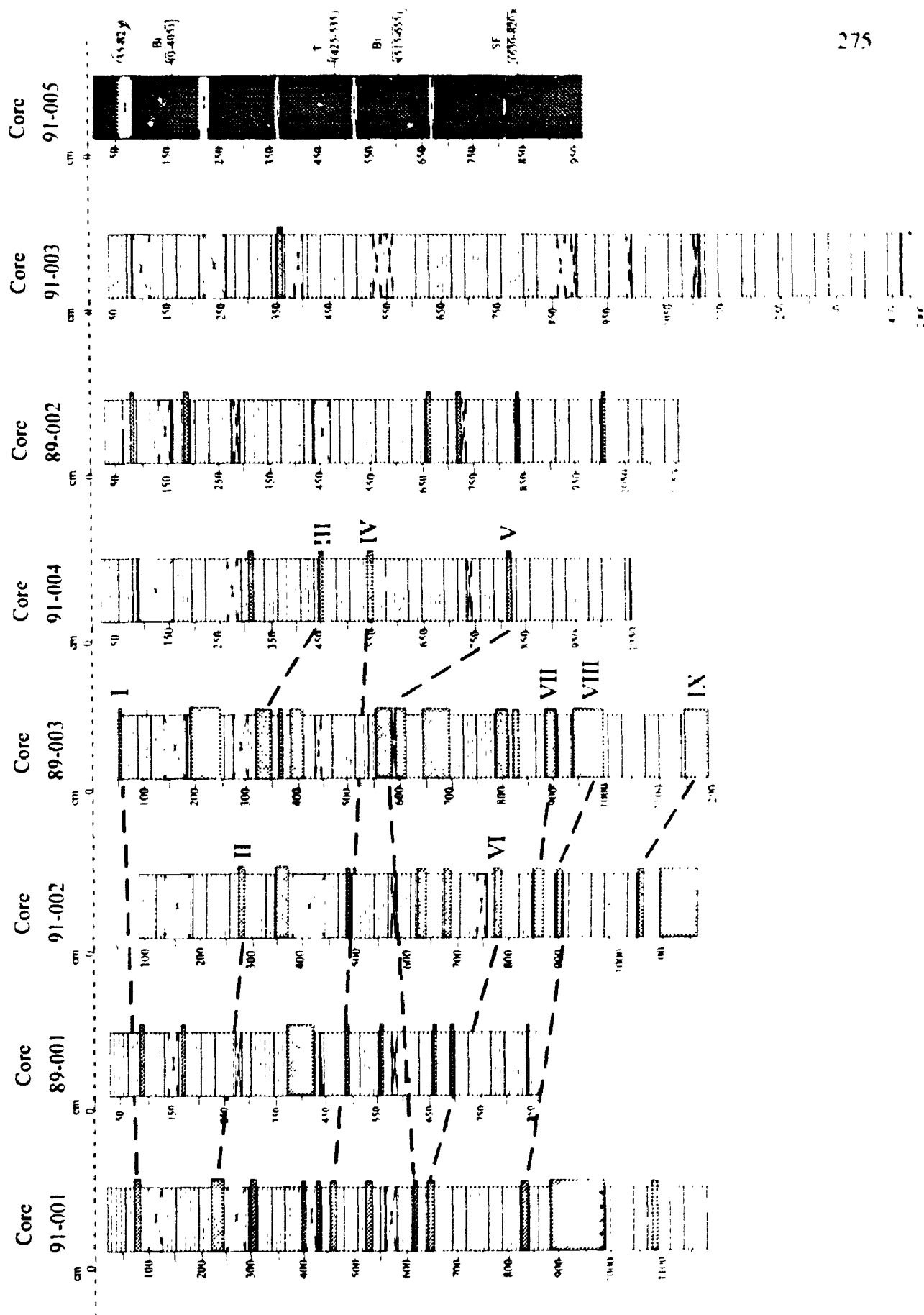
Note: Asterisk indicates presence of ¹³⁷Cs or ²¹⁰Pb. The massive layers of the two cores that lack ¹³⁷Cs and ²¹⁰Pb have not been correlated. Scenario (c) assumes layer I in TUL91A-001 and TUL89A-003 is 59 years old. See text for explanation of the adjustment method.

Scenario a: Massive layer correlations



Note: See Table 3-9 for ages.

Scenario b:



CHAPTER 4. CONCLUSIONS

The percentage of live foraminifera in Saanich Inlet decreases with increasing water depth, probably due to decreasing oxygen concentrations. The main environmental control is water circulation which is influenced by the presence of a sill. Different environmental parameters, including salinity, oxygen, and temperature, explain most of the clustering and the distribution of the dominant foraminiferal fauna. Other environmental controls are runoff from the land, contamination, and sediment texture, but these are also affected by the water circulation in the basin.

Certain foraminiferal species are closely linked to specific environmental parameters. Eggerella advena indicates contamination and brackish water conditions. Miliammina fusca reflects very brackish water conditions. Leptohalysis catella reflects deep water, low oxygen concentrations, high organic content, and a muddy (with some sand) substrate. Similarly, Stainforthia feylingi indicates deep water and, probably, low oxygen concentrations. Buccella frigida is indicative of normal temperate marine conditions.

There are five foraminiferal biofacies of distinct geographic distribution identified in Saanich Inlet. (1) Eggerella advena Biofacies of shallow nearshore environments near sewage outfalls and septic system drainage; (2) Eggerella advena-Spiroplectammina biformis Biofacies and (3) Miliammina fusca Biofacies, both located close to Biofacies 1 at shallow depths in brackish bays. Although there is relatively little freshwater runoff into Saanich Inlet, Biofacies 1, 2, and 3 indicate that localized ephemeral runoff affects the foraminiferal distribution; (4) Lobatula fletcheri

Biofacies, subdivided into (4A) Stainforthia feylingi Sub-biofacies dominant at greater depths where oxygen levels are low, and (4B) Buccella frigida Sub-biofacies at shallow depths within the bays of the inlet, reflecting poor mixing of normal marine seawater because of restricted circulation; (5) Leptohalysis catella-Spiroplectammina biformis Biofacies found at greater depths far from shore.

Data from eight piston cores show that late Holocene sediments in Saanich Inlet were deposited from suspension as varves, interrupted sporadically and locally by sediment gravity flows. Sedimentation rates decrease from north to south in the inlet, confirming that the main source of sediment is Cowichan River. However, variations in grain size between cores indicate that there are additional sources of sediment, probably ephemeral streams and possibly Goldstream River. Varve thicknesses do not vary with depth in the cores implying that for the last 1500 years, sedimentation has not changed significantly.

Massive layers interbedded with the varves are interpreted as sediment gravity flow deposits: (1) a Student t-test revealed that the particle size of samples of varves and massive sediments are not the same, implying different transport mechanisms; (2) basal contacts of massive layers are sharp, and some are clearly erosional; (3) massive layers contain brecciated varves and varve intraclasts, indicating that varves have been eroded and incorporated into the flow; (4) most massive layers have a lower zone of brecciated varves underlying massive mu 1; (5) most massive layers contain benthic foraminifera, implying that the sediment was transported from above the anoxic zone (< 150 m depth).

The massive layers are classified more precisely as debris flow deposits because: (1) none of the massive layers exhibits sedimentary structures and textures of a classic turbidite, i.e., Bouma-sequence; (2) there is no normal or inverse grading of grains; (3) most massive layers contain a basal zone of brecciated varves resulting from shearing at the base of a debris flow; (4) massive mud overlying the zone of brecciated varves is interpreted to be a plug or raft in the debris flow; and (5) varve intraclasts show no apparent directional fabric.

Varves were used with some success to date and correlate the massive layers. Uncertainties in age estimates result from the lack of a precise datum at the tops of the cores and from erosion of varves during the emplacement of debris flow deposits. Uncertainties in age increase downcore.

Correlation of the cores indicates that debris flows originated on the side walls of Saanich Inlet and did not travel the full length of the fiord. There are two possible triggering mechanisms. The first is oversteepening of sediment accumulations on the side walls. The second is seismic shaking.

The number of varves separating adjacent massive layers in the eight cores ranges from 15 to >754. The average is 116, which is broadly consistent with the expected periodicity of moderate to large earthquakes in the region.

Some massive layers may correspond to documented seismic events. Massive layers at the top of two cores may have been deposited during the 1946 Vancouver Island earthquake (M7.2). A massive layer, dating to about 200 years ago and found in two cores may have been emplaced during a strong earthquake in February 1793,

reported by Spanish explorers wintering on the west coast of Vancouver Island.

Another widespread massive layer, about 1050-1150 years old, may record a large crustal earthquake centered near Seattle, 140 km south-southeast of Saanich Inlet.

This earthquake may be linked to plate-boundary failure farther west. Some of the other massive layers probably record other prehistoric earthquakes, as yet undocumented elsewhere.

END

3 1 - 0 5 - 9 6

FIN